PHOTOCHEMISTRY AND ORGANOCATALYSIS FOR RADICAL-BASED CARBON-CARBON BOND-FORMING PROCESSES

Emilien Le Saux

UNIVERSITAT
ROVIRA i VIRGILI

Photochemistry and Organocatalysis for Radical-Based Carbon-Carbon Bond-Forming Processes

Emilien Le Saux

DOCTORAL THESIS
2023

UNIVERSITAT ROVIRA I VIRGILI
PHOTOCHEMISTRY AND ORGANOCATALYSIS FOR RADICAL-BASED CARBON-CARBON BOND-FORMING PROCESSES
Emilien Le Saux

UNIVERSITAT ROVIRA I VIRGILI
PHOTOCHEMISTRY AND ORGANOCATALYSIS FOR RADICAL-BASED CARBON-CARBON BOND-FORMING
PROCESSES
Emilien Le Saux

Emilien Le Saux

Photochemistry and Organocatalysis for Radical-Based Carbon-Carbon Bond-Forming Processes

Doctoral Thesis

Supervised by Prof. Paolo Melchiorre

ICIQ – Institut Català d'Investigació Química

UNIVERSITAT
ROVIRA i VIRGILI

ICIQ
Institut
Català
d'Investigació
Química

Tarragona

2023

UNIVERSITAT ROVIRA I VIRGILI
PHOTOCHEMISTRY AND ORGANOCATALYSIS FOR RADICAL-BASED CARBON-CARBON BOND-FORMING
PROCESSES
Emilien Le Saux

I, Prof. Paolo Melchiorre,

Professor at the University of Bologna, Italy, previously Group Leader at ICIQ

STATE

that the present study, entitled

"Photochemistry and Organocatalysis for Radical-Based Carbon-Carbon Bond-Forming Processes",

presented by EMILIEN LE SAUX for the award of the degree of Doctor, has been carried out under my supervision at the Institut Català d'Investigació Química (ICIQ).

Tarragona, March 23 2023

Doctoral Thesis Supervisor

Prof. Paolo Melchiorre

UNIVERSITAT ROVIRA I VIRGILI
PHOTOCHEMISTRY AND ORGANOCATALYSIS FOR RADICAL-BASED CARBON-CARBON BOND-FORMING
PROCESSES
Emilien Le Saux

Acknowledgements

A PhD is a long journey that would not be possible without the support of family, friends, and colleagues. In these three years and a half I was lucky to meet people who helped me in many different ways, and for this I would like to thank them.

First, I would like to express my gratitude to my supervisor Prof. Paolo Melchiorre for giving me the opportunity to join his research group for my doctoral studies and for his constant support and guidance throughout my PhD.

I would also like to thank Prof. Mariola Tortosa, Prof. Rubén Martín, and Prof. Karl Anker Jørgensen for their willingness to be part of my doctoral thesis committee, which I appreciate very much.

I am of course grateful to all my colleagues and friends from the Melchiorre group for helping me growing as a scientist and also for the good times spent together. A special mention to the 2.10*ers* who made me feel part of the group from the very beginning. In particular thank you to *Eugenio* (the quenching expert) for his good advice in chemistry, to *Nurtalya* for all the laughs and books/music recommendations, to *Pablo* for always being so calm, to *Eduardo* for the funny times after lockdown, to *Riccardo* whose despedida will never be forgotten, and to *Adri*. Thank you also to *Davide*, to *Matteo* and *Wei* (the Great) whom I started the PhD with, to *Laura* the best lunch partner, to *Yann*, to *Martin* for proofreading this thesis, to *Eleni* for always being "happy, happy, happy", to the best host *Vasileios*, to *Miguel* for his good jokes, and to our beloved visiting students: *Pietro*, *Davide C.*, *Elena*, *Enrico*, and *Gianluca*. A very special thanks goes to two postdocs I shared memorable times with and who taught me a lot: *Margherita* and her passion of Ferris wheel, and *Will* who has been an incredible support during my PhD, and who proofread most of this thesis.

I also want to express my gratitude to *Núria* for the administrative support, and to *Laia* for her help in the lab, and to all the research support units at ICIQ. In particular, the work presented here would not have been possible without the assistance of the NMR, mass, chromatography, spectroscopy, and photophysics units. Moltes gràcies to *Ariadna Roca* who made the cover of this thesis.

Un énorme merci à ma famille pour leur soutien sans faille non seulement pendant la thèse mais aussi pendant toutes les étapes qui ont précédé. Également, merci à tous mes amis qui sont derrière moi depuis toutes ces années, en particulier la team family et les copains de Montpellier.

List of Publications

Some of the results presented in this thesis have been published:

- <u>Le Saux, E.,</u>[+] Ma, D., [+] Bonilla, P., Holden, C. M., Lustosa, D., Melchiorre, P. "A General Organocatalytic System for Enantioselective Radical Conjugate Additions to Enals" *Angew. Chem. Int. Ed.* **2021**, *60*, 5357 – 5362.

- <u>Le Saux, E.,</u> Zanini, M., Melchiorre, P. "Photochemical Organocatalytic Benzylation of Allylic C-H Bonds" *J. Am. Chem. Soc.* **2022**, *144*, 1113 – 1118.

- <u>Le Saux, E.,</u> Georgiou, E., Dmitriev, I. A., Hartley, W. C., Melchiorre, P. "Photochemical Organocatalytic Functionalization of Pyridines via Pyridinyl Radicals" *J. Am. Chem. Soc*. **2023**, *145,* 47 – 52.

UNIVERSITAT ROVIRA I VIRGILI
PHOTOCHEMISTRY AND ORGANOCATALYSIS FOR RADICAL-BASED CARBON-CARBON BOND-FORMING PROCESSES
Emilien Le Saux

Table of Contents

UNIVERSITAT ROVIRA I VIRGILI
PHOTOCHEMISTRY AND ORGANOCATALYSIS FOR RADICAL-BASED CARBON-CARBON BOND-FORMING PROCESSES
Emilien Le Saux

Chapter I

General Overview

The research work described in this thesis focuses on the development of new organocatalytic methods for the construction of carbon-carbon bonds. Specifically, the photochemical activation of organocatalytic intermediates was studied as a means of achieving unconventional reactivity. The aim of this chapter is to introduce the concept of photochemistry and the different mechanisms of photoactivation of organic molecules. Seminal examples are discussed to highlight how photochemical activation has enabled the design of challenging radical-based transformations that are not feasible under thermal conditions, thus providing the context and the background that have motivated this research.

1.1 Photochemistry

All photochemical processes begin with an interaction between light and matter, in the form of absorption of a photon by a molecule.[1] This condition directly correlates to the principle of photochemical activation, also known as the Grotthuss–Draper law, which states that *"only the light absorbed is effective in producing a photochemical change"*. Although this statement may sound obvious, it is critical to understand photochemistry. The implication is that the light which is not absorbed does not result in a photochemical event. Behind this statement lies the quantum mechanical description of matter, whereby molecules possess quantized energy levels ranging from its low energy 'ground state' to a number of higher order states. The absorption of photons, packets of 'quantized' energy, can only take place if the photon is of *exactly* the same energy as the energy gap between an occupied energy state and an unoccupied energy state. Upon the absorption of light of adequate energy, a molecule can be electronically excited. This excited state comes from the transition of an electron from the highest occupied molecular orbital (HOMO) of the molecule, to its lowest unoccupied molecular orbital (LUMO, Figure 1.1.a). In the process, the molecule has gained a certain amount of energy (hv, the energy of the photon with h Planck's constant), which is inversely proportional to the wavelength of the absorbed light λ (Planck's equation, Eq. 1).

$$E = h \cdot (c/\lambda) = E_f - E_i \qquad \textbf{(Eq. 1)}$$

---

[1] Balzani, V., Ceroni, P., Juris, A. "Photochemistry and Photophysics: Concept, Research and Applications" Weinheim, Wiley-VCH, 2014.

These excited states are described by the wave functions Ψ, with Ψ_i associated to the ground state and Ψ_f to the excited state (Figure 1.1.b).
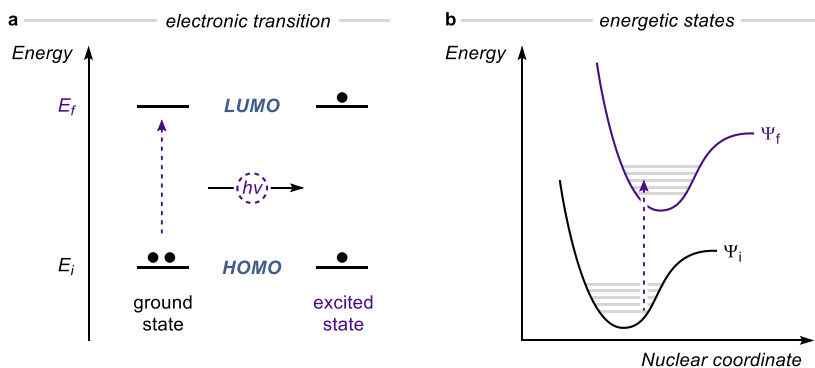
Figure 1.1. (**a**) Energy of the absorbed photon promotes the transition of an electron from the highest occupied molecular orbital (HOMO) to the lowest unoccupied molecular orbital (LUMO). (**b**) Electronic transition from the ground state Ψ_i to the excited state Ψ_f.

This electronic transition changes the physical and chemical properties of the molecule; therefore, an excited molecule can be considered a different compound from the ground state.[2] From the electronically excited state, a series of photophysical and photochemical events can take place. First, the excited molecule can return to the ground state S_0 through radiative and non-radiative deactivation pathways, including relaxation between vibrational levels, transitions between different excited states ($S_2 \rightarrow S_1$ or $S_1 \rightarrow T_1$) leading to luminescence from the lowest excited states, or thermal deactivation (Figure 1.2).[3] Another possibility for the excited molecule is to use this surplus of energy to initiate unimolecular or bimolecular photochemical processes, such as single-electron or energy transfers (SET and EnT), thus offering new-reactivity patterns that are unavailable under traditional thermal activation.
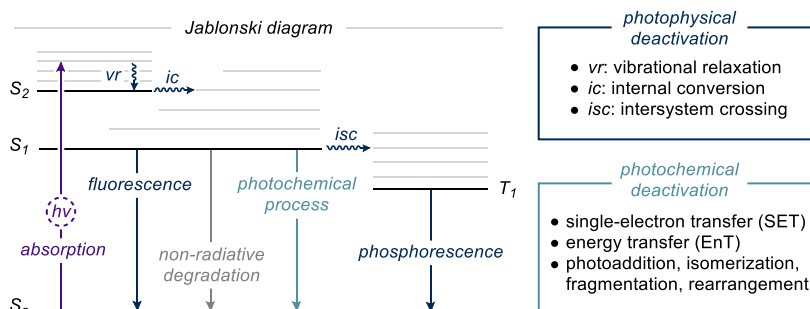
Figure 1.2. Photophysical and photochemical processes on a Jablonski diagram. Grey lines represent the different vibrational levels. *S*: singlet state; *T*: triplet state.

---

[2] Albini, A., Fagnoni, M. "Photochemically Generated Intermediates in Synthesis" John Wiley & Sons, 2013.
[3] Lakowicz, J. R. "Principles of Fluorescence Spectroscopy" Springer, 2006.

UNIVERSITAT ROVIRA I VIRGILI
PHOTOCHEMISTRY AND ORGANOCATALYSIS FOR RADICAL-BASED CARBON-CARBON BOND-FORMING
PROCESSES
Emilien Le Saux

3

The first reports of photochemical processes dated back to the 18th century.[4] However, organic photochemistry was only established as a field in the early 20th century, after Giacomo Ciamician and Paul Silber used sunlight to perform transformations of organic molecules in their pioneering studies.[5] From then until the late 2000s, only a few synthetic chemists were interested in photochemistry. Typically, the photochemical activation of colorless substrates required high-energy UV-light. Such potent irradiation does not tolerate a wide range of functionality, often leading to inefficient and unselective reactivity. Furthermore, these processes required specialized equipment that limited a broad application of photochemistry.

These shackles were removed with the introduction of colored photoredox catalysts as intermediaries between visible light and colorless substrates. The use of these catalysts initiated a renaissance of the field in 2008 and 2009 with seminal works from MacMillan,[6] Yoon,[7] and Stephenson.[8] These three reports disclosed the use of tris(bipyridine)ruthenium(II) complex $(Ru(bpy)_3{}^{2+})$[9] as a photocatalyst to mediate SET or EnT processes triggered by visible-light activation. This specific ruthenium catalyst had already been used extensively in the context of artificial photosynthesis or water splitting, [10] but its use in organic chemistry had found limited applications.[11]

In their report,[6] MacMillan and co-workers combined organo- and photocatalysis (Figure 1.3). Specifically, they used $[Ru(bpy)_3Cl_2]$ (**PC**) to generate radicals **II** by SET reduction of bromomalonates **2**. Meanwhile, condensation of MacMillan's imidazolidinone amine catalyst with aldehydes **1** generated the nucleophilic chiral enamine intermediate **I**, which could intercept the radicals **II** in a stereoselective fashion. The resulting α-amino radical **III** was then oxidized to iminium **IV** by the photoexcited Ru[II] complex. Eventually, hydrolysis of **IV** delivered the enantioenriched α-alkylated aldehydes **3**, while turning-over the organocatalyst.

[4] (a) Roth, H. D. "The Beginnings of Organic Photochemistry" *Angew. Chem. Int. Ed.* **1989**, *28*, 1193; (b) König, B. "Chemical Photocatalysis", Berlin/Boston, Walter de Gruyter GmbH, 2013.

[5] (a) Ciamician, G., Silber, P. "Chemische Lichtwirkungen" *Ber. Dtsch. Chem. Ges.* **1910**, *43*, 45; (b) Ciamician, G. "The Photochemistry of the Future", *Science*, **1912**, *926*, 385.

[6] Nicewicz, D. A., MacMillan, D. W. C. "Merging Photoredox Catalysis with Organocatalysis: The Direct Asymmetric Alkylation of Aldehydes" *Science* **2008**, *322*, 77.

[7] Ischay, M. A.; Anzovino, M. E.; Du, J.; Yoon, T. P. "Efficient Visible Light Photocatalysis of [2+2] Enone Cycloadditions" *J. Am. Chem. Soc.* **2008**, *130*, 12886.

[8] Narayanam, J. M. R.; Tucker, J. W.; Stephenson, C. R.J. "Electron-Transfer Photoredox Catalysis: Development of a Tin-Free Reductive Dehalogenation Reaction" *J. Am. Chem. Soc.* **2009**, *131*, 8756.

[9] Paris, J. P., Brandt, W. W., "Charge Transfer Luminescence of a Ruthenium(II) Chelate" *J. Am. Chem. Soc.* **1959**, *81*, 5001.

[10] (a) Grätzel, M. *Acc. Chem. Res*. **1981**, *14*, 376; (b) Meyer, T. J. *Acc. Chem. Res*. **1989**, *22*, 163.

[11] (a) Hedstrand, D. M.; Kruizinga, W. M.; Kellogg, R. M. "Light Induced and Dye Accelerated Reductions of Phenacyl Onium Salts by 1,4-Dihydropyridines" *Tetrahedron Lett*. **1978**, *19*, 1255; (b) Cano-Yelo, H.; Deronzier, A. "Photo-Oxidation of Some Carbinols by the Ru(II) Polypyridyl Complex-Aryl Diazonium Salt System" *Tetrahedron Lett*. **1984**, *25*, 5517; (c) Okada, K.; Okamoto, K.; Morita, N.; Okubo, K.; Oda, M. "Photosensitized Decarboxylative Michael Addition through *N*-(acyloxy)phthalimides *via* an Electron-Transfer Mechanism" *J. Am. Chem. Soc.* **1991**, *113*, 9401.

Later, Yoon and coworkers showed that, instead of the originally proposed two closed-loop catalytic cycles, a radical chain propagation mechanism was responsible for product formation. Here, the photoexcited ruthenium catalyst acted as an initiator, and the chain process was propagated by the reductive properties of the α-amino radical **III**.[12] The stereoselective intermolecular α-alkylation of aldehydes was a long-standing challenge in polar chemistry, which was finally overcome thanks to radical reactivity. Today, a large variety of photoredox catalysts are available and offer powerful tools to generate reactive intermediates through SET or energy transfer events.[13]
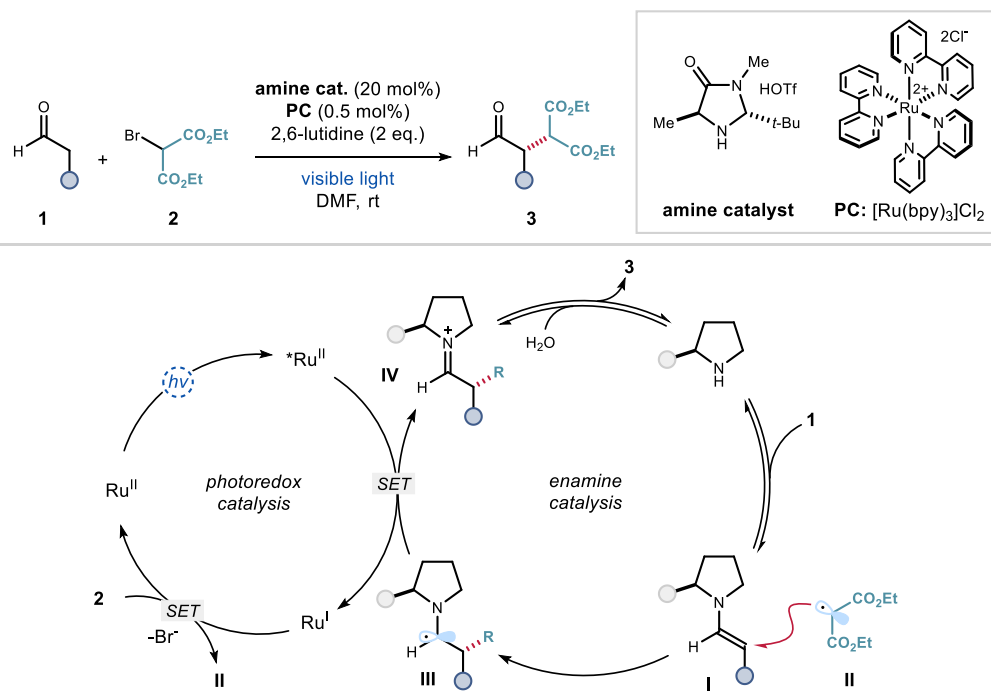
Figure 1.3. The merging of photoredox and organocatalysis for the enantioselective α-alkylation of aldehydes.

The use of a photoredox catalyst is not the only way to exploit the power of visible light in photocatalytic processes. It is also possible to excite colored organic intermediates to trigger the formation of radicals. Specific non-covalent aggregations between colorless electron-rich and electron-poor molecules can sometimes yield a change in the color of the solution. This type of aggregate is known as "electron donor-acceptor" or *EDA* complexes.[14] While the

---

[12] Cismesia, M. A. & Yoon, T. P. "Characterizing Chain Processes in Visible Light Photoredox Catalysis" *Chem. Sci.* **2015**, *6*, 5426.

[13] Shaw, M. H., Twilton, J., MacMillan, D. W. C. "Photoredox Catalysis in Organic Chemistry" *J. Org. Chem.* **2016**, *81*, 6898.

[14] Crisenza, G. E. M.; Mazzarella, D.; Melchiorre, P. "Synthetic Methods Driven by the Photoactivity of Electron Donor–Acceptor Complexes" *J. Am. Chem. Soc.* **2020**, *142*, 5461.

UNIVERSITAT ROVIRA I VIRGILI
PHOTOCHEMISTRY AND ORGANOCATALYSIS FOR RADICAL-BASED CARBON-CARBON BOND-FORMING
PROCESSES
Emilien Le Saux

5

individual components may not absorb visible light, the EDA aggregate usually does thanks to a new red-shifted charge transfer absorption band. The photoexcitation of such complexes can be harnessed for the generation of radical intermediates, and subsequent transformations. For example, our group discovered that mixing an enamine **I** with an electron-poor benzyl bromide **5** resulted in a color change of the solution from colorless to yellow (Figure 1.4). This observation was rationalized with the formation of an EDA complex between **I** and **5**.[15] Upon irradiation with visible light, an intracomplex SET triggered the fragmentation of the bromide and formation of the benzyl radical **V**, which subsequently added stereoselectively to the ground-state enamine **I** to ultimately afford α-benzyl aldehydes **6** with high enantioselectivity. This work showed that organocatalysis could be useful to generate photoactive intermediates that unlock distinct reaction pathways from those available under thermal activation.
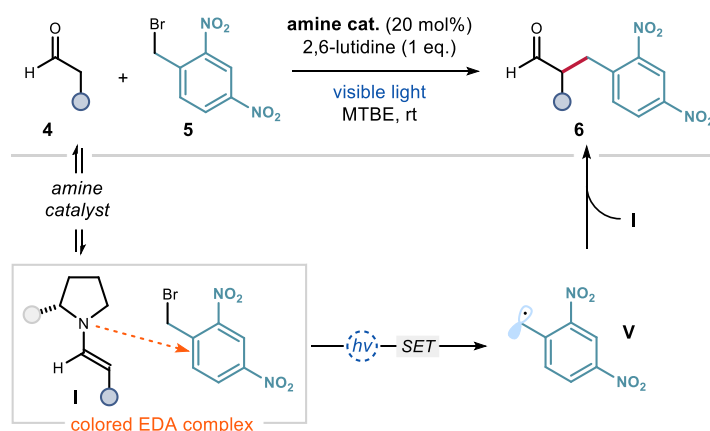
Figure 1.4. Photochemical stereoselective α-alkylation of aldehydes promoted by EDA complex formation.

We also found that some organocatalytic intermediates can directly absorb visible light without the need of an aggregate-based interaction with another species. Therefore, excited-state reactivity can be accessed directly upon light absorption. For example, enamine **I** can absorb near UV light (390 nm) to reach an electronically excited state (Figure 1.5). While enamines behave as nucleophiles in the ground state,[16] our group found that they act as strong SET reductants upon excitation.[17] This increased reducing power ($E^*(I^{•+}/I^*)$ = -2.5 V vs Ag^+/Ag) was exploited to generate malonyl radicals **II** from bromomalonates **2** which would

[15] Arceo, E.; Jurberg, I. D.; Álvarez-Fernández, A.; Melchiorre, P. "Photochemical Activity of a Key Donor-Acceptor Complex Can Drive Stereoselective Catalytic α-Alkylation of Aldehydes" *Nat. Chem.* **2013**, *5*, 750.

[16] Mukherjee, S., Yang, J. W., Hoffmann, S., List, B., "Asymmetric Enamine Catalysis", *Chem. Rev.* **2007**, *107*, 5471.

[17] Silvi, M.; Arceo, E.; Jurberg, I. D.; Cassani, C.; Melchiorre, P. "Enantioselective Organocatalytic Alkylation of Aldehydes and Enals Driven by the Direct Photoexcitation of Enamines" *J. Am. Chem. Soc.* **2015**, *137*, 6120.

UNIVERSITAT ROVIRA I VIRGILI
PHOTOCHEMISTRY AND ORGANOCATALYSIS FOR RADICAL-BASED CARBON-CARBON BOND-FORMING PROCESSES
Emilien Le Saux

6

not engage in EDA complex formation with enamines. The ground-state nucleophilic chiral enamine **I** subsequently intercepted **II** in an enantioselective fashion to afford the α-amino intermediate **III**. This species then reduced another molecule of substrate **2** to sustain a radical chain mechanism. The resulting iminium **IV** was eventually hydrolyzed to product **3**, while releasing the aminocatalyst. This work highlighted how a well-established intermediate in ground-state polar chemistry could be repurposed using light to trigger new radical processes by employing its excited state reactivity.[18]
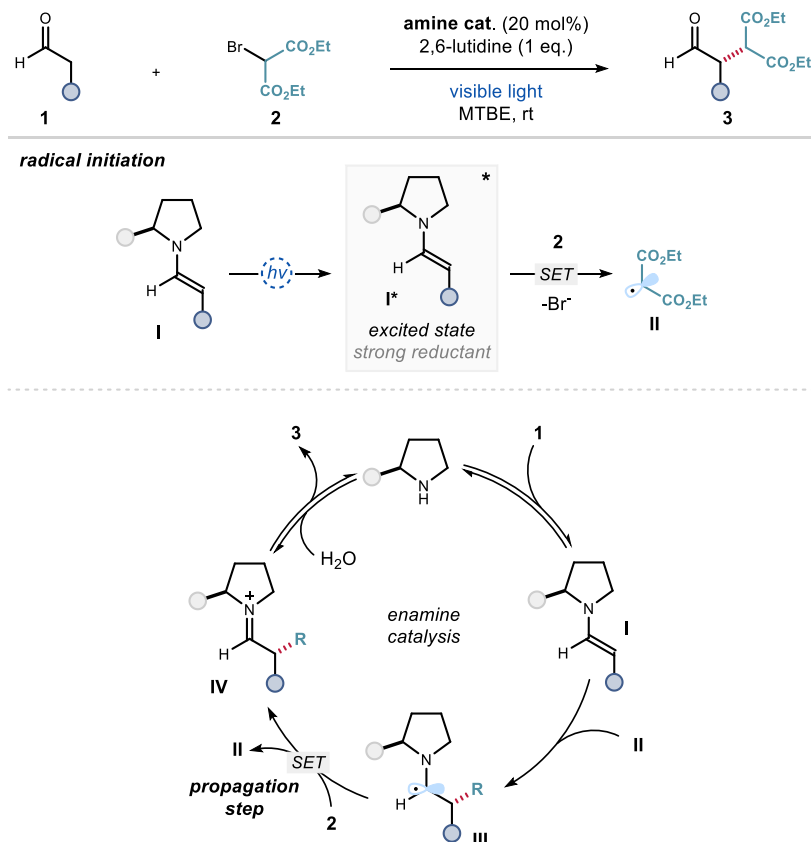
Figure 1.5. Direct photoexcitation of enamines **I** for the stereoselective α-alkylation of aldehydes.

Enamines (cornerstone intermediates of polar organocatalysis characterized by their nucleophilic reactivity) could be repurposed with photochemical activation to become strong SET reductants. By analogy, our group envisaged that electrophilic intermediates might act as SET oxidants in the excited state. The iminium ion[19] (the electrophilic sibling of the enamine in organocatalysis) also exhibits new reactivity in the photochemical realm. It was

---

[18] Silvi, M., Melchiorre, P. "Enhancing the Potential of Enantioselective Organocatalysis with Light" *Nature* **2018**, *554*, 41.

[19] Erkkilä, A.; Majander, I.; Pihko, P. M.; "Iminium Catalysis" *Chem. Rev.* **2007**, *107*, 5416.

UNIVERSITAT ROVIRA I VIRGILI
PHOTOCHEMISTRY AND ORGANOCATALYSIS FOR RADICAL-BASED CARBON-CARBON BOND-FORMING
PROCESSES
Emilien Le Saux

7

found that electrophilic chiral iminium ions **VI** could absorb visible light to reach an electronically excited state (Figure 1.6).[20] These excited iminium ions **VI*** acted as strong oxidants (E*(**VI***/**VIII**) = +2.40 V vs Ag$^+$/Ag) to generate radicals from organosilanes **8** through SET. The resulting benzylic and β-enaminyl radicals (**VII** and **VIII** respectively) coupled stereoselectively to eventually afford enantioenriched β-functionalized aldehydes **9**. This new reactivity enabled the enantioselective functionalization of enals **7** with non-nucleophilic partners **8** that did not undergo conjugate addition under thermal conditions.
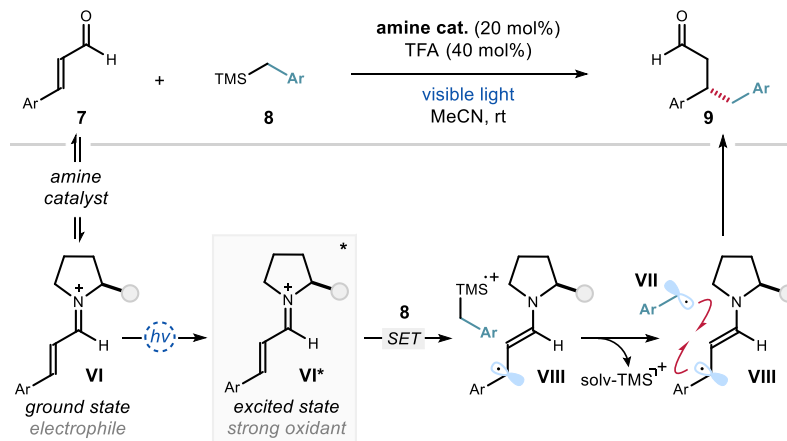
Figure 1.6. Photoexcitation of iminium ions for the enantioselective β-alkylation of enals. TMS: trimethylsilyl.

These examples highlight the power of combining organocatalysis with photochemistry to develop challenging stereoselective radical transformations. Intermediates with well-known reactivity in the polar domain can be activated directly with light, or form new visible-light-absorbing molecular aggregates, to achieve new radical reactivity.

Radical chemistry is now closely associated to photocatalysis, since access to reactive open-shell species can be achieved without the use of toxic organotin reagents or initiators.[13] Besides offering milder versions of previously known radical reactions, photocatalysis has stimulated creativity in organic chemistry by challenging traditional disconnections in retrosynthetic analyses. Radicals are particularly useful in the forgery of C-C bonds, owing to a versatile range of mechanistic pathways (Figure 1.7).[21] For example, carbon-centered radicals can add to unsaturated π-systems (e.g. Giese addition, Minisci reaction), they can be intercepted by transition metal catalysts and coupled with a variety of partners

[20] Silvi, M.; Verrier, C.; Rey, Y. P.; Buzzetti, L.; Melchiorre, P. "Visible-light excitation of iminium ions enables the enantioselective catalytic β-alkylation of enals" *Nat. Chem.* **2017**, *9*, 868.

[21] (a) Hart, D, J. "Free-Radical Carbon-Carbon Bond Formation in Organic Synthesis" *Science* **1984**, *223*, 883; (b) Giese, B. "Radicals in Organic Synthesis: Formation of Carbon–Carbon Bonds" Pergamon, 1986; (c) Fagnoni, M.; Dondi, D.; Ravelli, D.; Albini, A. "Photocatalysis for the Formation of the C-C Bond" *Chem. Rev.* **2007**, *107*, 2725.

UNIVERSITAT ROVIRA I VIRGILI
PHOTOCHEMISTRY AND ORGANOCATALYSIS FOR RADICAL-BASED CARBON-CARBON BOND-FORMING
PROCESSES
Emilien Le Saux

8

(metallaphotoredox),[22] or they can couple with other radicals either directly or via metal-catalyzed bimolecular homolytic substitution (S_H2) processes.[23]
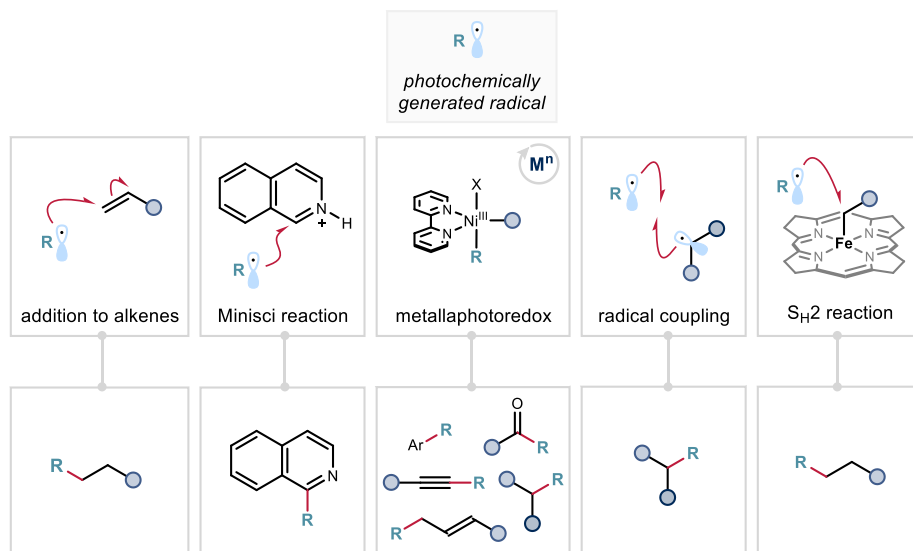
Figure 1.7. Carbon-carbon bond formation using radical reactivity.

The photochemical strategies and radical reactivity concepts described in this introduction were central to the design and development of the chemistry discussed in this doctoral thesis. The following section will summarize the general objectives of this research.

1.2 General objectives and summary

The principal objective of this doctoral thesis was to develop photo-organocatalytic carbon-carbon bond-forming reactions not achievable under thermal conditions. The three different photochemical activation manifolds discussed previously (photoredox catalysis, EDA complex formation, and direct excitation of organic catalysts) were used to generate radical intermediates under mild reaction conditions (Figure 1.8). In Chapter II, electrophilic iminium ions, formed from enals and a chiral amine catalyst, were used to trap a variety of carbon-centered radicals generated by an excited photoredox catalyst. The second and third projects (Chapters III and IV respectively) are closely related as they both rely on a dithiophosphoric

---

[22] Chan, A. Y.; Perry, I. B.; Bissonnette, N. B.; Buksh, B. F.; Edwards, G. A.; Frye, L. I.; Garry, O. L.; Lavagnino, M. N.; Li, B. X.; Liang, Y.; Mao, E.; Millet, A.; Oakley, J. V.; Reed, N. L.; Sakai, H. A.; Seath, C. P.; MacMillan, D. W. C. "Metallaphotoredox: The Merger of Photoredox and Transition Metal Catalysis" *Chem. Rev.* **2022**, *122*, 1485.

[23] Liu, W.; Lavagnino, M. N.; Gould, C. A.; Alcázar, J.; MacMillan, D. W. C. "A Biomimetic S_H2 Cross-Coupling Mechanism for Quaternary sp³-Carbon Formation" *Science*, **2021**, *374*, 1258.

UNIVERSITAT ROVIRA I VIRGILI
PHOTOCHEMISTRY AND ORGANOCATALYSIS FOR RADICAL-BASED CARBON-CARBON BOND-FORMING
PROCESSES
Emilien Le Saux

9

acid catalyst that, upon light irradiation, could act sequentially as a SET reductant and a hydrogen atom transfer (HAT) catalyst to activate allylic C-H bonds. The reducing properties of the catalyst were enabled either by EDA complex formation or by direct excitation. These two modes of activations were harnessed to develop C-H functionalization processes involving radical cross-coupling steps.
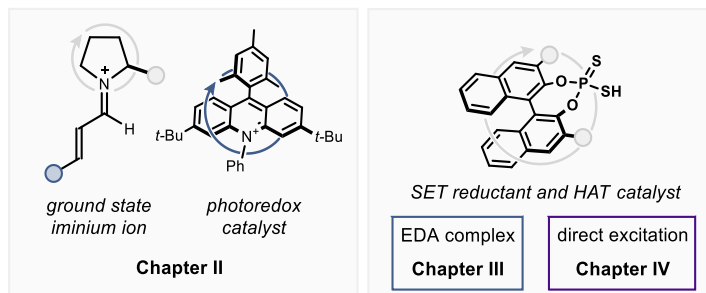
Figure 1.8. General photo-organocatalysis tools applied in this thesis.

1.2.1 Enantioselective radical conjugate addition to iminium ions

In chapter II, the stereoselective radical conjugate addition to iminium ions will be discussed. Previous strategies for the asymmetric β-functionalization of enals using *excited* iminium ions were limited to unsaturated aldehydes with an aromatic substituent at the β-position.[20] To overcome this drawback, we used *ground-state* chiral iminium ions to trap open-shell intermediates generated by an external photocatalyst under blue light (Figure 1.9). The two catalysts worked in concert in a redox-neutral process, which proved to be general in both enal substrates and radical precursors. Importantly, the use of tailored radical precursors allowed the synthesis of densely substituted piperidines in one-step thanks to an iminium ion-enamine cascade.
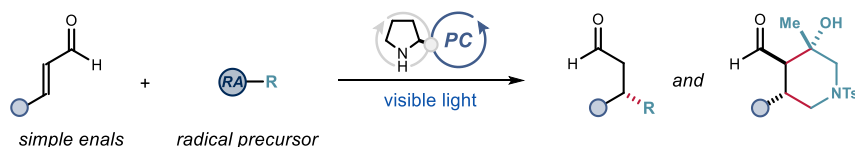
Figure 1.9. Dual-catalytic system for the enantioselective radical conjugate addition to iminium ions. RA: redox auxiliary.

This work was undertaken in collaboration with Dr. Catherine Holden, who discovered and optimized the reaction, Dr. Danilo Lustosa and Dr. Dengke Ma, who investigated part of the reaction scope, and Dr. Pablo Bonilla, who contributed to the mechanistic elucidation. I investigated the generality of the scope and conducted the mechanistic studies.

1.2.2 EDA-mediated benzylation of allylic C-H bonds

Chapter III details a different photochemical strategy. An electron-rich dithiophosphoric acid **A** was found to perform two distinct catalytic roles, sequentially acting as a donor in photoactive EDA complexes with electron-poor radical precursors, and hydrogen atom abstractor to activate allylic positions. Benzylic and allylic radicals were sequentially formed through these activation modes, and then coupled to afford the final allylic benzylation product (Figure 1.10.a). The overall process is an organocatalytic benzylation of allylic C-H bonds, relying on readily available starting materials. In order to expand the scope of the reaction to alkyl radical precursors, a three-component version of the process was developed (Figure 1.10.b). This time, benzylic radicals were generated by addition of electron-poor and non-stabilized alkyl radicals, still arising from EDA activation, to styrene derivatives.
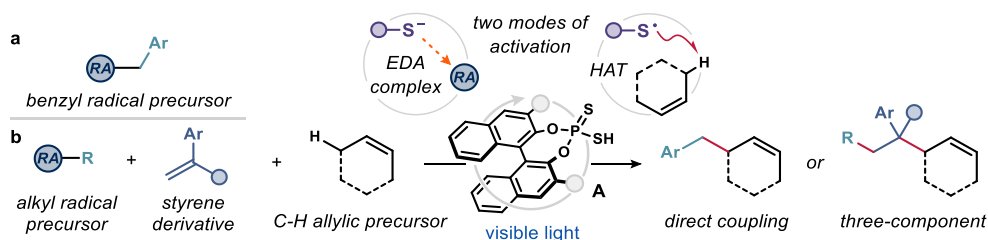
Figure 1.10. Photochemical organocatalytic benzylation of allylic C-H bonds through (**a**) a direct approach and (**b**) a three-component process. RA: redox auxiliary.

This project was carried out as a collaboration with Dr. Margherita Zanini. I discovered the reaction and performed the optimization studies. Investigation of the scope and mechanistic experiments were undertaken collaboratively.

1.2.3 Allylation of pyridines via direct excitation of dithiophosphoric acids

A new mode of photochemical activation available to dithiophosphoric acid **A** is discussed in chapter IV. We found that, upon UV light irradiation, the previously employed catalyst could be turned into a strong SET reductant. The organic catalyst now acts as a Brønsted acid for pyridine protonation, as a SET reductant for pyridinium ion reduction, and as a hydrogen atom abstractor for the activation of allylic C-H bonds. Through this sequence, pyridinyl and allyl radicals were formed and engaged in coupling processes with high regioselectivity, to ultimately afford C-H functionalized pyridines (Figure 1.11). This new reactivity pattern helped developing an otherwise elusive transformation.

UNIVERSITAT ROVIRA I VIRGILI
PHOTOCHEMISTRY AND ORGANOCATALYSIS FOR RADICAL-BASED CARBON-CARBON BOND-FORMING
PROCESSES
Emilien Le Saux

11
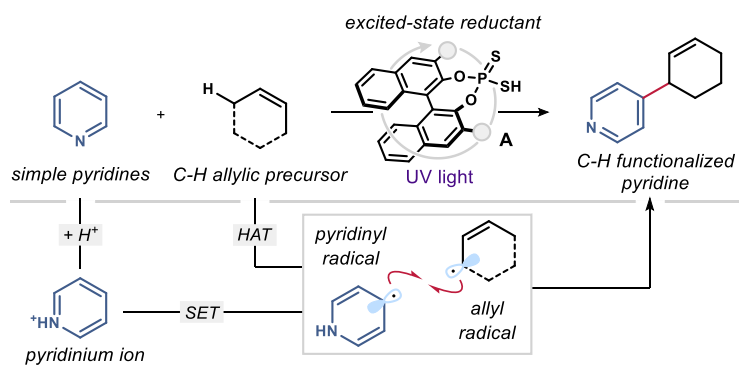
Figure 1.11. C-H allylation of pyridines using direct photoexcitation of dithiophosphoric acids.

This work was developed as a collaboration with Igor Dmitriev, who contributed to the initial optimization and the investigation of the process generality, and provided support for the mechanistic understanding. Eleni Georgiou took part to the scope and mechanistic elucidations, and Dr. Will Hartley performed computational experiments to support our mechanistic rationale. I discovered the reaction, contributed to the optimization and scope, and performed photophysical studies.

Chapter II

A General Organocatalytic System for Enantioselective Radical Conjugate Additions to Enals

Target

To develop a general catalytic system for the enantioselective conjugate addition of a wide range of carbon-centered radicals to β-substituted aliphatic and aromatic enals.
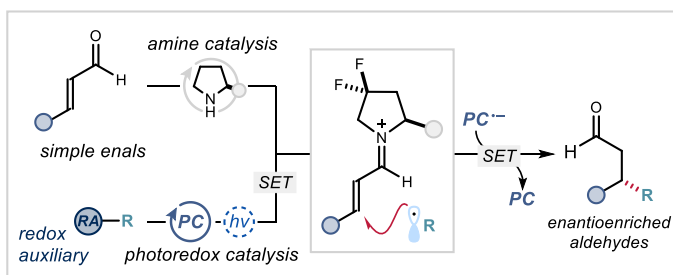
Tool

Simultaneous use of a photoredox catalyst, which promotes the generation of radicals from stable precursors, and a chiral secondary amine catalyst to generate electrophilic ground-state chiral iminium ions that trap open-shell intermediates with high enantioselectivity.[1]

2.1 General introduction

Iminium ion-based catalysis is a powerful method to activate α,β-unsaturated carbonyl compounds.[2] This mode of activation relies on the reversible condensation of small chiral amine catalysts with α,β-unsaturated carbonyl substrates to afford a conjugated iminium ion **I** (Figure 2.1). This intermediate exhibits enhanced electrophilicity with respect to the parent

---

[2] Erkkilä, A. Majander, I. Pihko, P. M. "Iminium Catalysis" *Chem. Rev.* **2007**, *107*, 12, 5416.

UNIVERSITAT ROVIRA I VIRGILI
PHOTOCHEMISTRY AND ORGANOCATALYSIS FOR RADICAL-BASED CARBON-CARBON BOND-FORMING
PROCESSES
Emilien Le Saux

13

substrate due to a decrease in energy of its lowest unoccupied orbital (LUMO). Consequently, iminium ions react readily with soft nucleophiles.[3]
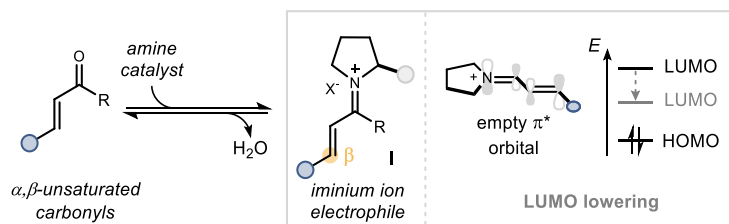
Figure 2.1. General concept of iminium ion activation.

Over the years, privileged catalysts were designed for asymmetric iminium ion catalysis, with secondary amines being particularly effective. These catalysts have to fulfil three requirements: (*i*) condense efficiently in a reversible manner with the unsaturated carbonyl substrate, (*ii*) control the double bond geometry of the resulting iminium ion, and (*iii*) selectively shield one of the prochiral faces of the intermediate to provide enantiofacial discrimination.

Diarylprolinol silyl ethers, developed independently by Jørgensen and Hayashi,[4] and imidazolidinones, developed by MacMillan (Figure 2.2), meet all three of these conditions and are used frequently in iminium ion-based catalysis.
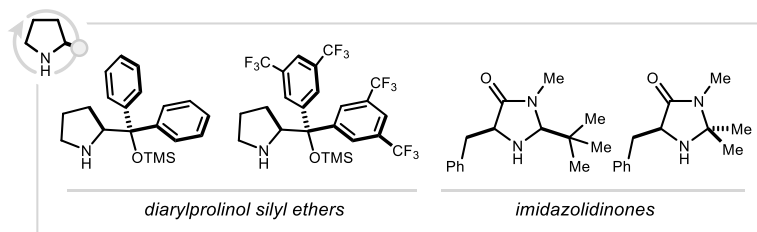
Figure 2.2. Selected secondary amine catalysts commonly encountered in iminium-ion activation.

Asymmetric iminium ion-based catalysis is commonly used for two types of reactions: cycloadditions and conjugate additions of nucleophiles. Although a number of nucleophiles are amenable to this second type of transformation, they are restricted by certain intrinsic structural requirements. For example, carbon sp^3 nucleophiles must be derived from

---

[3] Dalko, P. I. "Comprehensive Enantioselective Organocatalysis" 2013, Wiley-VCH Verlag.
[4] (a) Franzén, J. Marigo, M. Fielenbach, D. Wabnitz. T. C. Kjærsgaard, A. Jørgensen, K. A. "A General Organocatalyst for Direct α-Functionalization of Aldehydes: Stereoselective C−C, C−N, C−F, C−Br, and C−S Bond-Forming Reactions. Scope and Mechanistic Insights", *J. Am. Chem. Soc.* **2005**, *127*, 18296; (b) Hayashi, Y. Gotoh, H. Hayashi, T. Shoji, M. "Diphenylprolinol Silyl Ethers as Efficient Organocatalysts for the Asymmetric Michael Reaction of Aldehydes and Nitroalkenes", *Angew. Chem. Int. Ed.* **2005**, *44*, 4212.

adequately acidic C-H bonds, and carbon sp^2 nucleophiles are restricted to electron-rich systems (Figure 2.3).
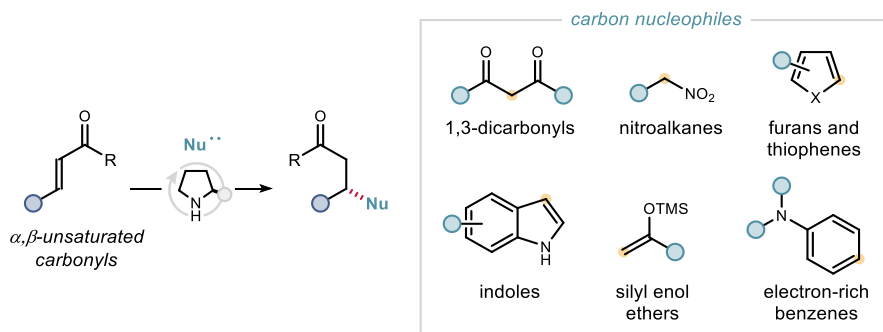
Figure 2.3. Asymmetric conjugate addition of carbon nucleophiles to chiral iminium ions.

In 2017, our group uncovered the ability of chiral iminium ions **I**, derived from aromatic enals **1**, to become strong oxidants in their excited state **I***.[5] This new mode of activation, enabled by the absorption of visible light, unlocked a new method for alkylating the β-position of enals in an enantioselective fashion (Figure 2.4). Specifically, the oxidative power of the excited iminium ion was harnessed to generate carbon-centered radicals upon single-electron transfer (SET) oxidation of stable non-nucleophilic precursors and trap them with high stereocontrol. This chemistry was proposed to proceed via a radical coupling event between the chiral β-enaminyl radical **IIIa**, arising from the iminium ion, and the open-shell intermediate **II** generated upon SET oxidation of benzylic trimethylsilanes **2**. Since **IIIa** has an allylic-benzylic character, it should benefit from sufficient stabilization to allow this coupling to happen.[6] The overall process delivered β-functionalized enantioenriched aldehydes **3**.

---

[5] Silvi, M.; Verrier, C.; Rey, Y. P.; Buzzetti, L.; Melchiorre, P. "Visible-light excitation of iminium ions enables the enantioselective catalytic β-alkylation of enals" *Nat. Chem.* **2017**, *9*, 868.

[6] Leifert, D.; Studer, A. "The Persistent Radical Effect in Organic Synthesis" *Angew. Chem. Int. Ed.* **2020**, *59*, 74.

UNIVERSITAT ROVIRA I VIRGILI
PHOTOCHEMISTRY AND ORGANOCATALYSIS FOR RADICAL-BASED CARBON-CARBON BOND-FORMING
PROCESSES
Emilien Le Saux

15
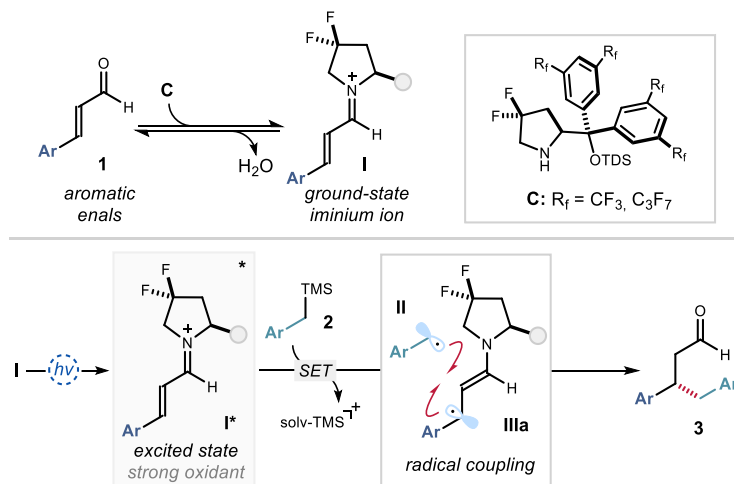
Figure 2.4. Excited-state iminium ion reactivity of aromatic enals. TDS: *tert*-hexyldimethylsilyl.

This study broadened the applicability of iminium ion catalysis to include radical reactivity. In subsequent reports,[7] the scope of radical precursors amenable to this chemistry was greatly expanded (Figure 2.5). However, the main limitation was the need for an aromatic substituent at the β-position of the starting enal **1**, since the presence of an aliphatic group completely shut down the excited-state reactivity of the chiral iminium ion.

silanes

dihydropyridines

toluene and xylene derivatives

cyclopropanols

alkenoic acids and alkenols

allenic acids
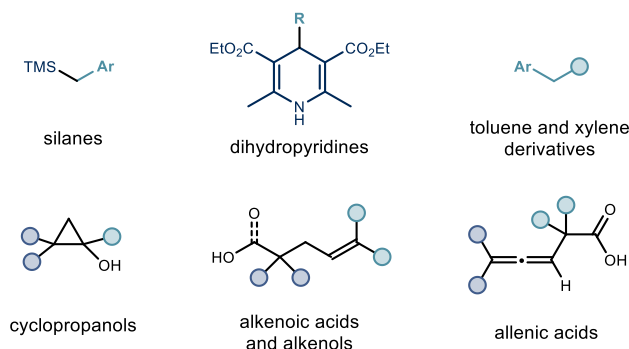
Figure 2.5. Radical precursors compatible with excited-state iminium ion chemistry.

---

[7] (a) Verrier, C.; Alandini, N.; Pezzetta, C.; Moliterno, M.; Buzzetti, L.; Hepburn, H. B.; Vega-Peñaloza, A.; Silvi, M; Melchiorre, P. "Direct Stereoselective Installation of Alkyl Fragments at the β-Carbon of Enals via Excited Iminium Ion Catalysis" *ACS Catal.* **2018**, *8*, 1062; (b) Mazzarella, D.; Crisenza, G.; Melchiorre, P. "Asymmetric Photocatalytic C–H Functionalization of Toluene and Derivatives" *J. Am. Chem. Soc.* **2018**, *140*, 8439; (c) Woźniak, Ł.; Magagnano, G.; Melchiorre, P. "Enantioselective Photochemical Organocascade Catalysis" *Angew. Chem. Int. Ed.* **2018**, *57*, 1068; (d) Bonilla, P.; Rey, Y. P.; Holden, C. M.; Melchiorre, P. "Photo-Organocatalytic Enantioselective Radical Cascade Reactions of Unactivated Olefins" *Angew. Chem. Int. Ed.* **2018**, *57*, 12819; (e) Perego, L. A.; Bonilla, P.; Melchiorre, P. "Photo-Organocatalytic Enantioselective Radical Cascade Enabled by Single-Electron Transfer Activation of Allenes" *Adv. Synth. Catal.* **2020**, *362*, 302.

We initially rationalized this lack of reactivity by the inability of aliphatic iminium ions to absorb light in the visible region. However, the use of shorter wavelengths did not change the outcome. A plausible explanation might be related to the inefficient radical coupling of the transient β-enaminyl radical **IIIb**, emerging from reduction of an aliphatic iminium ion, which is less stabilized (not benzylic) than its aromatic counterpart **IIIa** (Figure 2.6.a). In addition, aliphatic enals can form dienamines upon condensation with amine catalysts, due to the presence of an acidic C-H bond at the γ-position. The electronic properties of dienamines are vastly different from iminium ions, since they are nucleophiles (Figure 2.6.b). Dienamines can absorb visible light, but their electron-rich nature renders them strong reductants in the excited state, and therefore unable to perform SET oxidation of the aforementioned radical precursors **2**.[8]
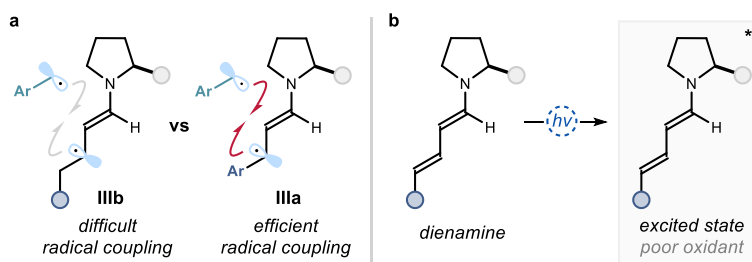
Figure 2.6. Rationalization for the lack of photoreactivity in aliphatic iminium ions based on (**a**) the stability of the β-enaminyl radical and (**b**) the electronic properties of photoexcited dienamines.

To overcome this limitation and enable aliphatic enals to intercept radicals, we surmised that decoupling the radical generation strategy from the stereo-determining C-C bond-forming event would be critical. With this in mind, this chapter discusses the design of a dual-catalytic platform that combines ground-state iminium ion catalysis with the action of an external photoredox catalyst, which secures the generation of radicals **II** and their stereocontrolled interception. The net reaction is an enantioselective radical conjugate addition to linear *aliphatic and aromatic* enals **1** via ground-state iminium ion-mediated catalysis affording β-disubstituted chiral aldehydes **3** (Figure 2.7).

---

[8] (a) Silvi, M.; Arceo, E.; Jurberg, I. D.; Cassani, C.; Melchiorre, P. "Enantioselective Organocatalytic Alkylation of Aldehydes and Enals Driven by the Direct Photoexcitation of Enamines" *J. Am. Chem. Soc.* **2015**, *137*, 6120; (b) Bamahonde, A.; Melchiorre, P. "Mechanism of the Stereoselective α-Alkylation of Aldehydes Driven by the Photochemical Activity of Enamines" *J. Am. Chem. Soc.* **2016**, *138*, 8019.

UNIVERSITAT ROVIRA I VIRGILI
PHOTOCHEMISTRY AND ORGANOCATALYSIS FOR RADICAL-BASED CARBON-CARBON BOND-FORMING
PROCESSES
Emilien Le Saux

17
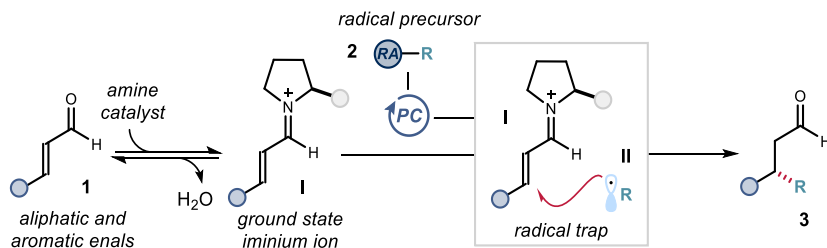
Figure 2.7. Proposed strategy for developing an enantioselective radical conjugate addition to aromatic and aliphatic enals. RA: redox auxiliary.

In the following sections, literature precedents for catalytic asymmetric radical conjugate addition reactions will be discussed, while providing the scientific background and previous studies that were essential to the development of the present research project.

2.2 Background

2.2.1 Catalytic radical conjugate additions with chiral Lewis acids

Carbon-centered radicals are prone to react with electron-deficient olefins.[9] Their conjugate addition to α,β-unsaturated carbonyl substrates represents a prominent C-C bond-forming process. However, developing a catalytic enantioselective variant is difficult because of the intrinsic high reactivity of radicals and their tendency to attack electron-poor olefins in the absence of catalytic activation. Herein lies the main problem in the development of enantioselective radical processes – the racemic background reaction. Over the past three decades, some solutions have been identified using chiral Lewis acids as catalysts.[10] In 1996, Sibi and Porter reported the first catalytic enantioselective radical conjugate addition.[11] They disclosed that a chiral Lewis acid complex, generated upon coordination of a chiral ligand L_1* to a metal cation derived from MgI_2 or $Zn(OTf)_2$, could activate acyclic enoates **4** while shielding one of the prochiral faces of the alkene (Figure 2.8.a). Stereocontrolled radical addition to the β-position delivered products **6** with moderate to good enantioselectivity. The main drawbacks of this system were the need for very low temperatures (–78 °C) and the stoichiometric amount of Lewis acid required to achieve high enantioselectivity. Both aspects highlighted the need to minimize the rate of a strong background racemic process. Substituting the flexible chiral bisoxazoline ligand L_1* for a more rigid scaffold L_2* increased

---

[9] (a) Giese, B. "The Stereoselectivity of Intermolecular Free Radical Reactions" *Angew. Chem. Int. Ed.* **1989**, *28*, 969; (b) Srikanth, G. S. C.; Castle, S. L. "Advances in radical conjugate additions" *Tetrahedron,* **2005**, *61*, 10377.

[10] Renaud, P.; Gerster, M. "Use of Lewis Acids in Free Radical Reactions" *Angew. Chem. Int. Ed.* **1998**, *37*, 2562.

[11] Sibi, M. P.; Ji, J.; Wu, J. H.; Gürtler, S.; Porter, N. A. "Chiral Lewis Acid Catalysis in Radical Reactions: Enantioselective Conjugate Radical Additions" *J. Am. Chem. Soc.* **1996**, *118*, 9200.

substantially the enantioselectivity and allowed the use of a lower amount of Lewis acid (10 mol% at –78 °C), and the use of ambient temperature when using 30 mol% of the chiral Lewis acid (Figure 2.8.b).[12]
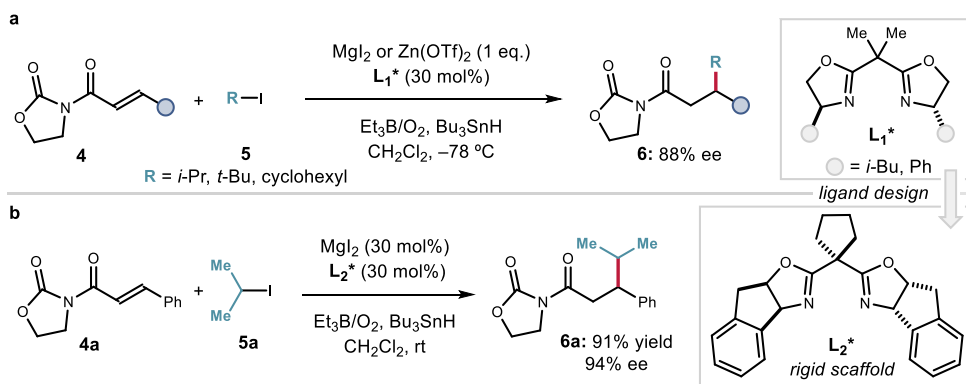
Figure 2.8. (**a**) The first catalytic enantioselective chiral Lewis acid-mediated radical conjugate addition. (**b**) An improved protocol enabled by ligand design.

Sibi later expanded this Lewis acid-based catalytic system to a variety of conjugated carbonyl substrates, including β-acyloxy acrylates,[13] imides,[14] acyloxy pyrones,[15] and α′-phosphoric enones.[16] Despite the excellent levels of enantioselectivity achieved, there are two main disadvantages to this strategy: (*i*) the substrates need to be judiciously prepared since they require a preinstalled moiety acting as an anchoring point to facilitate coordination and geometry control from the chiral Lewis acid; (*ii*) radicals are generated using undesirable tin and borane reagents in stoichiometric amounts.

The Sibi group also reported a radical conjugate addition to benzoate derivatives **7** (Figure 2.9). Even though enones possess only a single point for binding to the chiral Lewis acid complex, inclusion of a sterically demanding benzoate moiety in the substrates enabled stereo-discrimination between the prochiral faces of the exocyclic double bond, permitting high stereoselectivity.[17] Specifically, the lone pair of electrons on the carbonyl oxygen of substrate

[12] Sibi, M. P.; Ji, J. "Practical and Efficient Enantioselective Conjugate Radical Additions" *J. Org. Chem.* **1997**, *62*, 3800.

[13] Sibi, M. P.; Zimmerman, J.; Rheault, T. "Enantioselective Conjugate Radical Addition to β-Acyloxy Acrylate Acceptors: An Approach to Acetate Aldol-Type Products" *Angew. Chem. Int. Ed.* **2003**, *42*, 4521.

[14] Sibi, M. P.; Petrovic, G.; Zimmerman, J. "Enantioselective Radical Addition/Trapping Reactions with α,β-Disubstituted Unsaturated Imides. Synthesis of anti-Propionate Aldols" *J. Am. Chem. Soc.* **2005**, *127*, 2390.

[15] Sibi, M. P.; Zimmerman, J. "Pyrones to Pyrans: Enantioselective Radical Additions to Acyloxy Pyrones" *J. Am. Chem. Soc.* **2006**, *128*, 13346.

[16] Lee, S.; Kim, S. "Enantioselective Radical Conjugate Addition to α′-Phosphoric Enones" *Org. Lett.* **2008**, *10*, 4255.

[17] Sibi, M. P.; Nad, S. "Enantioselective Radical Reactions: Stereoselective Aldol Synthesis from Cyclic Ketones" *Angew. Chem. Int. Ed.* **2007**, *46*, 9231.

UNIVERSITAT ROVIRA I VIRGILI
PHOTOCHEMISTRY AND ORGANOCATALYSIS FOR RADICAL-BASED CARBON-CARBON BOND-FORMING
PROCESSES
Emilien Le Saux

19

7 coordinated to the chiral salen aluminum Lewis acid **[Al]**. The steric bulk induced by the benzoyl OR group enforced the alkene configuration in the most stable s-*cis*-geometry while pointing away from the axial groups of the cyclohexane ring of the salen ligand (Figure 2.9). Hence, the most stable transition state **TS-I** left the *si*-face of the alkene more exposed for radical addition, and delivered the enantioenriched products **8**.
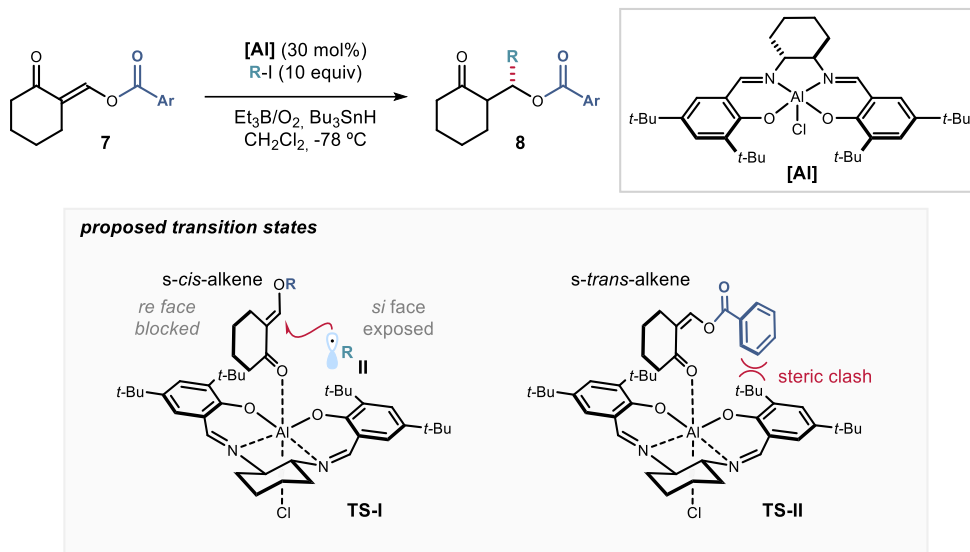
Figure 2.9. Radical conjugate addition to cyclic ketones bearing an exocyclic alkene and a benzoate ester.

With the advent of photoredox catalysis,[18] some of the problems associated with Sibi's strategy could be bypassed by using a photoredox catalyst to generate radicals under milder reaction conditions. Recently, the Yoon laboratory employed a Ru^{II}-based photoredox catalyst to generate nucleophilic α-aminoradicals **V** from α-silylamines **10** (Figure 2.10).[19] A scandium catalyst, coordinated with a chiral PyBox ligand **L***, could bind and activate a crotonate substrate bearing a pyrazolidinone moiety (**9**) to generate an electrophilic chiral intermediate **IV**. The radical **V**, generated upon SET oxidation of **10** and fragmentation of the trimethylsilyl group, could undergo radical conjugate addition to **IV** to deliver the enantioenriched β-functionalized product **11**. This system established the feasibility of combining a chiral Lewis acid with photocatalytically generated radicals to perform enantioselective radical conjugate additions.

[18] Shaw, M. H.; Twilton, J.; MacMillan, D. W. C. "Photoredox Catalysis in Organic Chemistry" *J. Org. Chem.* **2016**, *81*, 6898.
[19] Ruiz Espelt, L.; McPherson, I. S.; Wiensch, E. M.; Yoon, T. P. "Enantioselective Conjugate Additions of α-Amino Radicals via Cooperative Photoredox and Lewis Acid Catalysis" *J. Am. Chem. Soc.* **2015**, *137*, 2452.
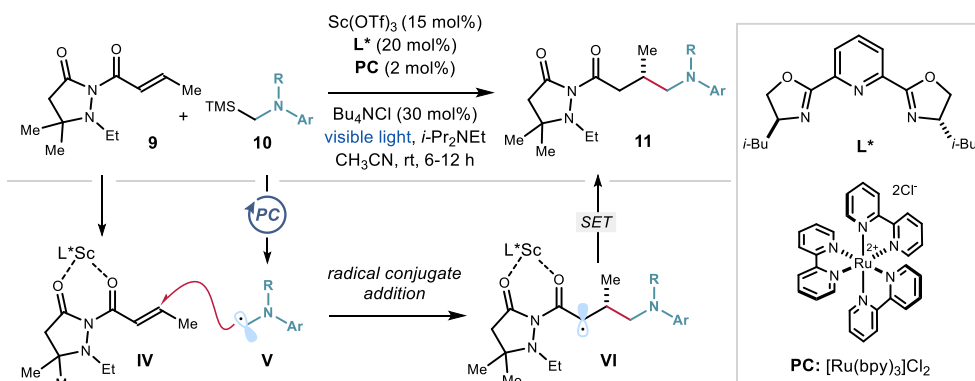
Figure 2.10. Asymmetric radical conjugate addition using photocatalytically generated α-amino radicals.

Meggers and co-workers expanded this dual strategy, where a chiral Lewis acid works in concert with a photoredox catalyst, using an octahedral chiral-at-metal Lewis acid catalyst (Figure 2.11).[20] The authors overcame the previous limitation of Yoon's system to α-amino radicals, using potassium trifluoroborate salts **13** as a source of alkyl radicals (benzylic, non-stabilized secondary and tertiary alkyl, and α-oxo radicals)
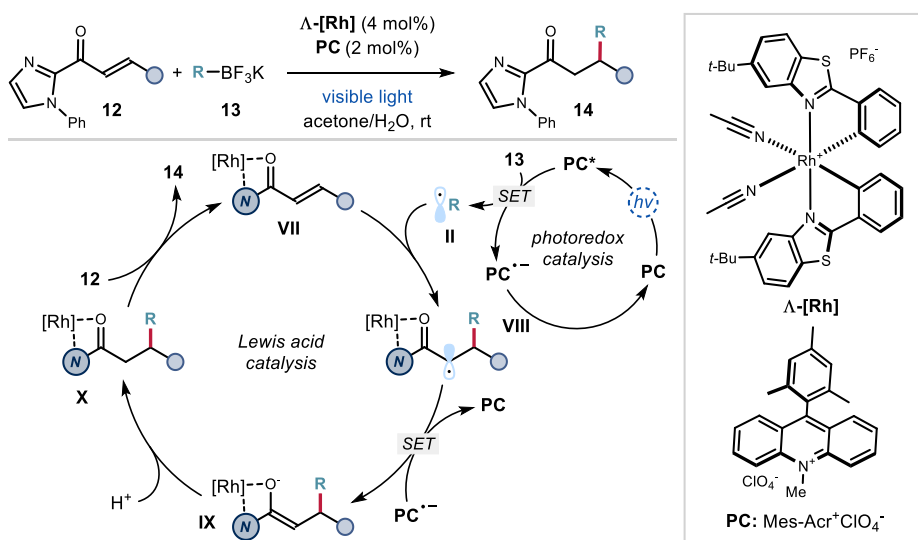
Figure 2.11. Photocatalytic asymmetric radical conjugate addition reaction using BF_3K salts as source of alkyl radicals.

The C2-symmetrical Rh^{III} catalyst **Λ-[Rh]** was able to lock the conformation of substrate **12** by coordination to the imidazole template. Oxidation of potassium trifluoroborate salt **13** by the excited organic photocatalyst **PC*** delivered an alkyl radical **II** (benzylic, α-oxo, or alkyl)

---

[20] Huo, H.; Harms, K.; Meggers, E. "Catalytic, Enantioselective Addition of Alkyl Radicals to Alkenes via Visible-Light-Activated Photoredox Catalysis with a Chiral Rhodium Complex" *J. Am. Chem. Soc.* **2016**, *138*, 6936.

UNIVERSITAT ROVIRA I VIRGILI
PHOTOCHEMISTRY AND ORGANOCATALYSIS FOR RADICAL-BASED CARBON-CARBON BOND-FORMING
PROCESSES
Emilien Le Saux

21

which was intercepted enantioselectively by **VII** to afford intermediate **VIII**. SET from the reduced form of the photocatalyst (**PC•⁻**) to **VIII** generated intermediate **IX** while turning-over the photoredox catalyst. Subsequent protonation of **IX** and ligand exchange eventually delivered product **14** in high yield and enantioselectivity while restarting the catalytic cycle. The versatility of this system was demonstrated in subsequent reports by the use of various radical precursors, such as dihydropyridines (DHPs)[21] and *N*-(acyloxy)phthalimides,[22] which reacted smoothly to afford β-functionalized products **14**.

A highly related transformation was recently reported based on the use of a chiral Ni^II complex **[Ni]**, generated in situ by coordination of a nickel salt with a dibenzofurandiyl-2,2′-bis(4-phenyloxazoline) chiral ligand **L*** (Figure 2.12).[23] However, this work diverged mechanistically from the aforementioned reports from Meggers and Yoon, since no exogenous photocatalyst was employed. Instead, the nickel complex acted both as a chiral Lewis acid and a photoredox catalyst for the enantioselective radical conjugate addition of α-amino radicals to *N*-acyl pyrazole-templated Michael acceptors **15**.
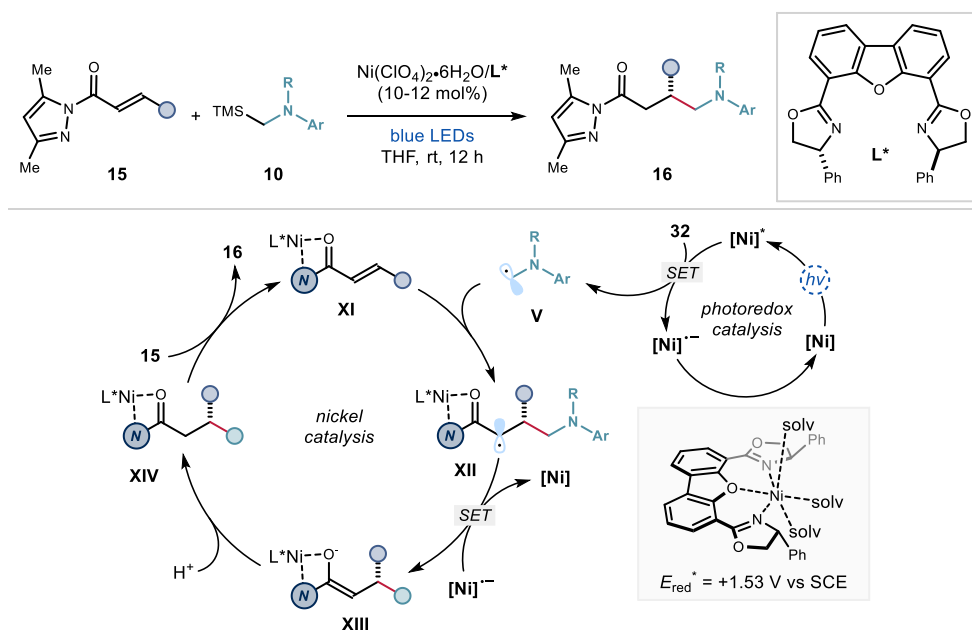
Figure 2.12. A nickel complex acting as bifunctional photoredox and chiral Lewis acid catalyst.

---

[21] de Assis, F. F.; Huang, X.; Akiyama, M.; Pilli, R. A.; Meggers, E. "Visible-Light-Activated Catalytic Enantioselective β-Alkylation of α,β-Unsaturated 2-Acyl Imidazoles Using Hantzsch Esters as Radical Reservoirs" *J. Org. Chem.* **2018**, *83*, 10922.

[22] Ma, J.; Lin, J.; Zhao, L.; Harms, K.; Marsch, M.; Xie, X.; Meggers, E. "Synthesis of β-Substituted γ-Aminobutyric Acid Derivatives through Enantioselective Photoredox Catalysis" *Angew. Chem. Int. Ed.* **2018**, *57*, 11193.

[23] Shen, X.; Li, Y.; Wen, Z.; Cao, S.; Hou, X.; Gong, L. "A Chiral Nickel DBFOX Complex as a Bifunctional Catalyst for Visible-Light-Promoted Asymmetric Photoredox Reactions" *Chem. Sci.* **2018**, *9*, 4562.

In the proposed mechanism, the colored Ni complex (**[Ni]**) reached an excited state **[Ni]***upon absorption of visible light. **[Ni]*** is a good oxidant able to generate α-amino radicals **V** through SET from the corresponding trimethylsilyl precursors **10**. Concomitantly, **[Ni]** coordinated substrate **15** thus enhancing its electrophilicity and promoting the radical conjugate addition of **V** to **XI**. This stereocontrolled step formed the radical **XII**. Single-electron reduction of **XII** by **[Ni]•⁻** followed by protonation delivered the intermediate **XIV**, which upon ligand exchange released the enantioenriched product **16** and restored **XI**.

The Xiao group reported an alternative method to circumvent the use of precious metals as catalysts, employing a novel octahedral Co^II-complex based on a chiral *N*4-ligand (**[Co]**) (Figure 2.13).[24] DHPs **17** were selected as a source of alkyl, benzyl, aryl, and acyl radicals for their conjugate addition to imidazole-bound enoates **12**.
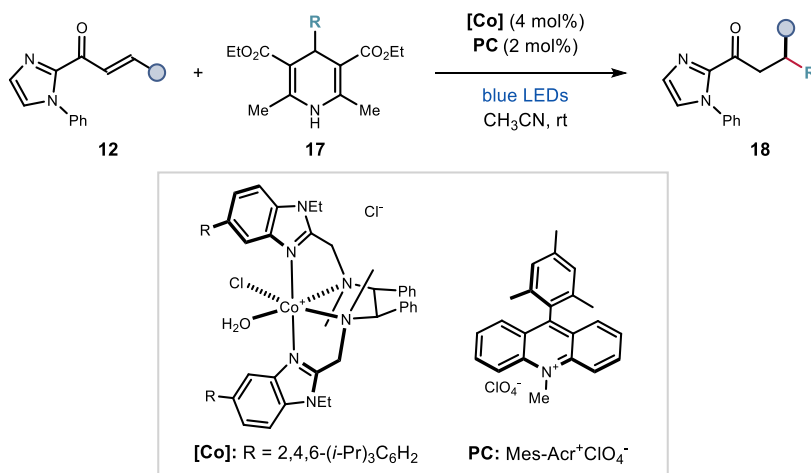
Figure 2.13. Asymmetric photochemical Giese reactions catalyzed by an octahedral chiral cobalt catalyst.

These recent examples showcase how modern photoredox catalysis has been harnessed to facilitate the development of catalytic enantioselective radical conjugate additions. However, the systems reported so far are limited by the need to preinstall a specific anchoring group (e.g. pyrazoles, imidazoles) within the substrate to facilitate coordination to a chiral Lewis acid complex to ensure optimal geometry control over the reactive intermediate.

---

[24] Zhang, K.; Lu, L.-Q.; Jia, Y.; Wang, Y.; Lu, F.-D.; Pan, F.; Xiao, W.-J. "Exploration of Novel Chiral Cobalt Catalyst for Visible-Light-Induced Enantioselective Radical Conjugate Addition" *Angew. Chem. Int. Ed.* **2019**, *58*, 13375.

UNIVERSITAT ROVIRA I VIRGILI
PHOTOCHEMISTRY AND ORGANOCATALYSIS FOR RADICAL-BASED CARBON-CARBON BOND-FORMING
PROCESSES
Emilien Le Saux

23

2.2.2 Organocatalytic asymmetric radical conjugate additions

In addition to the previously described transition metal-based systems, some metal-free methods have been developed for the asymmetric catalytic radical conjugate addition processes. In 2005, Bach and co-workers described an intramolecular radical addition of pyrrolidine **19** to afford spirocyclic compound **20** catalyzed by the chiral benzophenone **BP** (Figure 2.14).[25] Catalyst **BP** coordinated substrate **19** through hydrogen-bonding interactions thus effectively shielding one of the prochiral faces of the substrate. UV-light irradiation of the benzophenone moiety within intermediate **XV** promoted SET oxidation of the pyrrolidine unit that, upon proton loss, generated the α-amino radical intermediate (**XVI**). Cyclization and protonation delivered the enantioenriched product **20**.
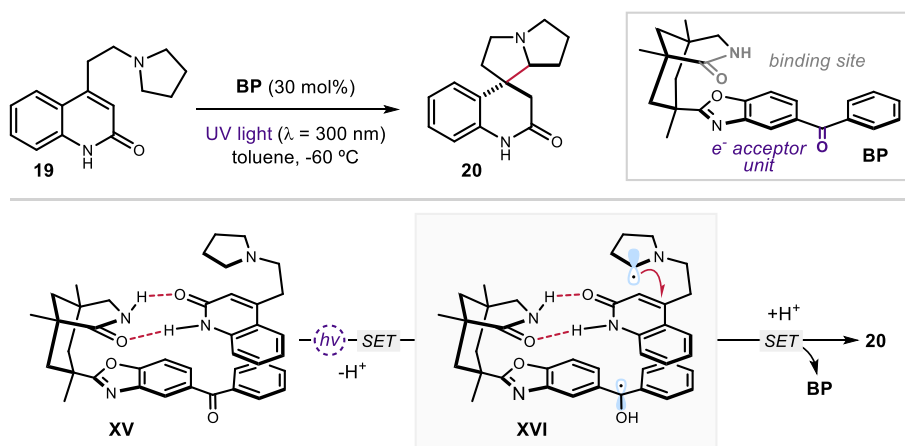
Figure 2.14. Enantioselective photoinduced-electron-transfer (PET)-catalyzed cyclization.

A strategy to functionalize more general scaffolds, such as cyclic enones, was reported by our research group. In particular, the combination of a chiral primary amine catalyst **A1** and a photoredox catalyst (**PC**) could promote a radical conjugate addition to β-substituted cyclic enones **21** to forge quaternary stereocenters in a stereoselective fashion (Figure 2.15).[26] Overall, this system was driven by an electron-relay mechanism. The 3π-radical cation **XVIII**, resulting from the addition of radical **II** to the electrophilic iminium ion **XVII**, underwent intramolecular SET from an electron-rich carbazole moiety, purposely placed within the chiral organocatalyst **A1**. The subsequent fast tautomerization from the enamine to the imine **XIX** avoided a back-electron transfer.[27] Finally, SET reduction of the carbazole radical cation **XIX** from the reduced photocatalyst restored the aminocatalyst **A1** and delivered the

[25] Bauer, A.; Westkämper, F.; Grimme, S.; Bach, T. "Catalytic enantioselective reactions driven by photoinduced electron transfer" *Nature*, **2005**, *436*, 1139.

[26] Murphy, J. J.; Bastida, D.; Paria, S.; Fagnoni, M.; Melchiorre, P. "Asymmetric Catalytic Formation of Quaternary Carbons by Iminium Ion Trapping of Radicals." *Nature,* **2016**, *532*, 218.

[27] Rappaport, Z., Ed. The Chemistry of Enamines; John Wiley and Sons: Chichester, 1994.

enantioenriched β-difunctionalized product **23**.[28] The presence of a β-substituent in the enone substrate helped to slow down the relative rate of the racemic background reaction.
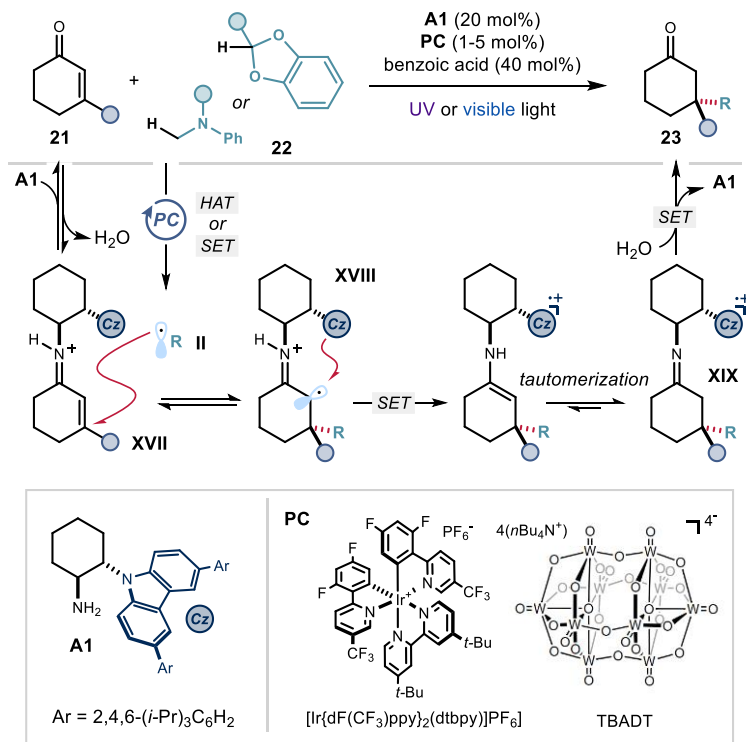
Figure 2.15. Photochemical organocatalytic strategy for the formation of quaternary stereocenters by radical conjugate addition to iminium ions. TBADT: tetrabutylammonium decatungstate.

In the course of this project, bright yellow crystals of the chiral iminium ion **XVII** were isolated. X-ray crystallographic analysis[29] established that this coloration was elicited by the formation of an electron donor-acceptor (EDA) complex between the electron-rich carbazole unit and the electron-deficient iminium ion moiety (Figure 2.16). Capitalizing upon this observation, the visible-light photoactivity of the intermediate EDA complex **XVII** was used to trigger radical conjugate additions to β-substituted cyclic enones **21** without the need for an external photocatalyst.[30] Condensation of the modified carbazole catalyst **A2** with a cyclic enone **21** generated a colored iminium ion **XVII**. Upon irradiation with visible light, an intramolecular SET was induced to give intermediate **XX**, which bears a persistent carbazole

[28] Bahamonde, A.; Murphy, J. J.; Savarese, M.; Brémond, E.; Cavalli, A.; Melchiorre, P. "Studies on the enantioselective iminium ion trapping of radicals triggered by an electron-relay mechanism" *J. Am. Chem. Soc.* **2017**, *139*, 4559.

[29] Crystallographic data for compound **XVII** has been deposited with the Cambridge Crystallographic Data Centre, accession number CCDC 1437991.

[30] Cao, Z.-Y.; Ghosh, T.; Melchiorre, P. "Enantioselective radical conjugate additions driven by a photoactive intramolecular iminium-ion-based EDA complex" *Nat Commun*, **2018**, *9*, 3274.

UNIVERSITAT ROVIRA I VIRGILI
PHOTOCHEMISTRY AND ORGANOCATALYSIS FOR RADICAL-BASED CARBON-CARBON BOND-FORMING
PROCESSES
Emilien Le Saux

25

radical cation. This moiety could act as a single-electron oxidant ($E(\mathbf{A1^{\bullet+}/A1}) = +1.09$ V vs. Ag$^+$/Ag in CH$_3$CN) to generate radicals **II** from suitable precursors such as **2** ($E_{red} < +1.09$ V). These two SET events constituted the initiation of a radical chain propagation. Interception of **II** by the ground-state iminium ion **XVII** and subsequent intramolecular SET afforded intermediate **XIX**, which propagated the radical-chain process through oxidation of **2**.
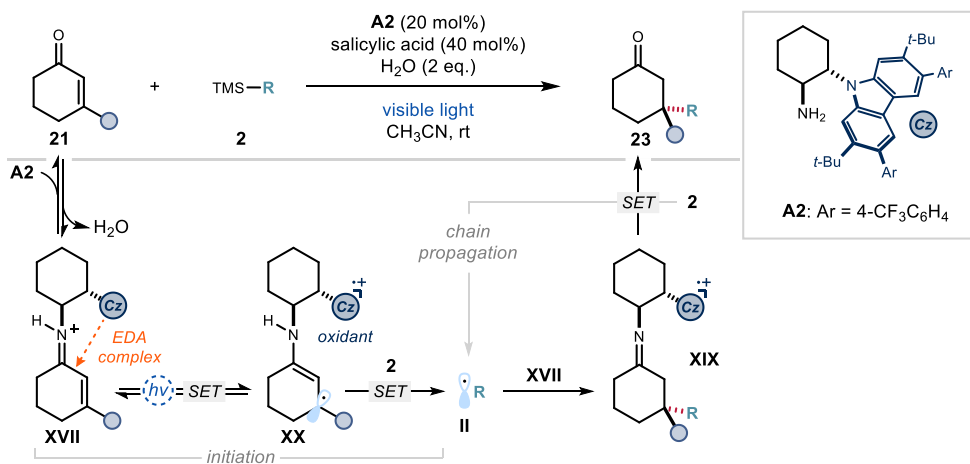
Figure 2.16. Intramolecular iminium ion-based EDA complex that triggers a photochemical asymmetric conjugate addition reaction.

Our group later showed that ground-state iminium ions derived from α,β-unsaturated aldehydes were also able to undergo stereocontrolled radical conjugate addition. Specifically, we found that the difluorinated secondary aminocatalyst **C**, which was purposely designed to promote the excited-state reactivity of iminium ions, had the potential to drive a stereocontrolled conjugate addition of acyl radicals **XXI** via ground-state iminium ion reactivity (Figure 2.17.a).[31] In this transformation, the radical generation strategy was based on the direct photolysis of 4-acyl-dihydropyridines **24** under visible light irradiation to generate nucleophilic acyl radicals **XXI**. Dihydropyridine **24** can absorb light up to 460 nm, which allowed for selective photoexcitation even in the presence of the photoabsorbing iminium ion. The ensuing open-shell intermediate **XXI** was then stereoselectively intercepted by the electrophilic ground-state chiral iminium ion **I**, formed upon condensation of aminocatalyst **C** with an enal.

[31] Goti, G.; Bieszczad, B.; Vega-Peñaloza, A.; Melchiorre, P. "Stereocontrolled Synthesis of 1,4-Dicarbonyl Compounds by Photochemical Organocatalytic Acyl Radical Addition to Enals" *Angew. Chem. Int. Ed.* **2019**, *58*, 1213.
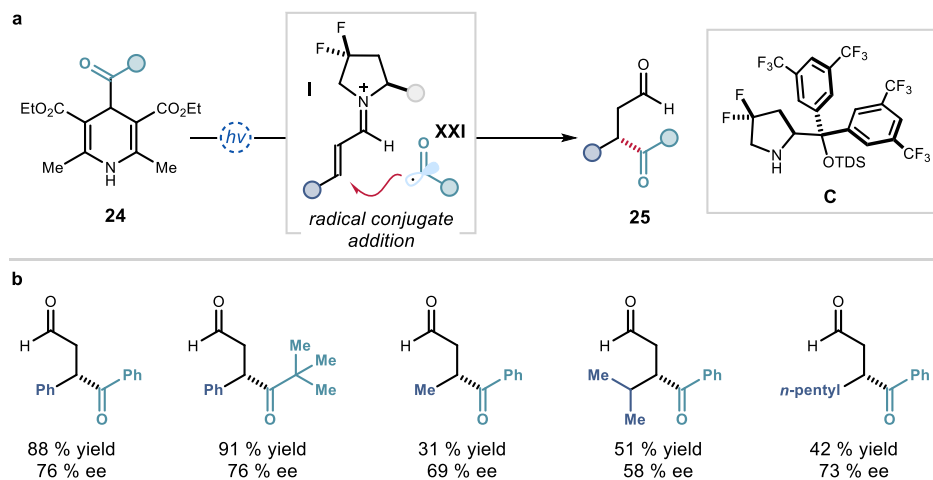
Figure 2.17. (**a**) Stereocontrolled conjugate addition of acyl radicals mediated by ground-state iminium ion reactivity. (**b**) Examples from the reaction scope; aliphatic substituents on the enals are also tolerated.

A variety of substituted acyl radicals were amenable to the radical conjugate addition with good yields but moderate enantioselectivity. Importantly, aliphatic enals also afforded the corresponding 1,4-dicarbonyl products with similar levels of enantiocontrol (Figure 2.17.b).

Overall, the reported organocatalytic strategies for asymmetric radical conjugate additions are mostly limited to β-substituted cyclic enones.[26,30] Enals, though amenable to such reactivity, only afforded moderate enantioselectivity in the process.

2.3 Design and target of the project

The present study was motivated by our interest in developing a general catalytic method for enantioselective radical conjugate additions to unmodified acyclic α,β-unsaturated carbonyl compounds. Our target was to develop a general system for the conjugate addition of a variety of radicals to readily available aliphatic and aromatic enals. We planned to fill this gap in synthetic methodology by using a dual catalytic system in which the radical formation and the stereo-determining step were decoupled. Specifically, we envisioned the use of an external photoredox catalyst,[32] which generates radicals from a wide variety of stable radical precursors, in combination with a chiral amine catalyst for iminium ion formation (Figure 2.18). Radical **II**, generated upon SET oxidation of precursor **2**, would be trapped by the ground-state electrophilic chiral iminium ion **I** in the stereodetermining step. The reduction of the resulting α-iminyl radical cation **XXII** would constitute the turnover event for the

---

[32] Zhao, J.-J.; Zhang, H.-H.; Shen, X.; Yu, S. Enantioselective Radical Hydroacylation of Enals with α-Ketoacids Enabled by Photoredox/Amine Cocatalysis. *Org Lett.* **2019**, *21*, 913.

UNIVERSITAT ROVIRA I VIRGILI
PHOTOCHEMISTRY AND ORGANOCATALYSIS FOR RADICAL-BASED CARBON-CARBON BOND-FORMING
PROCESSES
Emilien Le Saux

27

photocatalyst and would eventually afford the β-functionalized chiral aldehyde **3**. The main challenge to overcome will be the background addition of **II** to **1** leading to racemic product.
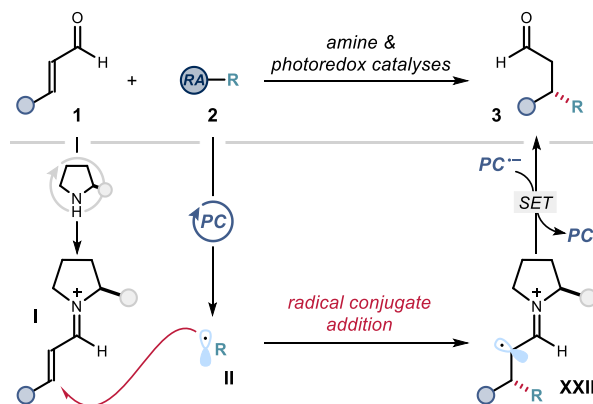
Figure 2.18. Our proposed strategy for a general radical conjugate addition to acyclic *aliphatic and aromatic* enals. RA = redox auxiliary.

2.4 Results and discussion

2.4.1 Optimization[33]

The α-silylamine substrate **2a**, bearing an oxidizable trimethylsilyl (TMS) group in α-position to nitrogen, was selected as the radical precursor. This is because the α-amino radical generated upon SET oxidation has a well-known tendency to undergo addition to electron-deficient alkenes.[34] Considering the oxidation potential of **2a** ((E (**2a**$^{•+}$/**2a**) = +1.78 V vs Ag$^+$/Ag), 3,6-di-*tert*-butyl-9-mesityl-10-phenylacridinium tetrafluoroborate (**PC-a**) was chosen as the photocatalyst (E^* (**PC-a***/**PC-a**$^{•-}$) = +2.08 V). Crotonaldehyde **1a** was selected as the model acceptor since this substrate was unsuitable for the previously developed β-functionalization radical strategy based on the direct excitation of chiral iminium ions (discussed in Figure 2.4).[5] In addition, the small size of the methyl fragment would challenge the ability of the chiral catalyst to infer high stereoselectivity in the radical conjugate addition. The experiments were conducted in CH$_3$CN using a blue high-power (HP) light-emitting-diode (LED, λ_{max} = 465 nm) with an irradiance set at 60 mW·cm^{-2}, as controlled by an external power supply[35] (details of the illumination set-up are reported in the experimental section).

---

[33] Preliminary investigations were conducted by Dr. Catherine M. Holden.
[34] Nakajima, K.; Miyake, Y.; Nishibayashi, Y. "Synthetic Utilization of α-Aminoalkyl Radicals and Related Species in Visible Light Photoredox Catalysis" *Acc. Chem. Res.* **2016**, *59*, 1946.
[35] The vial was placed into an aluminum block on a 3D-printed holder, fitted with a 460 nm high-power single LED. This setup secured a reliable irradiation while keeping a distance of 1 cm between the reaction vessel and the light source. The temperature was kept at -10 °C using a chiller connected to the irradiation plate.

UNIVERSITAT ROVIRA I VIRGILI
PHOTOCHEMISTRY AND ORGANOCATALYSIS FOR RADICAL-BASED CARBON-CARBON BOND-FORMING
PROCESSES
Emilien le Saux

28

Results are gathered in Table 2.1. We started our studies by screening chiral secondary amine catalysts with an established profile in promoting asymmetric iminium-ion-mediated processes.

Table 2.1. Optimization studies.
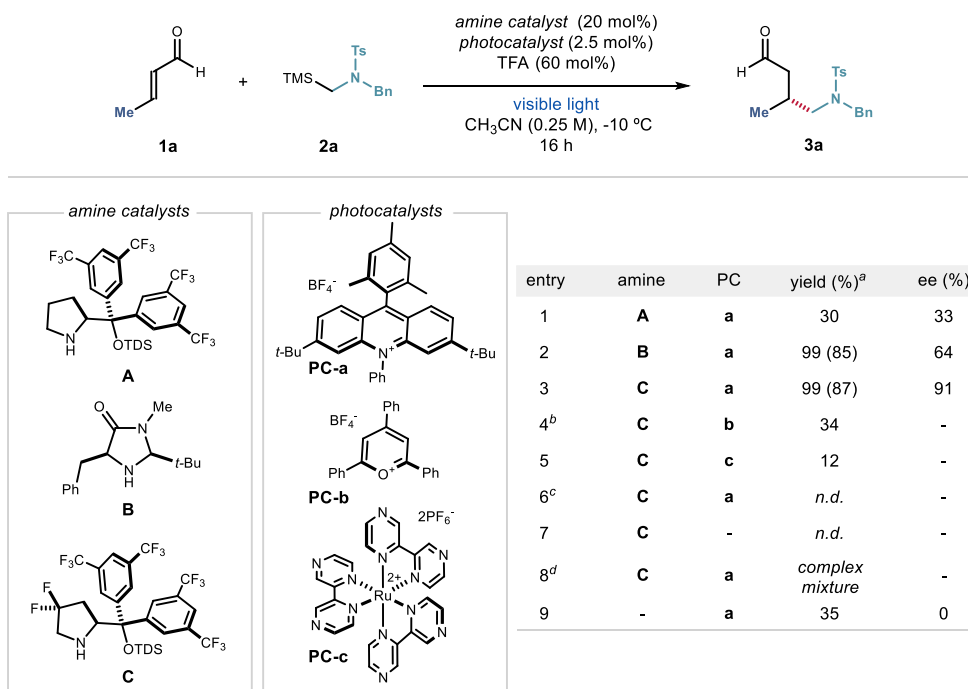
entry	amine	PC	yield (%)[a]	ee (%)
1	A	a	30	33
2	B	a	99 (85)	64
3	C	a	99 (87)	91
4[b]	C	b	34	-
5	C	c	12	-
6[c]	C	a	n.d.	-
7	C	-	n.d.	-
8[d]	C	a	complex mixture	-
9	-	a	35	0

Reactions performed on a 0.1 mmol scale using 2 equiv. of enal **1a** under illumination by a single high-power (HP) LED (λ_{max} = 465 nm) with an irradiance of 60 mW·cm^{-2}. [a]Yield of **3a** determined by ^{1}H NMR analysis of the crude reaction mixture using trichloroethylene as the internal standard. Yields of isolated **3a** are reported in parentheses. [b]Irradiation using a single HP LED (λ_{max} = 420 nm). [c]No light. [d]Reaction performed at room temperature. *n.d.*: not detected.

The diarylprolinol silyl ether **A**[36] afforded product **3a** with poor yield and stereocontrol (entry 1), while the MacMillan 2nd generation aminocatalyst **B** delivered product **3a** in excellent yield and increased enantiocontrol (entry 2, 64% ee). The *gem*-difluorinated diarylprolinol silylether catalyst **C**, specifically designed for the photoactivation of iminium ions,[5] offered the best result with **3a** formed in 87% yield and 91% ee (entry 3). Other strongly oxidizing photoredox catalysts were then tested in combination with organocatalyst **C**. Both triphenylpyrilium **PC-b** and the ruthenium-based catalyst **PC-c** afforded **3a** in low yield (entries 4 and 5). Control experiments indicated that the photocatalyst and light were both essential for the reaction (entries 6 and 7). When performing the reaction at room temperature (entry 8), a complex mixture of products was formed. The main aldehydic product was

---

[36] K. L. Jensen, G. Dickmeiss, H. Jiang, Ł. Albrecht, K. A. Jørgensen. "The Diarylprolinol Silyl Ether System: A General Organocatalyst" *Acc. Chem. Res.* **2012**, *45*, 248.

UNIVERSITAT ROVIRA I VIRGILI
PHOTOCHEMISTRY AND ORGANOCATALYSIS FOR RADICAL-BASED CARBON-CARBON BOND-FORMING PROCESSES
Emilien Le Saux

29

identified as a *p*-tolyl benzaldehyde. This product is most likely formed in a Michael addition/aldol condensation sequence involving dienamine and iminium ion intermediates (Figure 2.19). This type of polar pathway was reported under similar conditions.[37]
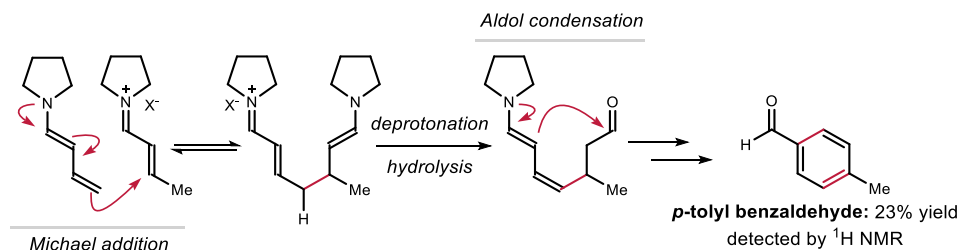
Figure 2.19. Tentative rationalization for the formation of *p*-tolyl benzaldehyde under standard conditions at room temperature. The substituent on the amine catalyst was omitted for clarity.

The reactivity observed in the absence of amine **C** (entry 9, Table 2.1) implies that the rate acceleration offered by iminium ion activation is large enough to overcome the racemic background process. A competition experiment between crotonaldehyde and methyl vinyl ketone (**MVK**) with and without amine catalyst **C** allowed us to qualitatively observe this rate enhancement (Table 2.2). It is assumed that the **MVK** product **3a'** does not decompose *in situ* and that the rates of both reactions are independent. In the absence of amine catalyst, addition of the α-amino radical to **MVK** is faster than to the β-substituted enal. However, in the presence of amine catalyst **C**, no product of conjugate addition to **MVK** was detected and only addition to enal **1a** was observed, with **3a** formed exclusively. In this experiment **MVK** mimics the background process, as condensation of **C** to this substrate is much slower than to enal **1a** (iminium ion formation is hampered by steric effects). These results show that the radical addition to the free substrate (background reaction) cannot compete with addition to the chiral iminium ion deriving from **C**, even though **1a** is present in a ten-fold excess at the beginning of the reaction. Similar rate enhancement in asymmetric radical conjugate addition has been described by Meggers and co-workers.[20]

---

[37] Song, X.; Zhang, X.; Zhang, S.; Li, H.; Wang, W. "Direct Transformation of Simple Enals to 3,4-Disubstituted Benzaldehydes under Mild Reaction Conditions via an Organocatalytic Regio- and Chemoselective Dimerization Cascade" *Chem. Eur. J.* **2012**, *18*, 9770.

Table 2.2. Competition experiment between crotonaldehyde **1a** and methyl vinyl ketone.
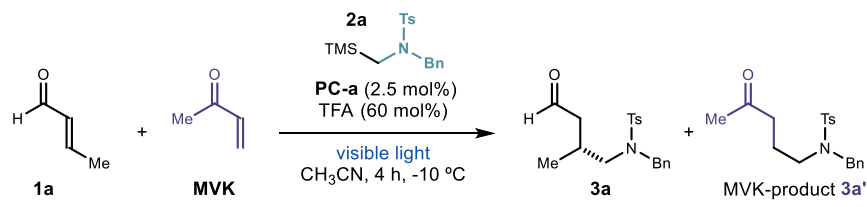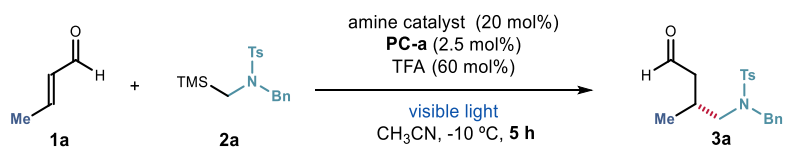
	yield **3a**[a]	yield **3a'**[a]	**3a : 3a'**
no amine catalyst **C**	6%	40%	0.15 : 1
with amine catalyst **C** (20 mol%)	36%	n.d.	>360: 1

Reactions performed on 0.1 mmol scale using 2 equiv. of **1a** or methyl vinyl ketone. [a]Yields determined by
^{1}H NMR analysis of the crude reaction mixture using trichloroethylene as the internal standard.

The results of this optimization campaign showed that the difluorinated amine **C** is clearly a
superior catalyst to well-established catalysts **A** and **B** for this radical transformation. While
the lower enantiomeric excess obtained with **B** can be ascribed to a less efficient face-
shielding of the iminium ion (see entries 2 and 3), the difference in yield and in particular
enantiomeric excess when using the structurally similar amine **A** prompted us to perform
additional experiments to understand the effect of the two fluorine atoms in **C**.

Our initial hypothesis was that catalyst **A** was decomposing under the reaction conditions due
to the highly oxidizing nature of catalyst **PC-a**. The introduction of fluorine substituents in
amine catalyst **C** significantly increases its reduction potential in comparison to **A** ($E(A^{•+}/A)$
= +1.57 V vs Ag$^+$/Ag in CH$_3$CN; $E(C^{•+}/C)$ = +2.20 V vs Ag$^+$/Ag in CH$_3$CN), making it less
sensitive to oxidation. However, a control of catalyst stability after 5 hours of reaction showed
that both **A** and **C** were partially destroyed to approximately the same extent during the
process (Table 2.3).

UNIVERSITAT ROVIRA I VIRGILI
PHOTOCHEMISTRY AND ORGANOCATALYSIS FOR RADICAL-BASED CARBON-CARBON BOND-FORMING
PROCESSES
Emilien Le Saux

31

Table 2.3. Evaluation of the catalyst's degradation under the reaction conditions.

entry	amine	yield (%)[a]	ee (%)	remaining cat. (%)[a]
1	A	14	33	69
2	C	41	91	52
3	-	20	-	-

Reactions performed on a 0.1 mmol scale using 2 equiv. of enal **1a** under illumination by a single high-power (HP) LED (λ_{max} = 465 nm) with an irradiance of 60 mW·cm^{-2}. [a]Yields determined by ^{1}H NMR analysis of the crude reaction mixture using trichloroethylene as the internal standard.

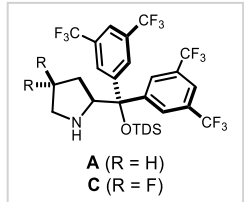The low stereoselectivity imparted by catalyst **A** (33% ee) in comparison to **C** (91% ee) might come from an insufficient rate enhancement offered by the iminium ion deriving from **A** compared to the background process (see entries 1 and 9 in Table 2.1: 30% yield with **A** against 35% yield without amine catalyst). This indicates that the iminium ion generated upon condensation of amine **A** with crotonaldehyde **1a** may not be electrophilic enough to provide adequate rate enhancement against the uncatalyzed reaction. In contrast, the rate acceleration offered by amine catalyst **C** is large enough to overcome the racemic background process. Overall, these results suggest that incorporating the electron-withdrawing fluorine atoms could facilitate the stereoselective radical trap by providing a chiral iminium ion with an enhanced electrophilicity. In consonance with this reasoning are previous reports by Mayr and co-workers, who conducted experimental studies to quantify the electrophilicities of different α,β-unsaturated iminium ions.[38] Their work established that iminium ions derived from catalyst **B** (**Ib**) are significantly more electrophilic than the ones derived from a parent amine to catalyst **A** (amine **Ia**, Figure 2.20). With a given nucleophile (a ketene acetal), the MacMillan catalyst-based iminium ion reacts 8 times faster than the diphenyl prolinol-based one. This may also explain the significantly enhanced product yield and enantioselectivity offered by catalyst **B** (99% yield, 64% ee) against catalysts **A** (30% yield, 33% ee) under the optimized conditions.

---

[38] (a) Lakhdar, S.; Tokuyasu, T.; Mayr, H. "Electrophilic Reactivities of α, β-Unsaturated Iminium Ions" *Angew. Chem. Int. Ed.* **2008**, *47*, 8723; (b) Lakhdar, S.; Ammer, J.; Mayr, H. "Generation of α,β-Unsaturated Iminium Ions by Laser Flash Photolysis" *Angew. Chem. Int. Ed.* **2011**, *50*, 9953.
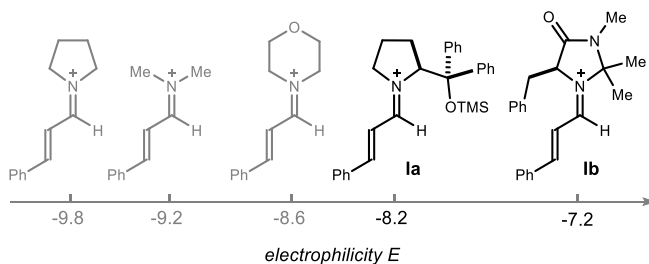
Figure 2.20. Electrophilicities of iminium ions deriving from the condensation of cinnamaldehyde with different secondary amines as studied by Mayr and co-workers (Ref. 38).

Since experimental results from the optimization studies have shown that the MacMillan catalyst **B** provided similar reactivity to the *gem*-difluorinated amine catalyst **C** in the model reaction, we considered it mechanistically relevant to compare the electrophilicity of iminium ions **Ib** and **Ic**, generated upon condensation of catalysts **B** and **C**, respectively, with crotonaldehyde. We used density functional theory (DFT) calculations (performed using B3LYP/6-31G(d)) to determine optimized structures of iminium ions of type **Ib** and **Ic**. From these minimized structures, the frontier molecular orbitals were calculated and their energies determined (Table 2.4). Our calculations indicated that the iminium ion **Ic**, generated from *gem*-difluorinated amine catalyst **C**, has a LUMO that lies slightly lower in energy than the highly electrophilic iminium ion **Ib**, suggesting greater electrophilicity. These theoretical results offer further support to our mechanistic interpretation that the presence of the electron-withdrawing fluorine atoms provides the chiral iminium ion **Ic** with an enhanced electrophilicity.

Table 2.4. Calculated energy levels for the frontier orbitals of iminium ions **Ib** and **Ic**.
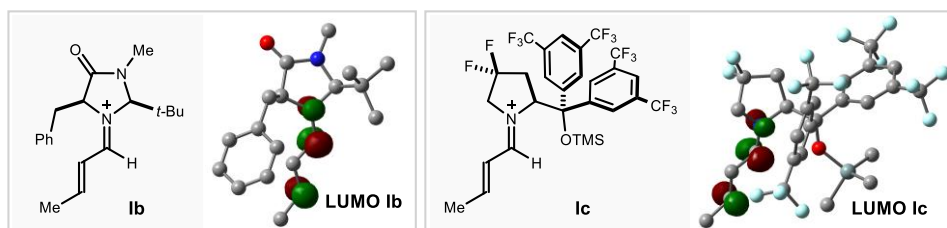
iminium ion	E_{HOMO} (eV)	E_{LUMO} (eV)	$\Delta E_{HOMO-LUMO}$ (eV)
Ib	-9.62	-6.35	3.27
Ic	-10.38	-6.39	3.99

UNIVERSITAT ROVIRA I VIRGILI
PHOTOCHEMISTRY AND ORGANOCATALYSIS FOR RADICAL-BASED CARBON-CARBON BOND-FORMING
PROCESSES
Emilien Le Saux

33

2.4.2 Generality of the system

Adopting the optimized conditions described in Table 2.1, entry 3, we evaluated the synthetic potential of the radical conjugate addition strategy. We first examined different enals as traps for the α-amino radical generated from substrate **2a**. A wide range of aliphatic substituents at the enals' β position was well tolerated (Figure 2.21), with the corresponding products being formed with consistently high stereoselectivity (products **3a-h**, ee ≥89%). The presence of a terminal olefin did not lead to undesired side reactions, smoothly affording product **3f**. A benzylic ether functionality was also tolerated (product **3g**). The reaction of (*E*)-3-cyclopropylacrylaldehyde led to the exclusive formation of the β-alkylated product **3h**, with the cyclopropyl fragment left untouched. Performing the model reaction on a 1 mmol scale only slightly affected the efficiency of the process (**3a** formed in 74% yield and 86% ee), showing that the method is amenable to synthetically useful purposes.

Aromatic enals were equally suitable substrates for the protocol (products **3i-p**). Different substitution patterns at the aromatic moiety of enals **1** were tolerated well, regardless of their electronic and steric properties and position on the phenyl ring. The reaction of a heteroaromatic enal was less effective but still delivered the β-alkylated benzothiophene product **3o** in high enantioselectivity. We also tested the ability of our protocol to stereoselectively forge quaternary carbon stereocenters. The reaction of β,β'-disubstituted (*E*)-3-phenylbut-2-enal led to the formation of the product **3p** with moderate yield and enantioselectivity.

Figure 2.21. Scope of aliphatic and aromatic enals. Reactions performed on a 0.1 mmol scale using 2 equiv. of enal **1**. Yields and enantiomeric excesses refer to isolated products **3** after purification (average of two runs per substrate). [a]Reaction performed on 1 mmol scale. Ts: toluenesulfonyl; Bn: benzyl.

Given the high reduction potential of the excited photocatalyst **PC-a** (E^*(**PC-a***/ **PC-a**•⁻) = +2.08 V vs Ag⁺/Ag in CH_3CN), we anticipated that a variety of radical precursors with redox potentials < +2.08 V would be amenable to the reaction conditions. First, we turned our attention towards other TMS-based radical precursors (Figure 2.22). Variation of the nitrogen protecting groups of **2a** were perfectly tolerated affording the desired products in good yields and excellent enantioselectivity (**3q-s**). The protocol enabled the stereoselective installation of nitrogen-containing heterocyclic fragments of pharmaceutical interest within products **3**, such as a carbazole and an indole moiety (**3t** and **3u**). Benzyl silanes, bearing both electron-releasing and electron-withdrawing substituents on the aryl ring, were successfully used (**3v-z**). We also found that α-silyl thioethers and ethers could be used in the radical conjugate addition (**3aa** and **3bb**).

UNIVERSITAT ROVIRA I VIRGILI
PHOTOCHEMISTRY AND ORGANOCATALYSIS FOR RADICAL-BASED CARBON-CARBON BOND-FORMING PROCESSES
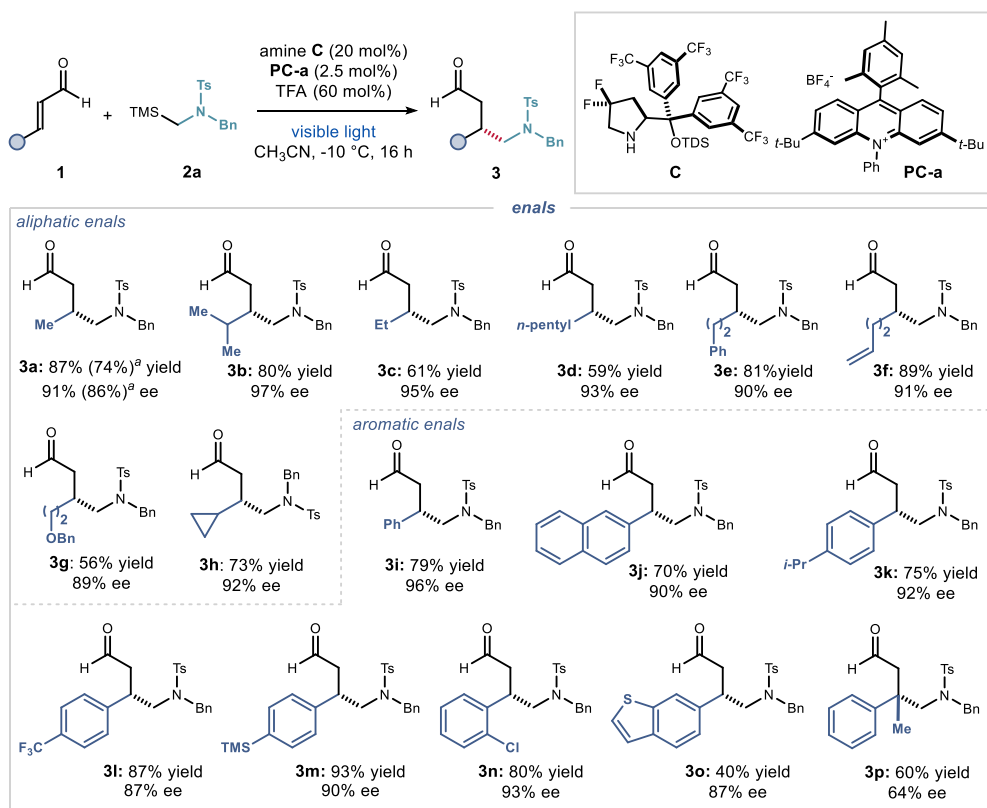Emilien Le Saux

35

Figure 2.22. Scope of TMS radical precursors. Reactions performed on a 0.1 mmol scale using 2 equiv. of enal **1**. Yields and enantiomeric excesses refer to isolated products **3** after purification (average of two runs per substrate). [a]Using a 3:1 mixture of CH_3CN/H_2O as solvent. TMS: trimethylsilyl; Ts: toluenesulfonyl; PMB: *p*-methoxybenzyl; Piv: pivaloyl; Boc: *tert*-butyloxycarbonyl.

We then tested the possibility of activating radical precursors bearing other redox auxiliary groups (Figure 2.23). The use of a trifluoroborate salt **26**[7a] enabled the incorporation of a cyclopentyl fragment at the β position of octenal (product **3cc**). The alkylsilicate **27**[39] could be used for the stereoselective incorporation of a cyclohexyl moiety in both aromatic and aliphatic enals (products **3dd** and **3ee**). Dihydropyridines[7a,40] **17** proved useful to stereoselectively functionalize cinnamaldehyde with an isopropyl moiety, a derivative of the insecticide *carbaryl,* and a 3,4-dihydroquinolone, leading to products **3ff-hh**.

[39] Ikarashi, G.; Morofuji, T.; Kano, N. "Terminal-Oxidant-Free Photocatalytic C–H Alkylations of Heteroarenes with Alkylsilicates as Alkyl Radical Precursors" *Chem. Commun.* **2020**, *56*, 10006.
[40] Crisenza, G. E. M.; Faraone, A.; Gandolfo, E.; Mazzarella, D.; Melchiorre, P. "Catalytic Asymmetric C–C Cross-Couplings Enabled by Photoexcitation" *Nat. Chem.* **2021**, *13*, 575.
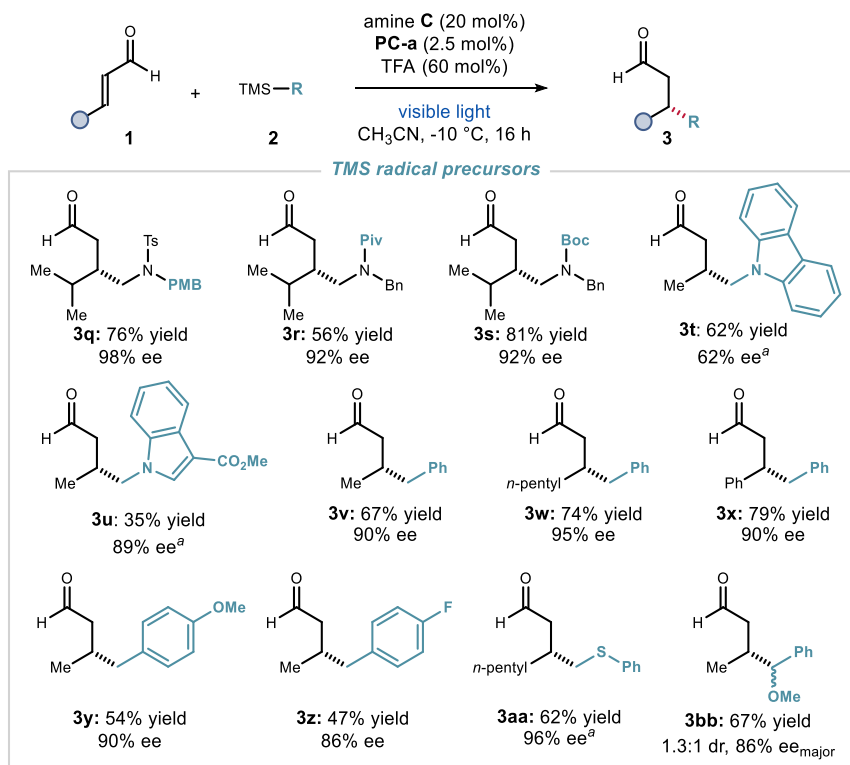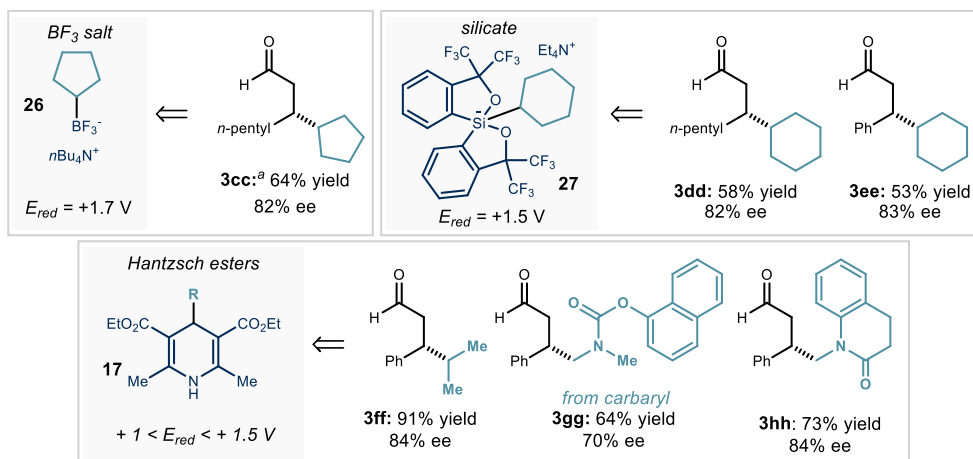
Figure 2.23. Scope of other radical precursors. Reactions performed on a 0.1 mmol scale using 2 equiv. of enal **1**. Yields and enantiomeric excesses refer to isolated products **3** after purification (average of two runs per substrate). [a]Using 1.1 equiv. of enal. Redox potentials vs Ag^{+}/Ag in acetonitrile.

Besides radical precursors bearing redox auxiliaries, we wondered if the direct oxidation of native functional groups for radical generation would be compatible with our system (Figure 2.24). Gratifyingly, we could use cyclopropanol **28** as a suitable radical precursor.[41] Upon SET oxidation-mediated ring-opening, the resulting non-stabilized primary radical could be effectively intercepted with high stereocontrol to afford products **3ii** and **3jj**. Moreover, the alkenoic acid **29**, which generates a tertiary radical upon SET oxidation-mediated anti-Markovnikov lactonization,[7d,42] afforded product **3kk**.

[41] Jia, K.; Zhang, F.; Huang, H.; Chen, Y. "Visible-Light-Induced Alkoxyl Radical Generation Enables Selective C(sp[3])–C(sp[3]) Bond Cleavage and Functionalizations" *J. Am. Chem. Soc.* **2016**, *138*, 1514.
[42] Hamilton, D. S.; Nicewicz, D. A. "Direct Catalytic Anti-Markovnikov Hydroetherification of Alkenols" *J. Am. Chem. Soc.* **2012**, *134*, 18577;

UNIVERSITAT ROVIRA I VIRGILI
PHOTOCHEMISTRY AND ORGANOCATALYSIS FOR RADICAL-BASED CARBON-CARBON BOND-FORMING PROCESSES
Emilien Le Saux

37
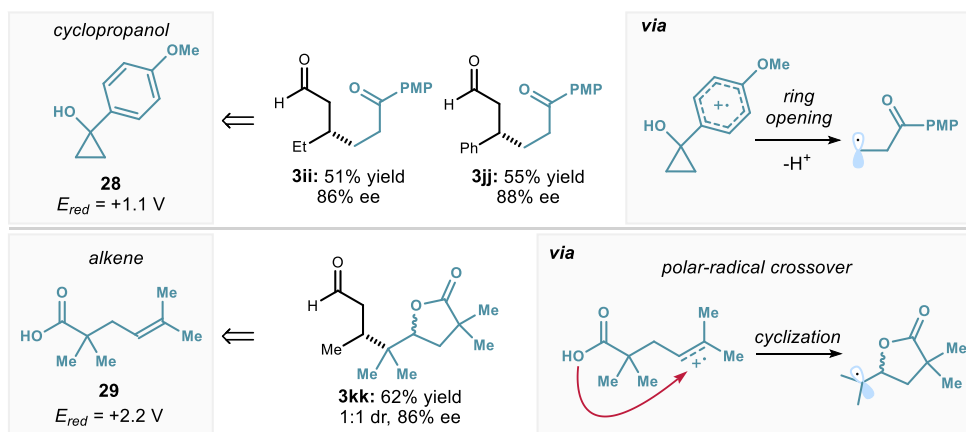
Figure 2.24. Examples of direct oxidation of functional groups without the need for a redox auxiliary. Reactions performed on a 0.1 mmol scale using 2 equiv. of enal **1**. Yields and enantiomeric excesses refer to isolated products **3** after purification (average of two runs per substrate). Redox potentials vs Ag+/Ag in acetonitrile. PMP: *p*-methoxyphenyl.

This last result motivated us to develop a different cascade process exploiting the intermediacy of a chiral enamine in the reaction mechanism. By using the radical precursor **2b** bearing an electrophilic ketone, a series of densely functionalized piperidines **30** could be synthesized in a single step (Figure 2.25). This cascade reaction is enabled by a radical-polar crossover process whereby the radical conjugate addition product, an enamine (grey panel in Figure 2.25) undergoes an intramolecular aldol reaction with the tethered ketone moiety. Products **30a-c** were obtained in good diastereo- and enantio-selectivity. Interestingly, the use of biphenyl as an additive was beneficial for this cascade process. When omitting this additive, **30** is formed in lower yields and the uncyclized product **3** was also detected in the mixture. As biphenyl has been previously reported to act as a redox mediator,[7c] a possible explanation for its role is to prevent the undesired oxidation of the key enamine intermediate, securing a more efficient cyclization step. Importantly, the stereochemistry of the major diastereoisomer of product **30c** was established by single crystal X-ray crystallographic analysis.[43]

---

[43] Crystallographic data for compound **30c** (major diastereoisomer) has been deposited with the Cambridge Crystallographic Data Centre, accession number CCDC 2008646.

Figure 2.25. Iminium ion – enamine cascade for the synthesis of complex piperidines. Reactions performed on a 0.2 mmol scale using 2 equiv. of enal **1**. Yields and enantiomeric excesses refer to isolated prod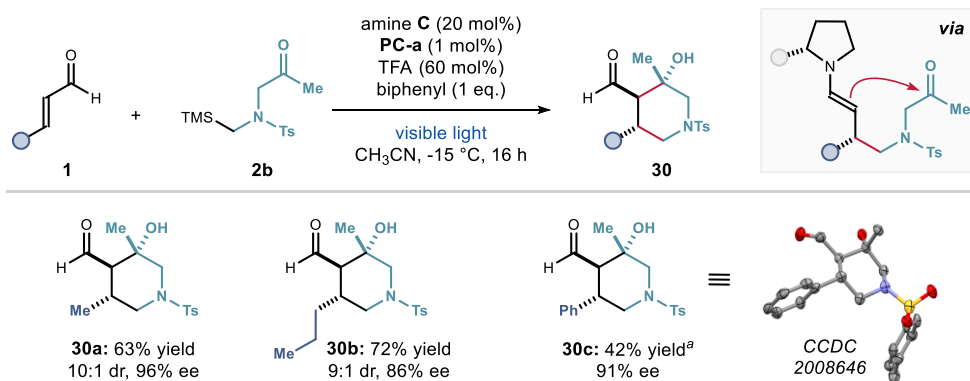ucts **30** after purification. Ts: toluenesulfonyl. *ᵃ*The process afforded a *d.r.* of 2:1, but the pure major diastereoisomer **30c** could be isolated. Ts: toluenesulfonyl.

We also implemented a different cascade (Figure 2.26), where the Michael acceptor **31** was intercepted intermolecularly by an enamine intermediate. After completion of the conjugate radical addition using catalyst **C**, the electron-poor alkene **31** was added along with aminocatalyst **D** (20 mol%), which assisted the enamine step of the cascade. This one-pot procedure granted access to the 2,3-disubsituted product **32** with high enantioselectivity and good *anti* diastereoselectivity.
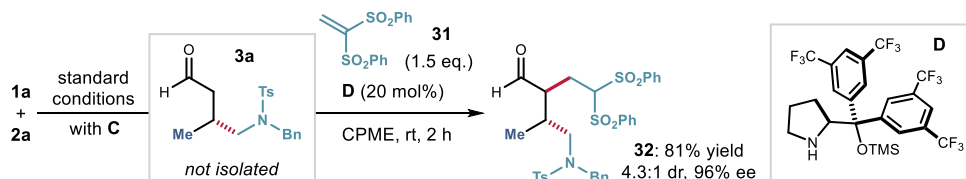
Figure 2.26. Iminium ion – enamine one-pot sequence for the synthesis of α,β-functionalized aldehydes. Reactions performed on a 0.1 mmol scale using 2 equiv. of enal **1a** using the conditions described in entry 4 of Table 2.1. Yields and enantiomeric excesses refer to isolated products **32** after purification. Ts: toluenesulfonyl; Bn: benzyl; CPME: cyclopentyl methyl ether.

Some radical precursors, selected because they had redox potentials in the range of **PC-a**, were poorly or not reactive under the reaction conditions (Figure 2.27). Allyl silane **33** afforded the desired product **3ll** with moderate yield and low enantioselectivity. Acylation of crotonaldehyde was attempted using phenylglyoxylic acid **34** as a radical precusor,[44] but the target 1,4-dicarbonyl **3mm** was obtained in a racemic form. Alkylation of octenal with cyclopentyl-DHP **36** afforded adduct **3cc** in low yield (due to poor substrate conversion), albeit with excellent enantioselectivity. Some radicals were not amenable to the reaction,

---

[44] Morack, T.; Mück-Lichtenfeld, C.; Gilmour, R. "Bioinspired Radical Stetter Reaction: Radical Umpolung Enabled by Ion-Pair Photocatalysis" *Angew. Chem. Int. Ed.* **2019**, *58*, 1208.

UNIVERSITAT ROVIRA I VIRGILI
PHOTOCHEMISTRY AND ORGANOCATALYSIS FOR RADICAL-BASED CARBON-CARBON BOND-FORMING
PROCESSES
Emilien Le Saux

39

including carbamoyl (from DHP **35**) and α-boryl (from silane **37**) ones. Finally, TMS **38** and simple Boc-piperidine **39** were not suitable to generate α-amino radicals in our system.
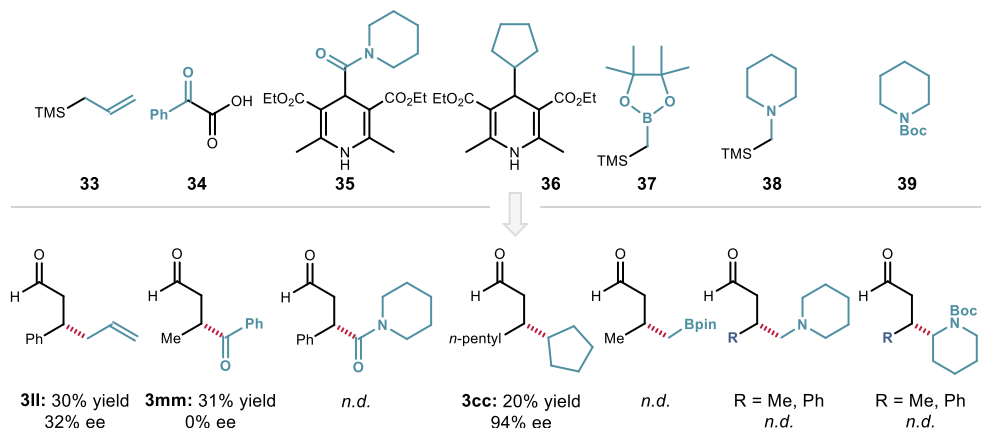
Figure 2.27. Moderately successful and unsuccessful substrates. Reactions performed on a 0.1 mmol scale using 20 mol% of catalyst **C**, and 2 equiv. of enal **1a**. Yields of determined by ^{1}H NMR analysis of the crude reaction mixtures using trichloroethylene as the internal standard. Bpin: pinacol boronic ester; Boc: *tert*-butyloxycarbonyl.

2.5 Mechanistic investigations

2.5.1 Control experiments with aromatic enals

A control experiment demonstrated that the model reaction of crotonaldehyde **1a** does not proceed in the absence of the acridinium photocatalyst **PC-a** (Table 2.1, entry 7). However, based on our previous reports,[5] a possible background reactivity arising from the photoexcitation of iminium ions had to be considered when using aromatic enals. All the radical precursors used in this study can be oxidized by the excited iminium ion ($E^*(I^*/I^{\bullet-})$ > +2.2 V vs Ag$^+$/Ag).[5] In particular, TMS radical precursors of type **2a**,[5] dihydropyridines **17**,[7a] and cyclopropanols **28**[7c] are amenable to photo-iminium ion chemistry. Although aromatic iminium ions absorb light up to 420 nm, we wanted to confirm that **PC-a** was the photoactive species under our reaction conditions also with aromatic enals.

Different cinnamaldehydes were submitted to the reaction with different radical sources in the presence and absence of **PC-a**. The results gathered in Figure 2.28 indicate that the radical conjugate addition products **3** can be formed to some extent also in the absence of the photocatalyst. The presence of the acridinium catalyst **PC-a** still proved to be highly beneficial, securing consistently higher chemical yields.
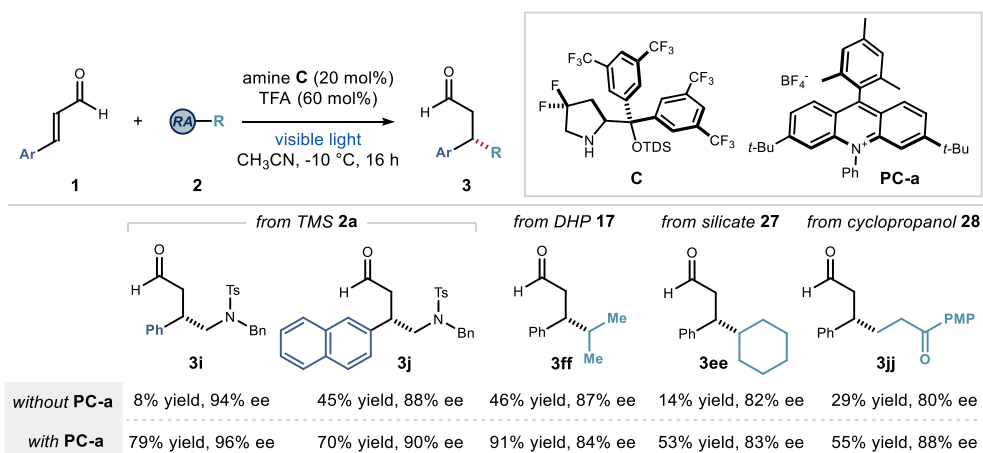
Figure 2.28. Study on the background reaction enabled by direct excitation of iminium ions from aromatic enals.

The tail of absorption of the iminium ion **I** obtained by condensation of cinnamaldehyde with **C** is around 420 nm while the HP single LED used in this study has an emission centered at 465 nm. By plotting these absorption and emission spectra together (Figure 2.29), we observed a slight overlap which may explain the excited iminium ion-based reactivity with aromatic enals.
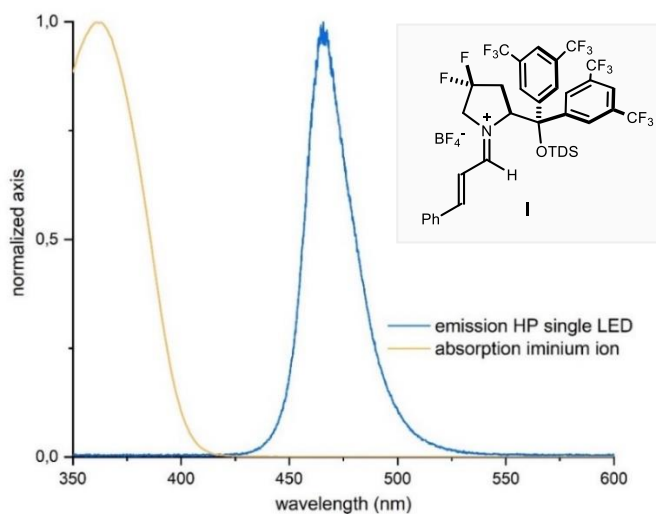
Figure 2.29. Normalized absorption of iminium ion **I** and emission of the blue HP LED used in this study.

We also performed the reaction between cinnamaldehyde and radical precursor **2a** using a Xenon lamp equipped with a band-pass filter centered at 450 nm (± 5 nm). This experiment should prevent the possibility to excite the iminium ion intermediate (Figure 2.30). In the absence of **PC-a**, no conversion was observed, while introduction of the photocatalyst

UNIVERSITAT ROVIRA I VIRGILI
PHOTOCHEMISTRY AND ORGANOCATALYSIS FOR RADICAL-BASED CARBON-CARBON BOND-FORMING
PROCESSES
Emilien Le Saux

41

restored the reactivity. Overall, these results provide evidence that acridinium **PC-a** was the key photoactive species mainly responsible for the radical conjugate addition.
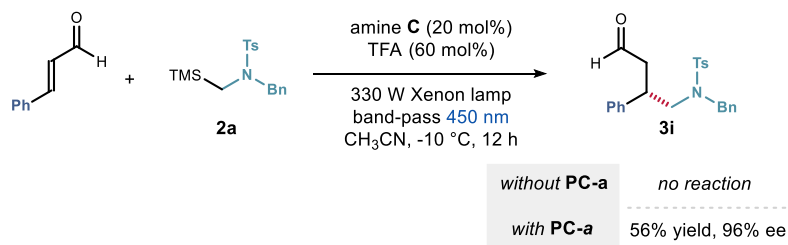
Figure 2.30. Selective excitation of photocatalyst **PC-a** using a band-pass filter.

2.5.2 Stern-Volmer quenching studies

Stern-Volmer (or emission) quenching experiments are useful to study and quantify the effect of a compound (the quencher) on the fluorescence of an excited-state species.[45] This fluorescence is caused by electronic relaxation of the fluorophore from its excited state to lower-energy levels. Since non-radiative events can decrease the efficiency of the fluorescence process, the emission of a fluorophore from its excited state is usually observed at a higher wavelength than the excitation wavelength (this phenomenon is referred to as Stokes shift). This shift is illustrated in Figure 2.31, which shows the normalized absorption and emission spectra of catalyst **PC-a**.
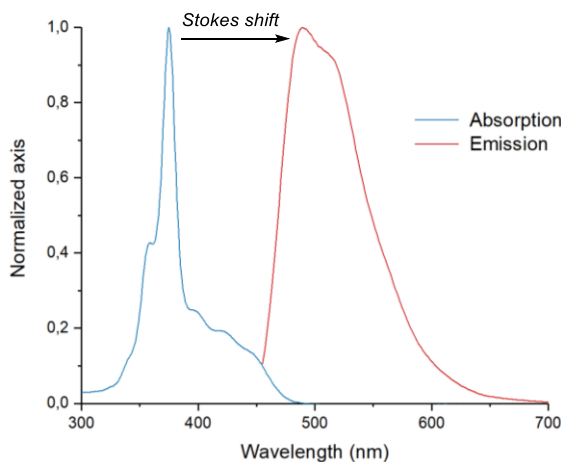
Figure 2.31. Normalized absorption and emission spectra of catalyst **PC-a**.

---

[45] (a) Lakowicz, J. R. "Principles of Fluorescence Spectroscopy" New York: Springer, 2006; (b) Balzani, V. Ceroni, P. Juris, A. "Photochemistry and Photophysics: Concept, Research and Applications" Weinheim, Wiley-VCH, 2014.

Dynamic quenching, is a phenomenon that occurs when a quencher Q undergoes collisional events with the emitting moiety and deactivates its fluorescence via single-electron transfer (SET), energy transfer (EnT), or formation of an exciplex (excited-state complex) and subsequent charge transfer. A linear dependence exists for the ratio I_0/I (I and I_0 are the luminescence intensities at a selected wavelength with and without quencher respectively) and the concentration of quencher in solution following Equation 1:

$$I_0/I = 1 + k_q\tau_0[Q] = 1 + K_{SV}[Q] \qquad \textbf{(Eq. 1)}$$

where k_q is the kinetic constant of the quenching process, while τ_0 is the excited-state lifetime in the absence of quencher. The product $k_q\tau_0$ is usually referred to as the Stern-Volmer constant, K_{SV}.

Thus, by measuring the decrease of emission intensity over addition of an increasing concentration of quencher, the Stern-Volmer constant can be deduced.

We performed emission quenching studies of the excited state of photocatalyst **PC-a** using the radical precursor **2a** as the quencher. Experimentally, a 4×10^{-6} M solution of **PC-a** in thoroughly degassed DCE was used. **PC-a** displayed an emission maximum at 500 nm when excited with 444 nm light. Sequential addition of a solution of **2a** caused a decrease in emission intensity (Figure 2.32, left panel). The Stern-Volmer plot was constructed (Figure 2.32, right panel) which highlighted a linear correlation between I_0/I and [**2a**]. From this data, a Stern-Volmer constant $\textbf{\textit{K}}_{SV} = \textbf{3.9 M}^{-1}$ was determined. A quenching constant $\textbf{\textit{k}}_q = \textbf{2.7} \cdot \textbf{10}^8$ $\textbf{M}^{-1}\cdot\textbf{s}^{-1}$ was calculated considering the lifetime of **PC-a** in the excited state (0.0144 μs).[46]

No change in the absorption spectrum of **PC-a** was observed upon additions of **2a**, thus excluding a possible ground-state association between these two species, which would lead to a decrease in emission intensity.

---

[46] Wu, Y.; Kim, D.; Teets, T., S. "Photophysical Properties and Redox Potentials of Photosensitizers for Organic Photoredox Transformations" *Synlett*, **2022**, *33*, 1154.

UNIVERSITAT ROVIRA I VIRGILI
PHOTOCHEMISTRY AND ORGANOCATALYSIS FOR RADICAL-BASED CARBON-CARBON BOND-FORMING
PROCESSES
Emilien Le Saux

43
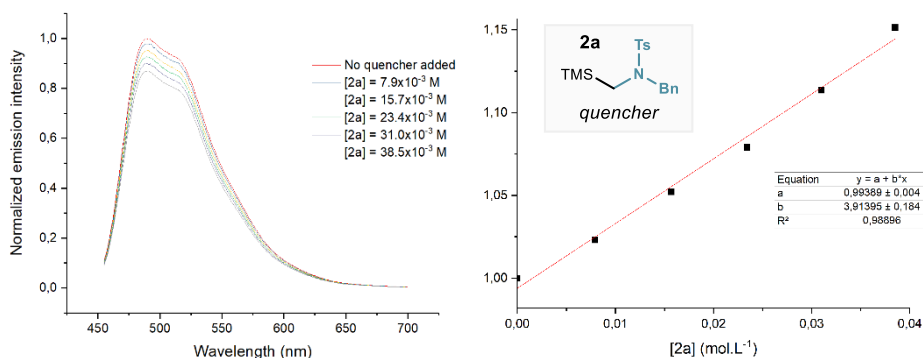
Figure 2.32. Quenching of the photocatalyst **PC-a** emission (4×10^{-6} M in DCE) in the presence of increasing amounts of tertiary amine **2a.**

These results support the excited-state role of photocatalyst **PC-a**, which likely oxidizes **2a** in a SET event, securing the generation of radicals in the reaction.

2.5.3 Proposed mechanism

Our proposed mechanism is depicted in Figure 2.33. Condensation of the chiral aminocatalyst **C** with the enal substrate **1** delivers the electrophilic ground-state iminium ion **I**. Simultaneously, SET oxidation of the radical precursor **2** by the excited state of the acridinium photocatalyst **PC-a** generates radical **II**. This SET event is supported by Stern-Volmer quenching studies ($k_q = 2.7 \cdot 10^8$ M^{-1}·s^{-1}). The ensuing radical intermediate **II** can undergo stereocontrolled conjugate addition to the iminium ion **I**, forming the 3π-radical cation **XXII**. At this stage, SET reduction of **XXII** from the reduced photocatalyst **PC-a**$^{\bullet-}$ delivers the enamine **XXIII**, which upon hydrolysis affords the enantioenriched β-functionalized product **3** and releases aminocatalyst **C**.
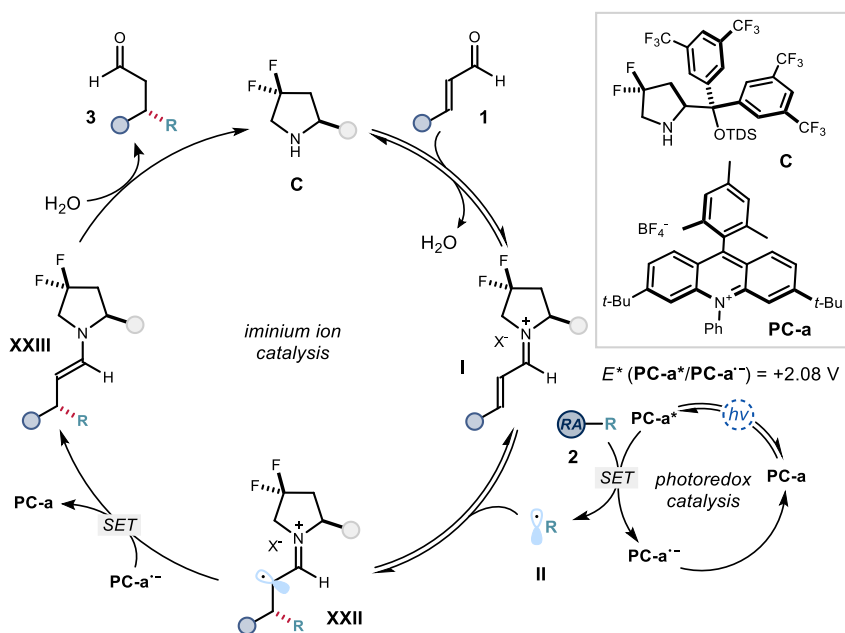
Figure 2.33. Proposed mechanism for the enantioselective radical conjugate addition to enals.

An alternative chain propagation mechanism, in which the radical precursor would be oxidized by the intermediate α-iminyl radical cation **XXII** to form the enamine **XXIII**, was also considered. Previous studies estimated the oxidation potential of the 3π-intermediates of type **XXIV**[5] to the corresponding enamine **XXV** at about +0.9 V (vs Ag$^+$/Ag in CH$_3$CN), as inferred by cyclic voltammetry studies on preformed enamines (Figure 2.34). We assumed that the redox properties of intermediate **XXV** are similar to the actual enamine intermediate **XXIII** involved in the mechanism. As shown in Figure 2.34, the α-iminyl radical cation of type **XXIV** should not be capable of oxidizing **2a**, which has a high redox potential (E (**2a**$^{•+}$/**2a**) = +1.78 V), therefore precluding a possible radical chain propagation mechanism. Additionally, we measured the quantum yield[47] of the reaction between 4-methylpent-2-enal and substrate **2a**, which was found to be as low as Φ = 0.02. This fractional value is far lower than the typical value measured for chain propagation mechanisms (Φ > 1), thus excluding this possibility.[48]

---

[47] Details about quantum yield determination can be found in the experimental section.
[48] (a) Cismesia, M. A. & Yoon, T. P. "Characterizing Chain Processes in Visible Light Photoredox Catalysis" *Chem. Sci.* **2015**, *6*, 5426; (b) Buzzetti, L.; Crisenza, G. E. M.; Melchiorre, P. "Mechanistic Studies in Photocatalysis" *Angew. Chem., Int. Ed.* **2019**, *58*, 3730.

UNIVERSITAT ROVIRA I VIRGILI
PHOTOCHEMISTRY AND ORGANOCATALYSIS FOR RADICAL-BASED CARBON-CARBON BOND-FORMING
PROCESSES
Emilien Le Saux

45
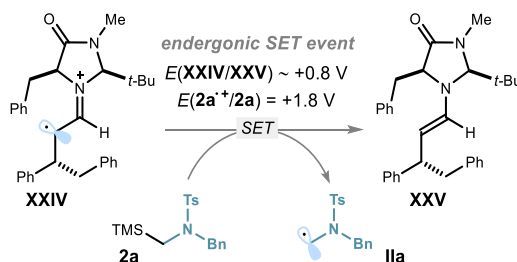
Figure 2.34. Key SET event for a possible chain mechanism.

Finally, another mechanistic scenario was considered, which is depicted in Figure 2.35. After oxidation of the radical precursor **2** by the excited photocatalyst **PC-a***, the reduced photocatalyst (E (**PC-a**/ **PC-a**$^{\bullet-}$) = -0.59 V vs SCE) could reduce the ground-state iminium ion **I** affording the chiral 5π electron intermediate **III** (E (**III/I**) = -0.38 V vs Ag/Ag$^+$). At this juncture, a radical coupling with the radical **II** generated beforehand could ensue, delivering the chiral β-alkylated enamine **XIII**. Subsequent hydrolysis of **XIII** would eventually afford the target compound **3**, and releasing the aminocatalyst **C**. In spite of the redox potentials indicating that this pathway could be thermodynamically possible, a radical coupling between **III** and **II** seems unlikely as they would be both generated in catalytic amounts (since 2.5 mol% of photocatalyst is used), and neither of them is kinetically stabilized.[6]
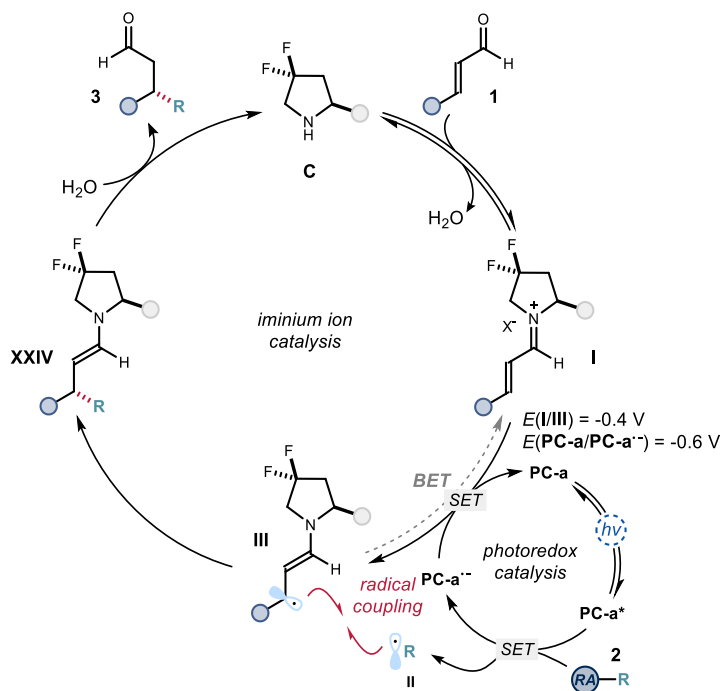
Figure 2.35. Alternative mechanism proceeding through the formation of 5π-intermediate.

2.6 Conclusions

In summary, we have developed a general iminium ion-based system for asymmetric radical conjugate additions to readily available aliphatic and aromatic enals. The method relies on an organic photoredox catalyst that generates radicals from stable precursors, in combination with highly electrophilic ground-state iminium ions, which can stereoselectively trap these open-shell intermediates. The system delivers highly enantioenriched chiral β-functionalized aldehydes, which cannot be accessed using previously reported strategies. A radical-polar crossover path exploiting the intermediacy of a chiral enamine was developed to stereoselectively synthesize complex piperidines. Mechanistic studies showed that the photocatalyst is indeed the photoactive species that oxidizes the radical precursors, although some reactivity was observed in its absence when using aromatic enals.

UNIVERSITAT ROVIRA I VIRGILI
PHOTOCHEMISTRY AND ORGANOCATALYSIS FOR RADICAL-BASED CARBON-CARBON BOND-FORMING
PROCESSES
Emilien Le Saux

47

2.7 Experimental section

General Information. The ^{1}H NMR, ^{19}F NMR, ^{13}C NMR spectra, HPLC and UPC[2] traces are available in the literature[1] and are not reported in the present dissertation.

The NMR spectra were recorded at 300 MHz, 400 MHz and 500 MHz for ^{1}H or at 75 MHz, 101 MHz and 126 MHz for ^{13}C, 376 MHz for ^{19}F, respectively. The chemical shifts (δ) for ^{1}H and [13]C{1H} are given in ppm relative to residual signals of the solvents (CHCl$_3$ @ 7.26 ppm ^{1}H NMR, 77.00 ppm ^{13}C NMR). Coupling constants are given in Hz. The following abbreviations are used to indicate the multiplicity: s, singlet; d, doublet; t, triplet; q, quartet; m, multiplet; br s, broad signal.

High-resolution mass spectra (HRMS) were obtained from the ICIQ High-Resolution Mass Spectrometry Unit on MicroTOF Focus and Maxis Impact (Bruker Daltonics) with electrospray ionization (ESI) or atmospheric pressure chemical ionization (APCI). X-ray data were obtained from the ICIQ X-Ray Unit using a Bruker-Nonius diffractometer equipped with an APPEX 2 4K CCD area detector. Optical rotations were measured on a Polarimeter Jasco P-1030 and are reported as follows: $[\alpha]_D$ ambient temperature (c in g per 100 mL, solvent). Cyclic voltammetry (CV) studies were carried out on a Princeton Applied Research PARSTAT 2273 potentiostat offering compliance voltage up to $\pm$ 100 V (available at the counter electrode), $\pm$ 10 V scan range and $\pm$ 2 A current range. UV-vis measurements were carried out on a Shimadzu UV-2401PC spectrophotometer equipped with photomultiplier detector, double beam optics and D2 and W light sources. The emission spectra were recorded using a Fluorolog Horiba Jobin Yvon spectrofluorimeter equipped with a photomultiplier detector, a double monochromator, and a 350W xenon light source.

Yield of isolated products refer to materials of > 95% purity as determined by ^{1}H NMR analysis.

General Procedures. All reactions were set up under an argon atmosphere in oven-dried glassware using standard Schlenk techniques, unless otherwise stated. Synthesis grade solvents were used as purchased. Anhydrous solvents were taken from a commercial SPS solvent dispenser. Chromatographic purification of products was accomplished using flash column chromatography (FC) on silica gel (35-70 mesh). For thin layer chromatography (TLC) analysis throughout this work, Merck precoated TLC plates (silica gel 60 GF$_{254}$, 0.25 mm) were used, using UV light as the visualizing agent and either phosphomolybdic acid in EtOH, or basic aqueous potassium permanganate (KMnO$_4$), and heat as developing agents. Organic solutions were concentrated under reduced pressure on a Büchi rotary evaporator (in vacuo at 40 ºC, ~5 mbar).

Determination of Diastereomeric Ratio. The diastereomeric ratio were determined by ^{1}H NMR analysis of the crude reaction mixture through integration of diagnostic signals.

Determination of Enantiomeric Purity. HPLC analysis on chiral stationary phase was performed on an Agilient 1200 series HPLC, using Daicel Chiralpak columns with i-PrOH/n-hexane as the eluent. UPC^2 analysis on chiral stationary phase was performed on a Waters Acquity instrument using, OJ-3, IC-3, ID-3 and IG-3 chiral columns. The exact conditions for the analyses are specified within the characterization section. HPLC and UPC^2 traces were compared to racemic samples prepared by running the reaction in the presence of a catalytic amount (20 mol%) of an approximately 1:1 mixture of (2R, 5R)- and (2S, 5S)-2-tert-butyl-3-methyl-5-benzyl-4-imidazolidinone, which are commercially available form Sigma Aldrich.

Materials. Commercial grade reagents and solvents were purchased at the highest commercial quality from Sigma Aldrich, Fluka, Acros Organics, Fluorochem, or Alfa Aesar and used as received, unless otherwise stated. The chiral secondary amine catalyst **C** was prepared according to the reported literature.[5] The photocatalyst **PC-a** was prepared according to the reported literature.[49] Some of the enal substrates **1**, including crotonaldehyde, (*E*)-4-methylpent-2-enal, (*E*)-pent-2-enal, (*E*)-oct-2-enal, and cinnamaldehyde are commercially available, and they were distilled prior to use. Other enals and radical precursors were prepared according to the literature procedures.[1]

2.7.1 Substrate synthesis

The α-silylamine **2a** was prepared following a reported procedure (Figure 2.36).
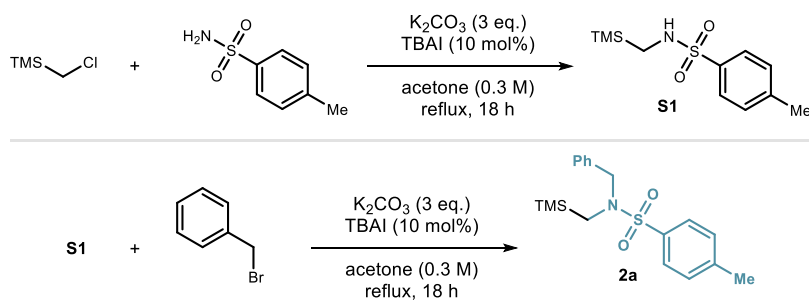
Figure 2.36. Preparation of radical precursor **2a**.

To a flame dried round bottom flask were added 4-methylbenzenesulfonamide (3.1 g, 1.2 equiv.), potassium carbonate (6.2 g, 3 equiv.) and tetrabutylammonium iodide (550 mg, 0.1 equiv.) in acetone (45 mL, 0.3 M) under atmosphere of argon. Then

[49] A. R. White, L. Wang, D. A. Nicewicz. "Synthesis and Characterization of Acridinium Dyes for Photoredox Catalysis" *Synlett*, **2019**, *30*, 827.

UNIVERSITAT ROVIRA I VIRGILI
PHOTOCHEMISTRY AND ORGANOCATALYSIS FOR RADICAL-BASED CARBON-CARBON BOND-FORMING
PROCESSES
Emilien Le Saux

49

(chloromethyl)trimethylsilane (2.1 mL, 15 mmol) was added at room temperature and the solution was refluxed in a pressure flask overnight. The solvent was removed under vacuum, the residue was dissolved in EtOAc (120 mL), washed with aqueous HCl (1.0 M, 100 mL), and brine. The organic phase was dried over magnesium sulfate, filtered and concentrated under vacuum. The crude material was purified by flash column chromatography (SiO_2, 10:90 EtOAc/hexanes) to afford **S1** (2.5 g, 9.7 mmol, 65% yield) as a white crystalline solid.

Intermediate **S1** (1.5 g, 5.8 mmol), potassium carbonate (2.4 g, 3 equiv.) and tetrabutylammonium iodide (320 mg, 0.15 equiv.) were dissolved in acetone (18 mL, 0.3 M) under an atmosphere of argon. (Bromomethyl)benzene (1.5 mL, 1.5 equiv.) was then added at room temperature and the solution was refluxed in a pressure flask overnight. After filtration, the solvent was removed under vacuum, and the crude material was purified by flash column chromatography (SiO_2, 10:90 EtOAc/hexanes) to afford **2a** (1.6 g, 4.5 mmol, 78 % yield) as a white crystalline solid.

N-benzyl-4-methyl-N-((trimethylsilyl)methyl)benzene sulfonamide (2a) ^{1}H NMR (400 MHz, $CDCl_3$) δ 7.73 – 7.68 (m, 2H), 7.36 – 7.23 (m, 5H), 4.22 (s, 2H), 2.49 (s, 2H), 2.44 (s, 3H), -0.09 (s, 9H).

^{13}C NMR (101 MHz, $CDCl_3$) δ 143.14, 136.60, 135.26, 129.57, 128.46, 128.40, 127.68, 127.65, 55.23, 39.73, 21.52, -1.62.

2.7.2 Cyclic voltammetry study of 2a

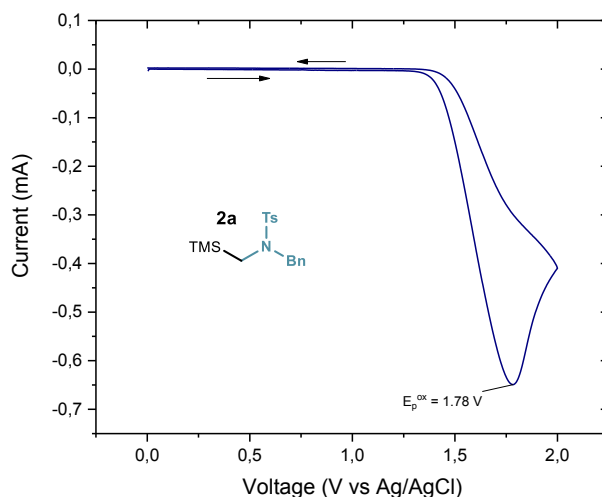**Figure 2.37.** Cyclic voltammogram of **2a** [5 mM] in [0.1 M] $TBAPF_6$ in CH_3CN. Sweep rate 100 mV.s^{-1}. Glassy carbon working electrode, Ag/AgCl reference electrode (NaCl 3 M), Pt wire auxiliary electrode. One irreversible wave observed at +1.78 V.

2.7.3 General procedure for the photochemical conjugate addition
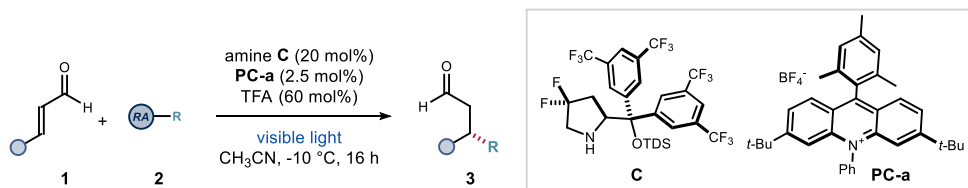
General procedure A. To an argon-purged glass vial containing the amine catalyst **C** (14.1 mg, 0.02 mmol), photocatalyst **PC-a** (1.4 mg, 2.5 μmol) and radical precursor **2** (0.1 mmol) was added enal **1** (0.2 mmol). Then, 400 μL of an argon-sparged 0.15 M acetonitrile solution of TFA (4.6 μL, 0.06 mmol) were added. The vial was sealed with Parafilm, and placed into an aluminum block on a 3D-printed holder, fitted with a 465 nm high-power single LED. The irradiance was fixed at 60 ± 2 mW/cm^2, as controlled by an external power supply and measured using a photodiode light detector at the start of each reaction. This setup secured a reliable irradiation while keeping a distance of 1 cm between the reaction vessel and the light source. The temperature was kept at -10 °C with a chiller connected to the irradiation plate (the setup is detailed in Figure 2.38). The reaction was stirred for 16 hours, then the solvent was evaporated and the crude mixture was purified by flash column chromatography on silica gel to furnish product **3**.

Figure 2.38. Detailed set-up and illumination system. The light source for illuminating the reaction vessel is a single 465 nm high-power LED.

UNIVERSITAT ROVIRA I VIRGILI
PHOTOCHEMISTRY AND ORGANOCATALYSIS FOR RADICAL-BASED CARBON-CARBON BOND-FORMING PROCESSES
Emilien Le Saux

51

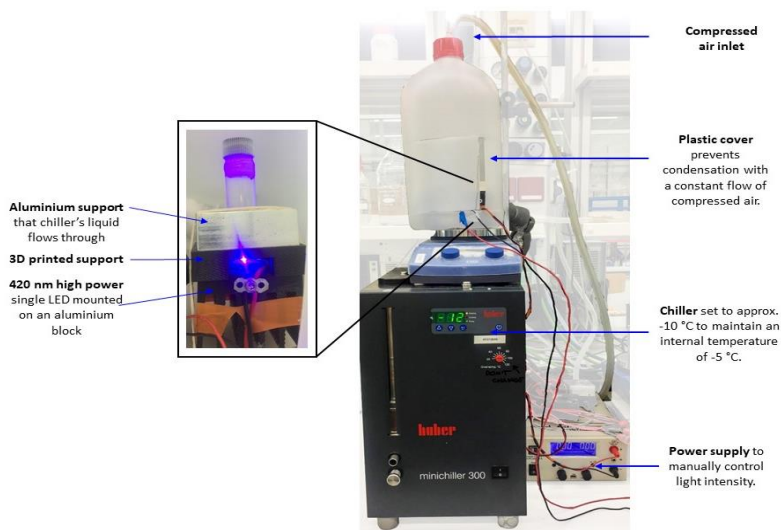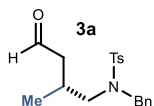## 2.7.4 Characterization of products

(S)-N-Benzyl-4-methyl-N-(2-methyl-4-oxobutyl)benzene sulfonamide (3a)

Prepared according to general procedure A using (E)-but-2-enal (16.5 µL, 0.2 mmol) and radical precursor **2a** (34.8 mg, 0.1 mmol). The crude mixture was purified by column chromatography (SiO$_2$, 5:95 to 15:85 EtOAc/hexanes) to afford product **3a** as a colorless oil (37 mg, 87% yield, average of two runs, 91% ee). The enantiomeric excess was determined by HPLC analysis on a Daicel Chiralpak IC-3 column (70:30 n-hexane/i-PrOH, 1.0 mL/min, 30 °C, λ = 230 nm: τ_{minor} = 26.3 min, τ_{major} = 36.2 min). [α]$_D^{26}$ = -15.7 (c = 0.77, CHCl$_3$, 91% ee).

<u>^{1}H NMR</u> (400 MHz, CDCl$_3$) δ 9.47 (dd, J = 2.0, 1.2 Hz, 1H), 7.75 – 7.69 (m, 2H), 7.37 – 7.33 (m, 2H), 7.33 – 7.24 (m, 5H), 4.39 (d, J = 14.8 Hz, 1H), 4.17 (d, J = 14.8 Hz, 1H), 3.08 (dd, J = 13.8, 8.3 Hz, 1H), 2.86 (dd, J = 13.9, 6.1 Hz, 1H), 2.46 (m, 4H), 2.13 – 2.02 (m, 2H), 0.79 (d, J = 6.4 Hz, 3H).

<u>^{13}C NMR</u> (101 MHz, CDCl$_3$) δ 201.80, 143.65, 136.42, 136.38, 129.93, 129.83, 128.75, 128.72, 128.13, 127.41, 54.92, 53.79, 48.03, 27.09, 21.66, 17.85.

<u>HRMS</u> (ESI$^+$) Calculated for C$_{23}$H$_{31}$NNaO$_3$S [M+Na]$^+$: 424.1917, found: 424.1918.

Note: 40% of the initial catalyst C could be isolated (as the corresponding TFA salt) after completion of the reaction.

(S)-N-Benzyl-N-(2-isopropyl-4-oxobutyl)-4-methylbenzene sulfonamide (3b)

Prepared according to general procedure A using (E)-4-methylpent-2-enal (23.3 µL, 0.2 mmol) and radical precursor **2a** (34.8 mg, 0.1 mmol). The crude mixture was purified by column chromatography (SiO$_2$, 10:90 EtOAc/hexanes) to afford product **3b** as a colorless oil (30 mg, 80% yield, average of two runs, 97% ee). The enantiomeric excess was determined by UPC^2 analysis on a Daicel Chiralpak IC-3 column (gradient: 1 min 100% CO$_2$; 5 min from 100% CO$_2$ to 60% CO$_2$ - 40% i-PrOH; flow rate 3.0 mL/min; λ = 229 nm: τ_{minor} = 4.8 min, τ_{major} = 5.4 min). [α]$_D^{26}$ = -14.2 (c = 0.7, CHCl3, 97% ee).

<u>^{1}H NMR</u> (500 MHz, CDCl$_3$) δ 9.43 (t, J = 1.8 Hz, 1H), 7.71 – 7.65 (m, 2H), 7.31 (d, J = 8.0 Hz, 2H), 7.29 – 7.21 (m, 5H), 4.28 (d, J = 14.8 Hz, 1H), 4.19 (d, J = 14.8 Hz, 1H), 3.03 – 2.93 (m, 2H), 2.43 (s, 3H), 2.29 – 2.17 (m, 2H), 1.90 (dq, J = 10.4, 6.8 Hz, 1H), 1.67 (pd, J = 6.9, 3.7 Hz, 1H), 0.67 (d, J = 6.8 Hz, 3H), 0.62 (d, J = 6.9 Hz, 3H).

<u>^{13}C NMR</u> (126 MHz, CDCl$_3$) δ 202.57, 143.85, 136.81, 136.56, 130.17, 129.07, 128.94, 128.30, 127.66, 54.01, 51.40, 42.90, 36.97, 28.10, 21.88, 19.86, 18.20.

<u>HRMS</u> (ESI⁺) Calculated for $C_{21}H_{27}NNaO_3S$ [M+Na]⁺: 396.1604, found: 396.1599.

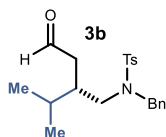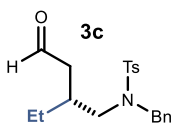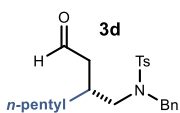**(R)-N-benzyl-N-(2-ethyl-4-oxobutyl)-4-methylbenzene sulfonamide (3c)**

Prepared according to general procedure A using (E)-pent-2-enal (23.2 μL, 0.2 mmol) and radical precursor **2a** (34.8 mg, 0.1 mmol). The crude mixture was purified by column chromatography (SiO₂, 10:90 EtOAc/hexanes) to afford product **3c** as a colorless oil (22.0 mg, 61%, average of two runs, 95% ee). The enantiomeric excess was determined by HPLC analysis on a Daicel Chiralpak ID-3 column (20:80 n-hexane:i-PrOH, 0.6 mL/min, 20 °C, λ = 215 nm: τ_{minor} = 39.8 min, τ_{major} = 41.4 min). $[\alpha]_D^{26}$ = -8.3 (c = 0.34, CHCl₃, 95% ee).

<u>¹H NMR</u> (500 MHz, CDCl₃) δ 9.47 – 9.44 (m, 1H), 7.70 (d, J = 8.3 Hz, 2H), 7.33 (d, J = 8.0 Hz, 2H), 7.31 – 7.25 (m, 4H), 4.26 (dd, J = 43.0, 14.8 Hz, 2H), 2.99 (ddd, J = 20.1, 13.8, 7.5 Hz, 2H), 2.45 (s, 3H), 2.39 (ddd, J = 17.2, 5.6, 1.3 Hz, 1H), 2.20 (ddd, J = 17.2, 7.0, 2.1 Hz, 1H), 1.86 (dp, J = 12.8, 6.5 Hz, 1H), 1.34 – 1.26 (m, 1H), 1.15 (tt, J = 14.3, 7.3 Hz, 1H), 0.68 (t, J = 7.5 Hz, 3H);

<u>¹³C NMR</u> (126 MHz, CDCl₃) δ 202.40, 143.87, 136.72, 136.55, 130.17, 129.02, 128.97, 128.35, 127.66, 54.10, 53.28, 45.91, 33.57, 25.00, 21.91, 11.25;

<u>HRMS</u> (ESI⁺) Calculated for $C_{20}H_{25}NNaO_3S^+$ [M+Na]⁺: 382.1453; found: 382.1446.

(R)-N-benzyl-4-methyl-N-(2-(2-oxoethyl)heptyl)benzene sulfonamide (3d)

Prepared according to general procedure A using (E)-oct-2-enal (29.8 μL, 0.2 mmol) and radical precursor **2a** (34.8 mg, 0.1 mmol). The crude mixture was purified by column chromatography (SiO₂, 10:90 EtOAc/hexanes) to afford product **3d** as a colorless oil (24 mg, 59% yield, average of two runs, 93%ee). The enantiomeric excess was determined by HPLC analysis on a Daicel Chiralpak IC-3 column (70:30 n-hexane:i-PrOH, 1.0 mL/min, 20 °C, λ = 230 nm: τ_{minor} = 28.5 min, τ_{major} = 49.4 min). $[\alpha]_D^{26}$ = -19.1 (c = 0.64, CHCl₃, 93% ee).

<u>¹H NMR</u> (500 MHz, CDCl₃) δ 9.43 (dd, J = 2.2, 1.4 Hz, 1H), 7.71 – 7.66 (m, 2H), 7.34 – 7.30 (m, 2H), 7.30 – 7.22 (m, 5H), 4.31 (d, J = 14.8 Hz, 1H), 4.17 (d, J = 14.7 Hz, 1H), 3.04 (dd, J = 13.8, 8.9 Hz, 1H), 2.91 (dd, J = 13.8, 6.2 Hz, 1H), 2.43 (s, 3H), 2.42 – 2.34 (m, 1H), 2.18 (ddd, J = 17.2, 7.0, 2.2 Hz, 1H), 1.95 – 1.81 (m, 1H), 1.22 – 1.12 (m, 3H), 1.10 – 0.99 (m, 4H), 0.81 (t, J = 7.3 Hz, 3H).

<u>¹³C NMR</u> (126 MHz, CDCl₃) δ 202.22, 143.64, 136.51, 136.36, 129.94, 128.80, 128.75, 128.12, 127.43, 53.89, 53.42, 46.13, 32.09, 31.93, 31.87, 26.39, 22.59, 21.66, 14.12.

UNIVERSITAT ROVIRA I VIRGILI
PHOTOCHEMISTRY AND ORGANOCATALYSIS FOR RADICAL-BASED CARBON-CARBON BOND-FORMING
PROCESSES
Emilien Le Saux

53

HRMS (ESI$^+$) Calculated for $C_{23}H_{31}NNaO_3S$ [M+Na]$^+$: 424.1917, found: 424.1918.
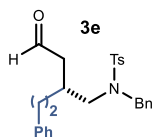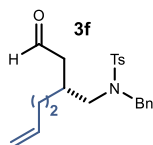
c(R)-N-benzyl-4-methyl-N-(4-oxo-2-phenethylbutyl)benzene sulfonamide (3e)

Prepared according to general procedure A using enal **1e** (32.0 mg, 0.2 mmol) and radical precursor **2a** (34.8 mg, 0.1 mmol). The crude mixture was purified by column chromatography (SiO$_2$, 10:90 EtOAc/hexanes) to afford product **3e** as a colorless oil (35.0 mg, 81% yield, average of two runs, 90% ee). The enantiomeric excess was determined by HPLC analysis on a Daicel Chiralpak ID-3 column (70:30 n-hexane:i-PrOH, 1.0 mL/min, 20 °C, $\lambda = 215$ nm: $\tau_{minor} = 19.6$ min, $\tau_{major} = 21.3$ min). [α]$_D^{26}$ = -2.1 (c = 0.29, CHCl$_3$, 90% ee).

^{1}H NMR (500 MHz, CDCl$_3$) δ 9.38 – 9.35 (m, 1H), 7.67 (d, J = 8.3 Hz, 126H), 7.34 – 7.28 (m, J = 6.3 Hz, 2H), 7.26 – 7.24 (m, J = 2.3, 1.7 Hz, 1H), 7.24 – 7.21 (m, J = 2.3, 1.7 Hz, 3H), 7.20 – 7.12 (m, 4H), 7.03 – 6.97 (m, 2H), 4.28 (d, J = 14.8 Hz, 68H), 4.13 (d, J = 15.0 Hz, 1H), 3.02 (ddd, J = 20.1, 13.7, 7.6 Hz, 2H), 2.60 – 2.50 (m, 1H), 2.43 (s, 3H), 2.42 – 2.35 (m, 2H), 2.33 – 2.21 (m, 2H), 1.96 (dp, J = 19.1, 6.4 Hz, 1H), 1.53 – 1.48 (m, 1H), 1.48 – 1.38 (m, 1H);

^{13}C NMR (126 MHz, CDCl$_3$) δ 202.05, 143.91, 141.80, 136.66, 136.53, 130.20, 129.01, 128.78, 128.61, 128.35, 127.65, 126.32, 54.03, 53.48, 46.21, 33.86, 33.21, 31.78, 21.91

HRMS (ESI$^+$) Calculated for $C_{26}H_{30}NO_3S$ [M+H]$^+$: 436.01946; found: 436.1940.

(R)-N-benzyl-4-methyl-N-(2-(2-oxoethyl)hept-6-en-1-yl)benzene sulfonamide (3f)

Prepared according to general procedure A using enal **1f** (24.8 mg, 0.2 mmol) and radical precursor **2a** (34.8 mg, 0.1 mmol). The crude mixture was purified by column chromatography (SiO$_2$, 10:90 EtOAc/hexanes) to afford product **3f** as a colorless oil (36.0 mg, 89% yield, average of two runs, 91% ee). The enantiomeric excess was determined by UPC^2 analysis on a Daicel Chiralpak IC-3 column (gradient: 1 min 100% CO$_2$; 5 min from 100% CO$_2$ to 60% CO$_2$ - 40% CH$_3$CN; flow rate 2.0 mL/min; λ = 230 nm: τ_{minor} = 4.3 min, τ_{major} = 4.6 min). [α]$_D^{26}$ = -20.3 (c = 0.45, CHCl$_3$, 91% ee).

^{1}H NMR (500 MHz, CDCl$_3$) δ 9.43 (dd, J = 2.0, 1.4 Hz, 1H), 7.67 (s, 2H), 7.31 (d, J = 7.9 Hz, 2H), 7.29 – 7.21 (m, 5H), 5.66 (ddt, J = 17.0, 10.3, 6.7 Hz, 1H), 4.94 – 4.89 (m, 1H), 4.89 – 4.87 (m, 1H), 4.24 (dd, J = 74.0, 14.8 Hz, 2H), 2.97 (ddd, J = 19.9, 13.8, 7.6 Hz, 2H), 2.47 – 2.37 (m, 4H), 2.18 (ddd, J = 17.3, 7.0, 2.1 Hz, 1H), 1.98 – 1.79 (m, 3H), 1.23 – 1.12 (m, 2H), 1.11 – 1.01 (m, 2H).

^{13}C NMR (126 MHz, CDCl$_3$) δ 202.25, 143.90, 138.67, 136.72, 136.54, 130.19, 129.04, 129.00, 128.39, 127.67, 115.06, 54.18, 53.59, 46.31, 33.96, 32.07, 31.84, 26.25, 21.91.

HRMS (ESI$^+$) Calculated for $C_{23}H_{30}NO_3S$ [M+H]$^+$: 400.1946; found: 400.1944.
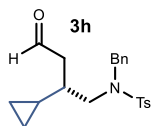
3g
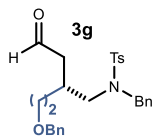
(R)-N-benzyl-N-(6-(benzyloxy)-2-(2-oxoethyl)hexyl)-4-methylbenzenesulfonamide (3g)

Prepared according to general procedure A using enal **1g** (43.7 mg, 0.2 mmol) and radical precursor **2a** (34.8 mg, 0.1 mmol). The crude mixture was purified by column chromatography (SiO$_2$, 10:90 EtOAc/hexanes) to afford product **3g** as colorless oil (27.4 mg, 56% yield, 89% ee). The enantiomeric excess was determined by UPC^2 analysis on a Daicel Chiralpak IC-3 column (gradient: 1 min 100% CO$_2$; 5 min from 100% CO$_2$ to 60% CO$_2$ - 40% CH$_3$CN; flow rate 2.0 mL/min; λ = 231 nm: τ_{minor} = 5.4, τ_{major} = 5.7 min,). [α]$_D^{26}$ = -14.7 (c = 0.85, CHCl$_3$, 89% ee).

^{1}H NMR (400 MHz, CDCl$_3$) δ 9.44 (t, J = 2.0 Hz, 1H), 7.69 (d, J = 8.3 Hz, 2H), 7.36 – 7.29 (m, 7H), 7.29 – 7.24 (m, 5H), 4.46 (s, 2H), 4.32 (d, J = 14.8 Hz, 1H), 4.17 (d, J = 14.8 Hz, 1H), 3.36 (t, J = 6.4 Hz, 2H), 3.05 (dd, J = 13.8, 8.9 Hz, 1H), 2.92 (dd, J = 13.8, 6.2 Hz, 1H), 2.47 – 2.36 (m, 4H), 2.20 (ddd, J = 17.3, 6.9, 2.1 Hz, 1H), 1.97 – 1.86 (m, 1H), 1.48 – 1.39 (m, 2H), 1.24 – 1.04 (m, 4H).

^{13}C NMR (101 MHz, CDCl$_3$) δ 201.9, 143.5, 138.5, 136.3, 136.1, 129.8, 128.6, 128.6, 128.3, 128.0, 127.6, 127.5, 127.3, 72.8, 69.9, 53.8, 53.2, 45.9, 31.8, 31.7, 29.6, 23.3, 21.5.

HRMS (ESI$^+$) Calculated for $C_{29}H_{36}NO_4S^+$ [M+H]$^+$: 494.2360; found: 494.2365.

3h

(S)-N-benzyl-N-(2-cyclopropyl-4-oxobutyl)-4-methylbenzenesulfonamide (3h)

Prepared according to general procedure A using enal **1h** (19.4 mg, 0.2 mmol) and radical precursor **2a** (34.8 mg, 0.1 mmol). The crude mixture was purified by column chromatography (SiO$_2$, 10:90 EtOAc/hexanes) to afford product **3h** as a yellowish oil (27.1 mg, 73% yield, average of two runs, 92% ee). The enantiomeric excess was determined by UPC^2 analysis on a Daicel Chiralpak IC-3 column (gradient: 1 min 100% CO$_2$, 5 min from 100% CO$_2$ to 60% CO$_2$ - 40% CH$_3$CN; flow rate 2.0 mL/min, λ = 351 nm: τ_{minor} = 4.6 min, τ_{major} = 4.8 min). [α]$_D^{26}$ = -2.6 (c = 0.21, CHCl$_3$, 92% ee).

^{1}H NMR (500 MHz, CDCl$_3$) δ 9.46 (dd, J = 2.9, 1.3 Hz, 1H), 7.72 – 7.67 (m, 2H), 7.34 – 7.30 (m, 2H), 7.28 – 7.24 (m, 2H), 7.19 (dt, J = 6.4, 2.3 Hz, 2H), 4.39 (d, J = 14.5 Hz, 1H), 4.09 (d, J = 14.5 Hz, 1H), 3.28 (dd, J = 14.2, 10.2 Hz, 1H), 2.96 (dd, J = 14.2, 4.8 Hz, 1H), 2.55 (ddd, J = 16.5, 4.7, 1.3 Hz, 1H), 2.43 (s, 3H), 2.26 (ddd, J = 16.5, 7.8, 2.9 Hz, 1H), 1.11 (dtd, J = 12.5, 9.7, 4.8 Hz, 1H), 0.36 – 0.30 (m, 2H), -0.12 (td, J = 4.7, 1.3 Hz, 2H).

^{13}C NMR (126 MHz, CDCl$_3$) δ 202.34, 143.88, 136.56, 136.41, 130.16, 129.21, 128.98, 128.46, 127.71, 77.64, 77.38, 77.13, 54.25, 53.50, 46.97, 38.94, 21.89, 14.34, 4.60, 4.38.

UNIVERSITAT ROVIRA I VIRGILI
PHOTOCHEMISTRY AND ORGANOCATALYSIS FOR RADICAL-BASED CARBON-CARBON BOND-FORMING
PROCESSES
Emilien Le Saux

55

HRMS (ESI$^+$) Calculated for C$_{21}$H$_{25}$NNaO$_3$S$^+$ [M+Na]$^+$: 394.1447; found: 394.1445.

(S)-N-benzyl-4-methyl-N-(4-oxo-2-phenylbutyl)benzene **sulfonamide (3i)**

Prepared according to general procedure A using (E)-cinnamaldehyde (25.2 uL, 0.2 mmol) and radical precursor **2a** (34.8 mg, 0.1 mmol). The crude mixture was purified by column chromatography (SiO$_2$, 10:90 EtOAc/hexanes) to afford product **3i** as a colorless oil (32.0 mg, 79%, average of two runs, 96% ee). The enantiomeric excess was determined by HPLC analysis on a Daicel Chiralpak IC-3 column (70:30 n-hexane/i-PrOH, 1.0 mL/min, 20 °C, λ = 215 nm: τ$_{major}$ = 24.7 min, τ$_{minor}$ = 27.6 min). [α]$_D^{26}$ = -35.0 (c = 0.97, CHCl$_3$, 96% ee).

^{1}H NMR (500 MHz, CDCl$_3$) δ 9.43 (dd, J = 2.2, 1.1 Hz, 1H), 7.69 – 7.65 (m, 2H), 7.32 – 7.26 (m, 5H), 7.25 – 7.16 (m, 5H), 7.01 – 6.94 (m, 2H), 4.19 (dd, J = 93.3, 14.7 Hz, 2H), 3.49 (dd, J = 14.1, 9.5 Hz, 1H), 3.21 (ddd, J = 14.9, 9.5, 5.6 Hz, 1H), 3.00 (dd, J = 14.1, 6.1 Hz, 1H), 2.86 (ddd, J = 17.3, 4.9, 1.1 Hz, 1H), 2.60 (ddd, J = 17.3, 9.5, 2.3 Hz, 1H), 2.43 (s, 3H).

^{13}C NMR (126 MHz, CDCl$_3$) δ 201.08, 143.83, 141.02, 136.60, 136.12, 130.08, 129.06, 129.04, 128.99, 128.42, 127.92, 127.58, 127.48, 54.36, 53.73, 46.93, 39.09, 21.80;

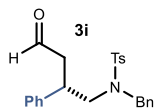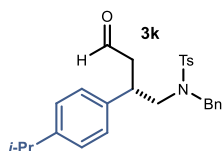HRMS (ESI$^+$) Calculated for C$_{24}$H$_{25}$NNaO$_3$S$^+$ [M+Na]$^+$: 430.1453; found: 430.1437.

(S)-N-benzyl-N-(2-(4-isopropylphenyl)-4-oxobutyl)-4-methyl benzenesulfonamide (3k)

Prepared according to general procedure A using enal **1k** (34.8 mg, 0.2 mmol) and radical precursor **2a** (34.8 mg, 0.1 mmol). The crude mixture was purified by column chromatography (SiO$_2$, 10:90 EtOAc/hexanes) to afford product **3k** as a colorless oil (33.8 mg, 75%, average of two runs, 92% ee). The enantiomeric excess was determined by HPLC analysis on a Daicel Chiralpak IC-3 (70:30 n-hexane/i-PrOH, 1.0 mL/min, 20 °C, λ = 215 nm: τ$_{minor}$ = 48.4 min, τ$_{major}$ = 66.9 min). [α]$_D^{26}$ = -56.8 (c = 0.65, CHCl$_3$, 96% ee).

^{1}H NMR (500 MHz, CDCl$_3$) δ 9.48 – 9.35 (m, 1H), 7.68 (d, J = 8.3 Hz, 2H), 7.33 – 7.26 (m, J = 5.9, 2.5 Hz, 5H), 7.19 – 7.16 (m, 2H), 7.08 (d, J = 8.1 Hz, 2H), 6.89 (d, J = 8.2 Hz, 2H), 4.20 (dd, J = 111.0, 14.7 Hz, 2H), 3.48 (dd, J = 14.1, 9.8 Hz, 1H), 3.26 – 3.12 (m, 1H), 2.98 (dd, J = 14.1, 5.8 Hz, 1H), 2.91 – 2.81 (m, 2H), 2.58 (ddd, J = 17.2, 9.6, 2.4 Hz, 1H), 2.43 (s, 4H), 1.20 (d, J = 6.9 Hz, 6H).

^{13}C NMR (126 MHz, CDCl$_3$) δ 201.00, 147.67, 143.40, 137.84, 136.24, 135.78, 129.66, 128.65, 128.57, 128.00, 127.40, 127.20, 126.68, 54.08, 53.32, 46.51, 38.31, 33.55, 23.82, 23.81, 21.40.

<u>HRMS</u> (ESI$^+$) Calculated for $C_{27}H_{31}NNaO_3S^+$ [M+Na]$^+$: 472.1922; found: 472.1901.

(S)-N-benzyl-4-methyl-N-(4-oxo-2-(4-(trifluoromethyl) phenyl)butyl) benzenesulfonamide (3l)

Prepared according to general procedure A using enal **1l** (40.0 mg, 0.2 mmol) and radical precursor **2a** (34.8 mg, 0.1 mmol). The crude mixture was purified by column chromatography (SiO$_2$, 10:90 EtOAc/hexanes) to afford product **3l** as a colorless oil (41.5 mg, 87%, average of two runs, 87% ee). The enantiomeric excess was determined by UPC^2 analysis on a Daicel Chiralpak ID-3 column (gradient: 1 min 100% CO$_2$; 5 min from 100% CO$_2$ to 60% CO$_2$ - 40% *i*-PrOH; flow rate 3.0 mL/min, λ = 230 nm: τ_{minor} = 3.9 min, τ_{major} = 4.0 min). $[\alpha]_D^{26}$ = -51.4 (c = 0.67, CHCl$_3$, 87% ee).

^{1}H NMR (500 MHz, CDCl$_3$) δ 9.48 (s, 1H), 7.66 (d, *J* = 8.3 Hz, 2H), 7.44 (d, *J* = 8.1 Hz, 2H), 7.34 – 7.26 (m, 5H), 7.15 (dd, *J* = 7.6, 1.8 Hz, 2H), 7.05 (d, *J* = 8.1 Hz, 2H), 4.34 (d, *J* = 14.5 Hz, 1H), 4.04 (d, *J* = 14.5 Hz, 1H), 3.43 (dd, *J* = 14.0, 8.8 Hz, 1H), 3.32 (ddd, *J* = 14.3, 8.8, 6.4 Hz, 1H), 3.04 (dd, *J* = 13.9, 6.6 Hz, 1H), 2.88 (ddd, *J* = 17.7, 5.2, 0.7 Hz, 1H), 2.63 (ddd, *J* = 17.8, 8.9, 1.8 Hz, 1H), 2.43 (s, 3H).

^{13}C NMR (126 MHz, CDCl$_3$) δ 200.24, 145.31, 144.15, 136.17, 135.96, 130.24, 129.86, 129.61, 129.14, 128.63, 128.43, 127.70, 125.98, 125.47, 54.11, 47.14, 38.89, 21.89.

<u>HRMS</u> (ESI$^+$) Calculated for $C_{25}H_{24}F_3NNaO_3S^+$ [M+Na]$^+$: 498.1327; found: 498.1320.

(S)-N-benzyl-4-methyl-N-(4-oxo-2-(4-(trimethylsilyl)phenyl) butyl)benzenesulfonamide (3m)

Prepared according to general procedure A using enal **1m** (40.9 mg, 0.2 mmol) and radical precursor **2a** (34.8 mg, 0.1 mmol). The crude mixture was purified by column chromatography (SiO$_2$, 10:90 EtOAc/hexanes) to afford product **3m** as yellowish oil (44.7 mg, 93% yield, 90% ee). The enantiomeric excess was determined by UPC^2 analysis on a Daicel Chiralpak IB-3 column (gradient: 1 min 100% CO$_2$; 5 min from 100% CO$_2$ to 60% CO$_2$ - 40% CH$_3$CN; flow rate 2.0 mL/min; λ = 223 nm: τ_{minor} = 3.7, τ_{major} = 3.9 min,). $[\alpha]_D^{26}$ = -57.5 (c = 1.1, CHCl$_3$, 90% ee).

^{1}H NMR (400 MHz, CDCl$_3$) δ 9.44 (dd, *J* = 2.3, 1.1 Hz, 1H), 7.70 – 7.65 (m, 2H), 7.40 – 7.35 (m, 2H), 7.32 – 7.27 (m, 5H), 7.21 – 7.15 (m, 2H), 6.99 – 6.92 (m, 2H), 4.34 (d, *J* = 14.6 Hz, 1H), 4.08 (d, *J* = 14.6 Hz, 1H), 3.49 (dd, *J* = 14.0, 9.8 Hz, 1H), 3.20 (tt, *J* = 9.8, 5.3 Hz, 1H), 2.99 (dd, *J* = 14.0, 5.8 Hz, 1H), 2.88 (ddd, *J* = 17.3, 4.8, 1.2 Hz, 1H), 2.61 (ddd, *J* = 17.3, 9.5, 2.3 Hz, 1H), 2.43 (s, 3H), 0.23 (s, 9H).

^{13}C NMR (101 MHz, CDCl$_3$) δ 200.9, 143.5, 141.2, 139.2, 136.2, 135.8, 133.8, 129.8, 128.8, 128.7, 128.1, 127.3, 127.0, 54.1, 53.5, 46.5, 38.7, 21.5, -1.2.

UNIVERSITAT ROVIRA I VIRGILI
PHOTOCHEMISTRY AND ORGANOCATALYSIS FOR RADICAL-BASED CARBON-CARBON BOND-FORMING
PROCESSES
Emilien Le Saux

57

HRMS (ESI$^+$) Calculated for $C_{27}H_{34}NO_3SSi^+$ [M+H]$^+$: 480.2023; found: 480.2023.
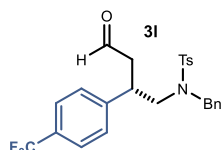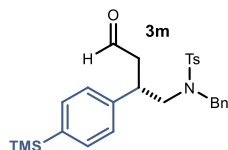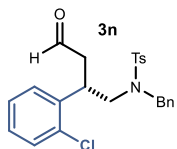
(S)-N-benzyl-N-(2-(2-chlorophenyl)-4-oxobutyl)-4-methyl benzenesulfonamide (3n)

Prepared according to general procedure A using enal **1n** (33.2 mg, 0.2 mmol) and radical precursor **2a** (34.8 mg, 0.1 mmol). The crude mixture was purified by column chromatography (SiO$_2$, 10:90 EtOAc/hexanes) to afford product **3n** as an off-white solid (35.5 mg, 80%, average of two runs, 93% ee). The enantiomeric excess was determined by HPLC analysis on a Daicel Chiralpak ID-3 column (70:30 n-hexane/i-PrOH, 1.0 mL/min, 20 °C, λ = 215 nm: τ_{major} = 29.5 min, τ_{minor} = 33.8 min). [α]$_D^{26}$ = -34.6 (c = 0.90, CHCl$_3$, 93% ee).

^{1}H NMR (500 MHz, CDCl$_3$) δ 9.33 (dd, J = 2.5, 0.8 Hz, 1H), 7.67 – 7.64 (m, 2H), 7.32 – 7.26 (m, 8H), 7.21 – 7.08 (m, 3H), 4.52 (d, J = 15.0 Hz, 1H), 4.09 (d, J = 15.0 Hz, 1H), 3.91 – 3.73 (m, 1H), 3.45 (dd, J = 13.9, 10.1 Hz, 1H), 3.12 (dd, J = 13.9, 5.5 Hz, 1H), 2.94 (ddd, J = 17.4, 5.0, 0.9 Hz, 1H), 2.68 (ddd, J = 17.4, 9.5, 2.6 Hz, 1H), 2.42 (s, 3H).

^{13}C NMR (126 MHz, CDCl$_3$) δ 200.77, 143.94, 138.19, 136.62, 136.37, 134.37, 130.34, 130.19, 129.01, 129.00, 128.72, 128.46, 127.71, 127.62, 53.79, 53.28, 46.03, 21.89.

HRMS (ESI$^+$) Calculated for $C_{24}H_{24}ClNNaO_3S$: 464.1058; found: 464.1059.
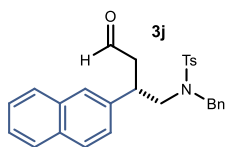
(S)-N-benzyl-4-methyl-N-(2-(naphthalen-2-yl)-4-oxobutyl)benzenesulfonamide (3j)

Prepared according to general procedure A using enal **1j** (36.4 mg, 0.02 mmol) and radical precursor **2a** (34.8 mg, 0.1 mmol). The crude mixture was purified by column chromatography (SiO$_2$, 10:90 EtOAc/hexanes) to afford product **3j** as an off-white solid (32.0 mg, 70%, average of two runs, 90% ee). The enantiomeric excess was determined by UPC^2 analysis on a Daicel Chiralpak IC-3 column (gradient: 1 min 100% CO$_2$; 5 min from 100% CO$_2$ to 60% CO$_2$ - 40% CH$_3$CN; flow rate 3.0 mL/min; λ = 223 nm: τ_{minor} = 5.4, τ_{major} = 5.6 min,). [α]$_D^{26}$ = -70.8 (c = 0.45, CHCl$_3$, 90% ee).

^{1}H NMR (500 MHz, CDCl$_3$) δ 9.48 (dd, J = 2.1, 1.2 Hz, 1H), 7.77 (dd, J = 6.5, 2.7 Hz, 1H), 7.72 (d, J = 8.6 Hz, 1H), 7.70 – 7.67 (m, 1H), 7.66 – 7.62 (m, 2H), 7.48 – 7.40 (m, 2H), 7.35 (s, 1H), 7.30 – 7.27 (m, 3H), 7.23 (d, J = 8.0 Hz, 2H), 7.20 (dd, J = 6.5, 3.0 Hz, 2H), 7.11 (dd, J = 8.5, 1.8 Hz, 1H), 4.21 (dd, J = 82.6, 14.7 Hz, 2H), 3.56 (dd, J = 14.1, 8.9 Hz, 1H), 3.47 – 3.29 (m, 1H), 3.14 (dd, J = 14.1, 6.6 Hz, 1H), 2.90 (ddd, J = 17.4, 5.1, 1.1 Hz, 1H), 2.72 (ddd, J = 17.4, 9.3, 2.2 Hz, 1H), 2.40 (s, 3H).

^{13}C NMR (126 MHz, CDCl$_3$) δ 200.76, 143.63, 138.25, 136.50, 135.97, 133.51, 132.72, 129.88, 128.91, 128.82, 128.69, 128.27, 127.80, 127.73, 127.39, 126.73, 126.35, 126.00, 125.61, 54.09, 53.54, 46.92, 39.01, 21.64.

HRMS (ESI$^+$) Calculated for C$_{28}$H$_{27}$NNaO$_3$S$^+$ [M+Na]$^+$: 480.1604; found: 480.1605.

(S)-N-(2-(benzo[b]thiophen-6-yl)-4-oxobutyl)-N-benzyl-4-methyl benzenesulfonamide (3o)

Prepared according to general procedure A using enal **1o** (37.6 mg, 0.02 mmol) and radical precursor **2a** (34.8 mg, 0.1 mmol). The crude mixture was purified by column chromatography (SiO$_2$, 10:90 EtOAc/hexanes) to afford product **3o** as a pale-yellow solid (19.0 mg, 40%, average of two runs, 87% ee). The enantiomeric excess was determined by UPC^2 analysis on a Daicel Chiralpak ID-3 column (gradient: 1 min 100% CO$_2$; 5 min from 100% CO$_2$ to 60% CO$_2$ - 40% i-PrOH; flow rate 3.0 mL/min; λ = 225 nm: τ_{minor} = 6.3 min, τ_{major} = 6.4 min). [α]$_D^{26}$ = -65.6 (c = 0.29, CHCl$_3$, 87% ee).

^{1}H NMR (500 MHz, CDCl$_3$) δ 9.44 (dd, J = 2.1, 1.1 Hz, 1H), 7.69 – 7.59 (m, 3H), 7.38 (d, J = 5.4 Hz, 1H), 7.35 – 7.32 (m, 1H), 7.29 – 7.26 (m, 3H), 7.26 – 7.25 (m, 2H), 7.24 – 7.23 (m, 1H), 7.22 – 7.12 (m, J = 6.6, 2.9 Hz, 2H), 6.97 (dd, J = 8.2, 1.6 Hz, 1H), 4.17 (dd, J = 78.3, 14.6 Hz, 2H), 3.52 (dd, J = 14.1, 8.8 Hz, 1H), 3.40 – 3.29 (m, 1H), 3.07 (dd, J = 14.1, 6.7 Hz, 1H), 2.86 (ddd, J = 17.3, 5.1, 1.1 Hz, 1H), 2.65 (ddd, J = 17.4, 9.3, 2.2 Hz, 1H), 2.40 (s, 3H).

^{13}C NMR (126 MHz, CDCl$_3$) δ 200.71, 143.67, 140.29, 138.88, 137.08, 136.54, 135.97, 129.91, 128.89, 128.83, 128.29, 127.39, 126.63, 124.03, 123.99, 123.62, 121.66, 54.27, 53.58, 47.14, 38.97, 21.66.

HRMS (ESI$^+$) Calculated for C$_{26}$H$_{26}$NO$_3$S$_2$$^+$ [M+H]$^+$: 464.1349; found: 464.1345
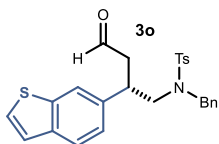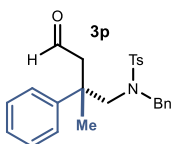
(S)-N-benzyl-4-methyl-N-(2-methyl-4-oxo-2-phenylbutyl) benzenesulfonamide (3p)

Prepared according to general procedure A using enal **1p** (29.2 mg, 0.2 mmol) and radical precursor **2a** (34.8 mg, 0.1 mmol). The crude mixture was purified by column chromatography (SiO$_2$, 10:90 EtOAc/hexanes) to afford product **3p** as a colorless oil (26.0 mg, 60%, average of two runs, 64% ee). The enantiomeric excess was determined by UPC^2 analysis on a Daicel Chiralpak ID-3 column (gradient: 1 min 100% CO$_2$, 5 min from 100% CO$_2$ to 60% CO$_2$ - 40% i-PrOH, flow rate 3.0 mL/min; λ = 225 nm: τ_{major} = 5.0 min, τ_{minor} = 5.5 min). [α]$_D^{26}$ = -1.1 (c = 0.44, CHCl$_3$, 64% ee).

^{1}H NMR (500 MHz, CDCl$_3$) δ 9.45 (t, J = 2.5 Hz, 1H), 7.69 – 7.58 (m, 2H), 7.26 (dd, J = 5.5, 2.3 Hz, 4H), 7.24 – 7.20 (m, 3H), 7.18 – 7.13 (m, 1H), 7.13 – 7.07 (m, 2H), 6.65 – 6.58 (m,

UNIVERSITAT ROVIRA I VIRGILI
PHOTOCHEMISTRY AND ORGANOCATALYSIS FOR RADICAL-BASED CARBON-CARBON BOND-FORMING PROCESSES
Emilien Le Saux

59

2H), 3.97 (s, 2H), 3.48 (dd, *J* = 66.4, 14.8 Hz, 2H), 3.00 (dd, *J* = 16.1, 1.8 Hz, 1H), 2.64 – 2.59 (m, 1H), 2.42 (s, 3H), 1.51 (s, 3H).

^{13}C NMR (126 MHz, CDCl$_3$) δ 202.24, 144.21, 143.85, 137.68, 135.84, 130.09, 129.17, 128.58, 128.38, 127.78, 127.75, 127.30, 126.87, 59.56, 53.54, 52.97, 41.63, 24.00, 21.89.

HRMS (ESI$^+$) m/z Calculated for C$_{25}$H$_{28}$NO$_3$S$^+$ [M+H]$^+$: 422.1712; found: 422.1783.
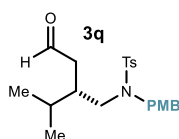
(*S*)-*N*-(2-isopropyl-4-oxobutyl)-*N*-(4-methoxybenzyl)-4-methylbenzene sulfonamide (3q)
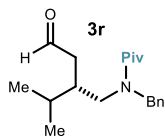
Prepared according to general procedure A using (*E*)-4-methylpent-2-enal (23.3 μL, 0.2 mmol) and radical precursor **2q** (37.8 mg, 0.1 mmol). The crude mixture was purified by column chromatography (SiO$_2$, 13:87 EtOAc/hexanes) to afford product **3q** as a colorless oil (30.7 mg, 76% yield, average of two runs, 98% ee). The enantiomeric excess was determined by UPC^2 analysis on a Daicel Chiralpak IC-3 column (gradient: 1 min 100% CO$_2$; 5 min from 100% CO$_2$ to 60% CO$_2$ - 40% CH$_3$CN; flow rate 3.0 mL/min, λ = 230 nm: τ$_{minor}$ = 4.4 min, τ$_{major}$ = 4.5 min). [α]$_D^{26}$ = -15.8 (c = 0.99, CHCl$_3$, 98% ee).

^{1}H NMR (400 MHz, CDCl$_3$) δ 9.49 (t, *J* = 1.8 Hz, 1H), 7.76 – 7.57 (m, 2H), 7.36 – 7.29 (m, 2H), 7.20 – 7.09 (m, 2H), 6.85 – 6.74 (m, 2H), 4.24 (d, *J* = 14.7 Hz, 1H), 4.13 (d, *J* = 14.7 Hz, 1H), 3.78 (s, 3H), 2.97 (m, 2H), 2.44 (s, 3H), 2.32 – 2.17 (m, 2H), 2.06 – 1.88 (m, 1H), 1.69 (pd, *J* = 6.9, 3.7 Hz, 1H), 0.70 (d, *J* = 6.9 Hz, 3H), 0.66 (d, *J* = 6.9 Hz, 3H).

^{13}C NMR (101 MHz, CDCl$_3$) δ 202.34, 159.39, 143.43, 136.27, 130.05, 129.78, 128.24, 127.29, 113.94, 55.30, 52.96, 50.68, 42.61, 36.69, 27.81, 21.52, 19.56, 17.91.

HRMS (ESI$^+$) Calculated for C$_{22}$H$_{29}$NNaO$_4$S [M+Na]$^+$: 426.1710, found: 426.1710.

(*S*)-*N*-benzyl-*N*-(2-isopropyl-4-oxobutyl)pivalamide (3r)

Prepared according to general procedure A using (*E*)-4-methylpent-2-enal (23 uL, 0.2 mmol) and radical precursor **2r** (27.7 mg, 0.1 mmol). The crude mixture was purified by column chromatography (SiO$_2$, 10:90 EtOAc/hexanes) to afford product **3r** as a colorless oil (17 mg, 56% yield, average of two runs, 92% ee). The enantiomeric excess was determined by HPLC analysis on a Daicel Chiralpak IC-3 column (90:10 *n*-hexane/*i*-PrOH, 1.0 mL/min, 20 ºC, λ = 215 nm: τ$_{major}$ = 13.8 min, τ$_{minor}$ = 18.9 min). [α]$_D^{28}$ = +5.1 (c = 0.68, CHCl$_3$, 92% ee).

^{1}H NMR (500 MHz, CDCl$_3$) δ 9.68 (t, *J* = 1.9 Hz, 1H), 7.33 (dd, *J* = 8.3, 6.8 Hz, 2H), 7.28 – 7.23 (m, 1H), 7.15 – 7.11 (m, 2H), 4.76 (d, *J* = 16.8 Hz, 1H), 4.63 (d, *J* = 16.8 Hz, 1H), 3.36 (dd, *J* = 13.7, 9.7 Hz, 1H), 3.10 (dd, *J* = 13.7, 5.1 Hz, 1H), 2.47 – 2.40 (m, 1H), 2.39 – 2.29

(m, 2H), 1.63 (pd, J = 6.9, 4.0 Hz, 1H), 1.25 (s, 9H), 0.82 (d, J = 6.9 Hz, 3H), 0.79 (d, J = 6.8 Hz, 3H).

^{13}C NMR (126 MHz, CDCl$_3$) δ 202.98, 179.17, 137.46, 129.14, 127.77, 127.05, 52.17, 49.20, 44.26, 39.84, 36.65, 29.99, 29.14, 20.15, 18.90.

HRMS (ESI$^+$) Calculated for C$_{19}$H$_{30}$NO$_2$ [M+H]$^+$: 304.2271, found: 304.2267.

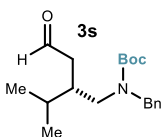**tert-Butyl (S)-benzyl(2-isopropyl-4-oxobutyl)carbamate (3s)**

Prepared according to general procedure A using (E)-4-methylpent-2-enal (23.3 μL, 0.2 mmol) and radical precursor **2s** (29.3 mg, 0.1 mmol). The crude mixture was purified by column chromatography (SiO$_2$, 10:90 EtOAc/hexanes) to afford product **3s** as a colorless oil (26 mg, 81% yield, average of two runs, 92% ee). The enantiomeric excess was determined by HPLC analysis on a Daicel Chiralpak IC-3 column (90:10 n-hexane/i-PrOH, 1.0 mL/min, 20 °C, λ = 215 nm: τ$_{minor}$ = 11.3 min, τ$_{major}$ = 13.2 min). [α]$_D^{28}$ = -8.2 (c = 0.64, CHCl$_3$, 92% ee).

^{1}H NMR (500 MHz, CDCl$_3$) δ 9.69 (s, 1H), 7.30 (dd, J = 8.0, 6.6 Hz, 2H), 7.26 – 7.12 (m, 3H), 4.54 – 4.15 (m, 2H), 3.36 – 2.96 (m, 2H), 2.50 – 2.17 (m, 3H), 1.69 (s, 1H), 1.44 (d, J = 24.2 Hz, 9H), 0.84 (dd, J = 7.0, 3.8 Hz, 6H).

^{13}C NMR (126 MHz, CDCl$_3$) δ 202.91, 173.19, 156.52, 138.57, 128.88, 127.59, 80.45, 50.92, 48.62, 44.01, 37.78, 28.75, 20.63, 20.16, 18.84.

HRMS (ESI$^+$) Calculated for C$_{19}$H$_{29}$NNaO$_3$ [M+Na]$^+$: 342.2040, found: 342.2038.
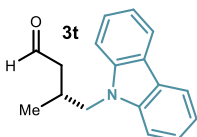
(R)-4-(9H-carbazol-9-yl)-3-methylbutanal (3t)

Prepared according to general procedure A using (E)-but-2-enal (16.5 μL, 0.2 mmol), radical precursor **2t** (31.5 mg, 0.1 mmol), and a 3:1 mixture of acetonitrile/water as solvent. The crude mixture was purified by column chromatography (SiO$_2$, 10:90 Et$_2$O/hexanes) to afford product **3t** as a colorless oil (15.6 mg, 62% yield, 62% ee). The enantiomeric excess was determined by UPC^2 analysis analysis on a Daicel Chiralpak IC-3 column (gradient: 1 min 100% CO$_2$, 5 min from 100% CO$_2$ to 60% CO$_2$ - 40% CH$_3$CN, flow rate 2 mL/min; λ = 340 nm: τ$_{minor}$ = 4.18 min, τ$_{major}$ = 4.27 min). [α]$_D^{26}$ = +9.2 (c = 0.76, CHCl$_3$, 60% ee).

^{1}H NMR (400 MHz, CDCl$_3$) δ 9.71 (dd, J = 1.9, 1.1 Hz, 1H), 8.13 (dt, J = 7.8, 1.0 Hz, 2H), 7.54 – 7.47 (m, 4H), 7.27 (ddd, J = 8.0, 6.5, 1.6 Hz, 2H), 4.29 (dd, J = 14.7, 7.5 Hz, 1H), 4.17 (dd, J = 14.7, 7.6 Hz, 1H), 2.96 – 2.86 (m, 1H), 2.54 (ddd, J = 17.4, 5.9, 1.1 Hz, 1H), 2.45 (ddd, J = 17.4, 7.4, 1.9 Hz, 1H), 1.08 (d, J = 6.7 Hz, 3H).

^{13}C NMR (101 MHz, CDCl$_3$) δ 201.07, 140.66, 125.81, 122.90, 120.40, 119.10, 108.92, 48.60, 48.57, 28.60, 18.32.

UNIVERSITAT ROVIRA I VIRGILI
PHOTOCHEMISTRY AND ORGANOCATALYSIS FOR RADICAL-BASED CARBON-CARBON BOND-FORMING PROCESSES
Emilien Le Saux

61

<u>HRMS</u> (ESI$^+$) Calculated for $C_{17}H_{17}NNaO$ [M+Na]$^+$: 274.1202, found: 274.1204.
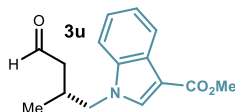
methyl (*R*)-1-(2-methyl-4-oxobutyl)-1H-indole-3-carboxylate (3u)

Prepared according to general procedure A using (*E*)-but-2-enal (16.5 μL, 0.2 mmol), radical precursor **2u** (26.1 mg, 0.1 mmol), and a 3:1 mixture of acetonitrile/water as solvent. The crude mixture was purified by column chromatography (SiO$_2$, 10:90 Et$_2$O/hexanes) to afford product **3u** as a colorless oil (9.0 mg, 35% yield, 89% ee). The enantiomeric excess was determined by UPC^2 analysis analysis on a Daicel Chiralpak IC-3 column (gradient: 1 min 100% CO$_2$, 5 min from 100% CO$_2$ to 60% CO$_2$ – 40% CH$_3$CN, flow rate 2 mL/min, 30 ºC; λ = 287 nm: τ_{minor} = 4.18 min, τ_{major} = 4.27 min). $[\alpha]_D^{26}$ = +2.8 (c = 0.28, CHCl$_3$, 89% ee).

<u>^{1}H NMR</u> (400 MHz, CDCl$_3$) δ 9.75 (t, *J* = 1.3 Hz, 1H), 8.23 – 8.18 (m, 1H), 7.81 (s, 1H), 7.49 – 7.44 (m, 1H), 7.35 – 7.30 (m, 2H), 4.20 (dd, *J* = 14.1, 6.8 Hz, 1H), 3.98 (dd, *J* = 14.1, 7.9 Hz, 1H), 3.94 (s, 3H), 2.74 (dq, *J* = 13.7, 6.8 Hz, 1H), 2.53 – 2.38 (m, 2H), 1.03 (d, *J* = 6.8 Hz, 3H).

<u>^{13}C NMR</u> (101 MHz, CDCl$_3$) δ 200.48, 165.43, 136.70, 134.56, 126.66, 123.00, 122.01, 121.85, 110.20, 107.36, 52.28, 51.03, 48.01, 28.87, 17.96.

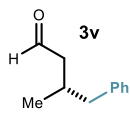<u>HRMS</u> (ESI$^+$) Calculated for $C_{15}H_{17}NNaO_3$ [M+Na]$^+$: 282.1101, found: 282.1102.

(*S*)-3-Methyl-4-phenylbutanal (3v)

Prepared according to general procedure A using (*E*)-but-2-enal (16.6 uL, 0.2 mmol) and benzyl trimethylsilane (16.4 mg, 0.1 mmol). The crude mixture was purified by column chromatography (SiO$_2$, 20:80 CH$_2$Cl$_2$/hexanes) to afford product **3v** as a colorless oil (16.4 mg, 67% yield, average of two runs, 90% ee). The enantiomeric excess of the corresponding 2,4-dinitrophenylhydrazone (obtained upon condensation with 2,4-dinitrophenylhydrazine) was determined by UPC^2 analysis on a Daicel Chiralpak OJ-3 column (gradient: 1 min 100% CO$_2$, 5 min from 100% CO$_2$ to 60% CO$_2$ – 40% CH$_3$CN; flow rate 2.0 mL/min, λ = 351 nm: τ_{minor} = 4.1 min, τ_{major} = 4.6 min). $[\alpha]_D^{28}$ = +1.0 (c = 0.59, CHCl$_3$, 90% ee).

<u>^{1}H NMR</u> (500 MHz, CDCl3) δ 9.69 (dd, J = 2.5, 1.6 Hz, 1H), 7.31 – 7.11 (m, 5H), 2.62 – 2.51 (m, 2H), 2.46 – 2.30 (m, 2H), 2.23 (ddd, J = 15.8, 7.6, 2.5 Hz, 1H), 0.97 (d, J = 6.6 Hz, 3H).

<u>^{13}C NMR</u> (126 MHz, CDCl3) δ 203.39, 140.87, 129.56, 128.73, 126.57, 50.61, 44.10, 30.61, 18.38.

<u>HRMS</u> (APCI$^+$) Calculated for $C_{11}H_{13}O^+$ [M-H]$^+$: 161.0961; found: 161.0960.
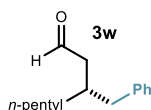
(*S*)-3-Benzyloctanal (3w)

Prepared according to general procedure A using (*E*)-oct-2-enal (30.0 μL, 0.2 mmol) and benzyl trimethylsilane (16.4 mg, 0.1 mmol). The crude mixture was purified by column chromatography (SiO$_2$, 20:80 CH$_2$Cl$_2$/hexanes) to afford product **3w** as a colorless oil (16.2 mg, 74% yield, average of two runs, 95% ee). The enantiomeric excess of the corresponding 2,4-dinitrophenylhydrazone (obtained upon condensation with 2,4-dinitrophenylhydrazine) was determined by UPC^2 analysis on a Daicel Chiralpak IG-3 column (gradient: 1 min 100% CO$_2$, 5 min from 100% CO$_2$ to 60% CO$_2$ – 40% CH$_3$CN; flow rate 2 mL/min, λ = 355 nm: τ_{minor} = 5.6 min, τ_{major} = 6.3 min). [α]$_D^{26}$ = +3.4 (c = 0.73, CHCl$_3$, 95% ee).

^{1}H NMR (500 MHz, CDCl$_3$) δ 9.64 (t, J = 2.0 Hz, 1H), 7.31 – 7.23 (m, 2H), 7.22 – 7.15 (m, 1H), 7.19 – 7.11 (m, 2H), 2.73 (dd, J = 13.6, 6.0 Hz, 1H), 2.48 (dd, J = 13.6, 7.8 Hz, 1H), 2.37 – 2.24 (m, 3H), 1.35 – 1.29 (m, 3H), 1.26 (ddd, J = 11.0, 5.4, 2.9 Hz, 5H), 0.87 (t, J = 7.0 Hz, 3H).

^{13}C NMR (126 MHz, CDCl$_3$) δ 204.06, 141.44, 129.61, 128.74, 126.52, 48.25, 40.98, 35.63, 34.46, 32.28, 31.26, 26.80, 22.93.

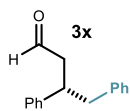HRMS (APCI$^+$) Calculated for C$_{15}$H$_{21}$O$^+$ [M-H]$^+$: 217.1587; found: 217.1585

(S)-3,4-Diphenylbutanal (3x)

Prepared according to general procedure A using (*E*)-cinnamaldehyde (25.2 uL, 0.2 mmol) and benzyltrimethylsilane (16.4 mg, 0.1 mmol). The crude mixture was purified by column chromatography (SiO$_2$, 20:80 CH$_2$Cl$_2$/hexanes) to afford product **3x** as a colorless oil (17.8 mg, 79% yield, average of two runs, 90% ee) that displayed spectroscopic data consistent with those reported previously. The enantiomeric excess was determined by HPLC analysis on a Daicel Chiralpak IC-3 column (90:10 *n*-hexane/*i*-PrOH, flow rate 0.6 mL/min, λ = 215 nm: τ_{major} = 13.2 min, τ_{minor} = 14.4 min). [α]$_D^{26}$ = -33.2 (c = 0.51, CHCl$_3$, 90% ee). The (*S*) absolute configuration of **3t** was established by correlation with value reported in the literature: Lit: [α]$_D^{26}$ = -45.8 (c = 0.49, CHCl$_3$, 88% ee for (*S*)-enantiomer).[5]

^{1}H NMR (400 MHz, CDCl$_3$) δ 9.62 (t, *J* = 2.0 Hz, 1H), 7.34 – 7.17 (m, 9H), 7.11 – 7.06 (m, 2H), 3.52 (p, *J* = 7.4 Hz, 1H), 3.03 – 2.87 (m, 2H), 2.86 – 2.71 (m, 2H).

^{13}C NMR (126 MHz, CDCl$_3$) δ 201.92, 143.59, 139.63, 129.58, 128.96, 128.79, 128.68, 128.59, 127.88, 127.84, 127.11, 126.71, 49.30, 43.69, 42.40.

UNIVERSITAT ROVIRA I VIRGILI
PHOTOCHEMISTRY AND ORGANOCATALYSIS FOR RADICAL-BASED CARBON-CARBON BOND-FORMING PROCESSES
Emilien Le Saux

63
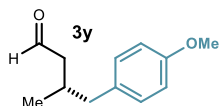
(S)-4-(4-Methoxyphenyl)-3-methylbutanal (3y)

Prepared according to general procedure A using (*E*)-but-2-enal (16.6 uL, 0.2 mmol) and radical precursor **2y** (19.4 mg, 0.1 mmol). The crude mixture was purified by column chromatography (SiO$_2$, 20:80 CH2Cl2/hexanes) to afford product **3y** as a colorless oil (10.3 mg, 54% yield, average of two runs, 90% ee). The enantiomeric excess was determined by UPC^2 analysis on a Daicel Chiralpak IG-3 column (gradient: 1 min 100% CO$_2$, 5 min from 100% CO$_2$ to 60% CO$_2$ - 40% CH$_3$CN; flow rate 2.0 mL/min, λ = 276 nm: τ_{minor} = 2.5 min, τ_{major} = 2.6 min). $[\alpha]_D^{26}$ = -0.82 (c = 0.48, CHCl$_3$, 90% ee).
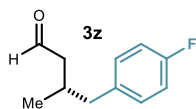
^{1}H NMR (500 MHz, CDCl$_3$) δ 9.68 (dd, *J* = 2.5, 1.8 Hz, 1H), 7.08 – 7.02 (m, 2H), 6.85 – 6.78 (m, 2H), 3.78 (s, 3H), 2.51 (d, *J* = 7.1 Hz, 2H), 2.40 (ddd, *J* = 16.0, 5.2, 1.8 Hz, 1H), 2.36 – 2.26 (m, 1H), 2.21 (ddd, *J* = 15.9, 7.9, 2.5 Hz, 1H), 0.96 (d, *J* = 6.6 Hz, 3H).

^{13}C NMR (126 MHz, CDCl$_3$) δ 202.99, 158.44, 132.39, 130.46, 114.14, 77.62, 77.37, 77.12, 55.61, 50.59, 42.68, 30.79, 20.30.

HRMS (ESI$^+$) Calculated for C$_{12}$H$_{15}$O$_2^+$ [M-H]$^+$: 191.1067; found: 191.1064.

(S)-4-(4-Fluorophenyl)-3-methylbutanal (3z)

Prepared according to general procedure A using (*E*)-but-2-enal (16.6 uL, 0.2 mmol) and radical precursor **2z** (18.2 mg, 0.1 mmol). The crude mixture was purified by column chromatography (SiO$_2$, 20:80 CH$_2$Cl$_2$/hexanes) to afford product **3z** as a colorless oil (8.4 mg, 47% yield, average of two runs, 86% ee). The enantiomeric excess of the corresponding 2,4-dinitrophenylhydrazone (obtained upon condensation with 2,4-dinitrophenylhydrazine) was determined by UPC^2 analysis on a Daicel Chiralpak OJ-3 column (gradient: 1 min 100% CO$_2$, 5 min from 100% CO$_2$ to 60% CO$_2$ - 40% CH$_3$CN; flow rate 2.0 mL/min, λ = 351 nm: τ_{minor} = 3.6 min, τ_{major} = 3.8 min). $[\alpha]_D^{26}$ = +2.1 (c = 0.36, CHCl$_3$, 86% ee).

^{1}H NMR (500 MHz, CDCl$_3$) δ 9.74 (dd, *J* = 2.3, 1.6 Hz, 1H), 7.16 – 7.10 (m, 2H), 7.03 – 6.97 (m, 2H), 2.57 (qd, *J* = 13.5, 6.9 Hz, 2H), 2.44 (ddd, *J* = 15.4, 4.9, 1.7 Hz, 1H), 2.41 – 2.31 (m, 1H), 2.28 (ddd, *J* = 15.6, 7.3, 2.3 Hz, 1H), 0.99 (d, *J* = 6.4 Hz, 3H).

^{13}C NMR (101 MHz, CDCl$_3$) δ 202.30, 162.71, 135.63, 130.54, 130.47, 115.24, 115.03, 50.18, 42.29, 30.27, 19.81.

HRMS (APCI$^+$) Calculated for C$_{11}$H$_{12}$FO$^+$ [M-H]$^+$: 179.0867; found: 179.0862.

(R)-3-((Phenylthio)methyl)octanal (3aa)

Prepared according to general procedure A using (*E*)-oct-2-enal (30.0 μL, 0.2 mmol), radical precursor **2aa** (19.6 mg, 0.1 mmol), and a 3:1 mixture

of acetonitrile/water as solvent. The crude mixture was purified by column chromatography (SiO$_2$, 20:80 CH$_2$Cl$_2$/hexanes) to afford product **3aa** as a colorless oil (15.5 mg, 62% yield, average of two runs, 96% ee). The enantiomeric excess was determined by UPC^2 analysis analysis on a Daicel Chiralpak IG-3 column (gradient: 1 min 100% CO$_2$, 5 min from 100% CO$_2$ to 60% CO$_2$ – 40% *i*-PrOH; flow rate 2 mL/min, 30 °C, $\lambda = 253$ nm: $\tau_{minor} = 2.7$ min, τ_{major} = 2.8 min). [α]$_D^{26}$ = +9.7 (c = 0.35, CHCl$_3$, 96% ee).

^{1}H NMR (500 MHz, CDCl$_3$) δ 9.73 (t, *J* = 1.9 Hz, 1H), 7.35 – 7.23 (m, 4H), 7.20 – 7.13 (m, 1H), 3.05 (dd, *J* = 13.1, 5.4 Hz, 1H), 2.84 (dd, *J* = 13.1, 7.6 Hz, 1H), 2.65 (ddd, *J* = 17.0, 6.4, 1.7 Hz, 1H), 2.44 (ddd, *J* = 17.0, 6.5, 2.0 Hz, 1H), 2.24 (dtd, *J* = 7.6, 6.5, 5.3 Hz, 1H), 1.53 – 1.32 (m, 2H), 1.31 – 1.16 (m, 6H), 0.86 (t, *J* = 7.0 Hz, 3H).

^{13}C NMR (126 MHz, CDCl$_3$) δ 201.99, 132.39, 128.98, 126.78, 123.84, 47.72, 37.68, 33.75, 33.03, 31.80, 30.41, 25.83, 22.51.

HRMS (APCI$^+$) Calculated for C$_{15}$H$_{23}$OS$^+$ [M+H]$^+$: 251.1464; found: 251.1463.

(*R*)-4-methoxy-3-methyl-4-phenylbutanal (3bb)
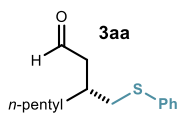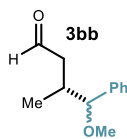
Prepared according to general procedure A using (*E*)-but-2-enal (16.5 μL, 0.2 mmol) and radical precursor **2bb** (19.4 mg, 0.1 mmol). The crude mixture was purified by column chromatography (SiO$_2$, 20:80 CH$_2$Cl$_2$/hexanes) to afford product **3bb** as a colorless oil (12.9 mg, 67% yield, average of two runs, 86% ee$_{maj}$ and 64% ee$_{min}$, 1.3:1 dr). The enantiomeric excess of the corresponding 2,4-dinitrophenylhydrazone (obtained upon condensation with 2,4-dinitrophenylhydrazine) was determined by UPC^2 analysis on a Daicel Chiralpak OJ-3 column (gradient: 1 min 100% CO$_2$, 5 min from 100% CO$_2$ to 60% CO$_2$ - 40% CH$_3$CN; flow rate 2.0 mL/min, $\lambda = 351$ nm: $\tau_{minor} = 3.6$ min, τ_{major} = 3.8 min. [α]$_D^{26}$ = -8.1 (c = 0.14, CHCl$_3$, 88% ee).

^{1}H NMR (400 MHz, CDCl$_3$) *major diastereoisomer:* δ 9.69 (dd, *J* = 2.4, 1.7 Hz, 1H), 7.40 – 7.35 (m), 7.35 – 7.24 (m), 4.07 (d, *J* = 5.3 Hz, 1H), 3.24 (s, 3H), 2.63 (ddd, *J* = 15.7, 6.3, 2.9 Hz, 1H), 2.35 (ddd, *J* = 15.7, 6.5, 1.9 Hz, 1H), 2.24 – 2.14 (m, 1H), 1.00 – 0.96 (m, 3H). *minor diastereoisomer:* δ 9.76 (dd, *J* = 2.9, 1.8 Hz, 1H), 7.40 – 7.35 (m), 7.35 – 7.24 (m), 3.80 (d, *J* = 8.1 Hz, 1H), 3.15 (s, 3H), 2.53 – 2.40 (m, 3H), 0.81 (d, *J* = 6.8 Hz, 3H).

^{13}C NMR (101 MHz, CDCl$_3$) *major diastereoisomer:* δ 202.18, 139.52, 128.27, 127.70, 127.31, 86.86, 57.08, 47.35, 34.99, 15.71. *minor diastereoisomer:* δ 202.23, 140.14, 128.37, 127.90, 127.41, 88.46, 56.63, 48.41, 35.93, 17.11.

HRMS (APCI$^+$) Calculated for C$_{12}$H$_{15}$O$_2^+$ [M-H]$^+$: 191.1067; found: 191.1063.

UNIVERSITAT ROVIRA I VIRGILI
PHOTOCHEMISTRY AND ORGANOCATALYSIS FOR RADICAL-BASED CARBON-CARBON BOND-FORMING
PROCESSES
Emilien Le Saux

65
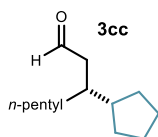
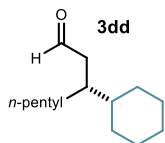### (*R*)-3-Cyclopentyloctanal (3cc)

Prepared according to general procedure A using (*E*)-oct-2-enal (30.0 μL, 0.11 mmol) and radical precursor **26** (37.9 mg, 0.1 mmol). The crude mixture was purified by column chromatography (SiO$_2$, 20:80 CH$_2$Cl$_2$/hexanes) to afford product **3cc** as a colorless oil (12.5 mg, 64% yield, average of two runs, 82% ee). The enantiomeric excess of the corresponding 2,4-dinitrophenylhydrazone (obtained upon condensation with 2,4-dinitrophenylhydrazine) was determined by UPC^2 analysis analysis on a Daicel Chiralpak IG-3 column (gradient: 1 min 100% CO$_2$, 5 min 100% CO$_2$ to 60% CO$_2$ – 40% EtOH; flow rate 2.0 mL/min, 30 °C, λ = 348 nm: τ_{major} = 4.5 min, τ_{minor} = 4.7 min). $[\alpha]_D^{26}$ = -3.4 (c = 0.23, CHCl$_3$, 82% ee).

^{1}H NMR (400 MHz, CDCl$_3$) δ 9.80 (t, *J* = 2.5 Hz, 1H), 2.48 – 2.32 (m, 2H), 1.94 – 1.86 (m, 1H), 1.82 – 1.73 (m, 2H), 1.67 – 1.59 (m, 2H), 1.54 (ttd, *J* = 7.8, 3.9, 1.8 Hz, 2H), 1.48 – 1.42 (m, 1H), 1.37 – 1.23 (m, 8H), 1.20 – 1.05 (m, 2H), 0.90 (t, *J* = 6.9 Hz, 3H).

^{13}C NMR (126 MHz, CDCl$_3$) δ 203.23, 48.51, 45.17, 39.49, 33.45, 32.52, 30.80, 26.65, 25.63, 20.69.

HRMS (APCI$^+$) Calculated for C$_{13}$H$_{23}$O$^+$ [M-H]$^+$: 195.1743; found: 195.1739.

(*R*)-3-cyclohexyloctanal (3dd)

Prepared according to general procedure A using (*E*)-oct-2-enal (22.4 μL, 0.15 mmol), radical precursor **27dd** (72.6 mg, 0.1 mmol), and photocatalyst **PC-a** (0.6 mg, 1.0 μmol, 1.0 mol%) in a 3:1 mixture of acetonitrile/water as solvent with an irradiance of 20±2 mW/cm^2. The crude mixture was purified by column chromatography (SiO$_2$, 20:80 CH$_2$Cl$_2$/hexanes) to afford product **3dd** as a colorless oil (12.2 mg, 58% yield, 82% ee). The enantiomeric excess of the corresponding 2,4-dinitrophenylhydrazone (obtained upon condensation with 2,4-dinitrophenylhydrazine) was determined by UPC^2 analysis analysis on a Daicel Chiralpak IG-3 column (gradient: 1 min 100% CO$_2$, 5 min from 100% CO$_2$ to 60% CO$_2$ – 40% EtOH; flow rate 2.0 mL/min, λ = 349 nm: τ_{major} = 4.7 min, τ_{minor} = 5.9 min). $[\alpha]_D^{24}$ = -10.0 (c = 0.1, CHCl$_3$, 82% ee).

^{1}H NMR (500 MHz, CDCl$_3$) δ 9.73 (t, *J* = 2.4 Hz, 1H), 2.39 (ddd, *J* = 16.2, 5.9, 2.3 Hz, 1H), 2.22 (ddd, *J* = 16.2, 7.1, 2.6 Hz, 1H), 1.83 (q, *J* = 6.2, 5.8 Hz, 1H), 1.75 – 1.71 (m, 2H), 1.67 – 1.62 (m, 1H), 1.58 (d, *J* = 12.4 Hz, 2H), 1.38 – 1.16 (m, 9H), 1.09 (dt, *J* = 12.8, 3.4 Hz, 1H), 1.04 – 0.91 (m, 2H), 0.86 (t, *J* = 7.1 Hz, 3H).

^{13}C NMR (101 MHz, CDCl$_3$) δ 203.84, 46.11, 40.78, 38.36, 32.09, 31.62, 30.35, 29.24, 27.10, 26.73, 26.69, 26.67, 22.60, 14.07.

HR-MS (ESI$^+$) Calculated for C$_{15}$H$_{30}$NaO$_2^+$ [M+MeOH+Na]$^+$: 265.2138; found: 265.2137.
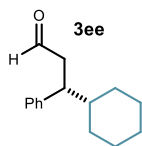
(*R*)-3-cyclohexyl-3-phenylpropanal (3ee)

3ee

Prepared according to general procedure A using (*E*)-cinnamaldehyde (38 μL, 0.3 mmol), radical precursor **27ee** (72.6 mg, 0.1 mmol), photocatalyst **PC-a** (0.6 mg, 1.0 μmol, 1.0 mol%) , and TFA (6.0 μL, 0.08 mmol) in a 3:1 mixture of acetonitrile/ water as solvent. The crude mixture was purified by column chromatography (SiO$_2$, 15:85 to 50:50 CH$_2$Cl$_2$/hexanes) to afford product **3ee** as a colorless oil (11.4 mg, 53% yield, 83% ee). The enantiomeric excess of the corresponding alcohol (obtained by reduction with NaBH$_4$) was determined by HPLC analysis on a Daicel Chiralpak IC-3 column (90:10 *n*-hexane/*i*-PrOH, 0.6 mL/min, 20 °C, λ = 215 nm: τ_{minor} = 13.0 min, τ_{major} = 15.8 min). $[\alpha]_D^{26}$ = -2.4 (c = 0.1, CHCl$_3$, 83% ee).

^{1}H NMR (500 MHz, CDCl3) δ 9.60 (t, *J* = 2.2 Hz, 1H), 7.31 – 7.26 (m, 2H), 7.22 – 7.17 (m, 1H), 7.16 – 7.12 (m, 2H), 2.98 (ddd, *J* = 9.6, 7.6, 5.4 Hz, 1H), 2.83 (ddd, *J* = 16.4, 5.4, 2.0 Hz, 1H), 2.72 (ddd, *J* = 16.4, 9.6, 2.5 Hz, 1H), 1.84 – 1.71 (m, 2H), 1.68 – 1.58 (m, 2H), 1.54 – 1.44 (m, 2H), 1.25 – 1.17 (m, 1H), 1.16 – 1.02 (m, 2H), 0.99 – 0.80 (m, 2H).

^{13}C NMR (126 MHz, CDCl$_3$) δ 202.6, 142.8, 128.4, 128.3, 126.5, 47.1, 46.2, 43.1, 31.1, 30.7, 26.4, 26.3.
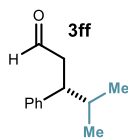
(*R*)-4-methyl-3-phenylpentanal (3ff)

3ff

Prepared according to general procedure A using (*E*)-cinnamaldehyde (25.2 uL, 0.2 mmol) and radical precursor **17ff** (29.5 mg, 0.1 mmol). The crude mixture was purified by column chromatography (SiO$_2$, 20:80 CH$_2$Cl$_2$/hexanes) to afford product **3ff** as a colorless oil (17.6 mg, 91% yield, average of two runs, 84% ee). The enantiomeric excess of the corresponding 2,4-dinitrophenylhydrazone (obtained upon condensation with 2,4-dinitrophenylhydrazine) was determined by UPC^2 analysis on a Daicel Chiralpak IG-3 column (gradient: 1 min 100% CO$_2$, 5 min from 100% CO$_2$ to 60% CO$_2$ - 40% CH$_3$CN; flow rate 2.0 mL/min, λ = 350 nm: τ_{minor} = 6.3 min, τ_{major} = 7.1 min). $[\alpha]_D^{24}$ = -1.0 (c = 0.1, CHCl$_3$, 84% ee). The (*R*) absolute configuration of **3z** was established by correlation with value reported in the literature: Lit: $[\alpha]_D^{26}$ = –14.3 (c = 0.57, CH$_2$Cl$_2$, 86% ee, for (*R*) enantiomer).[6a]

^{1}H NMR (400 MHz, CDCl$_3$) δ 9.64 – 9.62 (m, 1H), 7.34 – 7.28 (m, 3H), 7.25 – 7.20 (m, 1H), 7.19 – 7.15 (m, 2H), 2.98 (ddd, *J* = 9.5, 7.5, 5.5 Hz, 1H), 2.87 – 2.73 (m, 2H), 1.94 – 1.85 (m, 1H), 0.97 (d, *J* = 6.7 Hz, 3H), 0.80 (d, *J* = 6.7 Hz, 3H).

^{13}C NMR (101 MHz, CDCl$_3$) δ 202.53, 142.62, 128.39, 128.27, 126.55, 77.34, 77.02, 76.71, 47.21, 46.97, 33.44, 20.57, 20.29.

UNIVERSITAT ROVIRA I VIRGILI
PHOTOCHEMISTRY AND ORGANOCATALYSIS FOR RADICAL-BASED CARBON-CARBON BOND-FORMING
PROCESSES
Emilien Le Saux

67
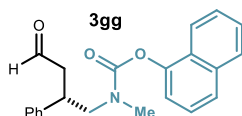
naphthalen-1-yl (*S*)-methyl(4-oxo-2-phenylbutyl)carbamate (3gg)

Prepared according to general procedure A using (*E*)-cinnamaldehyde (25.2 uL, 0.2 mmol), and radical precursor **17gg** (46.7 mg, 0.1 mmol. The crude mixture was purified by column chromatography (SiO$_2$, 2:98 CH$_2$Cl$_2$/EtOAc) to afford product **3gg** as a white solid (22.1 mg, 64% yield, 70% ee). The enantiomeric excess was determined by UPC^2 analysis analysis on a Daicel Chiralpak OJ-3 column (gradient: 1 min 100% CO$_2$, 5 min from 100% CO$_2$ to 60% CO$_2$ - 40% CH$_3$CN; flow rate 2 mL/min, λ = 279 nm: τ_{minor} = 4.22 min, τ_{major} = 3.99 min). [α]$_D^{26}$ = -29.3 (c = 1.1, CHCl$_3$, 70% ee).

^{1}H NMR (400 MHz, CDCl$_3$) δ 9.76 (dt, *J* = 10.2, 1.6 Hz, 1H), 7.88 (dt, *J* = 7.7, 2.0 Hz, 1H), 7.76 – 7.67 (m, 2H), 7.49 (dtt, *J* = 19.2, 7.9, 4.0 Hz, 3H), 7.40 (ddd, *J* = 11.1, 6.2, 2.9 Hz, 2H), 7.34 (dd, *J* = 7.2, 1.9 Hz, 3H), 7.25 – 7.02 (m, 1H), 3.94 – 3.49 (m, 3H), 3.06 (d, *J* = 51.9 Hz, 3H), 2.98 – 2.81 (m, 2H).

^{13}C NMR (101 MHz, CDCl$_3$) δ 200.77, 200.29, 155.16, 154.62, 147.11, 140.98, 140.69, 134.64, 129.06, 128.92, 127.97, 127.90, 127.84, 127.50, 127.35, 127.33, 126.31, 126.28, 125.59, 125.44, 121.27, 121.17, 118.24, 118.04, 55.07, 54.99, 53.45, 47.52, 47.23, 38.74, 38.21, 35.47.

HRMS (ESI$^+$) Calculated for C$_{22}$H$_{21}$NNaO$_3$ [M+Na]$^+$: 370.1403, found: 370.1414.
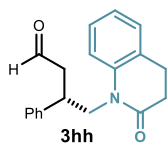
(*S*)-4-(2-oxo-3,4-dihydroquinolin-1(2H)-yl)-3-phenylbutanal (3hh)

Prepared according to general procedure A using (*E*)-cinnamaldehyde (25.2 uL, 0.2 mmol), and radical precursor **17hh** (41.2 mg, 0.1 mmol). The crude mixture was purified by column chromatography (SiO$_2$, 10:90 Et$_2$O/hexanes) to afford product **3hh** as a colorless oil (21.5 mg, 73% yield, 84% ee). The enantiomeric excess of the corresponding 2,4-dinitrophenylhydrazone (obtained upon condensation with 2,4-dinitrophenylhydrazine) was determined by UPC^2 analysis analysis on a Daicel Chiralpak OJ-3 column (gradient: 1 min 100% CO$_2$, 5 min from 100% CO$_2$ to 60% CO$_2$ - 40% CH$_3$CN; flow rate 2 mL/min, λ = 352 nm: τ_{minor} = 5.32 min, τ_{major} = 4.56 min). [α]$_D^{26}$ = -4.3 (c = 1.1, CHCl$_3$, 84% ee).

^{1}H NMR (400 MHz, CDCl$_3$) δ 9.68 (t, *J* = 1.5 Hz, 1H), 7.34 – 7.21 (m, 5H), 7.19 – 7.12 (m, 3H), 7.04 (td, *J* = 7.4, 1.1 Hz, 1H), 4.33 (dd, *J* = 14.2, 8.0 Hz, 1H), 4.27 – 4.19 (m, 1H), 3.69 (p, *J* = 7.5 Hz, 1H), 2.90 (dd, *J* = 7.2, 1.5 Hz, 2H), 2.74 (qd, *J* = 8.1, 4.0 Hz, 1H), 2.60 – 2.46 (m, 3H).

^{13}C NMR (101 MHz, CDCl$_3$) δ 200.78, 170.58, 140.55, 138.74, 128.66, 128.06, 127.74, 127.50, 127.28, 127.18, 123.05, 115.43, 47.66, 45.33, 37.16, 31.84, 25.27.

HRMS (ESI$^+$) Calculated for C$_{19}$H$_{19}$NNaO$_2$ [M+Na]$^+$: 316.1308, found: 316.1305.
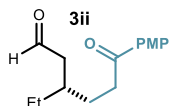
(*S*)-3-ethyl-6-(4-methoxyphenyl)-6-oxohexanal (3ii)

Prepared according to general procedure A using (*E*)-pent-2-enal (20 µL, 0.2 mmol) and radical precursor **28** (16.4 mg, 0.1 mmol) in 200 µL of an argon-sparged 0.3 M acetonitrile solution of TFA (4.5 µL, 0.06 mmol, 60 mol%). The crude mixture was purified by column chromatography (SiO$_2$, 9:91 EtOAc/hexanes) to afford product **3ii** as a yellow oil (12.8 mg, 51% yield, average of two runs, 86% ee). The enantiomeric excess was determined by HPLC analysis on a Daicel Chiralpak IC-3 column (85:15 *n*-hexane/*i*PrOH, 1.0 mL/min, 20 °C, λ = 215 nm: τ$_{major}$ = 45.5 min, τ$_{minor}$ = 49.5 min). [α]$_D^{26}$ = +2.6 (c = 0.12, CHCl$_3$, 86% ee).

^{1}H NMR (500 MHz, CDCl3) δ 9.79 (t, *J* = 2.2 Hz, 1H), 7.96 – 7.90 (m, 2H), 6.96 – 6.90 (m, 2H), 3.87 (s, 3H), 2.92 (t, *J* = 7.7 Hz, 2H), 2.48 – 2.35 (m, 2H), 2.02 (p, *J* = 6.5 Hz, 1H), 1.85 – 1.68 (m, 2H), 1.52 – 1.35 (m, 2H), 0.92 (t, *J* = 7.4 Hz, 3H).

^{13}C NMR (126 MHz, CDCl$_3$) δ 202.8, 198.5, 163.5, 130.3, 129.9, 113.7, 55.5, 48.1, 35.5, 34.0, 28.3, 26.5, 10.8.

HRMS (ESI$^+$) Calculated for C$_{15}$H$_{20}$NaO$_3$ [M+Na]$^+$: 271.1305, found: 271.1293.

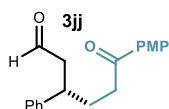### (*S*)-6-(4-methoxyphenyl)-6-oxo-3-phenylhexanal (3jj)

Prepared according to general procedure A using (*E*)-cinnamaldehyde (38 µL, 0.3 mmol) and radical precursor **28** (16.4 mg, 0.1 mmol) with amine catalyst **C** (21.1 mg, 0.03 mmol, 0.3 equiv.) in 200 µL of an argon-sparged 0.2 M acetonitrile solution of TFA (3.0 µL, 0.04 mmol, 40 mol%). The crude mixture was purified by column chromatography (SiO$_2$, 9:91 EtOAc/hexanes) to afford product **3jj** as a yellow oil (16.4 mg, 55% yield, average of two runs, 88% ee). The enantiomeric excess was determined by HPLC analysis on a Daicel Chiralpak IC-3 column (80:20 *n*-hexane/*i*-PrOH, 1.0 mL/min, 20 °C, λ = 215 nm: τ$_{major}$ = 52.3 min, τ$_{minor}$ = 56.4 min). [α]$_D^{26}$ = -30.9 (c = 0.10, CHCl$_3$, 88% ee).

^{1}H NMR (500 MHz, CDCl3) δ 9.68 (t, *J* = 1.9 Hz, 1H), 7.83 – 7.78 (m, 2H), 7.34 – 7.29 (m, 2H), 7.25 – 7.19 (m, 3H), 6.90 – 6.85 (m, 2H), 3.84 (s, 3H), 3.29 (dtd, *J* = 10.4, 7.3, 4.6 Hz, 1H), 2.87 – 2.76 (m, 3H), 2.71 (ddd, *J* = 17.0, 9.1, 5.1 Hz, 1H), 2.22 – 2.12 (m, 1H), 2.05 – 1.94 (m, 1H).

^{13}C NMR (126 MHz, CDCl$_3$) δ 201.5, 198.2, 163.4, 142.9, 130.2, 129.9, 128.8, 127.6, 126.9, 113.6, 55.4, 50.7, 39.5, 35.7, 30.8.

HRMS (ESI$^+$) Calculated for C$_{19}$H$_{20}$NaO$_3$ [M+Na]$^+$: 319.1305, found: 319.1303.

UNIVERSITAT ROVIRA I VIRGILI
PHOTOCHEMISTRY AND ORGANOCATALYSIS FOR RADICAL-BASED CARBON-CARBON BOND-FORMING PROCESSES
Emilien Le Saux

69
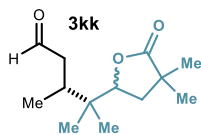
(3R)-4-(4,4-dimethyl-5-oxotetrahydrofuran-2-yl)-3,4-dimethylpentanal (3kk)

Prepared according to general procedure A using (E)-but-2-enal (16.5 μL, 0.2 mmol) and radical precursor **29** (15.6 mg, 0.1 mmol). The crude mixture was purified by column chromatography (SiO$_2$, 10:90 to 20:80 EtOAc/hexanes) to afford product **3kk** as a colorless oil (14.1 mg, 62% yield, average of two runs, 86% ee, 1:1 dr). The enantiomeric excess of the corresponding 2,4-dinitrophenylhydrazone (obtained upon condensation with 2,4-dinitrophenylhydrazine) was determined by UPC^2 analysis on a Daicel Chiralpak OJ-3 column, gradient: 1 min 100% CO$_2$, 5 min from 100% CO$_2$ to 60% CO$_2$ - 40% CH$_3$CN; flow rate 2 mL/min, λ = 345 nm. *Diastereoisomer A*: τ$_{Major}$ = 4.3 min, τ$_{Minor}$ = 4.1 min. *Diastereoisomer B*: τ$_{Major}$ = 4.4 min, τ$_{Minor}$ = 4.2 min. [α]$_D^{26}$ = +2.0 (c = 0.52, CHCl$_3$, 86% ee).

<u>^{1}H NMR</u> (500 MHz, CDCl$_3$) 1:1 mixture of diastereoisomers δ 9.73 (td, J = 2.7, 0.9 Hz, 2H), 4.36 (ddd, J = 9.8, 6.8, 2.0 Hz, 2H), 2.64 (dd, J = 16.7, 3.0 Hz, 1H), 2.61 – 2.56 (m, 1H), 2.27 – 2.10 (m, 4H), 1.94 – 1.85 (m, 4H), 1.26 (d, J = 2.1 Hz, 12H), 0.95 – 0.89 (m, 12H), 0.80 (s, 3H), 0.77 (s, 3H).

<u>^{13}C NMR</u> (126 MHz, CDCl$_3$) 1:1 mixture of diastereoisomers δ 202.75, 202.65, 182.08, 182.05, 81.33, 80.99, 77.65, 77.39, 77.13, 47.07, 47.03, 40.55, 40.52, 38.81, 38.60, 38.52, 38.37, 34.44, 34.28, 25.25, 24.96, 24.94, 19.89, 19.65, 19.14, 18.79, 15.63, 15.57.

<u>HRMS</u> (ESI$^+$) Calculated for C$_{13}$H$_{22}$NaO$_3^+$ [M+Na]$^+$: 249.1461; found: 249.1466.

2.7.5 Procedure for the 1 mmol reaction

A different setup was used for the scale up of the photochemical radical conjugate addition. It consisted of a 4 cm diameter jar fitted with a standard 29 sized ground glass joint. A commercial 1-meter blue LEDs strip (λ = 455 nm) was wrapped around the jar, followed by a layer of aluminium foil and cotton for insulation. An inlet and an outlet allow the circulation of liquid from a Huber Minichiller 300 inside the jar (Figure 2.39).

To a 10 mL flame-dried Schlenk tube, catalyst **C** (141 mg, 0.2 mmol), photocatalyst **PC-a** (14 mg, 25 μmol) and radical precursor **2a** (348 mg, 1.0 mmol) were sequentially added. The Schlenk tube was put under vacuum and backfilled with argon three times. Then, 4 mL of an argon-sparged 0.15 M acetonitrile solution of TFA (46 μL, 0.6 mmol, 60 mol%) were added, followed by crotonaldehyde **1a** (331 μL, 4.0 mmol). The Schlenk tube was sealed with Parafilm, and quickly placed into the reactor described above, with the temperature set at -10 °C. The reaction was stirred for 12 hours, then the solvent was evaporated and the crude mixture was purified by flash column chromatography on silica gel to furnish product **3a** (254 mg, 0.74 mmol, 74% yield, 86% ee) as a yellow oil.
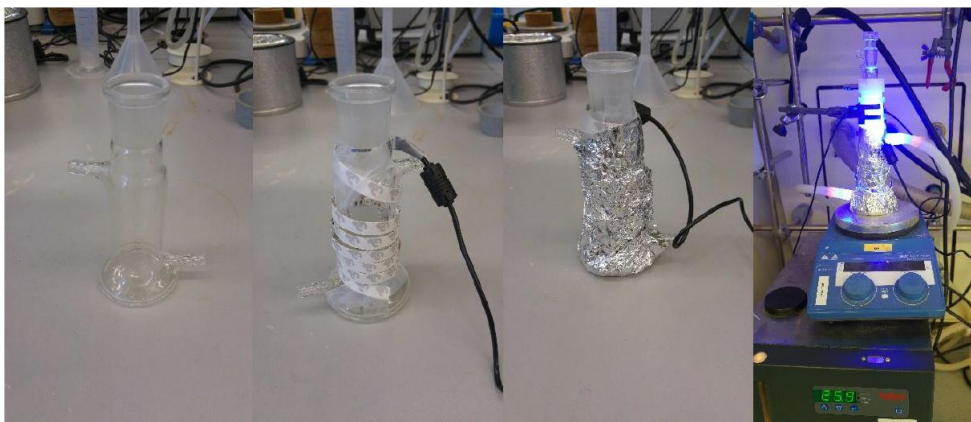
Figure 2.39. Fully assembled photoreactor for the 1 mmol scale photochemical radical conjugate addition.

2.7.6 General procedure for the synthesis of piperidines
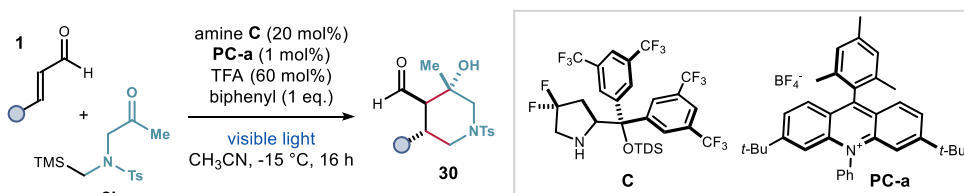
General procedure B. To an argon-purged glass vial containing the amine catalyst **C** (28.2 mg, 0.04 mmol), photocatalyst **PC-a** (1.2 mg, 2.0 μmol) and biphenyl (30.8 mg, 0.2 mmol) was added radical precursor **2b** (0.2 mmol) dissolved in 800 μL anhydrous acetonitrile. The solution was sparged with nitrogen for 5 minutes. Then, TFA (9.2 μL, 0.12 mmol) and enal **1** (0.4 mmol) were added. The vial was sealed with Parafilm, and placed in the photochemical reactor described Figure S2.3. The reaction was stirred for 18 hours at -10 ºC, then the solvent was evaporated and the crude mixture was purified by flash column chromatography on silica gel to furnish piperidines **30**.
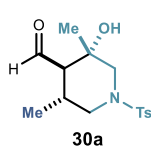
(3S,4R,5R)-3-Hydroxy-3,5-dimethyl-1-tosylpiperidine-4-carbaldehyde (30a)

Prepared according to general procedure B using (*E*)-but-2-enal (32.8 μL, 0.4 mmol) and radical precursor **2b** (62.6 mg, 0.2 mmol). The crude mixture was purified by column chromatography (solid load, RediSep column, Silica 12g, 75:25 hexanes:EtOAc) to afford product **30a** as a colorless gum (37 mg, 63% yield, average of two runs, 96% ee). The enantiomeric excess was determined by HPLC analysis on a Daicel

UNIVERSITAT ROVIRA I VIRGILI
PHOTOCHEMISTRY AND ORGANOCATALYSIS FOR RADICAL-BASED CARBON-CARBON BOND-FORMING PROCESSES
Emilien Le Saux

71

Chiralpak IC-3 column (gradient: 7 min, *i*-hexane with 0.1% acetic acid/*i*-PrOH with 0.1% acetic acid, from 85:15 to 50:50, flow rate: 1.0 mL/min, 40 °C; λ = 254 nm: τ_{minor} = 4.5 min, τ_{major} = 4.9 min).

^{1}H NMR (400 MHz, CDCl$_3$) δ = 9.82 (d, *J* = 2.3 Hz, 1H), 7.61 (d, *J* = 8.2 Hz, 2H), 7.33 (d, *J* = 7.9 Hz, 2H), 3.76 (ddd, *J* = 11.6, 4.7, 1.6 Hz, 1H), 3.54 (dd, *J* = 11.0, 1.7 Hz, 1H), 2.46 - 2.41 (m, 3H), 2.30 - 2.18 (m, 1H), 2.14 (d, *J* = 11.0 Hz, 1H), 1.94 (dd, *J* = 11.6, 2.3 Hz, 1H), 1.84 (t, *J* = 11.5 Hz, 1H), 1.39 (s, 3H), 0.92 (d, *J* = 6.5 Hz, 3H)

^{13}C NMR (101 MHz, CDCl$_3$) δ = 204.41, 143.89, 132.86, 129.81, 127.53, 71.39, 63.65, 57.85, 52.08, 28.90, 22.50, 21.53, 16.67

HRMS (ESI$^+$) Calculated for C$_{15}$H$_{21}$NO$_4$S [M+H]$^+$: 312.12641, found: 312.1265.

(3*S*,4*R*,5*R*)-3-Hydroxy-3-methyl-5-propyl-1-tosylpiperidine-4-carbaldehyde (30b)

Prepared according to general procedure B using (*E*)-hex-2-enal (46.3 µL, 0.4 mmol) and radical precursor **2b** (62.6 mg, 0.2 mmol). The crude mixture was purified by column chromatography (solid load, RediSep column, Silica 4g, 100:0 to 70:30 cyclohexane/EtOAc over 15 min) to afford product **30b** as a colorless gum (49 mg, 72% yield, average of two runs, 86% ee). The enantiomeric excess was determined by HPLC analysis on a Daicel Chiralpak IC-3 column (gradient: 7 min, *i*-hexane with 0.1% acetic acid/*i*-PrOH with 0.1% acetic acid, from 85:15 to 50:50, flow rate: 1.0 mL/min, 40 °C; λ = 254 nm: τ_{minor} = 4.2 min, τ_{major} = 4.6 min).

^{1}H NMR (400 MHz, CDCl$_3$) δ 9.80 (d, *J* = 2.8 Hz, 1H), 7.63 (d, *J* = 8.2 Hz, 2H), 7.34 (d, *J* = 7.9 Hz, 2H), 3.88 (ddd, *J* = 11.5, 4.7, 1.5 Hz, 1H), 3.52 (dd, *J* = 10.9, 1.7 Hz, 1H), 2.83 (br s, 1H), 2.45 (s, 3H), 2.26 - 2.18 (m, 1H), 2.16 (d, *J* = 11.2 Hz, 1H), 1.99 (dd, *J* = 11.5, 2.8 Hz, 1H), 1.89 (t, *J* = 11.2 Hz, 1H), 1.41 (s, 3H), 1.40 - 1.22 (m, 3H), 0.90 (t, *J* = 7.0 Hz, 3H)

^{13}C NMR (101 MHz, CDCl$_3$) δ 173.23, 143.66, 134.78, 129.51, 127.75, 50.49, 39.31, 21.53.

HRMS (ESI$^+$) Calculated for C$_{17}$H$_{26}$O$_4$NS [M+H]$^+$: 340.15771, found: 340.1577.

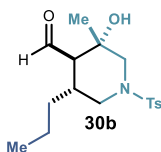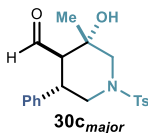### (3*S*,4*R*,5*S*)-3-hydroxy-3-methyl-5-phenyl-1-tosylpiperidine-4-carbaldehyde (30c$_{major}$)

Prepared according to general procedure B using (*E*)-cinnamaldehyde (52.8 µL, 0.4 mmol) and radical precursor **2b** (62.6 mg, 0.2 mmol). The crude mixture was purified by column chromatography (solid load, RediSep column, Silica 12g, 80:20 to 70:30 cyclohexane/EtOAc over 15 min) to afford the major diastereoisomer **30c$_{major}$** as a white solid (96 mg, 42% yield, average of two runs, 91% ee). The enantiomeric excess was determined by HPLC analysis on a Daicel Chiralpak IC-3 column (gradient: 7 min, *i*-

hexane with 0.1% acetic acid/i-PrOH with 0.1% acetic acid, from 85:15 to 50:50, flow rate: 1.0 mL/min, 40 °C; $\lambda = 254$ nm: $\tau_{major} = 5.0$ min, $\tau_{minor} = 5.5$ min). $[\alpha]_D^{20} = +86.3$ (c = 1.0, CHCl$_3$, 91% ee).

^{1}H NMR (400 MHz, CDCl$_3$) δ 9.48 (d, $J = 1.7$ Hz, 1H), 7.51 (d, $J = 8.3$ Hz, 2H), 7.27 - 7.16 (m, 5H), 7.13 - 7.08 (m, 2H), 3.84 (ddd, $J = 1.7, 4.6, 11.7$ Hz, 1H), 3.59 (dd, $J = 1.7, 11.1$ Hz, 1H), 3.26 (dt, $J = 4.6, 12.1$ Hz, 1H), 3.11 - 2.84 (m, 1H), 2.58 (dd, $J = 1.7, 12.6$ Hz, 1H), 2.35 (s, 4H), 2.23 (d, $J = 11.1$ Hz, 1H), 2.15 (t, $J = 11.7$ Hz, 1H), 1.41 (s, 3H)

^{13}C NMR (101 MHz, CDCl$_3$) δ 204.55, 143.94, 137.94, 132.86, 129.84, 129.18, 127.96, 127.93, 127.52, 71.48, 60.80, 57.53, 52.66, 41.05, 22.24, 21.53

HRMS (ESI$^+$) Calculated for C$_{20}$H$_{24}$NO$_4$S [M+H]$^+$: 374.14206; measured: 374.1425.
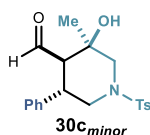
(3R,4R,5S)-3-hydroxy-3-methyl-5-phenyl-1-tosylpiperidine-4-carbaldehyde (30c$_{minor}$)

Prepared according to general procedure B using (E)-cinnamaldehyde (52.8 µL, 0.4 mmol) and radical precursor **2b** (62.6 mg, 0.2 mmol). The crude mixture was purified by column chromatography (solid load, RediSep column, Silica 12g, 80:20 to 70:30 cyclohexane/EtOAc over 15 min) to afford the minor diastereoisomer **30c$_{minor}$** as a white solid (48 mg, 24% yield, average of two runs, 99% ee). The enantiomeric excess was determined by HPLC analysis on a Daicel Chiralpak IC-3 column (gradient: 7 min, i-hexane with 0.1% acetic acid/i-PrOH with 0.1% acetic acid, from 85:15 to 50:50, flow rate: 1.0 mL/min, 40 °C; $\lambda = 254$ nm: $\tau_{minor} = 6.7$ min, $\tau_{major} = 6.9$ min).

^{1}H NMR (400 MHz, CDCl$_3$) δ 9.51 (d, $J = 4.2$ Hz, 1H), 7.63 (d, $J = 8.2$ Hz, 2H), 7.38 - 7.20 (m, 8H), 7.14 (br d, $J = 7.0$ Hz, 3H), 3.99 (ddd, $J = 1.5, 4.4, 11.7$ Hz, 1H), 3.73 – 3.60 (m, 2H), 2.89 (br S, 2H), 2.44 (s, 3H), 2.34 – 2.28 (m, 2H), 2.23 (t, $J = 11.8$ Hz, 1H), 1.32 (s, 5H).

^{13}C NMR (101 MHz, CDCl$_3$) δ 203.38, 144.20, 137.74, 132.87, 129.95, 129.09, 127.95, 127.63, 69.30, 60.58, 57.07, 51.79, 39.44, 25.07, 21.56.

UNIVERSITAT ROVIRA I VIRGILI
PHOTOCHEMISTRY AND ORGANOCATALYSIS FOR RADICAL-BASED CARBON-CARBON BOND-FORMING
PROCESSES
Emilien Le Saux

73

2.7.7 One-pot radical conjugate addition iminium cascade
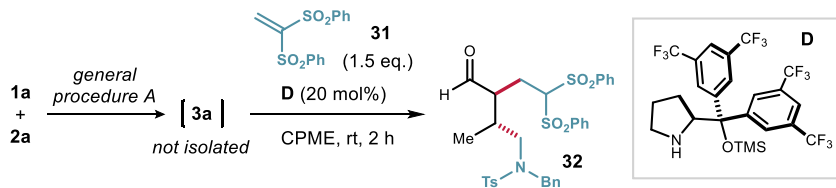
N-benzyl-N-((2R,3S)-3-formyl-2-methyl-5,5-bis(phenylsulfonyl)pentyl)-4

methylbenzene sulfonamide (32) The radical conjugate addition was performed following General Procedure A using (E)-but-2-enal (16.5 μL, 0.2 mmol) and radical precursors **2a** (34.8 mg, 0.1 mmol). After an irradiation time of 16 hours (465 nm, 60 mW/cm2), the reaction was allowed to reach room temperature. The amine catalyst (S)-**D** (12 mg, 0.02 mmol), cyclopentyl methyl ether (1 mL) and 1,1-bis(phenylsulfonyl)ethylene **31** (46 mg, 0.15 mmol) were added in this order and the reaction stirred for 2 hours at ambient temperature. The solvent was then removed under reduced pressure. The diastereomeric ratio (dr) was determined to be 4.3:1 (*anti/syn*) by ^{1}H NMR analysis of the crude mixture. The crude mixture was purified by column chromatography (SiO$_2$, 80:20 to 70:30 hexanes/EtOAc) to afford product **32** as a white solid (53 mg, 81% yield, 96% ee). The enantiomeric excess was determined by UPC^2 analysis analysis on a Daicel Chiralpak IC-3 column (gradient: 1 min 100% CO$_2$, 5 min from 100% CO$_2$ to 60% CO$_2$ - 40% CH$_3$CN, flow rate 2 mL/min, λ = 253 nm: τ_{Major} = 5.9 min, τ_{Minor} = 6.2 min). $[\alpha]_D^{26}$ = +29.4 (c = 0.29, CHCl$_3$, 96% ee).

^{1}H NMR (500 MHz, CDCl$_3$) δ 8.84 (s, 1H), 7.99 – 7.92 (m, 3H), 7.94 – 7.88 (m, 2H), 7.72 – 7.68 (m, 2H), 7.69 – 7.62 (m), 7.60 – 7.48 (m), 7.39 – 7.35 (m, 2H), 7.31 – 7.28 (m, 3H), 7.24 – 7.20 (m, 2H), 4.71 (t, J = 5.7 Hz, 1H), 4.46 (d, J = 13.8 Hz, 1H), 3.91 (d, J = 13.9 Hz, 1H), 3.07 (td, J = 7.0, 2.8 Hz, 1H), 3.00 (dd, J = 14.5, 9.6 Hz, 1H), 2.82 (dd, J = 14.6, 6.4 Hz, 1H), 2.62 – 2.54 (m, 1H), 2.46 (s, 3H), 1.95 (dd, J = 6.8, 2.9 Hz, 1H), 1.93 – 1.84 (m, 1H), 0.56 (d, J = 7.0 Hz, 3H).

^{13}C NMR (101 MHz, CDCl$_3$) δ 202.45, 144.06, 138.12, 137.52, 136.54, 135.31, 134.85, 134.57, 134.44, 134.38, 129.99, 129.77, 129.74, 129.52, 129.45, 129.40, 129.28, 129.18, 129.15, 129.05, 128.99, 128.89, 128.85, 128.56, 128.48, 128.24, 127.62, 127.42, 80.07, 77.35, 77.03, 76.72, 54.95, 52.46, 49.12, 33.47, 22.04, 21.59, 21.56, 13.45.

HRMS (ESI$^+$) Calculated for C$_{33}$H$_{35}$NNaO$_7$S$_3^+$ [M+Na]$^+$: 676.1468; found: 676.1460.

The relative configuration of product **32** was inferred considering the known absolute configuration of intermediate **3a**, formed upon iminium-ion-mediated radical conjugate addition, and on the basis of the stereochemical induction inferred by the silyl prolinol catalyst

of type **D** in the enamine-mediated addition of aldehydes to 1,1-bis(phenylsulfonyl)ethylene **31**, as reported by Alexakis and co-wokers.[50]

2.7.8 Quantum yield determination

A ferrioxalate actinometer solution was prepared by following the Hammond variation of the Hatchard and Parker procedure[51] outlined in the *Handbook of Photochemistry*.[52] Ferrioxalate actinometer solution measures the decomposition of ferric ions to ferrous ions, which are complexed by 1,10-phenanthroline and monitored by UV/Vis absorbance at 510 nm. The moles of iron-phenanthroline complex formed are related to moles of photons absorbed. The values of the quantum yield of potassium ferrioxalate are related to concentration and wavelength.

The solutions were prepared and stored in the dark (red light):

1. **Potassium ferrioxalate solution 0.012M**: 147.4 mg of potassium ferrioxalate (commercially available from Alfa Aesar) and 69.5 µL of sulfuric acid (96%) were added to a 25 mL volumetric flask, and filled to the mark with water (HPLC grade).

2. **Phenanthroline solution**: 0.2% by weight of 1,10-phenanthroline in water (100 mg in 50 mL volumetric flask or 50 mg in 25 mL).

3. **Buffer solution**: to a 100 mL volumetric flask 4.94 g of NaOAc and 1.0 mL of sulfuric acid (96%) were added and filled to the mark with water (HPLC grade).

4. **Internal standard solution**: 1.052 g of 1,3,5-trimethoxybenzene was added to a 5 mL volumetric flask which was filled up with HPLC grad acetonitrile (1.25 M).

Reaction setup:

1. **Reaction solution**: A Schlenk flask with stir bar was charged with amine catalyst **C** (35.3 mg, 0.05 mmol), **2a** (69.6 mg, 0.25 mmol), **4a** (3.5 mg, 6.25 µmol), acetonitrile (1 mL). After three cycles of freeze pump thaw (with septum), TFA (11.5 µL, 0.15 mmol) and (*E*)-4-methylpent-2-enal (58.3 µL, 0.5 mmol) were added and the tube was sealed with parafilm and put in the HP-LED 460 nm at 1 cm distance at -10 ºC with irradiance of 38 mW/cm^2. Four different reactions were setup and irradiated for different times: 15 min, 30 min, 45 min and 60 min. After each reaction was

[50] S. Sulzer-Mossé, A. Alexakis, J. Mareda, G. Bollot, G. Bernardinelli, Y. Filinchuk. "Enantioselective Organocatalytic Conjugate Addition of Aldehydes to Vinyl Sulfones and Vinyl Phosphonates as Challenging Michael Acceptors" *Chem. Eur. J.* **2009**, *15*, 3204.

[51] Hatchard, C. G.; Parker, C. A. "A New Sensitive Chemical Actinometer II. Potassium Ferrioxalate as a Standard Chemical Actinometer. *Proc. R. Soc. (London)*, **1956**, *A235*, 518.

[52] Montalti, M.; Credi, A.; Prodi, L.; Gandolfi, M. T. *Handbook of Photochemistry*, Taylor&Francis, **2006**, 601.

UNIVERSITAT ROVIRA I VIRGILI
PHOTOCHEMISTRY AND ORGANOCATALYSIS FOR RADICAL-BASED CARBON-CARBON BOND-FORMING
PROCESSES
Emilien Le Saux

75

finished, internal standard solution (200 µL, 0.25 mmol) was added. 500 µL of this solution was diluted with 4.5 mL of acetonitrile. From this solution were taken 100 µL, diluted to 1 mL and analyzed by GC-FID.

2. **Actinometer solutions:** A Schlenk flask of the same dimensions as used for the reaction mixtures was loaded with 1.0 mL of actinometer solution and placed on the HP-LED the same light intensity as the reaction (without freeze pump thaw). Four different actinometer solutions were irradiated in sequence for 5 s, 10 s, 15 s, 20 s and 25 s. To irradiate the Schlenk, it was placed on the holder with the light off and the light was turned on for the desired time. After each irradiation the actinometer solutions were carefully transferred into a 10 mL volumetric flask, then 0.5 mL of phenanthroline solution and 2.0 mL of buffer solution were added and the flask was filled up with water. The mixture was then analysed by UV-Vis (Figure 2.40).
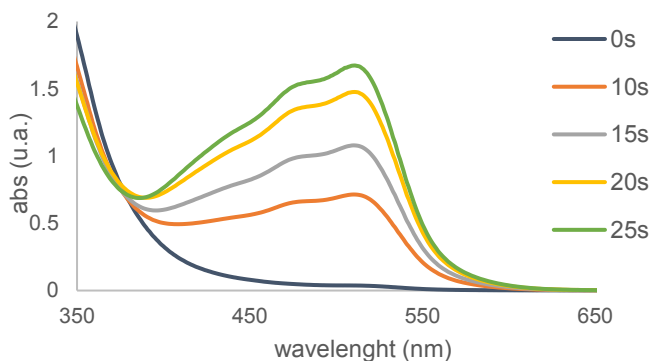
Figure 2.40. UV-Vis spectra of the actinometer solutions irradiated for different periods of times.

The moles of Fe^{2+} formed for each sample are determined using Beers' Law (Equation 2):

$$moles\ of\ Fe(II) = \frac{V_1\ V_3\ \Delta A(510\ nm)}{10^3\ V_2\ l\ \epsilon(510\ nm)} \quad (\textbf{Eq. 2})$$

Where V_1 is the irradiated volume (1 mL), V_2 is the aliquot of the irradiated solution taken for the determination of the ferrous ions (1 mL), V_3 is the final volume after complexation with phenanthroline (10 mL), l is the optical path-length of the irradiation cell (1 cm), $\Delta A(510$ nm) is the optical difference in absorbance between the irradiated solution and the one stored in the dark, $\epsilon(510$ nm) is the extinction coefficient the complex $Fe(phen)_3^{2+}$ at 510 nm (11100 L mol^{-1} cm^1).

The moles of Fe^{2+} formed (x) are plotted as a function of time (t) (Figure 2.41). The slope of this line was correlated to the moles of incident photons by unit of time ($q^0_{n,p}$) by the use of the following Equation 3:

$$\Phi(\lambda) = \frac{dx/dt}{q_{n,p}^0 [1 - 10^{-A(\lambda)}]} \quad (\textbf{Eq. 3})$$

where dx/dt is the rate of change of a measurable quantity (spectral or any other property), the quantum yield (Φ) for Fe^{2+} at 458 nm is 1.11,[25] $[1-10^{-A(\lambda)}]$ is the ratio of absorbed photons by the solution, and A(λ) is the absorbance of the actinometer at the wavelength used to carry out the experiments (460 nm). The absorbance at 460 nm ($A(460)$) was 1.04.
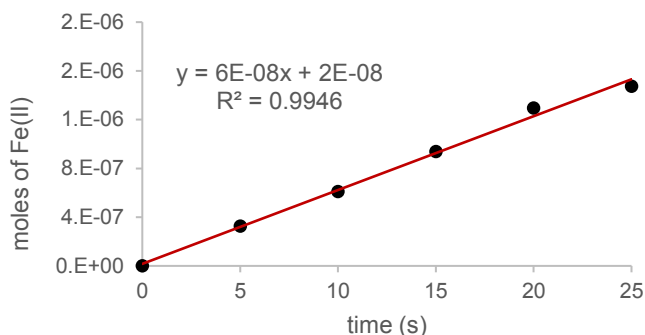
Figure 2.41. Plot of the moles of Fe^{2+} generated from the irradiation of the actinometer solutions, against time.

The photon flux, which is $q^0_{n,p}$, was determined as **1,81249x10^{-7} einstein s^{-1}**.

The moles of product per unit of time are plotted against the number of photons absorbed (Figure 2.42). The photons absorbed are correlated to the number of incident photons by the use of Equation 3. According to this, if we plot the moles of product (x-axis) versus the moles of incident photons ($q^0_{n,p}$dt), the slope is equal to:

$$\text{slope} = \Phi\left[1 - 10^{-A(460\ nm)}\right] \quad (\textbf{Eq. 4})$$

where Φ is the quantum yield to be determined and A(460 nm) is the absorption of the reaction under study. A(460 nm) was measured to be of 1.29 for the model reaction mixture.

UNIVERSITAT ROVIRA I VIRGILI
PHOTOCHEMISTRY AND ORGANOCATALYSIS FOR RADICAL-BASED CARBON-CARBON BOND-FORMING
PROCESSES
Emilien Le Saux

77

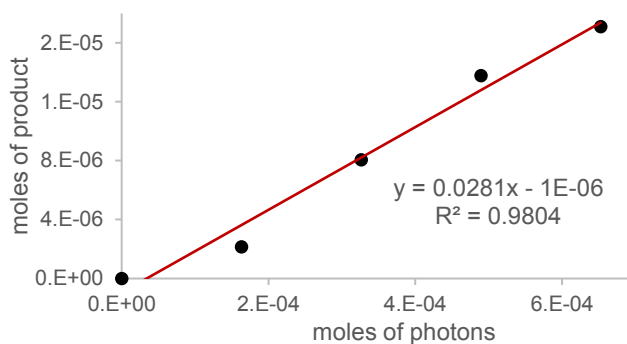**Figure 2.42.** Plot of the moles of products generated from the irradiation of the reaction solutions, against the moles of photons absorbed by each reaction solution.

The quantum yield Φ of the conjugate radical addition of **2a** to (E)-4-methylpent-2-enal was calculated to be **0.03** (the procedure was repeated a second time, $\Phi = 0.02$ was found.

Chapter III

Photochemical Organocatalytic Benzylation of Allylic C-H Bonds

Target

To develop a thiol-catalyzed benzylation of allylic C-H bonds using visible light activation.

Tool

Use of two distinct mechanisms of activation available to thiol catalysis to generate carbon-centered radicals: the formation of photoactive electron donor-acceptor (EDA) complexes and hydrogen atom abstraction from weak C-H bonds.[1]
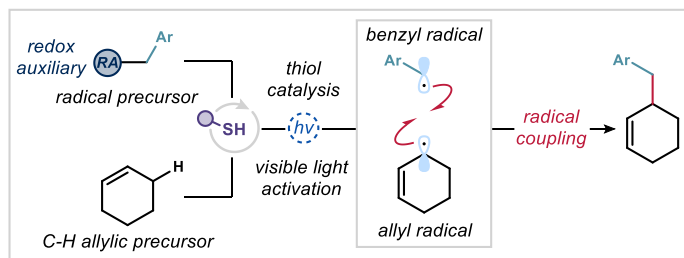
3.1 General introduction

Photoredox catalysis is a powerful and reliable strategy to secure the formation of reactive radical intermediates under mild conditions. The variety of available photocatalysts with distinct photophysical and redox properties offers a large toolbox from which synthetic chemists can pick to implement photocatalytic systems.[2] An alternative approach for radical formation has recently attracted the attention of the chemistry community, as it does not require an external photocatalyst as intermediary between visible light and substrates. Instead, this strategy exploits the formation of photoactive aggregates between colorless species.[3] These so-called electron donor-acceptor (EDA) complexes are formed by association of two compounds through generation of a new set of molecular orbitals. This is due to re-hybridization of the frontier orbitals of the two partners (HOMO for the donor and LUMO for

---

[1] The project discussed in this chapter has been conducted in collaboration with Dr. Margherita Zanini. I performed the initial experiments that led to the discovery of the reaction and the optimization. I was then involved in the investigation of the scope of the reaction and in the mechanistic elucidation. This study has been published: Le Saux, E.; Zanini, M.; Melchiorre, P. "Photochemical Organocatalytic Benzylation of Allylic C-H Bonds" *J. Am. Chem. Soc.* **2022**, *144*, 113.

[2] Shaw, M. H., Twilton, J., MacMillan, D. W. C. "Photoredox Catalysis in Organic Chemistry" *J. Org. Chem.* **2016**, *81*, 6898.

[3] Crisenza, G. E. M.; Mazzarella, D.; Melchiorre, P. "Synthetic Methods Driven by the Photoactivity of Electron Donor–Acceptor Complexes" *J. Am. Chem. Soc.* **2020**, *142*, 5461.

UNIVERSITAT ROVIRA I VIRGILI
PHOTOCHEMISTRY AND ORGANOCATALYSIS FOR RADICAL-BASED CARBON-CARBON BOND-FORMING
PROCESSES
Emilien Le Saux

79

the acceptor).[4] Although the two components, the acceptor (**A**) and the donor (**D**), may not absorb visible light themselves, the resulting EDA complex generally does (Figure 3.1.a). Irradiation of the ground-state EDA complex may result in an intracomplex single-electron transfer (SET) from the donor to the acceptor, triggering the formation of a radical ion pair (Figure 3.1.b). This radical ion pair may evolve to the formation of a radical, although this is usually hampered by fast and unproductive back-electron transfer (BET). A common strategy to promote the desirable radical generation pathway is to adorn one of the partners with a leaving group (LG) in order to push the radical generation through irreversible fragmentation of the radical ion.
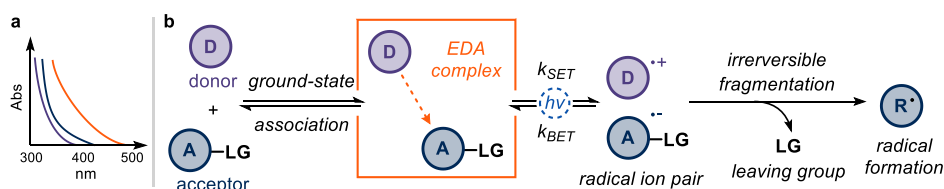
Figure 3.1. (**a**) UV-Vis absorption profile of an EDA complex. (**b**) Formation of a photoactive EDA complex between a donor **D** and an acceptor **A**.

In 2021, our group disclosed an unconventional way of using xanthates **A1** as electron-rich organic catalysts for the formation of photoactive EDA complexes with suitable radical precursors **1** (Figure 3.2).[5] A light-induced, intracomplex SET triggered the formation of a radical **I** via reduction of the radical precursor and subsequent fragmentation, while a sulfur-centered radical **A**• arose from the oxidation of the thiolate **A**⁻. Specifically, it was found that when using radical precursors bearing electron-poor phthalimides **RA-1** and pyridinium salts **RA-2** acting as both redox auxiliaries and leaving group, these donor catalysts allowed the generation of simple non-stabilized alkyl, electrophilic, α-heteroatom, or benzylic radicals. A key aspect of this work was to identify an effective turnover event of catalyst **A** from intermediate **A**•. This essential step was achieved either *via* hydrogen atom transfer (HAT) from a hydrogen atom donor or SET reduction to restore **A**⁻.

[4] Lima, C. G. S.; de M. Lima, T.; Duarte, M.; Jurberg, I. D.; Paixão, M. W. "Organic Synthesis Enabled by Light-Irradiation of EDA Complexes: Theoretical Background and Synthetic Applications" *ACS Catalysis* **2016**, *6*, 1389.

[5] de Pedro Beato, E.; Spinnato, D.; Zhou, W.; Melchiorre, P. "A General Organocatalytic System for Electron Donor−Acceptor Complex Photoactivation and Its Use in Radical Processes" *J. Am. Chem. Soc.* **2021**, *143*, 12304.
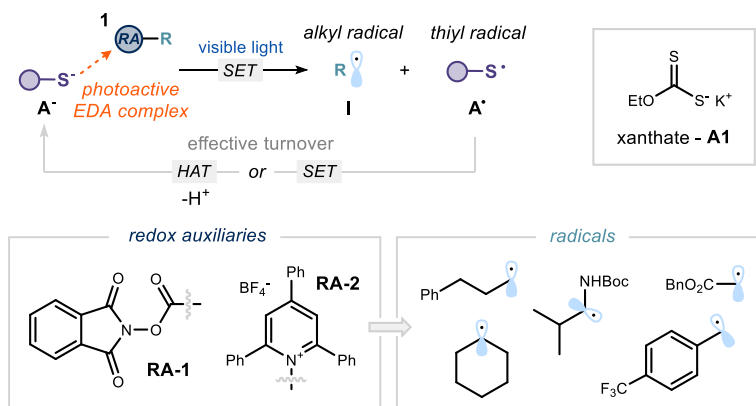
Figure 3.2. Generation of alkyl radicals using thiols as catalytic EDA donors.

We realized that the sulfur-centered radical, which in this report needed to be reduced to achieve catalyst turnover, has a rich chemistry in radical formation. In fact, sulfur-centered radicals have been previously used for the generation of open-shell species from simple $C(sp^3)$-H bonds using a HAT mechanism.[6] In particular, the relatively low bond-dissociation energy (BDE) of S-H bonds (around 87 kcal.mol^{-1})[7] makes thiyl radicals $A^\bullet$ ideal to abstract hydridic hydrogen atoms from allylic positions (BDE C-H of an allylic position is around 83 kcal.mol^{-1})[8] with high selectivity, thus generating allylic radicals **II** (Figure 3.3).
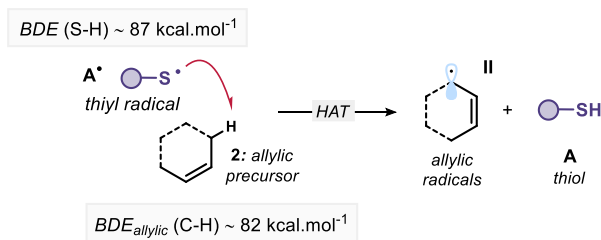
Figure 3.3. HAT-mediated generation of allylic radicals using sulfur-centered radicals.

Considering the tendency of sulfur anions to form EDA complexes and generate sulfur-centered radicals upon SET, and the ability of the latter to serve as HAT mediator, we sought to combine these two catalytic mechanisms to generate two radicals **I** and **II** through sequential EDA complex and HAT activation (Figure 3.4).

---

[6] These reports will be discussed in details later in the chapter.

[7] Denisov, E., Chatgilialoglu, C., Shestakov, A.; Denisova, T. "Rate Constants and Transition-State Geometry of Reactions of Alkyl, Alkoxyl, and Peroxyl Radicals with Thiols" *Int. J. Chem. Kinet*. **2009**, *41*, 284.

[8] Khursan, S. L., Mikhailov, D. A., Yanborisov, V. M.; Borisov, D. I. "AM1 Calculations of Bond Dissociation Energies. Allylic and Benzylic C–H Bonds" *React. Kinet. Catal. Lett*. **1997**, *61*, 91.

UNIVERSITAT ROVIRA I VIRGILI
PHOTOCHEMISTRY AND ORGANOCATALYSIS FOR RADICAL-BASED CARBON-CARBON BOND-FORMING
PROCESSES
Emilien Le Saux

81
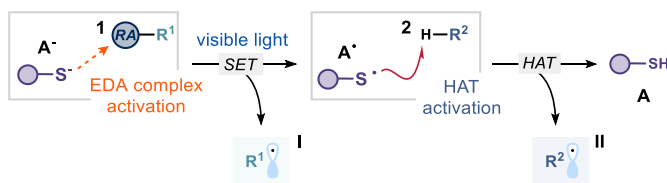
Figure 3.4. Envisioned radical generation strategy using thiol-mediated sequential EDA complex and HAT activation.

The two open-shell species could combine in a radical cross-coupling event to form a new C-C bond. To be feasible, this mechanistic scenario requires stabilized radicals to be formed, in order to favor the radical coupling step.[9] Thus, benzylic and allylic partners were selected as they are both resonance-stabilized radicals.[10]

In this chapter, we describe the catalytic benzylation of simple allylic C-H bonds proceeding via cross coupling of transient benzylic and allylic radicals (Figure 3.5). The system relies on a single organic thiol catalyst **A** sequentially acting as a donor for the formation of photoactive EDA complexes with radical precursors **1**, and as a hydrogen atom abstractor to activate C-H allylic bonds from alkenes **2**. Benzylic and allylic radicals (**I** and **II** respectively) are formed through SET and HAT events, respectively, before coupling with each-other to afford the cross-product **3**. While this direct approach afforded dimeric side products, a three-component version of the transformation was also developed, and granted complete cross-selectivity.
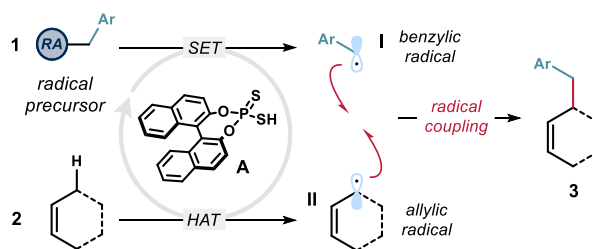
Figure 3.5. Thiol-catalyzed benzylation of allylic C-H bonds.

In the following sections, literature precedents on the formation of benzylic-allylic C-C bonds will be discussed. The scientific background and previous studies that were essential to the development of the present research project will also be detailed.

---

[9] Leifert, D.; Studer, A. "The Persistent Radical Effect in Organic Synthesis" *Angew. Chem. Int. Ed*. **2020**, *59*, 74.

[10] Sowndart, S. S. V.; St. John, P. C.; Paton, R. S. "A Quantitative Metric for Organic Radical Stability and Persistence Using Thermodynamic and Kinetic Features" *Chem. Sci*., **2021**, *12*, 13158.

UNIVERSITAT ROVIRA I VIRGILI
PHOTOCHEMISTRY AND ORGANOCATALYSIS FOR RADICAL-BASED CARBON-CARBON BOND-FORMING
PROCESSES
Emilienne Saux

82

3.2 Background

3.2.1 Catalytic allylic benzylation using benzylic nucleophiles

Transition metal-catalyzed allylic substitution has been the method of choice to perform allylic benzylation reactions. This well-studied chemistry proceeds via the formation of a metal-π-allyl complex formed upon oxidative addition of a low-valent metal catalyst into an allylic precursor bearing a leaving group (Figure 3.6).[11] These complexes are typically electrophilic and thus react with suitable nucleophiles. The modes of attack of the nucleophiles are classified depending on the pK_a of the corresponding pronucleophiles. While - according to hard and soft acids and bases (HSAB) theory - "soft" nucleophiles ($pK_a < 25$) react via an outer-sphere mechanism, "hard" counterparts ($pK_a > 25$) first add to the metal center to then couple with the allyl moiety through reductive elimination (inner-sphere mechanism).[12] Since benzylic pronucleophiles have pK_a's > 30, they belong to the latter category.
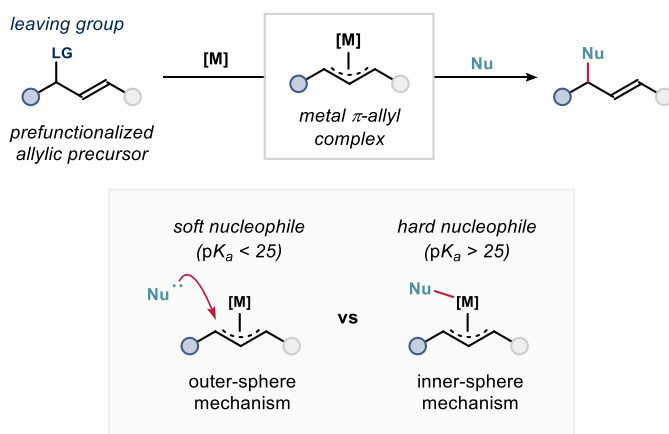
Figure 3.6. Metal-catalyzed allylic substitution and its mechanistic variance depending on the nucleophile.

In order to develop allylic substitution reactions with benzylic pronucleophiles, it was necessary to find ways to overcome such "hardness", as most strong non-nucleophilic bases do not have pK_a's high enough to deprotonate toluene derivatives **4** (pK_a for toluene = 44). A seminal report from the group of Trost used Lewis acids to lower the pK_a of picoline derivatives **4a** (Figure 3.7).[6] Later, they found that substituted diazines **4b** were acidic enough to omit the activating agent.[13]

---

[11] Van Vranken, D. L., Trost, B. M. "Asymmetric Transition Metal-Catalyzed Allylic Alkylations" *Chem. Rev.* **1996**, *96*, 395.

[12] Trost, B. M.; Thaisrivongs, D. A. "Strategy for Employing Unstabilized Nucleophiles in Palladium-Catalyzed Asymmetric Allylic Alkylations" *J. Am. Chem. Soc.* **2008**, *130*, 14092.

[13] Trost, B. M.; Thaisrivongs, D. A.; Hartwig, J. "Palladium-Catalyzed Asymmetric Allylic Alkylations of Polynitrogen- Containing Aromatic Heterocycles" *J. Am. Chem. Soc.* **2011**, *133*, 12439.

UNIVERSITAT ROVIRA I VIRGILI
PHOTOCHEMISTRY AND ORGANOCATALYSIS FOR RADICAL-BASED CARBON-CARBON BOND-FORMING
PROCESSES
Emilien Le Saux

83

Figure 3.7. Seminal reports of palladium-catalyzed allylic benzylation using benzylic nucleophiles under strongly basic conditions.

Using a different strategy, Walsh and co-workers introduced simple toluene derivatives, employing the corresponding (η^6-tolyl)Cr(CO)$_3$ complexes **4c** as pronucleophiles.[14] This method greatly expanded the scope of the chemistry, but required two additional steps to (*i*) first prepare the η^6-complex and then (*ii*) remove chromium from the products. Eventually, the same group showed that diarylmethane derivatives **4d** were amenable to the reaction without the need for activation.[15] Recent examples demonstrated that palladium could be replaced by nickel or rhodium.[16] These key reports proved the feasibility of using be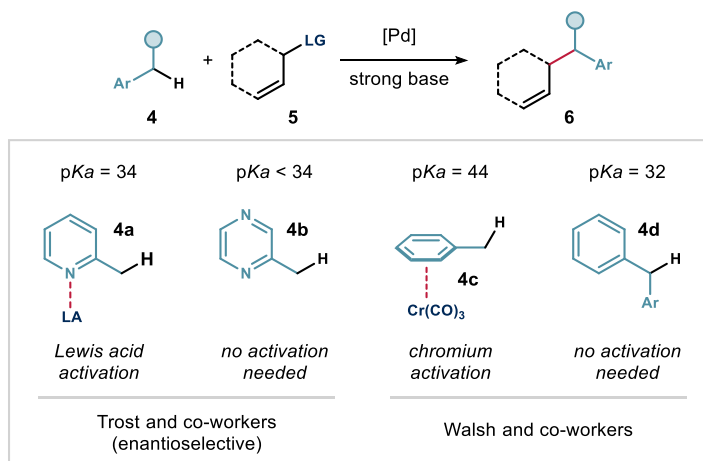nzylic nucleophiles in allylic substitution reactions, but the required strong base (typically silyl amides) significantly affected functional group tolerance, thus limiting a general applicability for these processes.

An inventive approach from Lungdren bypassed this limitation by making use of aryl acetic acids **7** as pronucleophiles (Figure 3.8.a).[17] Activation from the carboxylic acid allowed using milder bases, like DBU or *N*,O-bis(trimethylsilyl)acetamide (BSA), for the formation of benzyl anions in combination with iridium or palladium catalysts. Both linear and cyclic

---

[14] Zhang, J.; Stanciu, C.; Wang, B.; Hussain, M. M.; Da, C.; Carroll, P. J.; Dreher, S. D.; Walsh, P. J. "Palladium-Catalyzed Allylic Substitution with (η^6 -Arene–CH$_2$Z)Cr(CO)$_3$-Based Nucleophiles" *J. Am. Chem. Soc.* **2011**, *133*, 20552

[15] Sha, S. C.; Zhang, J.; Carroll, P. J.; Walsh, P. J. "Raising the pK$_a$ Limit of "Soft" Nucleophiles in Palladium-Catalyzed Allylic Substitutions: Application of Diarylmethane Pronucleophiles" *J. Am. Chem. Soc.* **2013**, *135*, 17602.

[16] (a) Sha, S. C.; Jiang, H.; Mao, J.; Bellomo, A.; Jeong, S. A.; Walsh, P. J. "Nickel-Catalyzed Allylic Alkylation with Diarylmethane Pronucleophiles: Reaction Development and Mechanistic Insights" *Angew. Chem., Int. Ed.* **2016**, *55*, 1070; (b) Pal, D.; Wright, T. B.; O'Connor, R.; Evans, P. A. "Regio- and Diastereoselective Rhodium-Catalyzed Allylic Substitution with Unstabilized Benzyl Nucleophiles" *Angew. Chem., Int. Ed.* **2021**, *60*, 2987.

[17] Moon, P. J.; Wei, Z.; Lundgren, R. J. "Direct Catalytic Enantioselective Benzylation from Aryl Acetic Acids" *J. Am. Chem. Soc.* **2018**, *140*, 17418.

allylic precursors were suitable (**8** and **9**, respectively). These conditions secured a better functional group tolerance, albeit with an additional decarboxylation step needed to obtain the final products **11** (Figure 3.8.b).
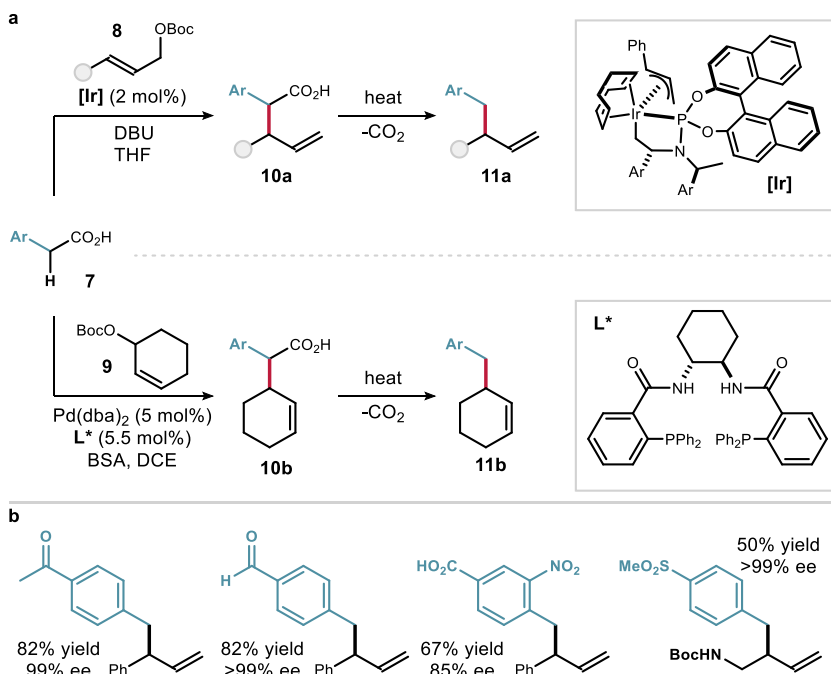
Figure 3.8. (**a**) Iridium and palladium-catalyzed asymmetric allylic alkylation using aryl acetic acids as benzylic pronucleophiles. (**b**) Selected examples from the scope.

Another approach combining palladium and photocatalysis was recently reported by Wang and co-workers (Figure 3.9).[18] In this system, the key benzyl anion **IV** was generated by SET reduction of a benzylic radical **III**, which was itself emerging from addition of an alkyl radical to a styrene derivative **13**. 5,7,12,14-Pentacenetetrone **PT** was used as a HAT catalyst to generate alkyl radicals from simple alkanes **12**, and presumably as the reductant for the formation of the benzylic nucleophiles. An interesting feature of this process was its multicomponent nature, which makes it versatile. Nonetheless, benzylic radicals are rather difficult to reduce (E_{red} for tolyl radical = -1.45 V vs SCE),[19] which mostly limited the scope to α-carbonyl styrenes.

---

[18] Shen, Y.; Dai, Z.-Y.; Zhang, C.; Wang, P.-S. "Palladium-Catalyzed Allylic Alkylation via Photocatalytic Nucleophile Generation" *ACS Catal.* **2021**, *11*, 6757.

[19] Sim, B. A.; Griller, D.; Wayner, D. D. M. "Reduction Potentials for Substituted Benzyl Radicals: pKa Values for the Corresponding Toluenes" *J. Am. Chem. Soc.* **1989**, *111*, 754.

UNIVERSITAT ROVIRA I VIRGILI
PHOTOCHEMISTRY AND ORGANOCATALYSIS FOR RADICAL-BASED CARBON-CARBON BOND-FORMING
PROCESSES
Emilien Le Saux

85

Figure 3.9. Three-component photocatalytic allylic benzylation.

3.2.2 Catalytic benzylic allylation using benzylic radicals

Because of the inherent challenges mentioned in the previous section, researchers turned their attention to benzylic radicals as surrogates for benzyl anions. Specifically, it was found that palladium π-allyl chemistry could be combined with radicals in lieu of nucleophiles, using an external photoredox catalyst and visible light to secure the generation of these radicals under mild conditions.
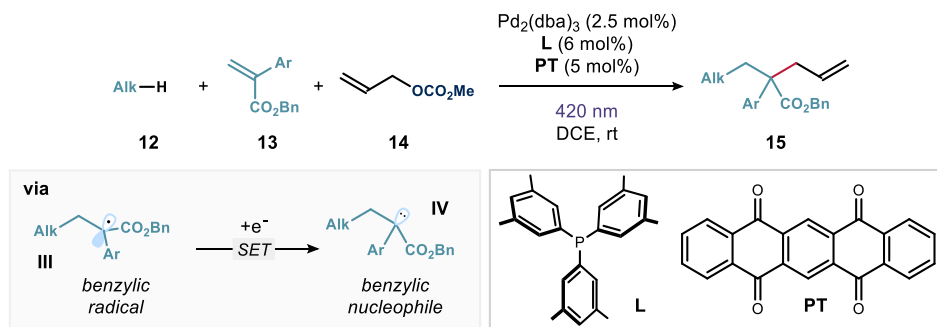
The first report of this kind came from the group of Tunge in 2014 (Figure 3.10).[20] In this innovative work, they designed a bifunctional reagent **16** bearing both the benzyl and allyl moieties. Mechanistically, oxidative addition of allyl ester **16** to Pd^0 afforded a Pd^{II}-π-allyl complex **V** and released the carboxylate intermediate **VI**. SET oxidation of **VI** by the excited iridium photocatalyst delivered a benzylic radical **I** upon decarboxylation.

The authors proposed that SET reduction of Pd^{II}-π-allyl to Pd^{I}-π-allyl **VII** by Ir^{II} led to the generation of an allyl radical **VIII** upon dissociation from the metal, while turning-over Pd^{I} to Pd^0. Eventually, radical-radical coupling between **I** and **VII** would afford the final product. An alternative pathway was also considered, where addition of **I** to complex **V** would afford a Pd^{III} intermediate before undergoing reductive elimination. Formation of the benzylic radicals was directly supported by the detection of dimers **18** in significant amounts, which limited the maximum yield of the reaction. An essential aspect of the transformation was the need for *para*-amino substituents on the benzyl moiety to facilitate the oxidation to the benzyl radical.

---

[20] Lang, S. B.; O'Nele, K. M.; Tunge, J. A. "Decarboxylative Allylation of Amino Alkanoic Acids and Esters via Dual Catalysis" *J. Am. Chem. Soc.* **2014**, *136*, 13606.

UNIVERSITAT ROVIRA I VIRGILI
PHOTOCHEMISTRY AND ORGANOCATALYSIS FOR RADICAL-BASED CARBON-CARBON BOND-FORMING
PROCESSES
Emilien Le Saux

86
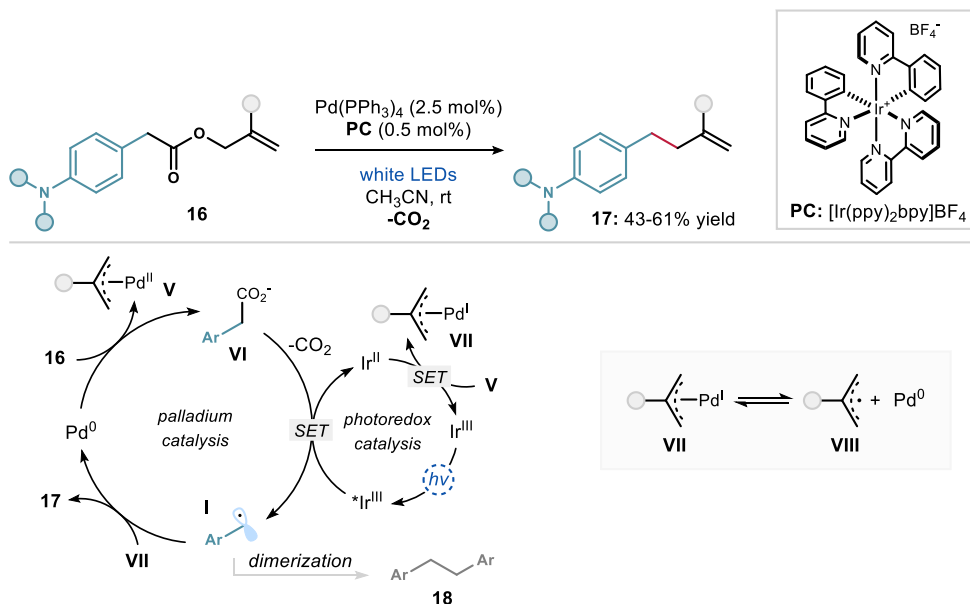
Figure 3.10. Seminal report on the use of benzylic radicals in an allylic benzylation reaction.

In the same report, Tunge and co-workers showed that they could also start from aryl acetic acids **19** and allyl carbonates **14** to generate identical products, avoiding the preformation of allyl esters **16** (Figure 3.11).
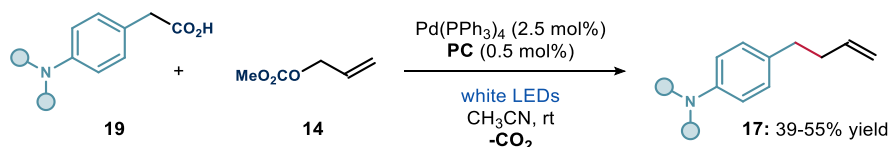
Figure 3.11. Seminal report on the use of benzylic radicals in an allylic benzylation reaction.

Later on, an enantioselective variant was developed by Yu, using Hantzsch ester derivatives **20** as sources of benzyl radicals (Figure 3.12).[21] The proposed mechanism involved the aforementioned Pd[III]-π-allyl intermediate **X**, which delivered the product upon reductive elimination. This time, the competitive formation of allyl radicals **XI** coming from dissociation of Pd[I]-π-allyl complexes was supported by the detection of allyl dimers by GC-MS.

---

[21] Zhang, H. H.; Zhao, J. J.; Yu, S. "Enantioselective Allylic Alkylation with 4-Alkyl-1,4-Dihydro-Pyridines Enabled by Photoredox/Palladium Cocatalysis" *J. Am. Chem. Soc.* **2018**, *140*, 16914.

UNIVERSITAT ROVIRA I VIRGILI
PHOTOCHEMISTRY AND ORGANOCATALYSIS FOR RADICAL-BASED CARBON-CARBON BOND-FORMING
PROCESSES
Emilien Le Saux

87
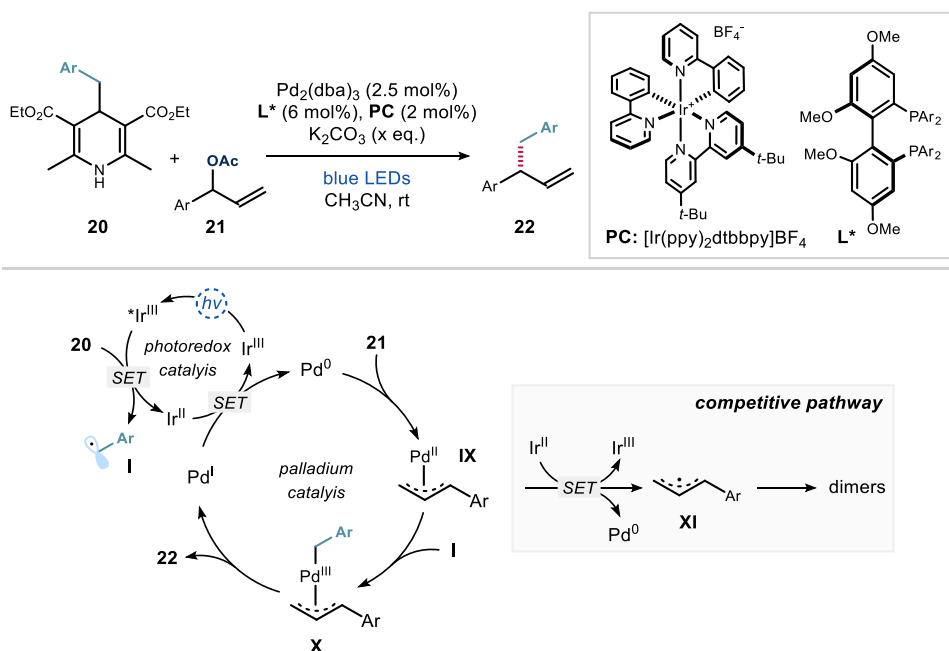
Figure 3.12. Dual photoredox-palladium asymmetric allylic benzylation using DHPs as source of benzylic radicals.

Despite these advances in the field of allylic substitution with benzyl nucleophiles or radicals, these strategies still relied on the use of precious transition metal catalysts and *prefunctionalized* allylic substrates.

3.2.3 Hydrogen Atom Transfer

A central goal in synthetic chemistry is to build molecular complexity from the simplest and/or most readily available starting materials. This challenge implies the necessity to use "native" functionalities to avoid pre-functionalization of the building blocks, with the final aim being the direct functionalization of late-stage intermediates. The most desirable bonds to functionalize are certainly C-H bonds because of their prevalence in organic molecules. While transition metal catalysis has found applications in the functionalization of C(sp^2)-H bonds mostly, the activation C(sp^3)-H bonds is more challenging, and the development of methods for their selective manipulations is still in its infancy.[22]

---

[22] (a) Goldman, A. S.; Goldberg, K. I. Organometallic C−H Bond Activation: An Introduction. In Activation and Functionalization of C− H Bonds; ACS Symposium Series 2004; Vol. 885, pp1−43; (b) Hartwig, J. F.; Larsen, M. A. "Undirected, Homogeneous C−H Bond Functionalization: Challenges and Opportunities" *ACS Cent. Sci.* **2016**, *2*, 281.

In this context, hydrogen atom transfer (HAT) has gained significant attention, as it allows to turn non-reactive $C(sp^3)$-H bonds into highly reactive carbon-centered radical which can engage in a variety of reactions.[23] HAT is defined as the concerted movement of a proton and an electron (a H·) between two substrates (Figure 3.13.a). The main factors influencing these processes are the bond dissociation energies (BDEs) of the two partners and their polarity match or mismatch, respectively. The comparison of the BDEs indicates the thermodynamic feasibility of the HAT, with the newly formed R-H bond needing to be stronger than the breaking C-H bond. The polarity of the partners plays an important role, and helps in predicting the selectivity of the HAT. An example is given in Figure 3.13.b, where the abstracting species is electrophilic. In the case of THF **23**, the C-H bond α-to the oxygen atom is both more hydridic (because of hyperconjugation) and weaker (it has a lower BDE than the other C-H bonds in the molecule), thus abstraction is mostly taking place at this position and leads to the α-oxo radical **XII**. For the 5-membered ring sulfone **24**, the situation is different: the C-H bond α-to the sulfone group is weaker because of conjugation, however it is not as hydridic as the C-H bonds in β-position. This time, the polarity effects take the lead, and the radical **XIII** at the β position is formed preferentially.[24] The main classes of hydrogen abstractors are also shown in Figure 3.13. They are mainly constituted of heteroatom-centered radicals (alkoxy, thiyl, aminium, and amidyl radicals), which are electrophilic abstractors. Methyl radicals or halogen atoms are also useful, as they have rather high BDEs. Finally, polyoxometalates, in particular the decatungstate anion, are commonly used as direct HAT catalysts: upon irradiation with UV light, a ligand-to-metal charge transfer (LMCT) triggers the formation of a HAT-active oxygen-centered radical on the metal complex.[25]

[23] (a) Capaldo, L.; Ravelli, D. "Hydrogen Atom Transfer (HAT): A Versatile Strategy for Substrate Activation in Photocatalyzed Organic Synthesis" *Eur. J. Org. Chem.* **2017**, 2056 (b) Capaldo, L.; Ravelli, D.; Fagnoni, M. "Direct Photocatalyzed Hydrogen Atom Transfer (HAT) for Aliphatic C–H Bonds Elaboration" *Chem. Rev.* **2022**, *122*, 1875.

[24] Sarver, P. J.; Bacauanu, V.; Schultz, D. M.; DiRocco, D. A.; Lam, Y-H. ; Sherer, E. C.; MacMillan, D. W. C. "The Merger of Decatungstate and Copper Catalysis to Enable Aliphatic $C(sp^3)$-H Trifluoromethylation" *Nat. Chem.* **2020**, *12*, 459.

[25] De Waele, V.; Poizat, O.; Fagnoni, M.; Bagno, A.; Ravelli, D. "Unraveling the Key Features of the Reactive State of Decatungstate Anion in Hydrogen Atom Transfer (HAT) Photocatalysis" *ACS Catal.* **2016**, *6*, 7174.
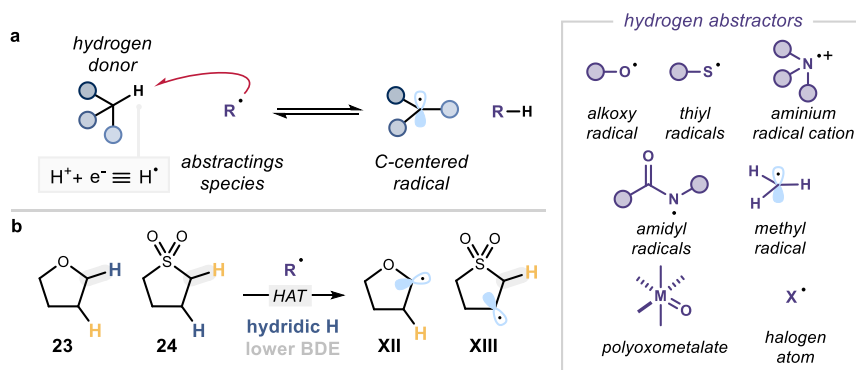
UNIVERSITAT ROVIRA I VIRGILI
PHOTOCHEMISTRY AND ORGANOCATALYSIS FOR RADICAL-BASED CARBON-CARBON BOND-FORMING PROCESSES
Emilien Le Saux

89

Figure 3.13. (a) General concept of hydrogen atom transfer. **(b)** Selectivity in HAT. Yellow hydrogen atoms are protic and blue ones are hydridic.

Figure 3.14 sums up the BDEs of some common molecules as well as their polarity (hydridic or protic hydrogen atoms). The BDE value is a direct indication of the stability of the radical formed upon H-abstraction: the lower the BDE, the more thermodynamically stable is the resulting radical.
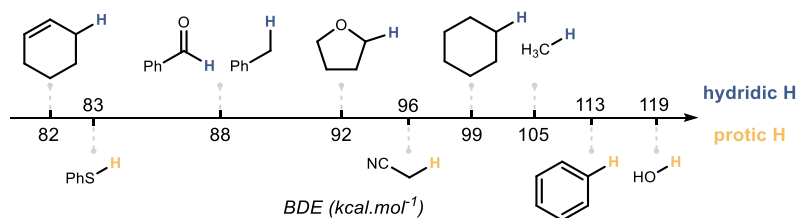
Figure 3.14. Bond-dissociation energies and polarity of some common substrates.

3.2.4 Thiols as HAT catalysts

Thiols are frequently used as HAT catalysts in combination with photoredox catalysis to secure the formation of the HAT-active thiyl radicals. In two pioneering reports from 2014, the group of MacMillan achieved the C-H functionalization of benzylic ethers **25** using a simple aliphatic thiol as HAT catalyst in combination with iridium-based photoredox catalysts (Figure 3.15).[26] The transformations were proposed to proceed *via* radical coupling between long-lived cyanoaryl or imido radical anions (**XV** and **XVI**, respectively) generated by SET reduction of cyanoarenes **26** or Schiff bases **27**, and benzylic radicals **XIV** generated by HAT from the benzylic ethers.

---

[26] (a) Qvortrup, K.; Rankic, D. A.; MacMillan, D. W. C. "A General Strategy for Organocatalytic Activation of C−H Bonds via Photoredox Catalysis: Direct Arylation of Benzylic Ethers" *J. Am. Chem. Soc.* **2014**, *136*, 626; (b) Hager, D.; MacMillan, D. W. C. "Activation of C−H Bonds via the Merger of Photoredox and Organocatalysis: A Coupling of Benzylic Ethers with Schiff Bases" *J. Am. Chem. Soc.* **2014**, *136*, 16986.

UNIVERSITAT ROVIRA I VIRGILI
PHOTOCHEMISTRY AND ORGANOCATALYSIS FOR RADICAL-BASED CARBON-CARBON BOND-FORMING PROCESSES
Emilien De Saux

90
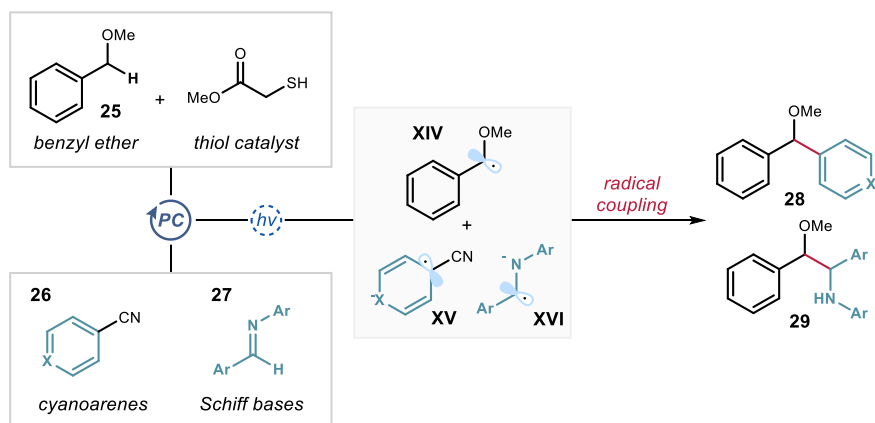
Figure 3.15. Original reports on the use of thiols as HAT catalysts.

The same group later showed that this strategy was also applicable to the formation and coupling of allylic radicals (Figure 3.16).[27] The mechanism is similar to the previous study using benzylic ethers **25**. The transformation relied on a radical coupling between persistent cyanoaryl radical anions **XV**, generated by reduction of cyanoarenes **26** from an excited iridium photocatalyst, and allyl radicals **II**, generated by HAT from simple alkenes **2**. The thiol catalyst (*i*-Pr)$_3$SiSH was oxidized to the HAT-active thiyl radical **A$^\bullet$** by the oxidized form of the photocatalyst, assisted by the presence of a base as proton scavenger.
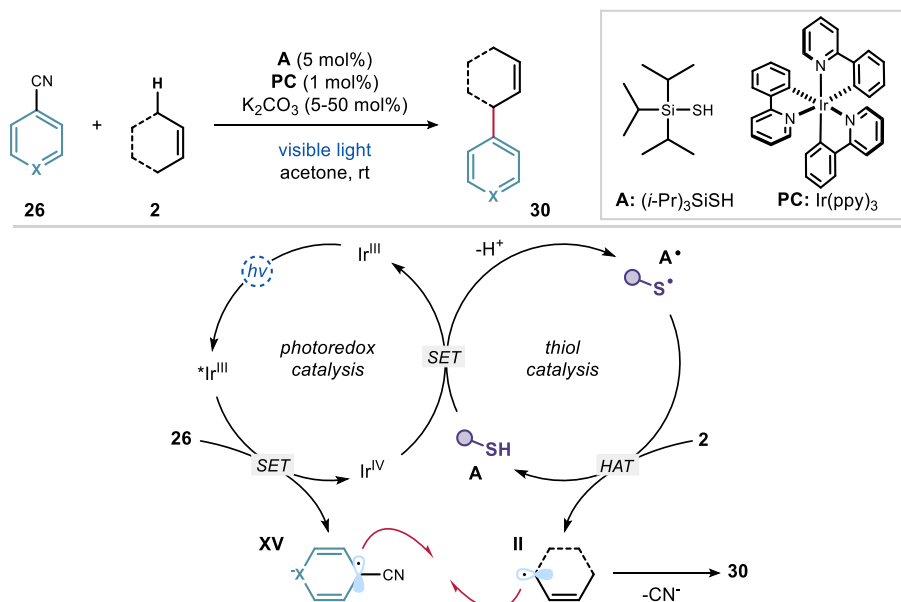
Figure 3.16. Dual photoredox-thiol arylation of allylic C-H bonds.

---

[27] Cuthbertson, J. D.; MacMillan, D. W. C. The Direct Arylation of Allylic *sp*^{3} C-H Bonds via Organic and Photoredox Catalysis. *Nature* **2015**, *519*, 74.

UNIVERSITAT ROVIRA I VIRGILI
PHOTOCHEMISTRY AND ORGANOCATALYSIS FOR RADICAL-BASED CARBON-CARBON BOND-FORMING
PROCESSES
Emilien Le Saux

91

While the coupling of cyanoaryl radicals and allyl radicals was already known,[28] this example showed that allylic radicals could be generated catalytically under mild reaction conditions using small organic catalysts. Similar strategies were used in subsequent work from other groups, who changed the coupling partners from cyanoarenes to long-lived ketyl or α-amido radical anions.[29]

In all these reports, the new C-C bonds were formed *via* radical cross-coupling events. Such processes are rarely synthetically valuable as cross-selectivity is difficult to achieve, because of the competing radical dimerization (Figure 3.17).[9] However, when the radicals are formed at equal rates and have different lifetimes, with one being longer-lived than the other, cross-coupling can become the dominant process. This phenomenon, known as the *persistent radical effect* (PRE), explains why the reactions showed in Figure 3.15 and 3.16 are efficient. Cyanoaryl and α-amido radical anions (**XV** and **XVI** respectively) are kinetically stabilized (they exhibit persistency), which allows them to engage in cross-coupling reactions with other transient radicals. As highlighted by Studer,[9] the term "persistent radical effect" is misleading as cross-selectivity can also be achieved with none of the radicals involved being persistent, but because their respective lifetime differs.
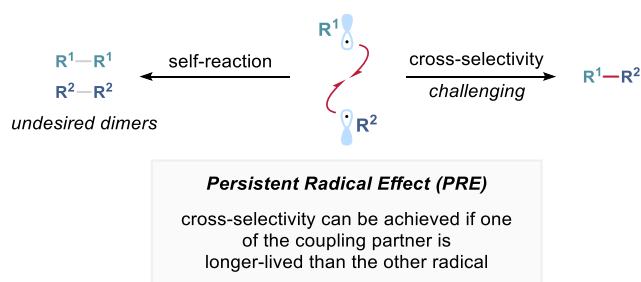
Figure 3.17. The persistent radical effect allows cross-selectivity in radical coupling reactions.

A subsequent example from the MacMillan group focused on the methylation of azines using methanol as methylating agent (Figure 3.18). [30] This Minisci-type reaction proceeded *via* addition of the nucleophilic radical **XVII**, generated by HAT from methanol **32**, to activated azine **XVIII**. After loss of a proton, radical **XIX** released one molecule of water upon spin-center shift (SCS) to afford the benzylic radical **XX**. The latter was eventually reduced to the anion by the excited photoredox catalyst and protonated to deliver the methylated azine **33**.

[28] Bernardi, R.; Caronna, T.; Morrocchi, S.; Traldi, P.; Vittimberga, B. M. *J.* "Photoinitiated Substitution Reactions of Heterocyclic Bases: Reaction with Alkenes" *Chem. Soc., Perkin Trans.* 1, **1981**, 1607.
[29] (a) Vu, M. D.; Das, M.; Guo, A.; Ang, Z. E.; Dokić, M.; Soo, H. Sen; Liu, X. W. "Visible-Light Photoredox Enables Ketone Carbonyl Alkylation for Easy Access to Tertiary Alcohols" *ACS Catal.* **2019**, *9*, 9009; (b) Jia, J.; Kancherla, R.; Rueping, M.; Huang, L. "Allylic C(sp^3)-H Alkylation via Synergistic Organo- And Photoredox Catalyzed Radical Addition to Imines" *Chem. Sci.* **2020**, *11*, 4954.
[30] Jin, J.; MacMillan, D. W. C. "Alcohols as alkylating agents in heteroarene C–H functionalization" *Nature*, **2015**, *525*, 87.
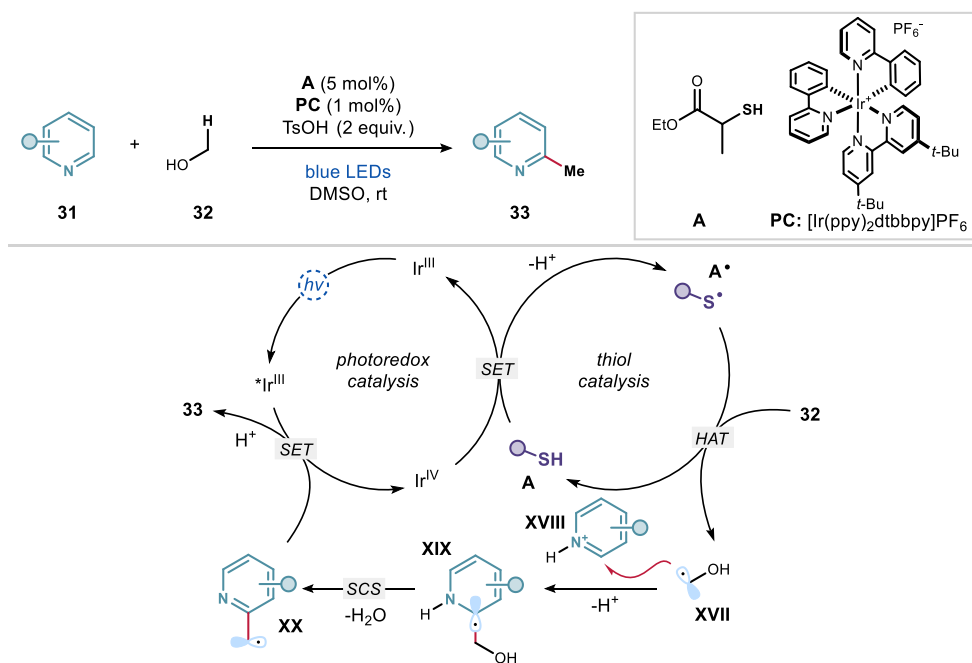
Figure 3.18. Spin-center shift (SCS)-mediated methylation of azines.

Another important class of catalysts was disclosed by Kanai and co-workers, who found that thiophosphoric acids **TPA** and imides **TPI**, with a rigid BINOL-based scaffold, could act as HAT catalysts (Figure 3.19).[31] They designed complex tri-catalytic systems combining HAT, photoredox, and metal catalysis for the dehydrogenation of tetrahydronaphthalenes **34a** and alcohols **34b**.

A strongly oxidizing acridinium photocatalyst ($E^* > +2$ V vs Ag$^+$/Ag) oxidized **TPA** or **TPI**, which ultimately afforded a sulfur-centered radical **A•** upon proton loss. The latter generated radicals **XXI** by abstraction of hydrogen atoms from activated positions. **XXI** then entered the metal catalytic cycle in which dehydrogenation took place. A turnover event, where the reduced acridinium reduced the metal catalyst, closed both catalytic cycles.

[31] (a) Kato, S.; Saga, Y.; Kojima, M.; Fuse, H.; Matsunaga, S.; Fukatsu, A.; Kondo, M.; Masaoka, S.; Kanai, M. "Hybrid Catalysis Enabling Room-Temperature Hydrogen Gas Release from N-Heterocycles and Tetrahydronaphthalenes" *J. Am. Chem. Soc.* **2017**, *139*, 2204; (b) Fuse, H.; Mitsunuma, H.; Kanai, M. "Catalytic Acceptorless Dehydrogenation of Aliphatic Alcohols" *J. Am. Chem. Soc.* **2020**, *142*, 4493.

UNIVERSITAT ROVIRA I VIRGILI
PHOTOCHEMISTRY AND ORGANOCATALYSIS FOR RADICAL-BASED CARBON-CARBON BOND-FORMING
PROCESSES
Emilien Le Saux

93
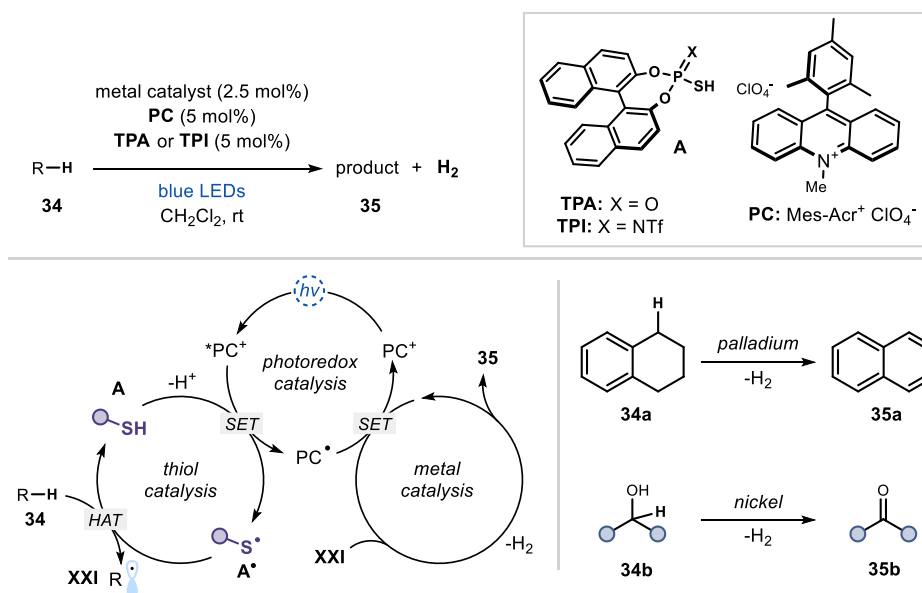
Figure 3.19. HAT-mediated dehydrogenation of carbocycles and alcohols.

A similar approach was reported for the chromium-catalyzed radical allylation of aldehydes using unactivated alkenes (Figure 3.20).[32] The allyl radical **XXII** arising from HAT from alkenes **37**, was intercepted by Cr^{II} to form intermediate **XXIII**. This allylchromium(III) species subsequently reacted with aldehyde **36** through a Zimmerman-Traxler-type transition state to produce the chromium alkoxide intermediate **XXIV** as the *anti*-diastereomer. Protonation of **XXIV** ultimately afforded the final homoallylic alcohol **38**, while the released Cr^{III} catalyst was turned-over to Cr^{II} by SET reduction from the reduced form of the photocatalyst.

---

[32] Tanabe, S.; Mitsunuma, H.; Kanai, M. "Catalytic Allylation of Aldehydes Using Unactivated Alkenes" *J. Am. Chem. Soc.* **2020**, *142*, 12374.
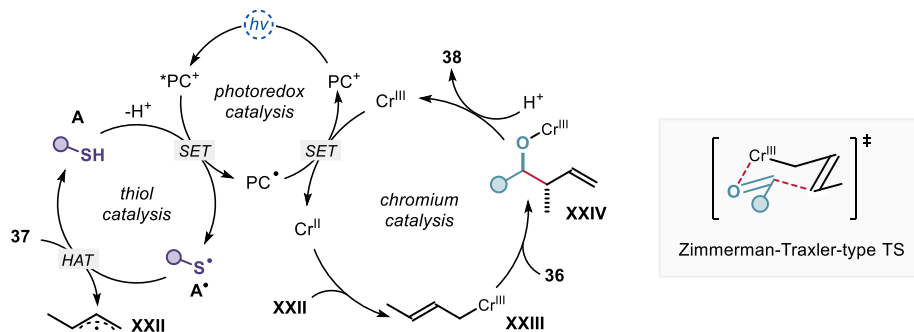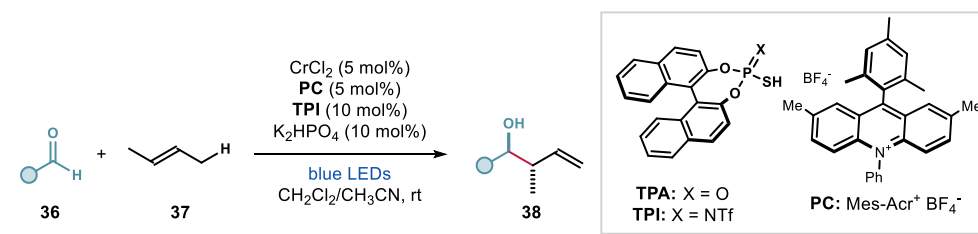
Figure 3.20. Ternary catalysis for the allylation of aldehydes using unactivated alkenes.

Aldehydes have relatively low BDEs (< 90 kcal·mol^{-1}) and could be activated directly to form acyl radicals through HAT. A hydroxyalkylation of azines **31** using aldehydes **36** as acylating agents was reported using the combination of **TPA**/acridinium salt (Figure 3.21).[33] The reaction followed a Minisci-type pathway where acyl radicals **XXV** attacked protonated azines **XVII**. A key spin-center shift of intermediate **XXVI** turned the acyl functionality into the final hydroxyalkyl moiety.
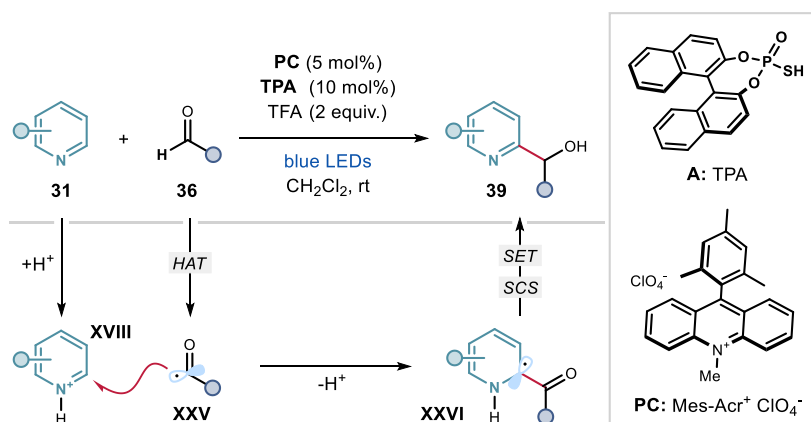
Figure 3.21. Ternary catalysis for the azination of aldehydes using *N*-heteroarenes.

[33] Fuse, H.; Nakao, H.; Saga, Y.; Fukatsu, A.; Kondo, M.; Masaoka, S.; Mitsunuma, H.; Kanai, M. "Photocatalytic Redox-Neutral Hydroxyalkylation of N-Heteroaromatics with Aldehydes" *Chem. Sci.*, **2020**, *11*, 12206.

UNIVERSITAT ROVIRA I VIRGILI
PHOTOCHEMISTRY AND ORGANOCATALYSIS FOR RADICAL-BASED CARBON-CARBON BOND-FORMING
PROCESSES
Emilien Le Saux

95

In summary, these reports highlighted the ability of thiol derivatives to act as hydrogen abstractors from activated positions to generate radicals from readily available substrates, without the need for pre-functionalization. Noteworthy, these organocatalysts are compatible with diverse conditions involving acidic or basic additives and even metal catalysts.

3.3 Design and target of the project

Our research group is interested in the discovery of new reactions exploiting the combination of visible light and organic catalysts. While allylic benzylation processes have been developed using transition metal catalysis, there are no organocatalytic methods available to forge such $C(sp^3)$-$C(sp^3)$ bonds. To achieve this target, we considered the ability of thiols to play distinct roles: first, thiolates are known to serve as effective donors in EDA complex formation; second, sulfur-centered radicals are good HAT catalysts for the activation of weak C-H bonds. We therefore wondered if a single thiol catalyst could perform those two roles sequentially for the generation and coupling of benzylic and allylic radicals.

Our reaction design is detailed in Figure 3.22. Upon deprotonation with a base, the thiol catalyst affords thiolate **A⁻** that engages in the formation of a photoactive EDA complex with a radical precursor **1**, adorned with an electron-poor redox auxiliary. Irradiation with visible light triggers an intra-complex SET which leads to the formation of a benzyl radical **I** (after fragmentation of the redox auxiliary) and a thiyl radical **A•**. The latter can sequentially abstract a hydrogen atom from a simple alkene **2**, thus affording an allyl radical **II**. This HAT step constitutes the turnover event of the catalytic cycle, since it regenerates the thiol catalyst. Radical coupling between **I** and **II** eventually affords the desired product **3**. We anticipated that cross-selectivity would be difficult to achieve, as both benzyl and allyl radicals are known to undergo fast dimerization.[34] Although neither of these intermediates is persistent, they are both stabilized by delocalization.[9]

---

[34] (a) Hefter, H. J.; Wu, C-H. S.; Hammond, G. S. "Rates of Termination of Radicals in Solution. VII. Allylic Radicals" *J. Am. Chem. Soc.* **1973**, *95*, 851; (b) Lehni, M.; Schuh, H.; Fischer, H. "Rate Constants for the Termination of Benzyl Radicals in Solution" *Int. J. Chem. Kinet.* **1979**, *11*, 705.
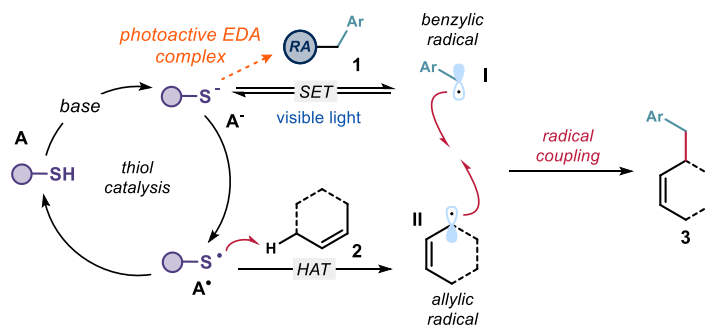
Figure 3.22. target of the project: developing a thiol-catalyzed benzylation of allylic C-H bonds through EDA and HAT activation.

3.4 Results and discussion

3.4.1 Optimization

We started our optimization campaign (Table 3.1) choosing the tetrachlorophthalimide ester **1a** as the precursor of benzyl radicals and an excess (20 equiv.) of cyclohexene **2a** as a C-H allylic precursor. The choice of **1a** was motivated by a previous report making use of such redox auxiliary as acceptors in EDA complexes,[35] while **2a** has been employed in various reports to generate allylic radicals by HAT.[27,29] A substoichiometric amount of base (Na$_2$HPO$_4$, 20 mol%) was added to facilitate initial deprotonation of the catalyst. The reactions were performed in acetone using a temperature-controlled photoreactor, irradiating with 455 nm LED strips at 35 °C.
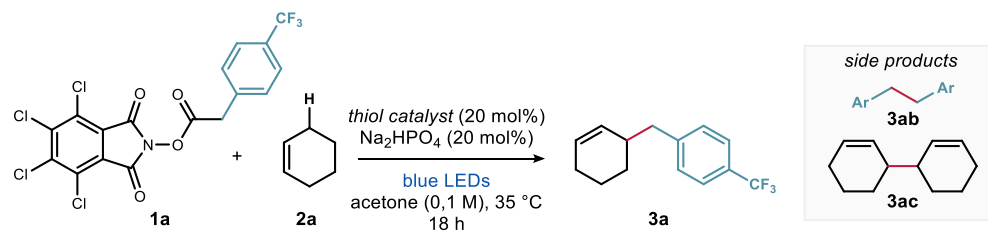
We started by screening different thiols known to act either as HAT catalyst or as donors in EDA complexes. The tri-isopropylsilane thiol **A1**[27] did not afford any product, even in the presence of an external photoredox catalyst (entries 1 and 2). A first hit was obtained with xanthate **A2**, which our group previously used as a donor for EDA complex catalysis.[5] Catalyst **A2** delivered the target product **3a** in 15% yield along with benzylic dimer **3ab** (entry 3). Thiobenzoic acid **A3** was ineffective in the reaction (entry 4).[36] We then turned our attention to Kanai's BINOL-based thiophosphoric acid **A4**, which afforded the desired product in 22% yield (entry 5).[31-33] We then thought of using a more electron-rich version of the thiophosphoric acid. We therefore prepared the dithiophosphoric acid **A5** and submitted

[35] Bosque, I.; Bach, T. "3-Acetoxyquinuclidine as Catalyst in Electron Donor–Acceptor Complex-Mediated Reactions Triggered by Visible Light" *ACS Catal.* **2019**, *9*, 9103.
[36] Kobayashi, F.; Fujita, M.; Ide, T.; Ito, Y.; Yamashita, K.; Egami, H.; Hamashima, Y. "Dual-Role Catalysis by Thiobenzoic Acid in Cα-H Arylation under Photoirradiation" *ACS Catal.* **2021**, *11*, 82.

UNIVERSITAT ROVIRA I VIRGILI
PHOTOCHEMISTRY AND ORGANOCATALYSIS FOR RADICAL-BASED CARBON-CARBON BOND-FORMING PROCESSES
Emilien Le Saux

97

it to the reaction conditions.[37] A significant boost in reactivity was observed, with **3a** formed in 45% yield (entry 6). Experiments showed that the reaction did not proceed in the absence of catalyst or light (entries 7 and 8). The base was found highly beneficial but not essential (entry 9).

Table 3.1. Optimization studies.

entry	catalyst	3a	3ab	3ac
1	A1	n.d.	n.d.	n.d.
2	A1 + Ir(ppy)$_3$	n.d.	n.d.	n.d.
3	A2	15	7	n.d.
4	A3	n.d.	n.d.	n.d.
5	A4	22	10	12
6	A5	45 (41)	11	20
7	-	n.d.	n.d.	n.d.
8	A5 (no light)	n.d.	n.d.	n.d.
9	A5 (no base)	12	3	8

Reaction performed on a 0.2 mmol scale using 20 equiv. of **2a** under irradiation with a 455 nm 14W LEDs strip. [a]Yields of **3** determined by ^{1}H NMR analysis of the crude reaction mixtures using trichloroethylene as the internal standard. Yields of isolated **3a** are reported in parentheses. *n.d.:* not detected.

Further optimization did not improve the reaction outcome. The moderate yield was a consequence of the competing formation of dimer **3ab**, which limited the overall efficiency of the reaction. Table 3.2 sums up the effect of the loading of **2a** on the reaction. Decreasing the loading of **2a** resulted in the formation of more dimer **3ab** at the expense of the desired cross-coupling product **3a**. Thus, the large excess of cyclohexene favored the cross-selectivity in the radical coupling over the dimerization process.

---

[37] Originally, such dithiophosphoric acids were used for their strong acidity and the nucleophilic character of the conjugate base, see: Shapiro, N. D.; Rauniyar, V.; Hamilton, G. L.; Wu, J.; Toste, F. D. "Asymmetric Additions to Dienes Catalysed by a Dithiophosphoric Acid" *Nature*. **2011**, *470*, 245.

Table 3.2. Effect of the loading of **2a** on cross-selectivity.
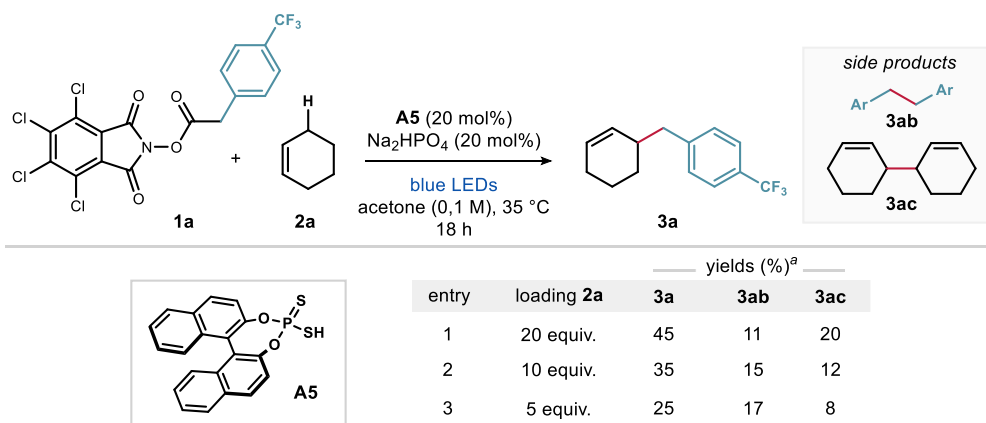
Reaction performed on a 0.2 mmol scale using 1 equiv. of **1a** under irradiation with a 455 nm 14 W LEDs strip. [a]Yields of **3** determined by ^{1}H NMR analysis of the crude reaction mixtures using trichloroethylene as the internal standard.

entry	loading **2a**	**3a**	**3ab**	**3ac**
1	20 equiv.	45	11	20
2	10 equiv.	35	15	12
3	5 equiv.	25	17	8

We then evaluated if the introduction of substituents at the 3,3'-positions of the BINOL-based phosphoric acid catalyst **A5**[38] could affect positively the reaction outcome. The phenyl (catalyst **A6**) and 2,4,6-triisopropyl analogues (**A7**) of **A5** were synthesized and tested in the model reaction (Table 3.3). While still catalytically active, none of them outcompeted the simple dithiophosphoric acid **A5**, which was easily prepared in one-step.

---

[38] Parmar, D.; Sugiono, E.; Raja, S.; Rueping, M. "Complete Field Guide to Asymmetric BINOL-Phosphate Derived Brønsted Acid and Metal Catalysis: History and Classification by Mode of Activation; Brønsted Acidity, Hydrogen Bonding, Ion Pairing, and Metal Phosphates" *Chem. Rev.* **2014**, *114*, 9047.

UNIVERSITAT ROVIRA I VIRGILI
PHOTOCHEMISTRY AND ORGANOCATALYSIS FOR RADICAL-BASED CARBON-CARBON BOND-FORMING PROCESSES
Emilien Le Saux

99

Table 3.3. Use of substituted catalysts in the model reaction.
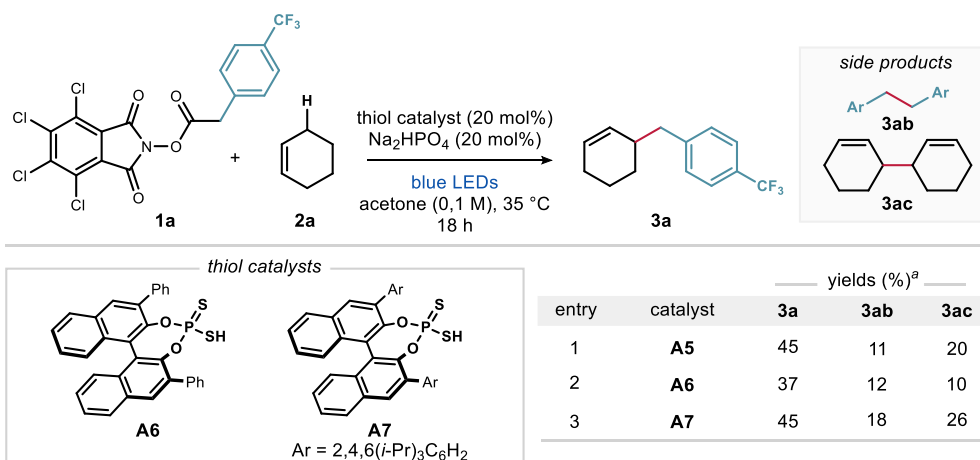
entry	catalyst	yields (%)[a]		
		3a	**3ab**	**3ac**
1	**A5**	45	11	20
2	**A6**	37	12	10
3	**A7**	45	18	26

Reaction performed on a 0.2 mmol scale using 20 equiv. of **2a** under irradiation with a 455 nm 14 W LEDs strip. [a]Yields of **3a** determined by ^{1}H NMR analysis of the crude reaction mixtures using trichloroethylene as the internal standard.

3.4.2 Mechanistic investigations

The dimers **3ab** and **3ac** detected during the optimization unambiguously indicated that both benzyl and cyclohexenyl radicals were formed during the reaction. Using DFT calculations (performed using B3LYP/6-31G(d,p)), the BDE of **A5** was estimated at **83.3 kcal·mol^{-1}**, which is higher than the one calculated for the C-H allylic bond in cyclohexene **2a** (82.2 kcal·mol^{-1}). These results suggested that HAT from cyclohexene **2a** by the sulfur-centered radical of **A5** is thermodynamically feasible.

A series of UV-Vis studies were then undertaken to probe the formation of an EDA complex between the anion of catalyst **A5$^-$** and the radical precursor **1a**. As shown in Figure 3.23, after mixing catalyst **A5** with **1a** in the presence of Na$_2$HPO$_4$, the absorption spectrum of the solution showed a bathochromic displacement in the visible region, thus indicating the formation of an EDA complex.[3] Overall, the only species absorbing in the visible region is the EDA complex aggregate, as the catalyst itself and its anion only absorb in the UV area (purple and grey lines).
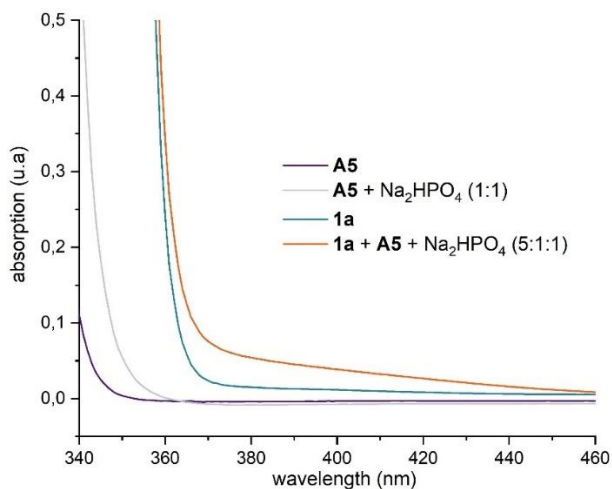
Figure 3.23. UV-Vis studies to probe the formation of an EDA complex between **A5** and **1a** in presence of a base.

These results support the proposed mechanism, which proceeds upon the formation of an EDA complex and HAT from alkene **2a**.

3.4.3 Generality of the system

Adopting the optimal conditions described in Table 3.1, entry 6, we evaluated the scope of the photochemical allylic C−H benzylation (Figure 3.24). We used tetrachlorophthalimide esters **1**, which are easily derived from carboxylic acids, as benzyl radical precursors. Primary (product **3a**), secondary (**3b** and **3c**), and tertiary (**3d**) benzylic groups could be coupled with cyclohexene **2a** in moderate yields. We also used nonsteroidal inflammatory drugs bearing a carboxylic moiety as radical precursors, which allowed us to install the *loxoprofen* (**3f**), *indomethacin* (**3g**), and *flurbiprofen* (**3h−k**) scaffolds within the allylation products. Other alkenes were suitable allyl radical precursors, including cyclopentene (product **3i**) and substituted cyclohexenes (**3j** and **3k**). Catalyst **A5** was also suitable for the activation of pyridinium salts **40**, a class of radical precursors prone to EDA complex formation acting as acceptors.[5] The phenylglycine-derived pyridinium salt afforded product **3l**.

UNIVERSITAT ROVIRA I VIRGILI
PHOTOCHEMISTRY AND ORGANOCATALYSIS FOR RADICAL-BASED CARBON-CARBON BOND-FORMING PROCESSES
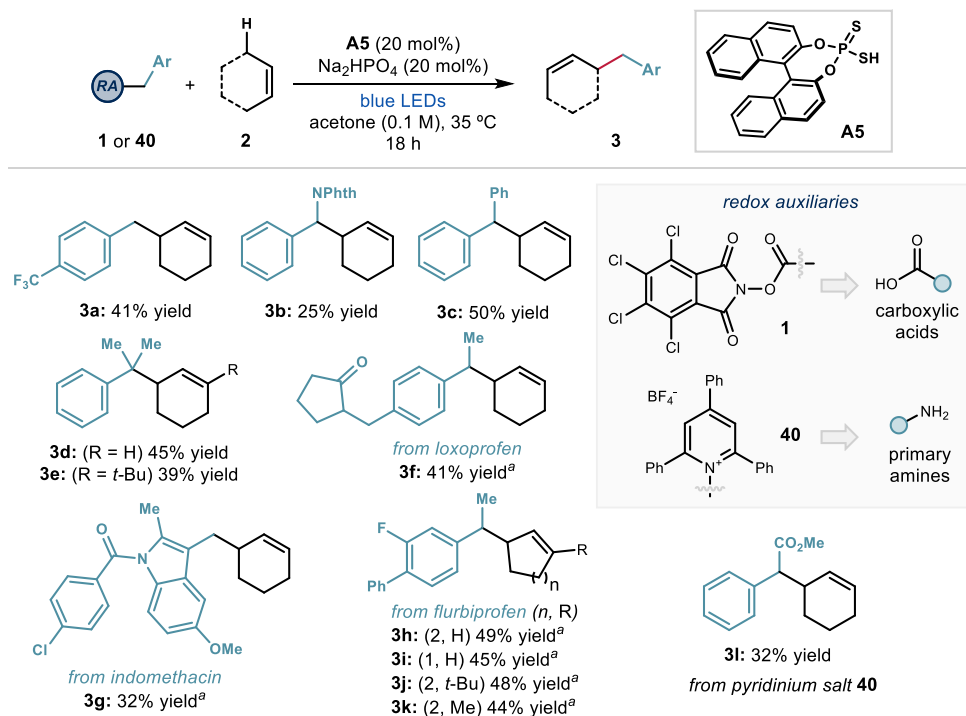Emilien Le Saux

101

Figure 3.24. Scope of the dithiophosphoric acid-catalyzed direct benzylation of allylic C-H bonds. Reactions performed on a 0.2 mmol scale using 20 equiv. of **2**. Yields refer to isolated products **3** after purification. When applicable, *d.r.* is ~ 1:1. [a]Reaction performed on a 0.1 mmol scale. Nphth: *N*-phthalimide.

As shown in Figure 3.25, a simple tolyl radical only afforded 15% of product, while linear C-H allylic partners remained unreactive. Some more complex cyclohexene derivatives afforded the target products, but in low yields.
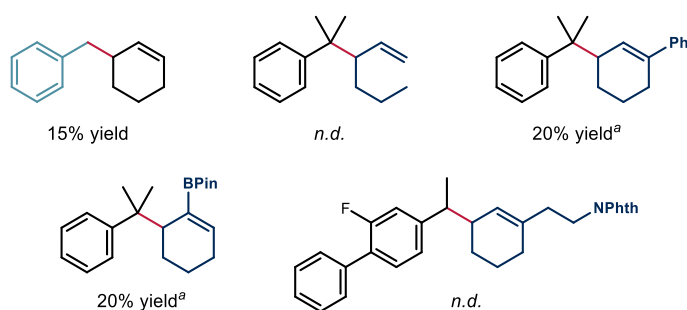
Figure 3.25. Moderately successful and unsuccessful substrates. Reactions performed on a 0.2 mmol scale using 20 equiv. of C-H partner **2** and 20 mol% of **A5**. Yields were determined by ^{1}H NMR analysis of the crude reaction mixtures using trichloroethylene as the internal standard. *n.d.*: not detected. [a]Using 10 equiv. of **2**. Bpin: pinacol boronic ester; NPhth: *N*-phthalimide.

After exploring the scope of benzylic radical precursors and some C-H partners, we wondered whether other alkyl radicals could undergo coupling with allyl fragments. As shown in Figure 3.26, neither non-stabilized alkyl nor alpha-amino radicals afforded the desired coupling

products. Instead, the formal decarboxylation products were formed in almost quantitative yields. This lack of reactivity is congruent with the radical coupling step envisaged in our mechanistic proposal, which requires the radical of type **I** to have enough stability (e.g., a benzylic radical) to engage in productive C−C bond formation with the allylic radical **II**. Though unsatisfactory, these results indicated that not only benzyl but also simple alkyl radicals could be generated using our system.
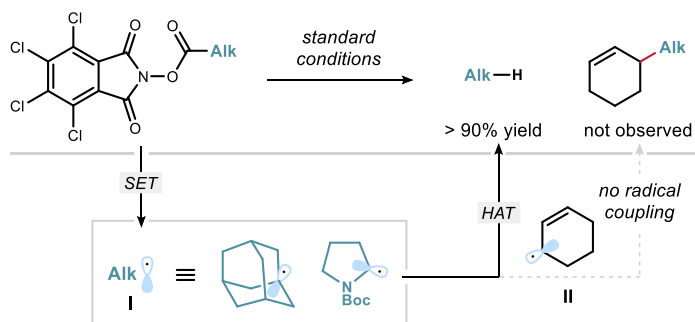
Figure 3.26. Attempts of using non-benzylic radicals in the coupling with cyclohexenyl radicals under the conditions described in Table 3.1 entry 6.

3.5 Expanding the system to unstabilized radicals

Willing to exploit the full potential of the radical generation strategy offered by EDA complex activation, we surmised that the key benzyl radical **I**, which is necessary to allow an efficient radical coupling with the ally radical, could be formed indirectly. Specifically, we sought to intercept unstabilized alkyl radicals **I**, formed through EDA complex activation, with styrene derivatives **41** (Figure 3.27). This radical trap would afford the stabilized benzylic intermediate **XXVII** which can couple efficiently with an allylic radical **II** to deliver the target product **42**, while restarting the catalytic cycle. In particular, when using α-aryl styrene derivatives, **XXVII** would then become a highly stabilized bis-benzylic radical ideal for radical coupling.[9] The overall transformation is now a three-component benzylation of allylic C-H bonds.

UNIVERSITAT ROVIRA I VIRGILI
PHOTOCHEMISTRY AND ORGANOCATALYSIS FOR RADICAL-BASED CARBON-CARBON BOND-FORMING
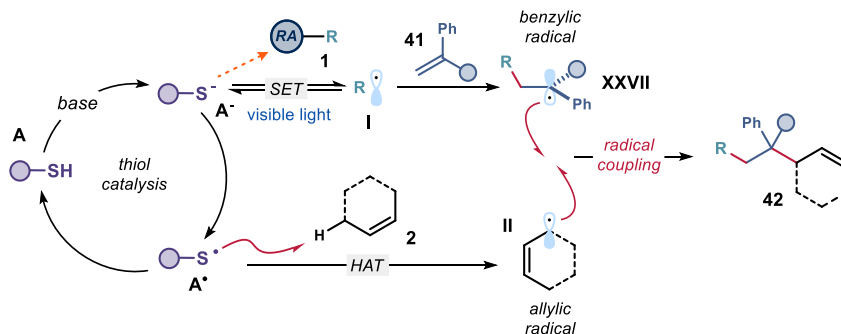PROCESSES
Emilien Le Saux

103

Figure 3.27. Design of a three-component process to perform allylic C-H benzylation.

The three-component reaction was optimized using the glycine-derived pyridinium salt **40b** as radical precursor, 1,1'-diphenylethylene **41a** as the intermediate trap, and cyclohexene **2a** as C-H allylic precursor (Table 3.4).

Table 3.4. Optimization studies.

entry	catalyst loading	loading **2a**	T (°C)	time (h)	yield **42a** (%)[a]
1	20 mol%	20 equiv.	35	48	75 (65)
2	20 mol%	10 equiv.	35	24	85
3	10 mol%	10 equiv.	35	28	85
4	**10 mol%**	**10 equiv.**	**60**	**8**	**96 (95)**
5	10 mol%	5 equiv.	60	8	70
6	-	10 equiv.	60	8	n.d.
7[b]	10 mol%	10 equiv.	60	8	n.d.

Reaction performed on a 0.1 mmol scale using 1 equiv. of **41a** under irradiation with a 455 nm 14 W LEDs strip. [a]Yields of **42a** determined by ^{1}H NMR analysis of the crude reaction mixtures using trichloroethylene as the internal standard. Yields of isolated **42a** are reported in parentheses. [b]No light. n.d.: not detected.

We started the optimization from the previous optimal conditions (entry 1), which afforded the desired three-component adduct **42a** in 75% yield. The reaction was extremely selective, since we did not observe dimers of the benzylic or allylic radicals and complete cross-selectivity was achieved. We therefore decreased the loading of the C-H allylic partner from 20 to 10 equiv. This resulted in an increased yield, since product **42a** was formed in 85% yield (entry 2). Decreasing the loading of catalyst **A5** to 10 mol% did not affect the chemical yield (entry 3), but a higher reaction time was required to obtain full conversion of the starting

material (28 h). Increasing the temperature to 60 °C diminished the reaction time to 8 hours, delivering **42a** in 95% yield after purification (entry 4). The loading of **2a** could be decreased to 5 equiv., albeit with a decreased yield (entry 5). Both catalyst and light were essential for reactivity (entries 6 and 7).

Using the conditions described in Table 3.4 entry 4, we explored the scope of the three-component process. A variety of radical precursors, either phthalimide esters **1** or pyridinium salts **40**, could be used, offering the corresponding products **42** in moderate to excellent yields (Figure 3.28). Pyridinium salts **40** were useful to generate electron-poor radicals α to electron-withdrawing groups, including esters (products **42a** and **42b**), nitriles (**42c**), or pyrimidine (**42d**). Importantly, the reaction could be scaled-up to 1 mmol without significant erosion of the yield.
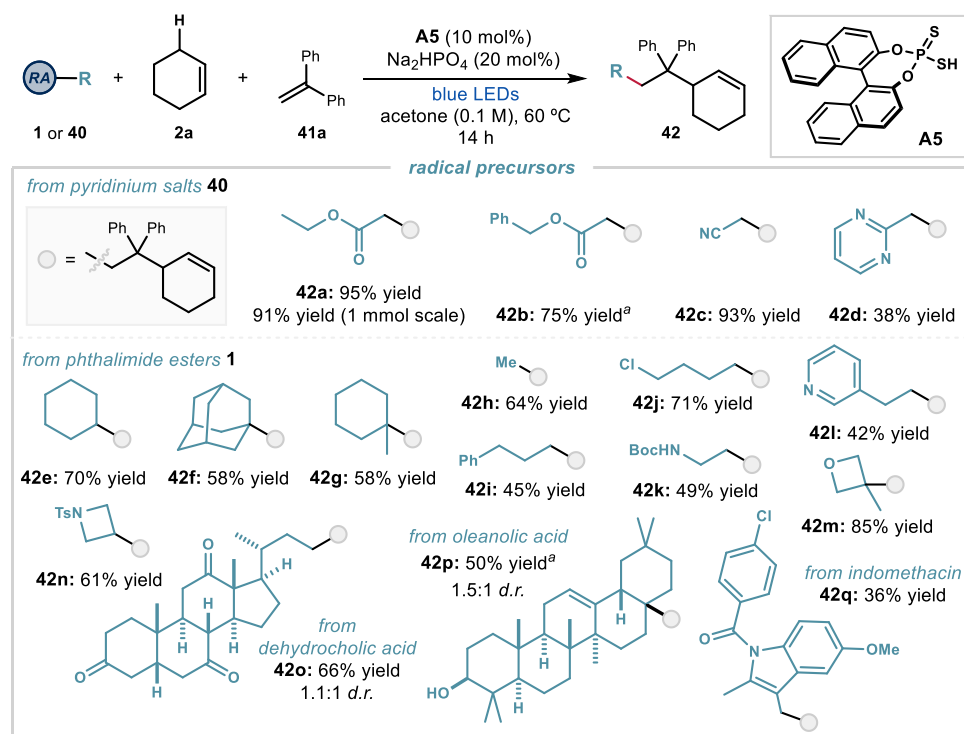
Figure 3.28. Scope of the radical precursors in the three-component allylic benzylation. Reactions performed on a 0.1 mmol scale using 5-10 equiv. of **2** and 1 equiv. of **41**. Yields refer to isolated products **42** after purification (average of two runs). [a]Yield determined by ^{1}H NMR analysis. Boc: *tert*-butyloxycarbonyl; Ts: tosyl.

A range of non-stabilized alkyl radicals were generated from phthalimide esters **1**. Non-stabilized primary (**42h−l**), secondary (**42e**), and tertiary (**42f−g** and **42m**) alkyl radicals were all amenable to this domino allylic benzylation process. Various heterocycles, including a pyridine (**42l**), an oxetane (**42m**), and an azetidine (**42n**), could be installed in the final products. Moreover, complex biorelevant molecules bearing non-protected functional groups,

UNIVERSITAT ROVIRA I VIRGILI
PHOTOCHEMISTRY AND ORGANOCATALYSIS FOR RADICAL-BASED CARBON-CARBON BOND-FORMING
PROCESSES
Emilien Le Saux

105

such as *dehydrocholic acid* (**42o**), *oleanolic acid* (**42p**), and *indomethacin* (**42q**), were successfully functionalized.

To improve the synthetic utility of the process, we wondered whether a one-pot telescoped sequence, starting from carboxylic acids **43** and without isolation of the phthalimide esters **1**, could be developed (Figure 3.29). A first attempt using cyclohexane carboxylic acid afforded **42e** with only a slight decrease in yield. After formation of the phthalimide ester **1**, the solvent was simply removed and the crude material submitted to the standard conditions. This strategy allowed us to use *D-biotin* as a radical precursor, affording product **42r** in 37% yield. Attempts to isolate the intermediate phthalimide ester of *D-biotin* were unsuccessful, since the intermediate decomposed on silica gel.

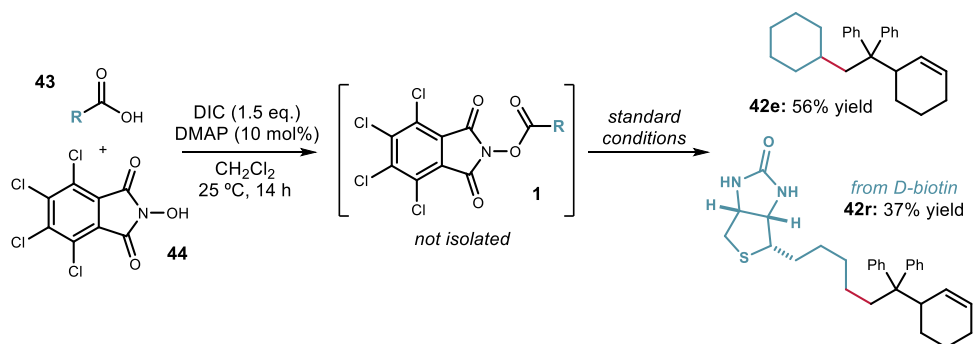**Figure 3.29.** Telescoped sequence for the direct use of carboxylic acids in the allylic benzylation process. Reactions performed on a 0.1 mmol scale using 1.2 equiv. of **43** and 1.2 equiv. of **44**. DIC: N,N'-diisopropylcarbodiimide.

We then studied the scope of the C-H allylic partners (Figure 3.30). While cyclopentene reacted smoothly to afford product **42s** in 75% yield, cyclooctene offered moderate reactivity (**42t** formed in 39% yield). Interestingly, catalyst **A5** secured high regioselectivity in the HAT activation of 1-substituted cyclohexenes (products **42u** and **42v**), promoting the formation of the less hindered allylic radical. Non-symmetrical C−H partners bearing a boronic ester (**42x**) and a phthalimide functional group (**42y**) were tolerated well. Our organocatalytic photochemical process was also suitable for the late-stage functionalization of *cholesterol*, which led to product **42z** in good yield. This coupling protocol was also useful to functionalize benzylic C−H bonds, including tetrahydronaphthalene and dihydrobenzofuran (products **42aa** and **42bb**).
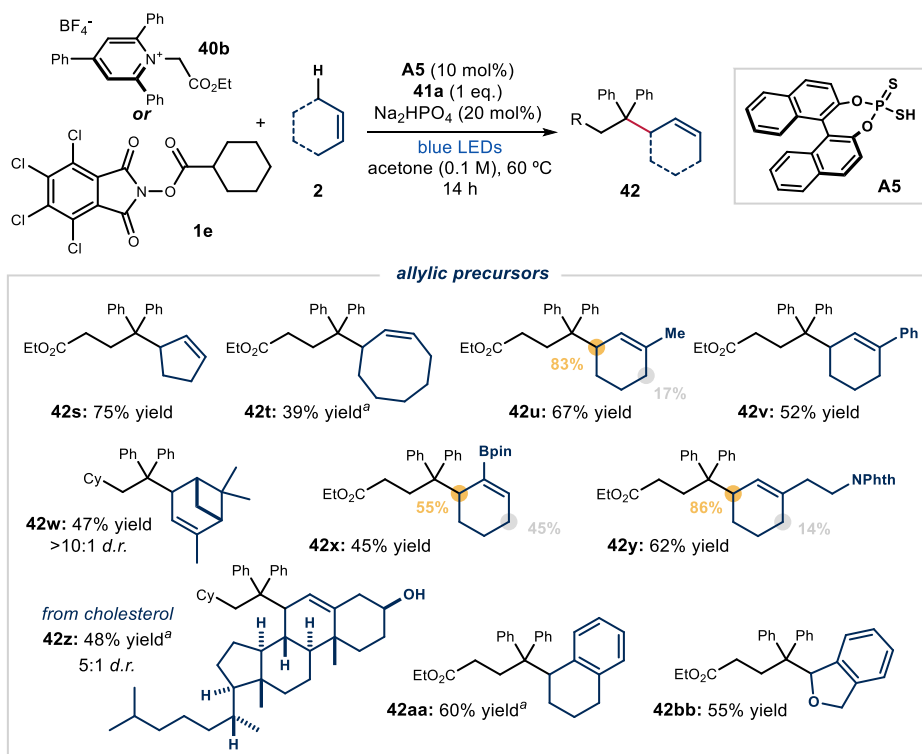
Figure 3.30. Scope of C-H allylic precursors **2.** Reactions performed on a 0.1 mmol scale using 5-10 equiv. of **2**. Yields refer to isolated products **42** after purification (average of two runs). [a]Yield determined by ^{1}H NMR analysis. Cy: cyclohexyl; NPhth: N-phthalimide; Bpin: pinacol boronic ester.

Eventually, styrene derivatives **41** were evaluated in the reaction (Figure 3.31). α-Aryl-styrene derivatives afforded the desired products in good to excellent yields (products **42cc−jj**). These results are congruent with the stabilization of the benzylic radical **XXVII**, emerging from the radical trap, which facilitates the radical coupling step (Figure 3.26).

Interestingly, a benzodioxole and an aldehyde moiety, despite being sensitive to HAT activation, were left untouched (compounds **42dd** and **42ff**). A derivative of *fenofibrate*, a marketed fibrate medication, was equally suitable for the transformation, delivering product **42jj**. Styrenes (products **42oo** and **42pp**) and α-alkyl styrene derivatives (**42kk−mm**) offered reduced reactivity, but they were still competent substrates. In particular, a protected piperidine (**42mm**) and a boronic ester (**42nn**) could be installed in the final products from suitably adorned styrenes.
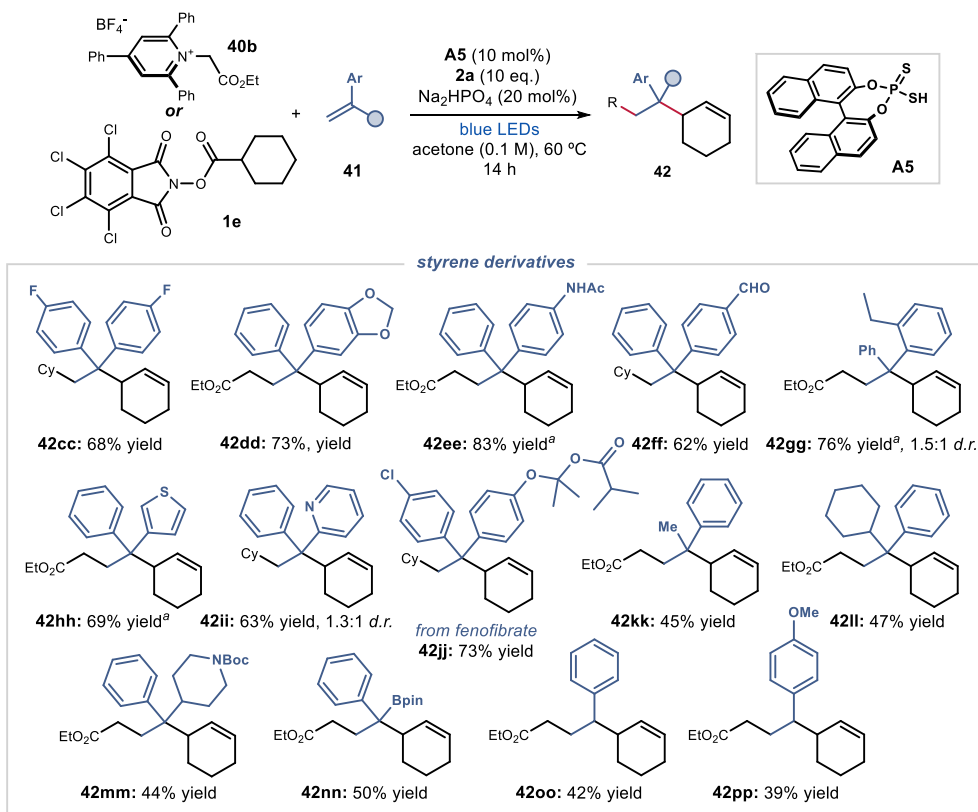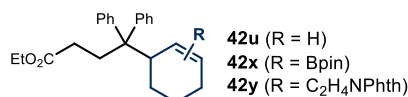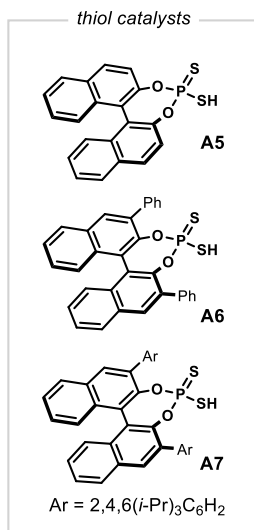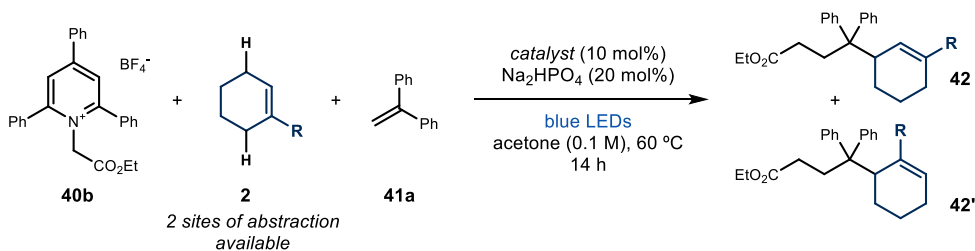
UNIVERSITAT ROVIRA I VIRGILI
PHOTOCHEMISTRY AND ORGANOCATALYSIS FOR RADICAL-BASED CARBON-CARBON BOND-FORMING
PROCESSES
Emilien Le Saux

107

Figure 3.31. Scope of styrene derivatives **41**. Reactions performed on a 0.1 mmol scale using 1 equiv. of **41**. Yields refer to isolated products **42** after purification (average of two runs). [a]Yield determined by ^{1}H NMR analysis. Cy: cyclohexyl; NPhth: N-phthalimide; Bpin: pinacol boronic ester; Boc: tert-butyloxycarbonyl.

3.6 Effect of the catalyst on the HAT regioselectivity

Because HAT processes are inherently sensitive to steric hindrance,[23] we wondered whether the regioselectivity of the abstraction, when using non-symmetrical cyclohexene derivatives, could be influenced by the catalyst's bulkiness. We performed a systematic study using catalysts **A5-7** in combination with Me-, C_2H_4NPhth-, and Bpin-substituted cyclohexene derivatives (Table 3.5). While the ratio of regioisomers was not affected for 1-Me cyclohexene (product **42u**, entries 1-3), the outcome was different for the two other substrates. With Bpin-cyclohexene (product **42x**), a switch of selectivity took place in favor of the less hindered position when using the more hindered catalysts **A6** and **A7** (entries 5 and 6). In the case of product **42y**, the ratio of regioisomers was significantly improved from 6:1 to 10:1 in favor of the less hindered site (entry 7 vs 9).

Overall, these results suggest that modulation of the BINOL scaffold of catalysts **A** could offer opportunities for tuning the site-selectivity of the HAT process.

Table 3.5. Regioselectivity studies when using non-symmetrical allylic precursors.

entry	R	catalyst	yield **42 + 42'** (%)[a]	**42:42'**
1		A5	67	5:1
2	Me	A6	37	5:1
3		A7	26	4:1
4		A5	45	1:1.2
5	Bpin	A6	50	4:1
6		A7	19	4:1
7		A5	62	6:1
8	C₂H₄NPhth	A6	54	7:1
9		A7	48	10:1

Reactions performed on a 0.1 mmol scale using 10 equiv. of **2** when R = Me and 5 equiv. when R = C_2H_4NPhth, Bpin. [a]Yields determined by ^1H NMR analysis.

3.7 Conclusion

This chapter summarizes our efforts towards the development of an organocatalytic platform for the benzylation of allylic C-H bonds under photochemical conditions. The chemistry exploits the ability of dithiophosphoric acids to play two distinct catalytic roles, serving sequentially as donors in the formation of photoactive EDA complexes, and then as hydrogen atom abstractors for the formation of allylic radicals from non-functionalized allylic precursors. The key bond-forming event relies on a cross-coupling between benzylic and allylic radicals. Importantly, the starting materials used in this chemistry are readily available carboxylic acids, primary amines, and alkenes used in combination with a cheap and easy-to-make catalyst. The need for an excess of allylic precursor to achieve cross-selectivity and moderate yields can be viewed as the major drawbacks. Nonetheless, the protocol's functional group tolerance enabled the functionalization of a variety of biologically relevant compounds and the design of a three-component radical process. This second strategy offered complete

UNIVERSITAT ROVIRA I VIRGILI
PHOTOCHEMISTRY AND ORGANOCATALYSIS FOR RADICAL-BASED CARBON-CARBON BOND-FORMING
PROCESSES
Emilien Le Saux

109

cross-selectivity in the radical coupling reaction by suppressing the formation of dimers. Finally, preliminary results indicated that tuning the catalyst's bulkiness could be useful to control the regioselectivity of the HAT process when more than one hydrogen atom is available for abstraction.

3.8 Experimental section

General Information. The ^{1}H NMR, ^{19}F NMR, and ^{13}C NMR spectra are available in the literature[1] and are not reported in the present dissertation.

The NMR spectra were recorded at 300 MHz, 400 MHz and 500 MHz for ^{1}H or at 75 MHz, 101 MHz and 126 MHz for ^{13}C, 376 MHz for ^{19}F, respectively. The chemical shifts (δ) for ^{1}H and ^{13}C{1H} are given in ppm relative to residual signals of the solvents (CHCl$_3$ @ 7.26 ppm ^{1}H NMR, 77.00 ppm ^{13}C NMR). Coupling constants are given in Hz. The following abbreviations are used to indicate the multiplicity: s, singlet; d, doublet; t, triplet; q, quartet; m, multiplet; br s, broad signal.

High-resolution mass spectra (HRMS) were obtained from the ICIQ High-Resolution Mass Spectrometry Unit on MicroTOF Focus and Maxis Impact (Bruker Daltonics) with electrospray ionization (ESI) or atmospheric pressure chemical ionization (APCI). UV-vis measurements were carried out on a Shimadzu UV-2401PC spectrophotometer equipped with photomultiplier detector, double beam optics and D2 and W light sources.

Yield of isolated products refer to materials of > 95% purity as determined by ^{1}H NMR analysis.

General Procedures. All reactions were set up under an argon atmosphere in oven-dried glassware using standard Schlenk techniques, unless otherwise stated. Synthesis grade solvents were used as purchased. Anhydrous solvents were taken from a commercial SPS solvent dispenser. Chromatographic purification of products was accomplished using flash column chromatography (FC) on silica gel (35-70 mesh). For thin layer chromatography (TLC) analysis throughout this work, Merck precoated TLC plates (silica gel 60 GF$_{254}$, 0.25 mm) were used, using UV light as the visualizing agent and either phosphomolybdic acid in EtOH, or basic aqueous potassium permanganate (KMnO$_4$), and heat as developing agents. Organic solutions were concentrated under reduced pressure on a Büchi rotary evaporator (*in vacuo* at 40 ºC, ~5 mbar).

Determination of Diastereomeric Ratio. The diastereomeric ratio were determined by ^{1}H NMR analysis of the crude reaction mixture through integration of diagnostic signals.

Materials. Commercial grade reagents and solvents were purchased at the highest commercial quality from Sigma Aldrich, Fluka, Acros Organics, Fluorochem, or Alfa Aesar and used as received, unless otherwise stated. Thiol catalysts **A1**, **A2** and **A3** are commercially available. The thiophosphoric acid **A4** was prepared according to a reported procedure.[31a]

UNIVERSITAT ROVIRA I VIRGILI
PHOTOCHEMISTRY AND ORGANOCATALYSIS FOR RADICAL-BASED CARBON-CARBON BOND-FORMING
PROCESSES
Emilien Le Saux

111

3.8.1 Substrate synthesis

Catalysts **A5-7** were prepared according to a reported procedure from the corresponding BINOLs.[37]
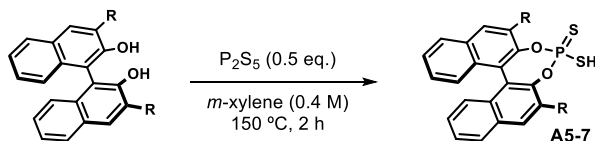

Figure 3.32. Synthesis of catalysts **A5-7**.

(11bS)-4-mercaptodinaphtho[2,1-d:1',2'-f][1,3,2]dioxaphosphepine 4-sulfide (A5) A flame dried flask was charged with (*S*)-1,1'-bi-2-naphtol (2.29 g, 8.0 mmol), P$_2$S$_5$ (889 mg, 4.0 mmol, 0.5 equiv), and anhydrous *m*-xylene (20 mL, 0.4 M). The flask was equipped with a condenser and placed in an oil-bath preheated to 150 ºC. The progress of the reaction was monitored by disappearance of the phenolic protons, as inferred by ^{1}H NMR analysis of the crude mixture. After 2 h, the reaction was completed and the mixture was cooled to ambient temperature. The solvent was removed *in vacuo*. The crude product was dissolved in a minimum amount of CH$_2$Cl$_2$ and treated with hexanes. The resulting fine precipitate was then collected by filtration and the operation repeated until no more precipitate was formed. Pure dithiophosphoric acid **A5** was obtained after washing the precipitates with cold hexanes.

^{1}H NMR (400 MHz, CDCl$_3$) δ 8.13 – 8.07 (m, 2H), 8.00 (dd, *J* = 8.1, 1.2 Hz, 2H), 7.60 (dd, *J* = 8.8, 1.4 Hz, 2H), 7.54 (ddt, *J* = 8.0, 6.8, 1.1 Hz, 2H), 7.48 – 7.42 (m, 2H), 7.36 (ddd, *J* = 8.4, 6.7, 1.3 Hz, 2H).

^{13}C NMR (75 MHz, CDCl$_3$) δ 147.2, 132.4, 132.0, 131.1, 128.6, 127.2, 126.9, 126.1, 122.6, 121.1.

^{31}P NMR (162 MHz, CDCl$_3$) δ 100.24.

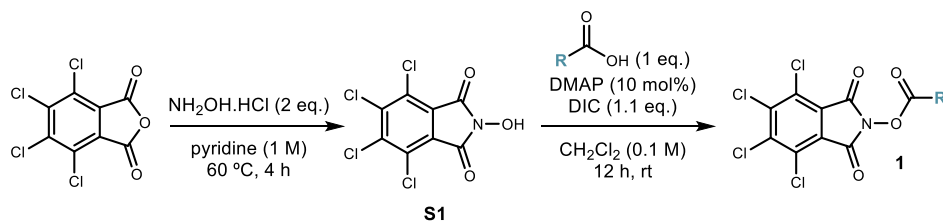Tetrachlorophthalimide esters **1** were prepared as depicted in Figure 3.33.

Figure 3.33. Synthesis of tetrachlorophthalimide esters from carboxylic acids.

***N*-hydroxy-tetrachlorophthalimide (S1)[39]** Tetrachlorophthalic anhydride (1.0 equiv.) and hydroxylamine hydrochloride (2.0 equiv.) were dissolved in pyridine (1 M). and stirred at 60 ºC for 4 hours. The resulting slurry was suspended in water and acidified with concentrated HCl until a solid precipitated. The solid was collected by filtration and washed, water and dried under high vacuum to affod **S1**.

Tetrachlorophthalimide esters (1) A round-bottom flask was charged with carboxylic acid (1.0 equiv), *N*-hydroxy-tetrachlorophthalimide **S1** (1.0 equiv.) and DMAP (0.1 equiv.). Dichloromethane was added (0.1 M), and the mixture was stirred vigorously. DIC (1.1 equiv.) was then added slowly, and the mixture was allowed to stir overnight. The mixture was filtered over Celite and rinsed with additional CH_2Cl_2. The solvent was removed under reduced pressure, and the crude mixture purified by column chromatography to afford the corresponding tetrachloro-phthalimide esters **1**.

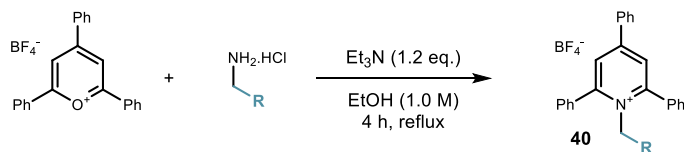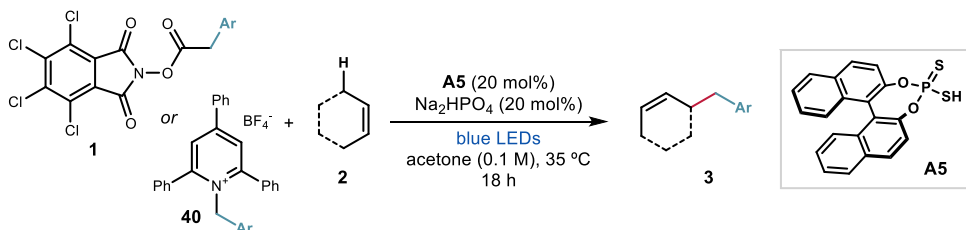Pyridinium salts **40** were prepared following a reported procedure.[40]

Figure 3.34. Synthesis of pyridinium salts.

To the amino acid salt (1.2 equiv.) were added EtOH (1.0 M) and Et_3N (1.2 equiv.). The resulting suspension was stirred at room temperature for 30 min and then 2,4,6-triphenylpyrylium tetrafluoroborate (1.0 equiv) was added in one portion. The reaction mixture was then heated under reflux for 4 h. The reaction was then allowed to cool to room temperature before Et_2O was added and the mixture stirred for an additional 1 h. The resulting solid was collected by filtration and thoroughly washed with H_2O and Et_2O. The remaining solid was then dried under reduced pressure to afford the pyridinium salt **40** without further purification.

[39] Horn, E. J.; Rosen, B. R.; Chen, Y.; Tang, J.; Chen, K.; Eastgate, M. D.; Baran, P. S. "Scalable and Sustainable Electrochemical Allylic C-H Oxidation" *Nature*, **2016**, *533*, 77.

[40] James, M. J.; Strieth-Kalthoff, F.; Sandfort, F.; Klauck, F. J. R.; Wagener, F.; Glorius, F. "Visible-Light-Mediated Charge Transfer Enables C−C Bond Formation with Traceless Acceptor Groups" *Chem. Eur. J.* **2019**, *25*, 8240.

UNIVERSITAT ROVIRA I VIRGILI
PHOTOCHEMISTRY AND ORGANOCATALYSIS FOR RADICAL-BASED CARBON-CARBON BOND-FORMING
PROCESSES
Emilien Le Saux

113

3.8.2 General procedure for the direct C-H allylic benzylation

General procedure A. To an argon-purged glass vial containing catalyst **A5** (0.2 equiv.), tetrachloro-phthalimide ester **1** or pyridinium salt **40** (1.0 equiv.), and Na$_2$HPO$_4$ (0.2 equiv.), was added the allylic precursor **2** (20 equiv.) followed by argon-sparged HPLC grade acetone (0.1M). The vial was sealed with Parafilm, and placed in the irradiation setup (detailed in Figure 3.35), maintained at a temperature of 35 ºC. The reaction was stirred for 18 h, then the solvent was evaporated and the crude mixture purified by flash column chromatography on silica gel to furnish the product **3**.
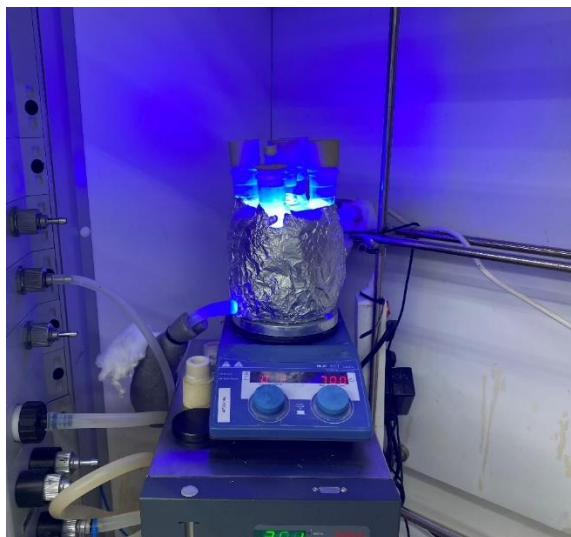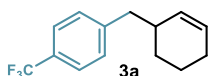

Figure 3.35. Fully assembled temperature-controlled photoreactor in operation.

3.8.3 Characterization of products 3

1-(cyclohex-2-en-1-ylmethyl)-4-(trifluoromethyl)benzene (3a)

Prepared according to General Procedure A using radical precursor **1a** (97.4 mg, 0.2 mmol) and cyclohexene **2a** (406 μL, 4.0 mmol). The crude mixture was purified
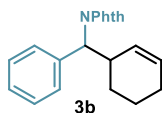
by column chromatography (SiO$_2$, 100% pentane) to afford product **3a** as a colorless oil (19.8 mg, 41% yield, average of two runs).

^{1}H NMR (400 MHz, CDCl$_3$) δ 7.53 (d, J = 8.0 Hz, 2H), 7.28 (d, J = 8.0 Hz, 2H), 5.71 (dtd, J = 9.8, 3.5, 2.2 Hz, 1H), 5.53 (dq, J = 10.1, 2.4 Hz, 1H), 2.69 (dd, J = 13.3, 7.2 Hz, 1H), 2.60 (dd, J = 13.3, 8.0 Hz, 1H), 2.39 (ddtq, J = 10.4, 7.6, 5.0, 2.7 Hz, 1H), 1.99 (dtt, J = 7.4, 5.2, 2.7 Hz, 2H), 1.71 (tdt, J = 12.6, 8.7, 4.3 Hz, 2H), 1.60 – 1.48 (m, 1H), 1.40 – 1.26 (m, 1H).

^{13}C NMR (101 MHz, CDCl$_3$) δ 145.0, 130.6, 129.4, 129.1 (q, J = 275.1 Hz), 127.9, 125.1 (q, J = 3.8 Hz), 42.5, 40.1, 37.0, 28.8, 26.0, 25.4, 25.3, 22.2, 21.2.

^{19}F NMR (376 MHz, CDCl$_3$) δ -62.4.

HRMS (APCI$^+$) Calculated for C$_{14}$H$_{14}$F$_3$ [M-H]$^-$: 239.1042, found: 239.1052.

2-(cyclohex-2-en-1-yl(phenyl)methyl)isoindoline-1,3-dione (3b)

Prepared according to General Procedure A using radical precursor **1b** (56.4 mg, 0.1 mmol), and cyclohexene **2a** (203 μL, 2.0 mmol). The crude mixture was purified by column chromatography (SiO$_2$, 20:1 Hexane/EtOAc) to afford product **3b** as a white solid (7.9 mg, 25% yield, 1.1:1 dr., average of two runs).

^{1}H NMR (500 MHz, CDCl$_3$) *1.1:1 mixture of diastereoiomers* δ 7.79 (ddd, J = 5.4, 3.8, 3.0 Hz, 2H), 7.67 (dd, J = 5.5, 3.0 Hz, 2H), 7.63 (tt, J = 8.1, 1.3 Hz, 2H), 7.37 – 7.30 (m, 2H), 7.29 – 7.24 (m, 1H), 5.78 (dtd, J = 9.8, 3.7, 2.0 Hz, 0.5H), 5.71 (dtd, J = 9.9, 3.7, 2.2 Hz, 0.5H), 5.56 – 5.50 (m, 0.5H), 5.33 – 5.26 (m, 0.5H), 5.00 (d, J = 12.3 Hz, 0.5H), 4.98 (d, J = 12.1 Hz, 0.5H), 3.83 – 3.71 (m, 0.5H), 2.05 – 1.99 (m, 2H), 1.83 – 1.68 (m, 0.5H), 1.68 – 1.48 (m, 0.5H), 1.37 – 1.27 (m, 0.5H), 1.16 (dddd, J = 12.9, 10.4, 7.9, 2.9 Hz, 0.5H).

^{13}C NMR (126 MHz, CDCl$_3$) *1.1:1 mixture of diastereoiomers* δ 168.4, 168.4, 138.8, 138.4, 133.9, 131.8, 131.8, 129.9, 129.4, 129.1, 129.1, 128.6, 128.0, 127.9, 127.5, 127.0, 127.0, 123.2, 123.2, 60.6, 60.0, 34.7, 34.1, 27.1, 26.6, 25.3, 25.2, 20.7, 20.5.

HRMS (ESI$^+$) Calculated for C$_{21}$H$_{19}$NNaO$_2$ [M+Na]$^+$: 340.1308, found: 340.1304
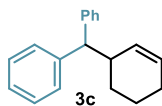
(cyclohex-2-en-1-ylmethylene)dibenzene (3c)

Prepared according to General Procedure A using radical precursor **1c** (49.5 mg, 0.1 mmol), and cyclohexene **2a** (203 μL, 2.0 mmol). The crude mixture was purified by column chromatography (SiO$_2$, 99:1 pentane/CH$_2$Cl$_2$) to afford product **3c** as a white solid (12.4 mg, 50% yield, average of two runs).

^{1}H NMR (400 MHz, CDCl$_3$) δ 7.34 – 7.29 (m, 2H), 7.29 – 7.22 (m, 6H), 7.17 – 7.10 (m, 2H), 5.66 (dtd, J = 9.9, 3.5, 2.0 Hz, 1H), 5.45 (dqd, J = 10.3, 2.2, 1.0 Hz, 1H), 3.59 (d, J = 11.4 Hz, 1H), 2.98 (dddp, J = 10.9, 8.0, 5.4, 2.7 Hz, 1H), 1.98 (qt, J = 5.1, 3.1 Hz, 2H), 1.76 – 1.66 (m, 1H), 1.65 – 1.56 (m, 1H), 1.56 – 1.44 (m, 1H), 1.19 (dddd, J = 12.8, 11.2, 8.6, 2.8 Hz, 1H).

UNIVERSITAT ROVIRA I VIRGILI
PHOTOCHEMISTRY AND ORGANOCATALYSIS FOR RADICAL-BASED CARBON-CARBON BOND-FORMING
PROCESSES
Emilien Le Saux

115

^{13}C NMR (101 MHz, CDCl$_3$) δ 144.2, 143.9, 130.0, 128.5, 128.4, 128.3, 128.2, 128.0, 126.1, 126.1, 58.1, 38.9, 28.3, 25.4, 21.5.
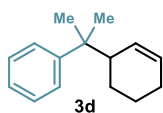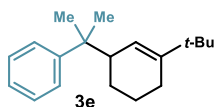
(2-(cyclohex-2-en-1-yl)propan-2-yl)benzene (3d)

Prepared according to General Procedure A using radical precursor **1d** (89.4 mg, 0.2 mmol), and cyclohexene **2a** (406 µL, 4.0 mmol). The crude mixture was purified by column chromatography (SiO$_2$, 100% pentane) to afford product **3d** as a colorless oil (18.0 mg, 45% yield, average of two runs).

^{1}H NMR (500 MHz, CDCl$_3$) δ 7.37 – 7.34 (m, 2H), 7.33 – 7.28 (m, 2H), 7.20 – 7.16 (m, 1H), 5.73 – 5.66 (m, 1H), 5.49 (dp, J = 10.3, 2.0 Hz, 1H), 2.46 (dddt, J = 10.2, 8.0, 5.2, 2.6 Hz, 1H), 1.92 (dddd, J = 9.0, 4.4, 3.3, 2.0 Hz, 2H), 1.77 – 1.69 (m, 1H),1.50 – 1.40 (m, 1H), 1.30 (s, 3H), 1.26 (s, 3H), 1.20 (tdd, J = 12.7, 10.7, 2.9 Hz, 2H).

^{13}C NMR (126 MHz, CDCl$_3$) δ 149.8, 129.0, 128.4, 127.9, 126.2, 125.4, 46.5, 40.2, 30.3 29.7, 25.3, 25.2, 25.0, 24.7, 22.8.

HRMS (APCI$^+$) Calculated for C$_{15}$H$_{21}$ [M+H]$^+$: 201.1638, found: 201.1633.

(2-(3-(tert-butyl)cyclohex-2-en-1-yl)propan-2-yl)benzene (3e)

Prepared according to General Procedure A using radical precursor **1d** (49.7 mg, 0.1 mmol), and 1-tert-Butyl-1-cyclohexene **2b** (170 µL, 1.0 mmol). The crude mixture was purified by column chromatography (SiO$_2$, 100% pentane) to afford product **3e** as a colorless oil (10 mg, single regioisomer, 39% yield, average of two runs).

^{1}H NMR (400 MHz, CDCl$_3$) δ 7.40 – 7.29 (m, 4H), 7.22 – 7.17 (m, 1H), 5.33 (tt, J = 2.2, 0.9 Hz, 1H), 2.43 (dddd, J = 10.5, 5.9, 4.0, 2.2 Hz, 1H), 2.06 – 1.98 (m, 1H), 1.91 – 1.82 (m, 1H), 1.82 – 1.73 (m, 1H), 1.54 – 1.46 (m, 1H), 1.41 – 1.33 (m, 1H), 1.31 (s, 3H), 1.27 (s, 3H), 1.09 (ddd, J = 12.6, 10.6, 3.2 Hz, 1H), 1.00 (s, 9H).

^{13}C NMR (101 MHz, CDCl$_3$) δ 150.0, 147.0, 127.8, 126.3, 125.3, 119.2, 46.7, 40.7, 35.5, 29.1, 25.3, 25.0, 24.8, 24.6, 23.5.

HRMS (APCI$^+$) Calculated for C$_{19}$H$_{29}$ [M+H]$^+$: 257.2264, found: 257.2256.
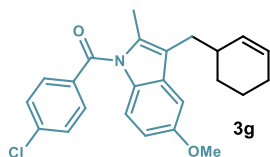
(4-chlorophenyl)(3-(cyclohex-2-en-1-ylmethyl)-5-methoxy-2-methyl-1H-indol-1-yl)methanone (3f)

Prepared according to General Procedure A using radical precursor **1e** (64.1 mg, 0.1 mmol), and cyclohexene **2a** (203 µL, 2.0 mmol). The crude mixture was purified by column chromatography (SiO$_2$, 98:2

hexanes/EtOAc) to afford product **3f** as a yellowish oil (12.6 mg, 32% yield, average of two runs).

<u>1</u>H NMR (500 MHz, CDCl$_3$) δ 7.68 – 7.64 (m, 2H), 7.52 – 7.47 (m, 2H), 6.96 – 6.86 (m, 2H), 6.67 (dd, J = 9.0, 2.6 Hz, 1H), 5.73 (td, J = 6.0, 2.9 Hz, 1H), 5.63 (dd, J = 10.1, 2.3 Hz, 1H), 3.85 (s, 3H), 2.68 (dd, J = 14.0, 7.3 Hz, 1H), 2.60 (dd, J = 14.0, 8.2 Hz, 1H), 2.47 (s, 1H), 2.34 (s, 3H), 2.03 (d, J = 5.7 Hz, 2H), 1.79 (dq, J = 10.1, 6.2, 5.4 Hz, 2H), 1.55 (s, 1H), 1.34 (td, J = 10.9, 8.5 Hz, 1H).

<u>13</u>C NMR (126 MHz, CDCl$_3$) δ 206.9, 168.3, 155.8, 139.0, 134.7, 134.3, 131.6, 131.3, 131.1, 131.0, 129.1, 127.6, 118.6, 114.9, 110.8, 101.9, 55.8, 35.8, 30.9, 30.7, 29.3, 25.4, 21.3, 13.6.

<u>HRMS</u> (ESI$^+$) Calculated for C$_{24}$H$_{24}$ClNNaO$_2$ [M+Na]$^+$: 416.1388, found: 416.1399.

3f

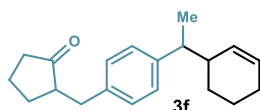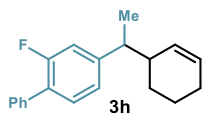### 2-(4-(1-(cyclohex-2-en-1-yl)ethyl)benzyl)cyclopentan-1-one (3g)

Prepared according to General Procedure A using radical precursor **1f** (52.9 mg, 0.1 mmol), and cyclohexene **2a** (203 µL, 2.0 mmol). The crude mixture was purified by column chromatography (SiO$_2$, 98:2 hexanes/EtOAc) to afford product **3g** as a colorless oil (12.4 mg, 44% yield, 1.1:1 dr, average of two runs).

<u>1</u>H NMR (400 MHz, CDCl$_3$) *1.1:1 mixture of diastereoiomers* δ 7.11 (s, 4H), 5.84 – 5.72 (m, 1H), 5.64 (dq, J = 10.1, 3.4 Hz, 0.5H), 5.38 (dd, J = 10.2, 2.3 Hz, 0.5H), 3.14 (dt, J = 13.9, 3.8 Hz, 1H), 2.68 – 2.48 (m, 2H), 2.43 – 2.32 (m, 2H), 2.30 – 2.21 (m, 1H), 2.19 – 2.06 (m, 2H), 1.97 (dtt, J = 8.4, 6.1, 3.3 Hz, 3H), 1.87 – 1.65 (m, 2H), 1.64 – 1.54 (m, 1H), 1.53 – 1.39 (m, 1H), 1.33 – 1.27 (m, 2H), 1.27 – 1.22 (m, 2H), 1.21 – 1.11 (m, 0.5H), 0.97 – 0.78 (m, 0.5H).

<u>13</u>C NMR (101 MHz, CDCl$_3$) *1.1:1 mixture of diastereoiomers* δ 144.5, 144.3, 137.4, 130.8, 129.6, 128.8, 128.6, 128.2, 127.9, 127.8, 127.5, 127.5, 51.1, 44.6, 44.2, 41.9, 41.9, 41.8, 38.3, 35.2, 35.2, 29.3, 27.6, 26.5, 25.4, 25.3, 22.0, 21.4, 20.6, 18.7, 18.7, 18.5, 15.6, -18.5.

<u>HRMS</u> (APCI$^+$) Calculated for C$_{20}$H$_{27}$O [M+H]$^+$: 283.2056, found: 283.2051.

3h

4-(1-(cyclohex-2-en-1-yl)ethyl)-2-fluoro-1,1'-biphenyl (3h)

Prepared according to General Procedure A using radical precursor **1g** (52.7 mg, 0.1 mmol), and cyclohexene **2a** (203 µL, 2.0 mmol). The crude mixture was purified by column chromatography (SiO$_2$, hexanes) to afford product **3h** as a colorless oil (13.8 mg, 49% yield, 1.1:1 dr, average of two runs).

<u>1</u>H NMR (400 MHz, CDCl$_3$) *1.1:1 mixture of diastereoiomers* δ 7.61 – 7.55 (m, 2H), 7.50 – 7.44 (m, 2H), 7.41 – 7.35 (m, 2H), 7.09 – 6.98 (m, 2H), 5.87 – 5.77 (m, 1H), 5.75 – 5.67 (m, 0.5H), 5.46 (ddd, J = 10.2, 2.3, 1.2 Hz, 0.5H), 2.67 (ddt, J = 14.5, 11.3, 7.4 Hz, 1H), 2.34

UNIVERSITAT ROVIRA I VIRGILI
PHOTOCHEMISTRY AND ORGANOCATALYSIS FOR RADICAL-BASED CARBON-CARBON BOND-FORMING
PROCESSES
Emilien Le Saux

117

(ddddd, J = 18.5, 11.5, 8.1, 5.3, 2.8 Hz, 1H), 2.00 (ddt, J = 6.0, 4.0, 2.1 Hz, 2H), 1.91 – 1.78 (m, 1H), 1.78 – 1.68 (m, 1H), 1.62 – 1.46 (m, 1H), 1.37 – 1.28 (m, 3H), 1.28 – 1.20 (m, 0.5H), 0.96 – 0.81 (m, 0.5H).

^{13}C NMR (101 MHz, CDCl$_3$) *1.1:1 mixture of diastereoiomers* δ 160.9, 158.4, 148.5, 135.9, 130.3, 130.3, 130.2, 129.2, 129.0, 128.9, 128.6, 128.4, 128.0, 127.4, 126.3, 123.8, 123.6, 115.3, 115.1, 114.8, 44.6, 44.3, 41.8, 41.7, 27.6, 26.5, 25.4, 25.3, 21.9, 21.4, 18.6, 18.4.

^{19}F NMR (376 MHz, CDCl$_3$) δ -118.8.

HRMS (APCI$^+$) Calculated for C$_{20}$H$_{22}$F [M+H]$^+$: 281.1700, found: 281.1701.
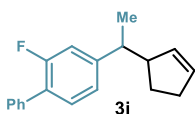
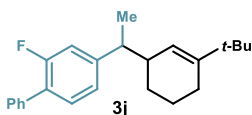### 4-(1-(cyclopent-2-en-1-yl)ethyl)-2-fluoro-1,1'-biphenyl (3i)

Prepared according to General Procedure A using radical precursor **1g** (52.7 mg, 0.1 mmol) and cyclopentene **2c** (176 µL, 2.0 mmol). The crude mixture was purified by column chromatography (SiO$_2$, 30:1 hexanes/CH$_2$Cl$_2$) to afford product **3i** as a colorless oil (12.1 mg, 45% yield, 1.1:1 dr, average of two runs).

^{1}H NMR (500 MHz, CDCl$_3$) *1.1:1 mixture of diastereoisomers* δ 7.56 (dt, J = 7.9, 1.5 Hz, 2H), 7.48 – 7.40 (m, 2H), 7.39 – 7.32 (m, 2H), 7.04 (dd, J = 7.9, 1.7 Hz, 1H), 7.00 (dt, J = 12.1, 1.8 Hz, 1H), 5.87 – 5.80 (m, 1H), 5.73 (dq, J = 5.8, 2.3 Hz, 0.5H), 5.45 (dq, J = 6.0, 2.1 Hz, 0.5H), 2.95 – 2.84 (m, 1H), 2.64 – 2.54 (m, 1H), 2.35 – 2.20 (m, 2H), 2.10 (dtd, J = 12.7, 8.1, 4.5 Hz, 0.5H), 1.85 (dtd, J = 13.4, 8.6, 5.0 Hz, 0.5H), 1.62 – 1.53 (m, 0.5H), 1.45 (ddt, J = 12.9, 9.0, 6.3 Hz, 0.5H), 1.31 (d, J = 6.9 Hz, 1.5H), 1.28 (d, J = 7.0 Hz, 1.5H), 1. 29 – 1.26 (m, 1H).

^{13}C NMR (126 MHz, CDCl$_3$) *1.1:1 mixture of diastereoisomers* δ 160.6, 158.7, 148.8 (d, J = 7.1 Hz), 148.7 (d, J = 7.3 Hz), 135.9, 133.6, 132.8, 132.0, 131.2, 130.3 (d, J = 3.4 Hz), 130.2 (d, J = 3.4 Hz), 128.9 (d, J = 3.1 Hz), 128.4, 127.4, 126.3 (d, J = 4.0 Hz), 126.2 (d, J = 3.7 Hz), 123.6 (d, J = 3.3 Hz), 123.5 (d, J = 3.4 Hz), 115.0 (d, J = 4.4 Hz), 114.8 (d, J = 4.3 Hz), 52.8, 52.5, 45.1, 44.9, 32.3, 31.9, 28.6, 28.2, 19.8, 19.8.

^{19}F NMR (376 MHz, CDCl$_3$) δ -118.7.

HRMS (APCI$^+$) Calculated for C$_{19}$H$_{20}$F [M+H]$^+$: 267.1544, found: 267.1541.

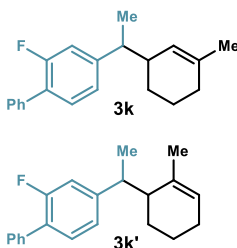### 4-(1-(3-(tert-butyl)cyclohex-2-en-1-yl)ethyl)-2-fluoro-1,1'-biphenyl (3j)

Prepared according to General Procedure A using radical precursor **1g** (52.7 mg, 0.1 mmol) and 1-tert-Butyl-1-cyclohexene **2b** (170 µL, 1.0 mmol). The crude mixture was purified by column chromatography (SiO$_2$, hexanes) to afford product **3j** as a colorless oil (16 mg, 48% yield, 1.1:1 dr, single regioisomer, average of two runs).

^{1}H NMR (400 MHz, CDCl$_3$) *1.1:1 mixture of diastereoisomers* δ 7.62 – 7.55 (m, 2H), 7.46 (ddt, *J* = 8.2, 6.1, 0.9 Hz, 2H), 7.41 – 7.35 (m, 2H), 7.08 – 6.98 (m, 2H), 5.60 (d, *J* = 2.6 Hz, 0.5H), 5.29 – 5.26 (m, 0.5H), 2.77 – 2.61 (m, 1H), 2.32 (dtq, *J* = 10.8, 5.5, 2.5 Hz, 1H), 2.05 (dd, *J* = 17.1, 4.7 Hz, 1H), 1.99 – 1.85 (m, 1H), 1.84 – 1.70 (m, 1H), 1.54 – 1.39 (m, 2H), 1.35 (d, *J* = 7.0 Hz, 1.5H), 1.30 – 1.28 (m, 1.5H), 1.07 (s, 4.5H), 1.00 (s, 4.5H), 0.92 (d, *J* = 3.6 Hz, 1H).

^{13}C NMR (101 MHz, CDCl$_3$) *1.1:1 mixture of diastereoisomers* δ 160.83, 158.37, 148.68 (d, *J* = 7.2 Hz), 148.47 (d, *J* = 7.1 Hz), 136.01, 130.06 (dd, *J* = 7.9, 4.0 Hz), 128.96 (d, *J* = 3.0 Hz), 128.38, 127.35, 123.98 (d, *J* = 3.0 Hz), 123.68 (d, *J* = 3.2 Hz), 120.81, 119.56, 115.36, 115.15 (d, *J* = 3.2 Hz), 114.94, 44.87, 44.66, 42.27, 41.98, 35.53, 35.39, 29.15, 29.06, 27.37, 26.06, 24.75, 24.68, 22.77, 22.32, 18.53, 17.61.

^{19}F NMR (376 MHz, CDCl$_3$) δ -119.0.

HRMS (APCI$^+$) Calculated for C$_{20}$H$_{30}$F [M+H]$^+$: 337.2326, found: 337.2324.

2-fluoro-4-(1-(3-methylcyclohex-2-en-1-yl)ethyl)-1,1'-biphenyl (3k + 3k')

Prepared according to General Procedure A using radical precursor **1g** (52.7 mg, 0.1 mmol) and 1-Methyl-1-cyclohexene **2d** (237 μL, 2.0 mmol). The crude mixture was purified by column chromatography (SiO$_2$, hexanes) to afford product **3k** as a colorless oil (12.8 mg, 44% yield, 1.5:1 *r.r.;* major regioisomer (**3k**) 1.4:1 *d.r.,* minor regioisomer (**3k'**) 1.5:1 *d.r.*, average of two runs). Product **3k** was isolated together with an unidentified isomeric product.

^{1}H NMR (400 MHz, CDCl$_3$) *major regioisomer (3k)* 1.4:1 *mixture of diastereoimers* δ 7.56 (ddddd, *J* = 7.2, 5.8, 4.3, 2.7, 1.6 Hz), 7.48 – 7.39 (m), 7.39 – 7.30 (m), 7.06 – 6.94 (m), 5.54 – 5.48 (m, 1.4H), 5.15 (dd, *J* = 2.8, 1.4 Hz, 1H), 2.59 (p, *J* = 7.2 Hz, 2.4H), 2.40 – 2.18 (m, 2.4H), 1.99 – 1.84 (m), 1.84 – 1.75 (m), 1.69 (dt, *J* = 2.3, 1.1 Hz, 3H), 1.62 (dt, *J* = 2.4, 1.2 Hz, 3H), 1.72– 1.60 (m), 1.47 (dddd, *J* = 15.0, 10.4, 5.5, 2.7 Hz), 1.32 (d, *J* = 6.9 Hz, 3H), 1.25 (d, *J* = 7.0 Hz, 3H), 1.37 – 1.24 (m).

^{1}H NMR (400 MHz, CDCl$_3$) *minor regioisomer (3k')* 1.5:1 *mixture of diastereoimers* δ 7.56 (ddddd, *J* = 7.2, 5.8, 4.3, 2.7, 1.6 Hz), 7.48 – 7.39 (m), 7.39 – 7.30 (m), 7.06 – 6.94 (m), 5.66 (s, 1.5H), 5.58 (s, 1H), 2.79 (q, *J* = 7.2 Hz, 1H), 2.69 (qd, *J* = 7.4, 3.8 Hz, 1.5H), 1.99 – 1.84 (m), 1.84 – 1.75 (m), 1.71 (s, 3H), 1.72– 1.60 (m), 1.54 (s, 4.5H), 1.47 (dddd, *J* = 15.0, 10.4, 5.5, 2.7 Hz), 1.31 (d, *J* = 7.1 Hz, 3H), 1.28 (d, *J* = 7.3 Hz, 4.5H) 1.37 – 1.24 (m).

^{13}C NMR (126 MHz, CDCl$_3$) *mixture of regioisomers and diasteroisomers* δ 160.6, 158.7, 136.0, 135.8, 135.0, 130.2, 130.2, 128.9, 128.9, 128.4, 128.4, 127.4, 127.3, 124.4, 123.8, 123.8, 123.6, 123.6, 123.2, 115.3, 115.1, 115.0, 114.8, 49.3, 47.8, 45.3, 45.0, 44.8, 44.5, 42.0,

UNIVERSITAT ROVIRA I VIRGILI
PHOTOCHEMISTRY AND ORGANOCATALYSIS FOR RADICAL-BASED CARBON-CARBON BOND-FORMING
PROCESSES
Emilien Le Saux

119

42.0, 33.6, 31.8, 30.2, 30.1, 27.4, 26.2, 25.4, 25.1, 25.1, 24.5, 24.1, 23.9, 22.3, 21.7, 19.1, 18.7, 18.5, 15.9, 15.6, 14.1, 12.8.

<u>^{19}F NMR</u> (376 MHz, CDCl$_3$) δ -118.9, -119.0, -119.1, -119.4.

<u>HRMS</u> (APCI$^+$) Calculated for C$_{21}$H$_{23}$F [M+H]$^+$: 295.1857, found: 295.1858.
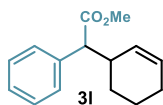
methyl 2-(cyclohex-2-en-1-yl)-2-phenylacetate (3l)

Prepared according to General Procedure A using radical precursor **40a** (109 mg, 0.2 mmol), and cyclohexene **2a** (203 μL, 2.0 mmol). The crude mixture was purified by column chromatography (SiO$_2$, 50:50 hexanes/toluene) to afford product **3l** as a colorless oil (14.6 mg, 32% yield, 1.1:1 dr, average of two runs).

<u>^{1}H NMR</u> (500 MHz, CDCl$_3$)1.1:1 *mixture of diastereoiomers* δ 7.37 – 7.30 (m, 4H), 7.29 – 7.24 (m, 1H), 5.79 (dtd, *J* = 9.8, 3.7, 2.0 Hz, 0.5H), 5.67 – 5.60 (m, 1H), 5.18 – 5.13 (m, 0.5H), 3.67 (s, 3H), 3.66 (s, 3H), 3.32 (dd, *J* = 11.2, 1.1 Hz, 1H), 2.86 (dtdt, *J* = 18.8, 8.0, 5.2, 2.6 Hz, 1H), 1.98 (tt, *J* = 5.7, 4.0, 2.0 Hz, 2H), 1.93 – 1.86 (m, 1H), 1.82 – 1.71 (m, 1H), 1.67 – 1.54 (m, 1H), 1.46 (dtt, *J* = 13.3, 6.5, 3.0 Hz, 1H), 1.42 – 1.27 (m, 1H), 1.06 (dddd, *J* = 13.3, 10.7, 8.0, 2.9 Hz, 1H).

<u>^{13}C NMR</u> (126 MHz, CDCl$_3$)1.1:1 *mixture of diastereoiomers* δ 174.0, 174.0, 137.6, 137.4, 129.2, 128.9, 128.8, 128.7, 128.6, 128.5, 128.4, 127.9, 127.3, 57.5, 57.4, 51.8, 51.8, 38.5, 38.4, 29.7, 27.9, 26.3, 25.3, 25.2, 21.1, 20.7.

3.8.4 General procedure for the three-component allylic C-H benzylation

General procedure B. To an argon-purged glass vial containing catalyst **A5** (3.8 mg, 0.01 mmol, 0.1 equiv.), tetrachloro-phthalimide ester **1** or pyridinium salt **40** (0.1 mmol, 1.0 equiv.), and Na$_2$HPO$_4$ (2.8 mg, 0.02 mmol, 0.2 equiv.), was added alkene **5** (0.1 mmol, 1.0 equiv.) and allylic precursor **2** (1 mmol, 10 equiv.). Then, 800 μL (0.1 M) of argon-sparged HPLC grade acetone were added. The vial was sealed with Parafilm, and placed in the irradiation setup, maintained at a temperature of 60 ºC. The reaction was stirred for 14 h, then the solvent was evaporated and the crude mixture purified by flash column chromatography on silica gel to furnish the product **42**.

3.8.5 Characterization of products 42
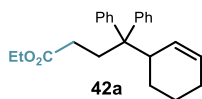
Ethyl 4-(cyclohex-2-en-1-yl)-4,4-diphenylbutanoate (42a)

Prepared according to General Procedure B using radical precursor **40b** (48.1 mg, 0.1 mmol), cyclohexene **2a** (101 μL, 1.0 mmol), and 1,1-diphenylethylene **41a** (17.7 μL, 0.1 mmol). The crude mixture was purified by column chromatography (SiO$_2$, 50:50 hexanes/toluene) to afford product **42a** as a colorless oil (33.0 mg, 95% yield, average of two runs).

^{1}H NMR (400 MHz, CDCl$_3$) δ 7.33 – 7.20 (m, 10H), 5.81 (dt, J = 10.4, 2.1 Hz, 1H), 5.62 (dddd, J = 9.8, 5.1, 2.7, 1.3 Hz, 1H), 4.07 (q, J = 7.2 Hz, 2H), 3.19 (ddt, J = 9.3, 6.9, 2.4 Hz, 1H), 2.59 (ddd, J = 13.9, 11.8, 4.6 Hz, 1H), 2.48 – 2.37 (m, 1H), 2.07 (ddd, J = 16.3, 11.7, 4.6 Hz, 1H), 1.98 – 1.82 (m, 3H), 1.76 – 1.49 (m, 3H), 1.22 (t, J = 7.1 Hz, 3H), 0.94 (tdd, J = 12.5, 10.4, 3.6 Hz, 1H).

^{13}C NMR (126 MHz, CDCl$_3$) δ 173.9, 145.2, 142.9, 129.7, 129.3, 129.0, 128.9, 127.7, 127.1, 126.0, 125.9, 60.3, 53.7, 41.6, 33.9, 30.1, 25.0, 24.7, 22.4, 14.2.

HRMS (APCI$^+$) Calculated for C$_{24}$H$_{29}$O$_2$ [M+H]$^+$: 349.2162, found: 349.2164.
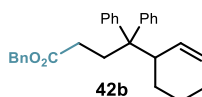
Benzyl 4-(cyclohex-2-en-1-yl)-4,4-diphenylbutanoate (42b)

Prepared according to General Procedure B using radical precursor **40c** (54.3 mg, 0.1 mmol), cyclohexene **2a** (101 μL, 1.0 mmol), and 1,1-diphenylethylene **41a** (17.7 μL, 0.1 mmol). The crude mixture was purified by column chromatography (SiO$_2$, 70:30 hexanes/toluene) to afford product **42b** as a colorless oil (27.7 mg, 68% yield, average of two runs). Multiple purifications by column chromatography resulted in poor separation from several unidentified byproducts. The yield (75%, average of two runs) of **42b** was inferred by ^{1}H NMR analysis of the crude reaction mixture using trichloroethylene as the internal standard. An analytical amount of pure compound was isolated by preparative TLC (80:20 hexanes/toluene) to obtain a colorless oil.

^{1}H NMR (400 MHz, CDCl$_3$) δ 7.42 – 7.19 (m, 15H), 5.82 (dq, J = 10.4, 2.0 Hz, 1H), 5.62 (ddt, J = 10.2, 4.9, 2.4 Hz, 1H), 5.06 (s, 2H), 3.25 – 3.16 (m, 1H), 2.63 (ddd, J = 13.9, 11.7, 4.6 Hz, 1H), 2.46 (ddd, J = 13.9, 11.6, 5.3 Hz, 1H), 2.22 – 2.10 (m, 1H), 2.02 (ddd, J = 16.5, 11.7, 5.3 Hz, 1H), 1.90 (tt, J = 15.0, 2.9 Hz, 2H), 1.77 – 1.49 (m, 3H), 0.98 (tdd, J = 12.3, 10.3, 3.7 Hz, 1H).

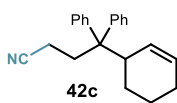^{13}C NMR (101 MHz, CDCl$_3$) δ 173.7, 145.2, 142.8, 135.9, 129.7, 129.3, 129.0, 128.9, 128.5, 128.2, 128.2, 127.8, 127.7, 127.1, 127.1, 126.0, 125.9, 66.2, 53.8, 41.6, 33.9, 30.1, 25.0, 24.7, 22.4.

HRMS (ESI$^+$) Calculated for C$_{29}$H$_{30}$NaO$_2$ [M+Na]$^+$: 433.2138, found: 433.2129.

UNIVERSITAT ROVIRA I VIRGILI
PHOTOCHEMISTRY AND ORGANOCATALYSIS FOR RADICAL-BASED CARBON-CARBON BOND-FORMING PROCESSES
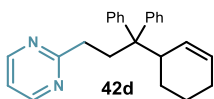Emilien Le Saux

121

4-(cyclohex-2-en-1-yl)-4,4-diphenylbutanenitrile (42c)

Prepared according to General Procedure B using radical precursor **40d** (43.4 mg, 0.1 mmol), cyclohexene **2a** (101 μL, 1.0 mmol), and 1,1-diphenylethylene **41a** (17.7 μL, 0.1 mmol). The crude mixture was purified by column chromatography (SiO$_2$, 50:50 hexanes/toluene) to afford product **42c** as a colorless oil (28.1 mg, 93% yield, average of two runs).

^{1}H NMR (400 MHz, CDCl$_3$) δ 7.37 – 7.24 (m, 6H), 7.21 (ddd, J = 7.1, 3.2, 1.8 Hz, 4H), 5.76 (dt, J = 10.5, 2.0 Hz, 1H), 5.69 – 5.61 (m, 1H), 3.23 – 3.12 (m, 1H), 2.65 (ddd, J = 14.0, 11.8, 4.6 Hz, 1H), 2.47 (ddd, J = 13.9, 11.7, 5.5 Hz, 1H), 2.08 (ddd, J = 16.4, 11.7, 4.5 Hz, 1H), 1.96 – 1.82 (m, 3H), 1.75 – 1.52 (m, 3H), 0.98 (tdd, J = 12.1, 10.3, 3.7 Hz, 1H).

^{13}C NMR (101 MHz, CDCl$_3$) δ 143.97, 141.62, 129.58, 129.42, 129.09, 128.23, 128.14, 127.51, 126.56, 126.52, 120.07, 53.97, 41.54, 35.09, 24.93, 24.73, 22.23, 13.25, 1.03.

HRMS (APCI$^+$) Calculated for C$_{22}$H$_{24}$N [M+H]$^+$: 302.1903, found: 302.1902.

2-(3-(cyclohex-2-en-1-yl)-3,3-diphenylpropyl)pyrimidine (42d)

Prepared according to General Procedure B using radical precursor **40e** (48.7 mg, 0.1 mmol), cyclohexene **2a** (101 μL, 1.0 mmol), and 1,1-diphenylethylene **41a** (17.7 μL, 0.1 mmol). The crude mixture was purified by column chromatography (SiO$_2$, 80:20 hexanes/EtOAc) to afford product **42d** as a white solid (14.5 mg, 41% yield, average of two runs).

^{1}H NMR (400 MHz, CDCl$_3$) δ 8.63 (d, J = 4.9 Hz, 2H), 7.37 – 7.27 (m, 8H), 7.26 – 7.18 (m, 2H), 7.09 (t, J = 4.9 Hz, 1H), 5.88 (dt, J = 10.4, 2.1 Hz, 1H), 5.66 – 5.58 (m, 1H), 3.32 (ddd, J = 11.0, 5.5, 3.0 Hz, 1H), 2.80 – 2.67 (m, 2H), 2.66 – 2.57 (m, 2H), 1.98 (dd, J = 12.5, 3.7 Hz, 1H), 1.84 (s, 1H), 1.74 – 1.64 (m, 1H), 1.56 (ddt, J = 13.7, 10.7, 5.5 Hz, 2H), 1.04 – 0.96 (m, 1H).

^{13}C NMR (101 MHz, CDCl$_3$) δ 171.7, 156.9, 145.7, 143.4, 129.9, 129.4, 129.4, 128.7, 127.7, 127.0, 125.8, 125.8, 118.3, 54.2, 41.6, 37.8, 35.0, 25.0, 24.7, 22.4.

HRMS (ESI$^+$) Calculated for C$_{25}$H$_{26}$NaN$_2$ [M+Na]$^+$: 355.2169, found: 355.2175.
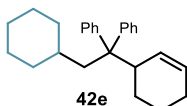
(1-(cyclohex-2-en-1-yl)-2-cyclohexylethane-1,1-diyl)dibenzene (42e)

Prepared according to General Procedure B using radical precursor **1h** (49.3 mg, 0.12 mmol), cyclohexene **2a** (101 μL, 1.0 mmol), and 1,1-diphenylethylene **41a** (17.7 μL, 0.1 mmol). The crude mixture was purified by column chromatography (SiO$_2$, pentane) to afford product **42e** as a colorless oil (24.2 mg, 70% yield, average of two runs).

^{1}H NMR (400 MHz, CDCl$_3$) δ 7.30 – 7.19 (m, 10H), 5.94 – 5.88 (m, 1H), 5.60 (ddt, J = 10.1, 5.0, 2.5 Hz, 1H), 3.22 (ddq, J = 9.7, 4.7, 2.3 Hz, 1H), 2.08 (dd, J = 14.1, 3.9 Hz, 1H), 2.01 – 1.96 (m, 1H), 1.93 – 1.83 (m, 1H), 1.74 – 1.61 (m, 2H), 1.48 (ddd, J = 12.3, 8.2, 5.1 Hz, 3H), 1.17 (dtd, J = 14.8, 6.8, 3.8 Hz, 2H), 1.11 – 0.98 (m, 4H), 0.91 (tdd, J = 10.1, 5.6, 2.2 Hz, 3H), 0.85 – 0.69 (m, 2H).

^{13}C NMR (101 MHz, CDCl$_3$) δ 146.2, 144.7, 129.9, 129.8, 129.6, 128.6, 127.3, 126.8, 125.7, 125.6, 54.9, 46.7, 41.4, 3.5, 35.2, 33.7, 33.3, 26.6, 26.5, 26.3, 25.1, 22.5.

HRMS (APCI$^+$) Calculated for C$_{26}$H$_{33}$ [M+H]$^+$: 345.2577, found: 345.2578.
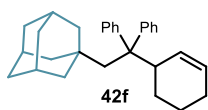
1-(2-(cyclohex-2-en-1-yl)-2,2-diphenylethyl)adamantane (42f)

Prepared according to General Procedure B using radical precursor **1i** (55.6 mg, 0.12 mmol), cyclohexene **2a** (101 µL, 1.0 mmol), and 1,1-diphenylethylene **41a** (17.7 µL, 0.1 mmol). The crude mixture was purified by column chromatography (SiO$_2$, pentane) to afford product **42f** as a colorless oil (23.0 mg, 58% yield, average of two runs).

^{1}H NMR (500 MHz, CDCl$_3$) δ 7.38 – 7.14 (m, 10H), 5.89 (dt, J = 10.6, 2.1 Hz, 1H), 5.51 (ddt, J = 10.3, 5.0, 2.5 Hz, 1H), 3.46 (ddh, J = 9.5, 4.8, 2.5 Hz, 1H), 2.18 (d, J = 14.8 Hz, 1H), 2.07 (d, J = 15.2 Hz, 1H), 2.05 – 2.01 (m, 2H), 1.88 – 1.78 (m, 1H), 1.71 (p, J = 3.2 Hz, 3H), 1.67 – 1.49 (m, 7H), 1.43 (dq, J = 12.2, 2.1 Hz, 3H), 1.30 – 1.23 (m, 2H), 1.16 (dq, J = 12.3, 2.7 Hz, 3H).

^{13}C NMR (126 MHz, CDCl$_3$) δ 146.2, 145.6, 130.4, 130.2, 129.7, 128.0, 127.9, 127.6, 127.1, 126.8, 126.3, 125.7, 125.5, 54.0, 52.4, 43.5, 43.1, 41.2, 36.8, 36.7, 34.7, 29.7, 28.9, 28.5, 25.4, 25.0, 22.4.

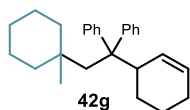HRMS (APCI)$^+$ Calculated for C$_{30}$H$_{36}$ [M+H]$^+$: 397.2890, found: 397.2887.

(1-(cyclohex-2-en-1-yl)-2-(1-methylcyclohexyl)ethane-1,1-diyl)dibenzene (42g)

Prepared according to General Procedure B using radical precursor **1j** (51.0 mg, 0.12 mmol), cyclohexene **2a** (101 µL, 1.0 mmol), and 1,1-diphenylethylene **41a** (17.7 µL, 0.1 mmol). The crude mixture was purified by column chromatography (SiO$_2$, pentane) to afford product **42g** as a colorless oil (21.9 mg, 58% yield, average of two runs).

^{1}H NMR (400 MHz, CDCl$_3$) δ 7.37 – 7.30 (m, 2H), 7.31 – 7.14 (m, 8H), 5.86 (dt, J = 10.5, 2.0 Hz, 1H), 5.51 (ddt, J = 10.3, 5.1, 2.5 Hz, 1H), 3.57 – 3.38 (m, 1H), 2.31 (d, J = 14.8 Hz, 1H), 2.26 (d, J = 15.0 Hz, 1H), 2.10 – 1.97 (m, 1H), 1.82 (dt, J = 19.3, 3.2 Hz, 1H), 1.67 – 1.47 (m, 4H), 1.33 (tdd, J = 9.5, 6.8, 3.8 Hz, 3H), 1.24 – 1.05 (m, 4H), 0.96 (dd, J = 7.2, 3.8 Hz, 2H), 0.93 – 0.86 (m, 2H), 0.83 (t, J = 5.9 Hz, 2H), 0.65 (s, 3H).

UNIVERSITAT ROVIRA I VIRGILI
PHOTOCHEMISTRY AND ORGANOCATALYSIS FOR RADICAL-BASED CARBON-CARBON BOND-FORMING PROCESSES
Emilien Le Saux

123

^{13}C NMR (101 MHz, CDCl$_3$) δ 145.8, 145.5, 130.2, 129.6, 128.0, 127.0, 126.2, 125.6, 125.5, 54.2, 41.5, 39.8, 39.8, 34.7, 29.6, 26.2, 25.3, 25.0, 22.4, 21.9, 21.9.

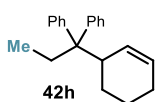HRMS (APCI$^+$) Calculated for C$_{27}$H$_{35}$ [M+H]$^+$: 359.2733, found: 359.2730.

(1-(cyclohex-2-en-1-yl)propane-1,1-diyl)dibenzene (42h)

Prepared according to General Procedure B using radical precursor **1k** (41.2 mg, 0.12 mmol), cyclohexene **2a** (101 μL, 1.0 mmol), and 1,1-diphenylethylene **41a** (17.7 μL, 0.1 mmol). The crude mixture was purified by column chromatography (SiO$_2$, pentane) to afford product **42h** as a colorless oil (17.8 mg, 64% yield, average of two runs).

^{1}H NMR (400 MHz, CDCl$_3$) δ 7.31 – 7.21 (m, 10H), 5.90 – 5.84 (m, 1H), 5.64 – 5.58 (m, 1H), 3.22 (ddq, J = 9.8, 4.8, 2.4 Hz, 1H), 2.22 – 2.16 (m, 2H), 1.88 (dddd, J = 14.0, 5.8, 2.7, 1.4 Hz, 2H), 1.74 – 1.62 (m, 1H), 1.03 – 0.84 (m, 3H), 0.64 (t, J = 7.3 Hz, 3H).

^{13}C NMR (101 MHz, CDCl$_3$) δ 146.0, 144.2, 129.9, 129.6, 129.6, 128.5, 127.3, 126.8, 125.6, 125.4, 54.5, 40.3, 31.6, 25.0, 24.6, 22.5, 8.9.

HRMS (APCI$^+$) Calculated for C$_{21}$H$_{25}$ [M+H]$^+$: 277.1951, found: 277.1948.
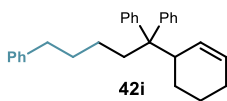
(1-(cyclohex-2-en-1-yl)pentane-1,1,5-triyl)tribenzene (42i)

Prepared according to General Procedure B using radical precursor **1l** (53.7 mg, 0.12 mmol), cyclohexene **2a** (101 μL, 1.0 mmol), and 1,1-diphenylethylene **41a** (17.7 μL, 0.1 mmol). The crude mixture was purified by column chromatography (SiO$_2$, 95:5 hexanes/CH$_2$Cl$_2$) to afford product **42i** as a colorless oil (17.2 mg, 45% yield, average of two runs).

^{1}H NMR (500 MHz, CDCl$_3$) δ 7.31 – 7.20 (m, 13H), 7.13 – 7.09 (m, 2H), 5.85 (dp, J = 10.5, 1.8 Hz, 1H), 5.64 – 5.58 (m, 1H), 3.21 (ddh, J = 9.3, 4.6, 2.4 Hz, 1H), 2.54 – 2.49 (m, 2H), 2.19 – 2.14 (m, 2H), 1.92 – 1.83 (m, 2H), 1.72 – 1.64 (m, 1H), 1.61 – 1.51 (m, 4H), 1.14 – 1.03 (m, 2H), 0.97 (tdd, J = 12.1, 10.3, 3.8 Hz, 1H).

^{13}C NMR (101 MHz, CDCl$_3$) δ 146.3, 144.3, 142.7, 129.8, 129.5, 129.5, 128.5, 128.2, 128.2, 127.4, 126.9, 125.7, 125.5, 125.5, 54.3, 40.9, 39.1, 35.7, 32.2, 25.0, 24.7, 24.1, 22.5.

HRMS (APCI$^+$) Calculated for C$_{29}$H$_{33}$ [M+H]$^+$: 381.2577, found: 381.2577.

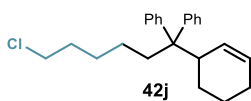**(6-chloro-1-(cyclohex-2-en-1-yl)hexane-1,1-diyl)dibenzene (42j)**

Prepared according to General Procedure B using radical precursor 1m (50.3 mg, 0.12 mmol), cyclohexene **2a** (101 μL, 1.0 mmol), and 1,1-diphenylethylene **41a**

(17.7 µL, 0.1 mmol). The crude mixture was purified by column chromatography (SiO$_2$, pentane) to afford product **42i** as a colorless oil (25 mg, 71% yield, average of two runs).

<u>^{1}H NMR</u> (500 MHz, CDCl$_3$) δ 7.31 – 7.26 (m, 4H), 7.26 – 7.19 (m, 6H), 5.84 (dd, J = 10.5, 2.2 Hz, 1H), 5.61 (ddt, J = 10.3, 5.1, 2.6 Hz, 1H), 3.44 (t, J = 6.7 Hz, 2H), 3.21 (ddd, J = 10.2, 4.7, 2.3 Hz, 1H), 2.17 – 2.09 (m, 2H), 1.92 – 1.84 (m, 2H), 1.73 – 1.63 (m, 3H), 1.57 (dt, J = 8.9, 3.1 Hz, 2H), 1.36 (dq, J = 9.4, 7.5 Hz, 2H), 1.07 – 0.92 (m, 3H).

<u>^{13}C NMR</u> (126 MHz, CDCl$_3$) δ 146.3, 144.1, 129.8, 129.4, 128.6, 127.4, 126.9, 125.8, 125.6, 54.3, 45.1, 41.1, 39.1, 32.4, 27.6, 25.1, 24.8, 23.7, 22.5.

<u>HRMS</u> (APCI$^+$) Calculated for C$_{24}$H$_{30}$Cl [M+H]$^+$: 353.2031, found: 353.2021.

Tert-butyl (4-(cyclohex-2-en-1-yl)-4,4-diphenylbutyl)carbamate (42k)

Prepared according to General Procedure B using radical precursor **1o** (47.2 mg, 0.1 mmol), cyclohexene **2a** (101 µL, 1.0 mmol), and 1,1-diphenylethylene **41a** (17.7 µL, 0.1 mmol). The crude mixture was purified by column chromatography (SiO$_2$, 80:20 hexanes/EtOAc) to afford product **42k** as a colorless oil (19.7 mg, 49% yield, average of two runs).

<u>^{1}H NMR</u> (500 MHz, CDCl$_3$) δ 7.30 – 7.19 (m, 10H), 5.82 (dt, J = 10.3, 2.2 Hz, 1H), 5.65 – 5.57 (m, 1H), 4.35 (s, 1H), 3.23 – 3.16 (m, 1H), 3.02 (d, J = 7.1 Hz, 2H), 2.19 – 2.07 (m, 2H), 1.90 – 1.83 (m, 2H), 1.68 (dtd, J = 13.6, 7.5, 6.8, 4.2 Hz, 1H), 1.55 (dtt, J = 13.4, 7.7, 3.3 Hz, 2H), 1.44 (s, 9H), 1.20 – 1.09 (m, 2H), 1.00 – 0.95 (m, 1H).

<u>^{13}C NMR</u> (101 MHz, CDCl$_3$) δ 155.8, 146.0, 143.8, 129.7, 129.3, 129.2, 128.7, 127.5, 126.9, 125.8, 125.7, 54.0, 41.0, 36.3, 28.4, 25.0, 24.7, 22.4.

<u>HRMS</u> (ESI$^+$) Calculated for C$_{27}$H$_{35}$NNaO$_2$ [M+Na]$^+$: 428.2560, found: 428.2552.

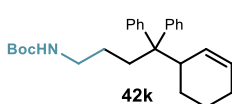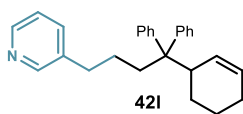**3-(4-(cyclohex-2-en-1-yl)-4,4-diphenylbutyl)pyridine (42l)**

Prepared according to General Procedure B using radical precursor **1n** (43.4 mg, 0.1 mmol), cyclohexene **2a** (101 µL, 1.0 mmol), and 1,1-diphenylethylene **41a** (17.7 µL, 0.1 mmol). The crude mixture was purified by preparative TLC (SiO$_2$, 90:10 toluene/acetone) to afford product **42l** as a colorless oil (15.3 mg, 42% yield, average of two runs).

<u>^{1}H NMR</u> (500 MHz, CDCl$_3$) δ 8.42 (dd, J = 4.8, 1.7 Hz, 1H), 8.36 – 8.32 (m, 1H), 7.34 – 7.30 (m, 1H), 7.27 – 7.24 (m, 3H), 7.24 – 7.20 (m, 2H), 7.20 – 7.15 (m, 5H), 5.80 (dp, J = 10.5, 1.8 Hz, 1H), 5.62 – 5.56 (m, 1H), 3.22 – 3.13 (m, 1H), 2.49 (t, J = 7.5 Hz, 2H), 2.22 – 2.07 (m, 2H), 1.90 – 1.77 (m, 2H), 1.72 – 1.64 (m, 2H), 1.60 – 1.46 (m, 2H), 1.41 – 1.29 (m, 2H), 0.98 – 0.89 (m, 1H).

UNIVERSITAT ROVIRA I VIRGILI
PHOTOCHEMISTRY AND ORGANOCATALYSIS FOR RADICAL-BASED CARBON-CARBON BOND-FORMING
PROCESSES
Emilien Le Saux

125

^{13}C NMR (101 MHz, CDCl$_3$) δ 149.9, 147.2, 146.0, 143.8, 137.3, 135.7, 129.7, 129.4, 129.2, 128.6, 127.5, 126.9, 125.8, 125.7, 123.2, 54.2, 41.1, 38.4, 33.3, 25.6, 25.0, 24.7, 22.4.

HRMS (ESI) Calculated for C$_{27}$H$_{30}$N [M+H]$^+$: 368.2373, found: 368.2374.
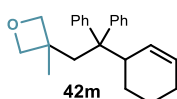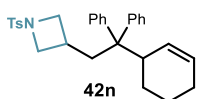
3-(2-(cyclohex-2-en-1-yl)-2,2-diphenylethyl)-3-methyloxetane (42m)

Prepared according to General Procedure B using radical precursor **1p** (47.9 mg, 0.12 mmol), cyclohexene **2a** (101 μL, 1.0 mmol), and 1,1-diphenylethylene **41a** (17.7 μL, 0.1 mmol). The crude mixture was purified by column chromatography (SiO$_2$, 20:1 hexanes/Et$_2$O) to afford product **42m** as a white solid (28.2 mg, 85% yield, average of two runs).

^{1}H NMR (400 MHz, CDCl$_3$) δ 7.37 – 7.15 (m, 10H), 5.75 (dp, J = 10.4, 1.8 Hz, 1H), 5.54 (ddt, J = 10.3, 5.0, 2.4 Hz, 1H), 3.85 (d, J = 5.7 Hz, 1H), 3.80 (d, J = 5.7 Hz, 1H), 3.65 (d, J = 5.7 Hz, 1H), 3.62 (d, J = 5.7 Hz, 1H), 3.37 – 3.27 (m, 1H), 2.69 (d, J = 14.6 Hz, 1H), 2.46 (d, J = 14.6 Hz, 1H), 1.98 – 1.89 (m, 1H), 1.88 – 1.77 (m, 1H), 1.62 (dddd, J = 12.8, 6.2, 4.5, 2.5 Hz, 1H), 1.58 – 1.48 (m, 2H), 1.33 (s, 3H), 0.98 – 0.81 (m, 1H).

^{13}C NMR (101 MHz, CDCl$_3$) δ 144.1, 142.9, 129.9, 129.7, 128.8, 128.7, 127.6, 126.7, 126.3, 126.0, 83.9, 83.3, 54.2, 46.8, 42.9, 39.7, 25.4, 25.0, 24.9, 22.3.

HRMS (APCI$^+$) Calculated for C$_{24}$H$_{29}$O [M+H]$^+$: 333.2213, found: 333.2207.

3-(2-(cyclohex-2-en-1-yl)-2,2-diphenylethyl)-1-tosylazetidine (42n)

Prepared according to General Procedure B using radical precursor **1q** (64.4 mg, 0.12 mmol), cyclohexene **2a** (101 μL, 1.0 mmol), and 1,1-diphenylethylene **41a** (17.7 μL, 0.1 mmol). The crude mixture was purified by column chromatography (SiO$_2$, 95:5 hexanes/EtOAc) to afford product **42n** as a colorless oil (28.9 mg, 61% yield, average of two runs).

^{1}H NMR (500 MHz, CDCl$_3$) δ 7.58 – 7.54 (m, 2H), 7.35 – 7.30 (m, 2H), 7.25 – 7.19 (m, 6H), 7.05 (ddd, J = 7.7, 3.5, 1.6 Hz, 4H), 5.70 (dp, J = 10.4, 1.8 Hz, 1H), 5.56 (ddq, J = 10.3, 4.9, 2.4 Hz, 1H), 3.41 (t, J = 8.1 Hz, 1H), 3.25 (t, J = 8.1 Hz, 1H), 3.03 (ddt, J = 6.9, 4.6, 2.5 Hz, 1H), 2.83 (dd, J = 8.1, 7.0 Hz, 1H), 2.71 (dd, J = 8.1, 6.9 Hz, 1H), 2.45 (s, 3H), 2.44 – 2.34 (m, 1H), 2.21 – 2.14 (m, 2H), 2.00 (dd, J = 14.2, 7.3 Hz, 1H), 1.82 (d, J = 17.9 Hz, 1H), 1.76 – 1.67 (m, 1H), 1.55 – 1.41 (m, 1H), 0.79 (tdd, J = 12.3, 10.2, 3.4 Hz, 1H).

^{13}C NMR (126 MHz, CDCl$_3$) δ 144.6, 143.8, 142.7, 131.5, 129.5, 129.4, 129.2, 129.1, 128.4, 128.3, 127.9, 127.1, 126.3, 126.2, 56.4, 56.2, 53.7, 43.5, 41.3, 25.5, 24.9, 24.6, 22.3, 21.6.

HRMS (ESI$^+$) Calculated for C$_{30}$H$_{33}$NNaO$_2$S [M+Na]$^+$: 494.2124, found: 494.2117
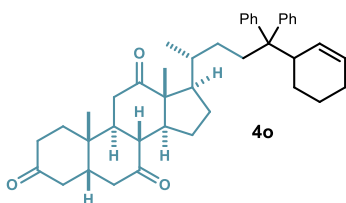
(5S,8R,9S,10S,13R,14S,17R)-17-(6-(cyclohex-2-en-1-yl) 6,6-diphenylhexan-2-yl)-10,13-dimethyldodecahydro-3H-cyclopenta[a]phenanthrene-3,7,12(2H,4H)-trione (42o)
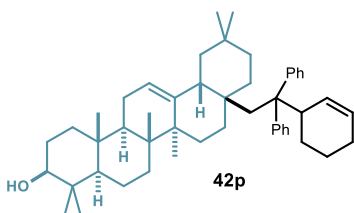
Prepared according to General Procedure B using radical precursor **1s** (68.5 mg, 0.1 mmol), cyclohexene **2a** (101 μL, 1.0 mmol), and 1,1-diphenylethylene **41a** (17.7 μL, 0.1 mmol). The crude mixture was purified by column chromatography (SiO₂, 90:10 toluene/EtOAc) to afford product **42o** as a white solid (40.7 mg, 66% yield, 1.1:1 *d.r.*, average of two runs).

[underline]H NMR (500 MHz, CDCl₃) *1.1:1 mixture of diastereoiomers* δ 7.31 – 7.17 (m, 10H), 5.83 (t, *J* = 8.7 Hz, 1H), 5.63 – 5.55 (m, 1H), 3.20 (s, 1H), 2.96 – 2.79 (m, 3H), 2.38 – 2.21 (m, 6H), 2.17 – 2.02 (m, 5H), 2.01 – 1.79 (m, 6H), 1.71 – 1.52 (m, 5H), 1.25 (d, *J* = 24.8 Hz, 6H), 1.16 – 1.06 (m, 2H), 1.03 (d, *J* = 2.4 Hz, 3H), 0.89 – 0.74 (m, 2H), 0.66 (dd, *J* = 9.3, 6.5 Hz, 3H).

[underline]C NMR (126 MHz, CDCl₃) *1.1:1 mixture of diastereoiomers* δ 212.0, 209.0, 208.8, 146.4, 144.6, 144.1, 129.8, 129.8, 129.5, 129.5, 129.4, 128.5, 128.4, 127.3, 126.9, 126.8, 125.6, 125.6, 125.4, 56.9, 54.5, 54.3, 51.7, 49.0, 46.8, 46.0, 46.0, 45.5, 45.0, 42.8, 41.4, 40.7, 39.7, 39.5, 38.6, 36.5, 36.2, 36.0, 35.9, 35.8, 35.3, 29.7, 29.2, 27.7, 27.7, 25.1, 25.0, 24.8, 24.7, 22.5, 22.4, 21.9, 21.4, 21.3, 18.9, 11.8.

[underline]HRMS (ESI⁺) Calculated for $C_{43}H_{54}NaO_3$ [M+Na]⁺: 641.3965, found: 641.3964.

(3S,4aR,6aR,6bS,12aR,14aR,14bR)-8a-(2-(cyclohex-2-en-1-yl)-2,2-diphenylethyl)-4,4,6a,6b,11,11,14b-heptamethyl 1,2,3,4,4a,5,6,6a,6b,7,8,8a,9,10,11,12,12a,14,14a,14b-icosahydropicen-3-ol (42p)

Prepared according to General Procedure B using radical precursor **1r** (74.0 mg, 0.1 mmol), cyclohexene **2a** (101 μL, 1.0 mmol), and 1,1-diphenylethylene **41a** (17.7 μL, 0.1 mmol). Multiple purifications by column chromatography resulted in poor separation from the simple decarboxylation product. The yield (49%, 1.5:1 dr, average of two runs) of **42p** was inferred by ¹H NMR analysis of the crude reaction mixture using trichloroethylene as the internal standard. An analytical amount of 86% pure compound (containing 14% of the simple decarboxylation product as estimated by ¹H NMR) was isolated by preparative TLC (90:10 hexanes/EtOAc) to obtain a colorless oil.

[underline]H NMR (500 MHz, CDCl₃) *1.5:1 mixture of diastereoiomers* δ 7.46 – 7.13 (m, 10H), 5.84 (d, *J* = 10.6 Hz, 0.5H), 5.71 (d, *J* = 11.0 Hz, 0.5H), 5.55 – 5.45 (m, 1H), 5.09 – 5.05 (m, 0.5H),

UNIVERSITAT ROVIRA I VIRGILI
PHOTOCHEMISTRY AND ORGANOCATALYSIS FOR RADICAL-BASED CARBON-CARBON BOND-FORMING
PROCESSES
Emilien Le Saux

127

4.96 (t, J = 3.6 Hz, 0.5H), 3.57 – 3.37 (m, 1H), 3.28 – 3.20 (m, 1H), 2.49 (d, J = 15.2 Hz, 0.5H), 2.43 – 2.32 (m, 1H), 2.21 (d, J = 11.5 Hz, 0.5H), 2.07 – 1.93 (m, 2H), 1.92 – 1.73 (m, 5H), 1.69 – 1.53 (m, 14H), 1.44 (qd, J = 12.5, 3.2 Hz, 5H), 1.08 (d, J = 4.6 Hz, 2H), 1.04 – 1.00 (m, 6H), 0.98 (d, J = 4.1 Hz, 4H), 0.95 – 0.89 (m, 4H), 0.81 (d, J = 2.3 Hz, 3H), 0.75 (d, J = 1.6 Hz, 4H), 0.54 (d, J = 6.2 Hz, 2H).

<u>13C NMR</u> (126 MHz, CDCl₃) *1.5:1 mixture of diastereoiomers* δ 145.4, 145.1, 129.7, 129.5, 128.3, 127.1, 127.0, 126.2, 126.1, 125.6, 125.5, 125.4, 122.2, 122.0, 79.0, 55.2, 55.1, 54.6, 54.2, 47.7, 47.6, 47.5, 46.7, 46.6, 44.9, 44.1, 43.9, 41.8, 40.9, 40.8, 39.9, 38.7, 38.5, 38.4, 37.2, 37.1, 36.9, 36.8, 35.7, 34.4, 34.3, 33.6, 33.3, 33.0, 32.3, 32.1, 31.1, 30.9, 30.6, 30.3, 30.2, 29.2, 28.0, 28.0, 27.2, 26.9, 26.9, 26.2, 26.1, 25.4, 25.0, 23.9, 23.8, 23.7, 23.6, 23.6, 22.7, 22.2, 18.3, 16.9, 16.8, 15.6, 15.5, 15.5, 15.5, 15.3.

<u>HRMS</u> (APCI⁺) Calculated for $C_{49}H_{69}O$ [M+H]⁺: 673.5343, found: 673.5337.

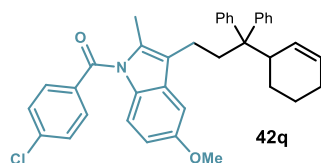### (4-chlorophenyl)(3-(3-(cyclohex-2-en-1-yl)-3,3-diphenylpropyl)-5-methoxy-2-methyl-1H-indol-1-yl)methanone (42q)

Prepared according to General Procedure B using radical precursor **1e** (64.1 mg, 0.1 mmol), cyclohexene **2a** (101 μL, 1.0 mmol), 1,1-diphenylethylene **41a** (35.3 μL, 0.2 mmol), and catalyst **A5** (7.6 mg, 0.2 mmol). The crude mixture was purified by column chromatography (SiO₂, 98:2 hexanes/EtOAc) to afford product **42q** as a yellowish oil (20.8 mg, 36% yield, average of two runs).

<u>1H NMR</u> (500 MHz, CDCl₃) δ 7.66 – 7.63 (m, 2H), 7.49 – 7.45 (m, 2H), 7.38 – 7.29 (m, 8H), 7.28 – 7.22 (m, 2H), 6.86 (d, J = 9.0 Hz, 1H), 6.63 (dd, J = 9.0, 2.6 Hz, 1H), 6.47 (d, J = 2.5 Hz, 1H), 5.95 (d, J = 10.4 Hz, 1H), 5.67 (ddd, J = 10.4, 4.8, 2.5 Hz, 1H), 3.78 (s, 3H), 3.38 (s, 1H), 2.45 – 2.37 (m, 1H), 2.36 – 2.25 (m, 3H), 2.18 (s, 3H), 2.01 – 1.87 (m, 2H), 1.77 – 1.66 (m, 1H), 1.34 (d, J = 24.8 Hz, 1H), 1.15 – 1.03 (m, 1H), 0.96 – 0.84 (m, 1H).

<u>13C NMR</u> (101 MHz, CDCl₃) δ 168.3, 155.8, 146.2, 144.0, 138.9, 134.3, 133.5, 131.0, 131.0, 130.9, 129.9, 129.6, 129.1, 129.0, 129.0, 127.7, 127.1, 126.0, 125.9, 120.2, 115.1, 111.4, 100.6, 55.7, 54.5, 40.3, 39.3, 25.1, 24.9, 22.5, 18.9, 13.1.

<u>HRMS</u> (ESI⁺) Calculated for $C_{38}H_{36}ClNNaO_2$ [M+Na]⁺: 596.2327, found: 596.2336.
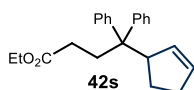
Ethyl 4-(cyclopent-2-en-1-yl)-4,4-diphenylbutanoate (42s)

Prepared according to General Procedure B using radical precursor **40b** (48.1 mg, 0.1 mmol), cyclopentene **2c** (110 μL, 1.0 mmol), and 1,1-diphenylethylene **41a** (17.7 μL, 0.1 mmol). The crude mixture was purified by column

chromatography (SiO$_2$, 70:30 hexanes/toluene) to afford product **42s** as a colorless oil (25.0 mg, 75% yield, average of two runs).

^{1}H NMR (500 MHz, CDCl$_3$) δ 7.29 – 7.19 (m, 10H), 5.83 (dq, *J* = 6.0, 2.0 Hz, 1H), 5.64 (dq, *J* = 5.8, 2.3 Hz, 1H), 4.07 (q, *J* = 7.2 Hz, 2H), 3.76 (ddt, *J* = 8.5, 6.0, 2.5 Hz, 1H), 2.53 (ddd, *J* = 13.9, 11.7, 4.8 Hz, 1H), 2.39 (ddd, *J* = 13.8, 11.6, 5.2 Hz, 1H), 2.12 (ddd, *J* = 16.4, 11.7, 4.8 Hz, 1H), 2.07 – 1.98 (m, 3H), 1.54 – 1.46 (m, 1H), 1.22 (t, *J* = 7.2 Hz, 3H), 0.94 – 0.84 (m, 1H).

^{13}C NMR (126 MHz, CDCl$_3$) δ 173.9, 145.9, 144.1, 133.3, 131.8, 129.8, 129.2, 127.4, 127.2, 125.9, 125.8, 60.3, 53.5, 51.3, 34.8, 31.6, 30.0, 25.7, 14.1.

HRMS (ESI[+]) Calculated for C$_{23}$H$_{26}$NaO$_2$ [M+Na][+]: 357.1825, found: 357.1818.

Ethyl (Z)-4-(clyclooct-2-en-1-yl)-4,4-diphenylbutanoate (42t)
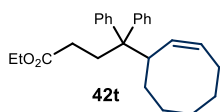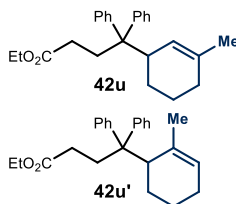
Prepared according to General Procedure B using radical precursor **40b** (48.1 mg, 0.1 mmol), Z-cyclooctene **2e** (130 μL, 1.0 mmol), and 1,1-diphenylethylene **41a** (17.7 μL, 0.1 mmol). Multiple purifications by column chromatography resulted in poor separation from several unidentified byproducts. The yield (39%, average of two runs) of **42t** was inferred by ^{1}H NMR analysis of the crude reaction mixture using trichloroethylene as the internal standard. An analytical amount of pure compound was isolated by preparative TLC (50:50 hexanes/toluene) to obtain a colorless oil.

^{1}H NMR (400 MHz, CDCl$_3$) δ 7.32 – 7.25 (m, 4H), 7.25 – 7.18 (m, 6H), 5.66 (td, *J* = 9.6, 7.0 Hz, 1H), 5.27 (ddd, *J* = 10.8, 9.5, 1.4 Hz, 1H), 4.01 (q, *J* = 7.1 Hz, 2H), 3.50 – 3.40 (m, 1H), 2.38 (dd, *J* = 9.0, 7.7 Hz, 2H), 2.14 (ddd, *J* = 13.4, 7.3, 3.7 Hz, 1H), 1.93 (td, *J* = 7.9, 6.3 Hz, 2H), 1.90 – 1.81 (m, 1H), 1.74 (ddd, *J* = 13.6, 7.5, 3.7 Hz, 1H), 1.66 – 1.46 (m, 4H), 1.45 – 1.29 (m, 2H), 1.17 (t, *J* = 7.1 Hz, 3H), 0.76 (tt, *J* = 12.7, 5.0 Hz, 1H).

^{13}C NMR (101 MHz, CDCl$_3$) δ 173.8, 145.3, 144.0, 130.6, 130.3, 129.5, 127.6, 127.1, 126.1, 125.9, 60.2, 53.1, 39.6, 35.7, 31.1, 29.8, 29.6, 26.7, 26.7, 25.9, 14.1.

HRMS (ESI[+]) Calculated for C$_{26}$H$_{32}$NaO$_2$ [M+Na][+]: 399.22875 found: 399.2287.

Ethyl 4-(3-methylcyclohex-2-en-1-yl)-4,4-diphenylbutanoate (42u + 42u')

Prepared according to General Procedure B using radical precursor **40b** (48.1 mg, 0.1 mmol), 1-methylcyclohexene **2d** (118 μL, 1.0 mmol), and 1,1-diphenylethylene **41a** (17.7 μL, 0.1 mmol). The crude mixture was purified by column chromatography (SiO$_2$, 70:30 hexanes/toluene) to afford product **42u** as a colorless oil (24.3 mg, 67% yield, 5:1 *r.r.*, average of two runs).

UNIVERSITAT ROVIRA I VIRGILI
PHOTOCHEMISTRY AND ORGANOCATALYSIS FOR RADICAL-BASED CARBON-CARBON BOND-FORMING PROCESSES
Emilien Le Saux

129

^{1}H NMR (400 MHz, CDCl$_3$) *5:1 mixture of regioisomers* δ 7.33 – 7.15 (m, 12H), 5.47 (brs, 1H), 5.46 – 5.42 (m, 0.2H), 4.09 – 3.99 (m, 2.4H), 3.19 – 3.08 (m, 1.2H), 2.55 (ddd, *J* = 13.9, 11.8, 4.5 Hz, 1H), 2.48 – 2.41 (m, 0.2H), 2.36 (ddd, *J* = 14.0, 11.8, 5.3 Hz, 1H), 2.24 (td, *J* = 15.3, 14.6, 3.2 Hz, 0.2H), 2.06 – 1.98 (m, 1.2H), 1.96 – 1.90 (m, 1H), 1.90 – 1.85 (m, 0.2H), 1.86 – 1.76 (m, 1.2H), 1.70 (dd, *J* = 15.9, 5.5 Hz, 1.2H), 1.57 (s, 0.8H), 1.52 (dd, *J* = 2.3, 1.3 Hz, 3H), 1.23 – 1.15 (m, 3.6H), 0.85 – 0.79 (m, 1.2H).

^{13}C NMR (101 MHz, CDCl$_3$) *major regioisomer* δ 173.9, 145.5, 143.0, 135.8, 129.7, 129.3, 127.6, 127.6, 126.9, 125.8, 125.8, 123.0, 60.2, 53.9, 41.7, 33.9, 30.1, 29.8, 24.4, 23.9, 22.5, 14.1.

HRMS (ESI$^+$) Calculated for C$_{25}$H$_{30}$NaO$_2$ [M+Na]$^+$: 385.2138 found: 385.2139.
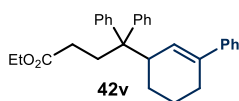
**Ethyl 4,4-diphenyl-4-(3,4,5,6-tetrahydro-[1,1'-biphenyl]-3-yl)butanoate (42v)**

Prepared according to General Procedure B using radical precursor **40b** (48.1 mg, 0.1 mmol), 1-phenylcyclohexene **2f** (160 µL, 1.0 mmol), and 1,1-diphenylethylene **41a** (17.7 µL, 0.1 mmol). The crude mixture was purified by column chromatography (SiO$_2$, 70:30 hexanes/toluene) to afford product **42v** as a colorless oil (22.0 mg, 52% yield, average of two runs).

^{1}H NMR (400 MHz, CDCl$_3$) δ 7.32 – 7.29 (m, 5H), 7.28 – 7.17 (m, 9H), 6.17 (dt, *J* = 2.6, 1.4 Hz, 1H), 4.08 (q, *J* = 7.2 Hz, 2H), 3.37 (d, *J* = 9.5 Hz, 1H), 2.62 (ddd, *J* = 14.0, 11.6, 4.8 Hz, 1H), 2.49 (ddd, *J* = 14.0, 11.5, 5.6 Hz, 1H), 2.38 – 2.29 (m, 1H), 2.12 – 1.93 (m, 5H), 1.81 – 1.74 (m, 1H), 1.72 – 1.64 (m, 1H), 1.23 (t, *J* = 7.1 Hz, 3H), 1.03 (tdd, *J* = 12.7, 10.2, 3.3 Hz, 1H).

^{13}C NMR (101 MHz, CDCl$_3$) δ 173.8, 145.1, 142.9, 142.8, 138.4, 129.7, 129.3, 128.1, 127.8, 126.7, 126.6, 126.1, 126.0, 125.3, 60.3, 54.2, 42.1, 34.1, 30.1, 27.4, 24.2, 22.7, 14.1.

HRMS (ESI$^+$) Calculated for C$_{30}$H$_{32}$NaO$_2$ [M+Na]$^+$: 447.2295 found: 447.2293.
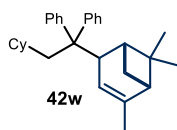
(1S,5R)-4-(2-cyclohexyl-1,1-diphenylethyl)-2,6,6-trimethylbicyclo[3.1.1]hept-2-ene (42w)

Prepared according to General Procedure B using radical precursor **1h** (49.3 mg, 0.12 mmol), α-pinene **2g** (158 µL, 1.0 mmol), and 1,1-diphenylethylene **41a** (17.7 µL, 0.1 mmol). The crude mixture was purified by column chromatography (SiO$_2$, cyclohexane) to afford product **42w** as a colorless oil (19.4 mg, 49% yield, >10:1 *d.r.*, average of two runs).

^{1}H NMR (500 MHz, CDCl$_3$) δ 7.28 – 7.19 (m, 10H), 5.49 (p, *J* = 1.8 Hz, 1H), 3.33 (q, *J* = 2.3 Hz, 1H), 2.21 (tt, *J* = 5.8, 1.9 Hz, 1H), 2.14 (dd, *J* = 14.1, 3.5 Hz, 1H), 1.87 (dd, *J* = 14.1, 5.2

Hz, 1H), 1.66 (td, J = 5.4, 1.3 Hz, 1H), 1.59 (dd, J = 2.5, 1.6 Hz, 3H), 1.55 – 1.41 (m, 6H), 1.23 (s, 3H), 1.03 (td, J = 11.3, 4.4 Hz, 3H), 0.97 (s, 3H), 0.95 – 0.84 (m, 3H), 0.72 – 0.63 (m, 1H).

^{13}C NMR (101 MHz, CDCl$_3$) δ 147.0, 145.5, 129.6, 129.4, 127.2, 126.9, 125.5, 125.4, 116.8, 54.0, 46.9, 46.2, 44.8, 42.0, 41.3, 35.6, 35.1, 33.6, 26.6, 26.4, 26.3, 25.4, 23.2, 20.7.

HRMS (APCI$^+$) Calculated for C$_{30}$H$_{39}$ [M+H]$^+$: 399.3046 found: 399.3036.
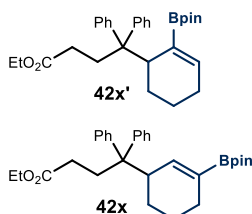
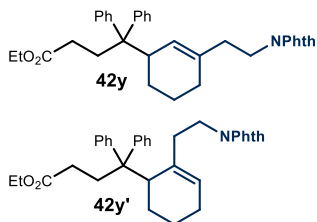**ethyl 4,4-diphenyl-4-(2-(4,4,5,5-tetramethyl-1,3,2-dioxaborolan-2-yl)cyclohex-2-en-1-yl)butanoate (42x + 42x')**

Prepared according to General Procedure B using radical precursor **40b** (48.1 mg, 0.1 mmol), 2-(cyclohex-1-en-1-yl)-4,4,5,5-tetramethyl-1,3,2-dioxaborolane **2i** (110 μL, 0.5 mmol), and 1,1-diphenylethylene **41a** (17.7 μL, 0.1 mmol). The crude mixture was purified by column chromatography (SiO$_2$, 50:50 hexanes/toluene) to afford product **42x** as a colorless oil (21.3 mg, 45% yield, 1:1.2 *r.r.*, average of two runs). When using catalyst **A6**, the yield (50% yield, 4:1 *r.r.*) of **42x** was inferred by ^{1}H NMR analysis of the crude reaction mixture using trichloroethylene as the internal standard.

^{1}H NMR (500 MHz, CDCl$_3$) *1.2:1 mixture of regioisomers* δ 7.43 – 7.39 (m, 1H), 7.36 – 7.29 (m, 3H), 7.27 – 7.20 (m, 6H), 6.68 (d, J = 2.6 Hz, 0.5H), 6.61 (ddd, J = 4.9, 3.4, 1.2 Hz, 0.5H), 4.06 (q, J = 7.1 Hz, H), 3.99 (qd, J = 7.1, 0.9 Hz, 1H), 3.60 – 3.55 (m, 1H), 2.56 – 2.44 (m, 1H), 2.43 – 2.32 (m, 1H), 2.20 (ddd, J = 15.1, 11.6, 5.3 Hz, 1H), 1.98 (dd, J = 9.3, 7.4 Hz, 1H), 1.75 (qd, J = 6.1, 3.0 Hz, 1H), 1.70 – 1.63 (m, 1H), 1.28 (d, J = 2.2 Hz, 1H), 1.26 (s, 4H), 1.24 (s, 3H), 1.21 (d, J = 2.0 Hz, 3H), 1.20 – 1.19 (m, 3H), 1.17 (d, J = 7.1 Hz, 1H), 1.07 – 0.99 (m, 1H), 0.95 – 0.82 (m, 2H), 0.73 – 0.64 (m, 0.5H).

^{13}C NMR (101 MHz, CDCl$_3$) *1.2:1 mixture of regioisomers* δ 174.0, 173.9, 146.9, 143.8, 143.3, 143.0, 130.6, 130.4, 129.8, 129.4, 127.8, 127.4, 127.0, 126.0, 125.9, 83.2, 82.9, 60.3, 60.0, 56.7, 53.9, 41.9, 40.1, 36.3, 33.9, 30.7, 30.0, 26.3, 25.1, 25.0, 24.9, 24.4, 24.3, 22.5, 19.4, 14.1.

HRMS (ESI$^+$) Calculated for C$_{30}$H$_{39}$NaO$_4$^{10}B [M+Na]$^+$: 496.2870 found: 496.2864.

ethyl 4-(3-(2-(1,3-dioxoisoindolin-2-yl)ethyl)cyclohex-2-en-1-yl)-4,4-diphenylbutanoate (42y + 42y')
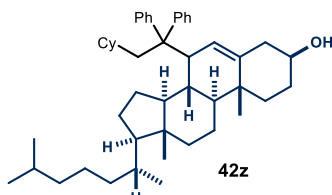
Prepared according to General Procedure B using radical precursor **40b** (48.1 mg, 0.1 mmol), 2-(2-(cyclohex-1-en-1-yl)ethyl)isoindoline-1,3-dione **2h** (128 mg, 5.0 mmol), and 1,1-diphenylethylene **41a** (17.7 μL, 0.1 mmol). The crude

UNIVERSITAT ROVIRA I VIRGILI
PHOTOCHEMISTRY AND ORGANOCATALYSIS FOR RADICAL-BASED CARBON-CARBON BOND-FORMING PROCESSES
Emilien Le Saux

131

mixture was purified by column chromatography (SiO$_2$, 90:10 hexanes/EtOAc) to afford product **42y** as a colorless oil (32.3 mg, 62% yield, 5:1 *r.r.*, average of two runs). When using catalyst **A7**, **42y** was obtained as a colorless oil (25 mg, 48% yield, 10:1 *r.r.*).

^{1}H NMR (500 MHz, CDCl$_3$) *5:1 mixture of regioisomers* δ 7.88 (dd, *J* = 5.4, 3.1 Hz, 2H), 7.79 (td, *J* = 5.4, 2.3 Hz, 2H), 7.22 – 7.11 (m, 6H), 7.11 – 7.06 (m, 2H), 7.03 – 6.98 (m, 2H), 5.47 (s, 1H), 5.26 (m, 0.2H), 4.04 (q, *J* = 7.2 Hz, 2H), 3.70 – 3.63 (m, 1H), 3.60 (ddd, *J* = 13.4, 7.8, 5.3 Hz, 1H), 3.02 (d, *J* = 9.2 Hz, 1H), 2.46 (ddd, *J* = 14.0, 11.2, 5.2 Hz, 1H), 2.35 (ddd, *J* = 13.9, 11.1, 5.9 Hz, 1H), 2.20 (dt, *J* = 15.0, 7.6 Hz, 1H), 2.13 (dt, *J* = 12.8, 6.2 Hz, 1H), 1.97 – 1.90 (m, 2H), 1.86 (dt, *J* = 13.5, 4.1 Hz, 2H), 1.70 – 1.61 (m, 2H), 1.58 – 1.49 (m, 1H), 1.20 (t, *J* = 7.2 Hz, 3H), 0.90 – 0.81 (m, 1H).

^{13}C NMR (126 MHz, CDCl$_3$) *major regioisomer* δ 173.8, 168.1, 145.1, 142.8, 135.9, 133.8, 132.2, 129.7, 129.1, 127.6, 126.9, 126.0, 125.9, 125.8, 123.1, 60.2, 53.7, 41.3, 36.9, 36.4, 33.9, 29.9, 27.6, 24.2, 22.5, 14.1.

HRMS (ESI$^+$) Calculated for C$_{34}$H$_{35}$NNaO$_4$ [M+Na]$^+$: 544.2458 found: 544.2469.


(3S,8S,9S,10R,13R,14S,17R)-7-(2-cyclohexyl-1,1-diphenylethyl)-10,13-dimethyl-17-((R)-6-methylheptan-2-yl)-2,3,4,7,8,9,10,11,12,13,14,15,16,17-tetradecahydro-1H-cyclopenta[a]phenanthren-3-ol (42z)

Prepared according to General Procedure B using radical precursor **1h** (49.3 mg, 0.12 mmol), cholesterol **2j** (193 mL, 0.5 mmol), and 1,1-diphenylethylene **41a** (17.7 μL, 0.1 mmol). The crude mixture was purified by column chromatography (SiO$_2$, 95:5 hexanesEtOAc) to afford product **42y** as a white solid. The yield (48% yield, 5:1 *d.r.*, average of two runs) of **42z** was inferred by ^{1}H NMR analysis of the crude reaction mixture using trichloroethylene as the internal standard.

^{1}H NMR (500 MHz, CDCl$_3$) *5:1 mixture of diastereoisomers* δ 7.63 – 6.97 (m, 10H), 5.61 – 5.35 (m, 1H), 3.58 – 3.40 (m, 1H), 3.25 (d, *J* = 71.6 Hz, 1H), 2.37 (d, *J* = 14.0 Hz, 1H), 2.25 – 2.14 (m, 1H), 2.02 – 1.95 (m, 1H), 1.90 (td, *J* = 11.5, 7.5 Hz, 2H), 1.86 – 1.74 (m, 3H), 1.72 (d, *J* = 3.5 Hz, 2H), 1.64 – 1.49 (m, 7H), 1.39 (ddt, *J* = 33.2, 17.5, 7.1 Hz, 9H), 1.25 – 1.12 (m, 10H), 1.11 – 0.99 (m, 4H), 0.94 (d, *J* = 6.5 Hz, 3H), 0.90 (dt, *J* = 6.6, 2.6 Hz, 7H), 0.74 – 0.58 (m, 1H), 0.16 (q, *J* = 12.0, 10.8 Hz, 1H), -0.21 (d, *J* = 12.5 Hz, 1H), -0.57 (s, 2H).

^{13}C NMR (126 MHz, CDCl$_3$) *5:1 mixture of diastereoisomers* δ 146.9, 142.2, 140.9, 129.1, 126.1, 126.1, 125.6, 125.4, 71.1, 60.4, 59.0, 56.7, 56.4, 49.7, 46.3, 44.8, 43.1, 42.3, 41.8, 39.5, 38.5, 37.6, 37.4, 36.2, 36.1, 34.8, 34.7, 34.3, 31.6, 28.8, 28.1, 28.0, 26.8, 26.4, 26.0, 24.1, 24.0, 22.8, 22.6, 19.1, 19.0, 15.5, 13.2, 11.1.

HRMS (APCI$^+$) Calculated for C$_{47}$H$_{69}$O [M+H]$^+$: 649.5186, found: 649.5180.
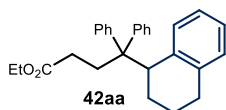
Ethyl 4,4-diphenyl-4-(1,2,3,4-tetrahydronaphthalen-1-yl)butanoate (42aa)

Prepared according to General Procedure B using radical precursor **40b** (48.1 mg, 0.1 mmol), tetralin **2k** (136 µL, 1.0 mmol), and 1,1-diphenylethylene **41a** (17.7 µL, 0.1 mmol). Multiple purifications by column chromatography resulted in poor separation from several unidentified byproducts. The yield (60%, average of two runs) of **42aa** was inferred by ^{1}H NMR analysis of the crude reaction mixture using trichloroethylene as the internal standard. An analytical amount of pure compound was isolated by preparative TLC (50:50 hexanes/toluene) to obtain a colorless oil.

^{1}H NMR (500 MHz, CDCl$_3$) δ 7.30 – 7.16 (m, 7H), 7.16 – 7.10 (m, 3H), 7.09 – 7.02 (m, 4H), 6.81 (d, J = 7.3 Hz, 1H), 4.06 (qd, J = 7.2, 3.0 Hz, 2H), 2.67 (ddd, J = 14.0, 11.6, 4.1 Hz, 1H), 2.37 (ddd, J = 14.1, 12.1, 5.3 Hz, 1H), 2.28 – 2.20 (m, 1H), 2.16 (ddd, J = 16.1, 12.1, 4.0 Hz, 1H), 2.05 – 1.96 (m, 1H), 1.88 (ddt, J = 14.3, 11.8, 5.9 Hz, 1H), 1.67 (ddd, J = 16.1, 11.7, 5.3 Hz, 1H), 1.57 – 1.50 (m, 1H), 1.22 (t, J = 7.1 Hz, 3H), 1.15 (dddd, J = 16.7, 10.3, 6.1, 3.0 Hz, 1H), 0.80 – 0.70 (m, 1H).

^{13}C NMR (126 MHz, CDCl$_3$) δ 173.8, 143.5, 137.0, 130.8, 130.3, 130.2, 128.5, 127.8, 127.8, 127.4, 127.2, 126.3, 126.0, 125.9, 124.7, 60.2, 57.4, 44.2, 35.5, 30.7, 29.1, 25.1, 23.2, 14.2, 14.2.

HRMS (ESI$^+$) Calculated for C$_{28}$H$_{30}$NaO$_2$ [M+Na]$^+$: 421.2138, found: 421.2138.
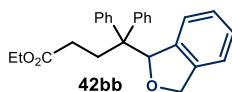
Ethyl 4-(1,3-dihydroisobenzofuran-1-yl)-4,4-diphenylbutanoate (42bb)

Prepared according to General Procedure B using radical precursor **40b** (48.1 mg, 0.1 mmol), 1,3-dihydrobenzofuran **2l** (109 µL, 1.0 mmol), and 1,1-diphenylethylene **41a** (17.7 µL, 0.1 mmol). The crude mixture was purified by column chromatography (SiO$_2$, 60:40 hexanes/toluene) to afford product **42bb** as a colorless oil (21.4 mg, 55% yield, average of two runs).

^{1}H NMR (400 MHz, CDCl$_3$) δ 7.39 – 7.33 (m, 2H), 7.27 – 7.13 (m, 9H), 7.08 – 6.97 (m, 2H), 6.44 (d, J = 7.7 Hz, 1H), 6.20 (d, J = 3.0 Hz, 1H), 4.88 (d, J = 12.1 Hz, 1H), 4.48 (dd, J = 12.2, 3.1 Hz, 1H), 4.07 (q, J = 7.1 Hz, 2H), 2.78 (ddd, J = 14.0, 11.5, 4.9 Hz, 1H), 2.45 (ddd, J = 14.0, 11.4, 5.7 Hz, 1H), 2.28 – 2.13 (m, 2H), 1.22 (t, J = 7.1 Hz, 3H).

^{13}C NMR (101 MHz, CDCl$_3$) δ 173.8, 144.1, 142.8, 140.8, 138.6, 129.7, 129.5, 127.6, 127.5, 126.4, 126.3, 126.2, 123.6, 120.4, 88.9, 72.9, 60.2, 56.3, 31.6, 30.5, 14.1, 1.0.

HRMS (ESI$^+$) Calculated for C$_{26}$H$_{26}$NaO$_3$ [M+Na]$^+$: 409.1774 found: 409.1776.

UNIVERSITAT ROVIRA I VIRGILI
PHOTOCHEMISTRY AND ORGANOCATALYSIS FOR RADICAL-BASED CARBON-CARBON BOND-FORMING
PROCESSES
Emilien Le Saux

133
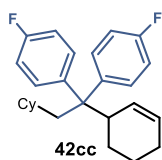
4,4'-(1-(cyclohex-2-en-1-yl)-2-cyclohexylethane-1,1-diyl)bis(fluorobenzene) (42cc)

Prepared according to General Procedure B using radical precursor **1h** (49.3 mg, 0.12 mmol), cyclohexene **2a** (101 µL, 1.0 mmol), and 4,4'-(ethene-1,1-diyl)bis(fluorobenzene) **41b** (21.6 mg, 0.1 mmol). The crude mixture was purified by column chromatography (SiO$_2$, pentane) to afford product **42cc** as a colorless oil (25.8 mg, 68% yield, average of two runs).

<u>^{1}H NMR</u> (500 MHz, CDCl$_3$) δ 7.17 (pd, J = 6.6, 6.2, 3.1 Hz, 4H), 6.96 (td, J = 8.8, 6.3 Hz, 4H), 5.81 (dt, J = 10.4, 2.2 Hz, 1H), 5.62 (ddt, J = 10.3, 5.1, 2.6 Hz, 1H), 3.15 (ddq, J = 9.6, 4.7, 2.3 Hz, 1H), 2.03 – 1.82 (m, 4H), 1.66 (dddd, J = 19.4, 8.8, 4.4, 2.2 Hz, 1H), 1.52 – 1.47 (m, 3H), 1.11 (tt, J = 7.5, 3.4 Hz, 1H), 1.07 – 0.96 (m, 5H), 0.93 – 0.86 (m, 2H), 0.85 – 0.74 (m, 3H).

<u>^{13}C NMR</u> (126 MHz, CDCl$_3$) δ 162.0 (d, J = 16.2 Hz), 160.0 (d, J = 16.3 Hz), 141.7 (d, J = 3.4 Hz), 140.1 (d, J = 3.3 Hz), 131.2 (d, J = 7.5 Hz), 131.0 (d, J = 7.6 Hz), δ 129.2, 128.8, 114.1 (d, J = 20.8 Hz), 113.5 (d, J = 20.6 Hz), 54.0, 46.9, 41.4, 35.4, 35.2, 33.7, 26.5 (d, J = 8.6 Hz), 26.2, 25.0 (d, J = 3.9 Hz), 22.3.

<u>^{19}F NMR</u> (376 MHz, CDCl$_3$) δ -117.7

<u>HRMS</u> (APCI$^+$) Calculated for C$_{26}$H$_{31}$F$_2$ [M+H]$^+$: 381.2388, found: 381.2380.

Ethyl 4-(benzo[d][1,3]dioxol-5-yl)-4-(cyclohex-2-en-1-yl)-4-phenylbutanoate (42dd)
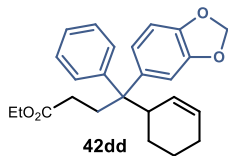
Prepared according to General Procedure B using radical precursor **40b** (48.1 mg, 0.1 mmol), cyclohexene **2a** (101 µL, 1.0 mmol), 5-(1-phenylvinyl)benzo[d][1,3]dioxole **41c** (22.4 mg, 0.1 mmol), and catalyst **A5** (7.6 mg, 0.02 mmol). The crude mixture was purified by column chromatography (SiO$_2$, 60:40 hexanes/toluene) to afford product **42dd** as a colorless oil (29.5 mg, 73% yield, 1.1:1 dr, average of two runs).

<u>^{1}H NMR</u> (400 MHz, CDCl$_3$) *1.1:1 mixture of diastereoisomers* δ 7.32 – 7.19 (m, 5H), 6.79 – 6.66 (m, 3H), 5.98 – 5.94 (m, 2H), 5.85 – 5.73 (m, 1H), 5.67 – 5.61 (m, 1H), 4.07 (dq, J = 9.3, 7.1 Hz, 2H), 3.13 (d, J = 8.5 Hz, 1H), 2.50 (ddd, J = 13.8, 11.8, 4.7 Hz, 1H), 2.36 (ddd, J = 11.6, 7.8, 5.8 Hz, 1H), 2.04 (ddd, J = 16.3, 11.6, 4.7 Hz, 1H), 1.99 – 1.91 (m, 1H), 1.90 (d, J = 5.2 Hz, 2H), 1.80 – 1.68 (m, 1H), 1.58 – 1.48 (m, 1H), 1.23 (q, J = 7.0 Hz, 3H), 1.07 – 0.95 (m, 1H), 0.93 – 0.84 (m, 1H).

<u>^{13}C NMR</u> (101 MHz, CDCl$_3$) *1.1:1 mixture of diastereoisomers* δ 173.9, 173.8, 147.3, 146.7, 145.6, 145.3, 143.0, 139.3, 137.0, 129.7, 129.3, 129.1, 129.0, 129.0, 127.8, 127.2, 126.0, 126.0, 122.7, 122.4, 110.6, 110.0, 107.3, 106.8, 100.9, 100.8, 60.3, 53.6, 42.0, 41.7, 34.3, 34.1, 30.2, 30.1, 25.1, 25.0, 24.8, 24.7, 22.4, 14.2.

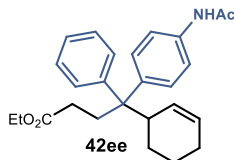<u>HRMS</u> (ESI$^+$) Calculated for $C_{25}H_{28}NaO_4$ [M+Na]$^+$: 415.1880, found: 415.1882.
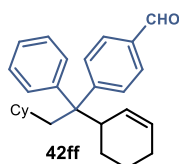

Ethyl 4-(4-acetamidophenyl)-4-(cyclohex-2-en-1-yl)-4-phenylbutanoate (42ee)

Prepared according to General Procedure B using radical precursor **40b** (48.1 mg, 0.1 mmol), cyclohexene **2a** (101 μL, 1.0 mmol), N-(4-(1-phenylvinyl)phenyl)acetamide **41d** (23.7 mg, 0.1 mmol), and catalyst **A5** (7.6 mg, 0.02 mmol). Multiple purifications by column chromatography resulted in poor separation from several unidentified byproducts. The yield (83%,1.1:1 dr, average of two runs) of **42ee** was inferred by ^{1}H NMR analysis of the crude reaction mixture using trichloroethylene as the internal standard. An analytical amount of the pure compound was isolated by preparative TLC (90:10 hexanes/EtOAc) to obtain a colorless oil.

<u>^{1}H NMR</u> (400 MHz, CDCl$_3$) *1.1:1 mixture of diastereoisomers* δ 7.43 (d, *J* = 8.6 Hz, 2H), 7.31 – 7.27 (m, 1H), 7.25 – 7.14 (m, 6H), 5.77 (d, *J* = 10.8 Hz, 1H), 5.60 (d, *J* = 10.8 Hz, 1H), 4.06 (qd, *J* = 7.2, 2.2 Hz, 2H), 3.15 (s, 1H), 2.54 (ddd, *J* = 13.9, 11.7, 4.5 Hz, 1H), 2.45 – 2.33 (m, 1H), 2.20 (s, 3H), 2.10 – 1.99 (m, 1H), 1.97 – 1.82 (m, 3H), 1.61 (s, 4H), 1.22 (td, *J* = 7.1, 1.3 Hz, 3H), 0.95 (dd, *J* = 24.8, 12.4 Hz, 1H).

<u>^{13}C NMR</u> (101 MHz, CDCl$_3$) *1.1:1 mixture of diastereoisomers* δ 173.8, 168.1, 145.1, 138.9, 135.8, 130.3, 129.9, 129.6, 129.2, 129.0, 128.9, 127.7, 127.1, 126.0, 125.9, 119.0, 118.4, 60.3, 53.4, 41.6, 34.0, 30.0, 25.0, 24.6, 22.3, 14.1, 1.0.

<u>HRMS</u> (ESI$^+$) Calculated for $C_{26}H_{31}NaNO_3$ [M+Na]$^+$: 428.2196, found: 428.2184.

4-(1-(cyclohex-2-en-1-yl)-2-cyclohexyl-1-phenylethyl)benzaldehyde (42ff)

Prepared according to General Procedure B using radical precursor **1h** (49.3 mg, 0.12 mmol), cyclohexene **2a** (101 μL, 1.0 mmol), 4-(1-phenylvinyl)benzaldehyde **41e** (20.8 mg, 0.1 mmol), and catalyst **A5** (7.6 mg, 0.02 mmol). The crude mixture was purified by column chromatography (SiO$_2$, 95:5 hexanes/CH$_2$Cl$_2$) to afford product **42ff** as a colorless oil (23 mg, 62% yield,1.1:1 dr, average of two runs).

<u>^{1}H NMR</u> (500 MHz, CDCl$_3$) *1.1:1 mixture of diastereoisomers* δ 10.02 (d, *J* = 3.3 Hz, 1H), 7.83 – 7.77 (m, 2H), 7.44 (dd, *J* = 8.6, 7.0 Hz, 2H), 7.31 – 7.18 (m, 5H), 5.89 (dq, *J* = 10.3, 2.0 Hz, 0.5H), 5.82 (dp, *J* = 10.4, 1.8 Hz, 0.5H), 5.62 (ddt, *J* = 10.3, 4.9, 2.5 Hz, 1H), 3.32 – 3.22 (m, 1H), 2.09 (ddd, *J* = 14.0, 8.0, 3.9 Hz, 1H), 2.03 (ddd, *J* = 14.2, 4.9, 2.7 Hz, 1H), 1.99 – 1.92 (m, 1H), 1.87 (d, *J* = 17.3 Hz, 1H), 1.56 (qdd, *J* = 10.6, 4.6, 2.5 Hz, 3H), 1.51 – 1.44 (m, 3H), 1.13 (tt, *J* = 7.0, 3.9 Hz, 1H), 1.08 – 0.94 (m, 5H), 0.88 (dddd, *J* = 11.1, 7.4, 5.4, 1.9 Hz, 1H), 0.84 – 0.74 (m, 2H).

UNIVERSITAT ROVIRA I VIRGILI
PHOTOCHEMISTRY AND ORGANOCATALYSIS FOR RADICAL-BASED CARBON-CARBON BOND-FORMING
PROCESSES
Emilien Le Saux

135

^{13}C NMR (101 MHz, CDCl$_3$) *1.1:1 mixture of diastereoisomers* δ 192.2, 192.1, 154.1, 152.4, 145.3, 143.7, 134.1, 134.0, 130.5, 130.4, 129.7, 129.5, 129.3, 129.2, 128.8, 128.7, 128.2, 127.6, 127.0, 126.0, 126.0, 55.6, 46.5, 41.4, 41.2, 35.4, 35.4, 35.2, 35.2, 33.7, 33.6, 26.5, 26.5, 26.4, 26.2, 26.1, 25.0, 25.0, 22.4, 22.3.

HRMS (ESI$^+$) Calculated for C$_{27}$H$_{32}$NaO [M+Na]$^+$: 395.2345, found: 395.2348.
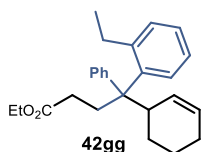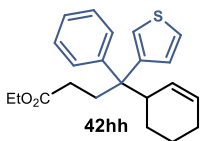
Ethyl 4-(cyclohex-2-en-1-yl)-4-(2-ethylphenyl)-4-phenylbutanoate (42gg)

Prepared according to General Procedure B using radical precursor **40b** (48.1 mg, 0.1 mmol), cyclohexene **2a** (101 µL, 1.0 mmol), 1-ethyl-2-(1-phenylvinyl)benzene **41f** (20.8 mg, 0.1 mmol), and catalyst **A5** (7.6 mg, 0.02 mmol). Multiple purifications by column chromatography resulted in poor separation from several unidentified byproducts. The yield (76%, 1.5:1 *d.r.*, average of two runs) of **42gg** was inferred by ^{1}H NMR analysis of the crude reaction mixture using trichloroethylene as the internal standard. An analytical amount of the pure compound was isolated by preparative TLC (20:80 hexanes/toluene) to obtain a colorless oil.

^{1}H NMR (400 MHz, CDCl$_3$) *Major diastereoisomer* δ 7.48 (t, J = 7.0 Hz,), 7.32 – 7.01 (m), 5.97 (d, J = 10.5 Hz, 1H), 5.77 (dq, J = 10.3, 3.4 Hz, 1H), 4.11 – 4.04 (q, 2H), 3.13 (m, J = 2.8 Hz, 1H), 2.87 (ddd, J = 20.8, 11.6, 5.2 Hz), 2.47 – 2.22 (m), 2.09 (ddt, J = 26.8, 14.7, 7.3 Hz), 1.92 – 1.74 (m), 1.71 – 1.61 (m), 1.22 (t, J = 7.1, 3H), 1.18 – 1.00 (m), 0.87 (t, J = 7.5 Hz, 3H). *Minor diastereoisomer* δ 7.48 (t, J = 7.0 Hz,), 7.32 – 7.01 (m), 5.86 (s, 1H), 5.54 (dd, J = 10.4, 3.5 Hz, 1H), 4.11 – 4.04 (q, 2H), 3.24 (s, 1H), 2.87 (ddd, J = 20.8, 11.6, 5.2 Hz), 2.47 – 2.22 (m), 2.09 (ddt, J = 26.8, 14.7, 7.3 Hz), 1.92 – 1.74 (m), 1.71 – 1.61 (m), 1.22 (t, J = 7.1, 3H), 1.18 – 1.00 (m), 0.87 (t, J = 7.5 Hz, 3H).

^{13}C NMR (101 MHz, CDCl$_3$) *1.5:1 mixture of diastereoisomers* δ 173.9, 144.3, 141.9, 141.8, 131.6, 131.3, 130.0, 129.4, 129.0, 128.7, 128.5, 127.6, 127.3, 127.0, 126.4, 125.6, 125.6, 124.6, 124.5, 60.3, 60.2, 52.8, 52.5, 30.9, 30.5, 30.1, 30.0, 29.7, 26.7, 26.2, 25.9, 25.1, 25.0, 24.0, 22.9, 21.5, 15.3, 15.1, 14.1, 1.0.

HRMS (ESI$^+$) Calculated for C$_{26}$H$_{32}$NaO$_2$ [M+Na]$^+$: 399.2295, found: 399.2281.

Ethyl 4-(cyclohex-2-en-1-yl)-4-phenyl-4-(thiophen-3-yl)butanoate (42hh)

Prepared according to General Procedure B using radical precursor **40b** (48.1 mg, 0.1 mmol), cyclohexene **2a** (101 µL, 1.0 mmol), 3-(1-phenylvinyl)thiophene **41g** (18.6 mg, 0.1 mmol), and catalyst **A5** (7.6 mg, 0.02 mmol). Multiple purifications by column chromatography resulted in poor separation from several unidentified byproducts. The yield (69%, 1.1:1 dr, average of two runs) of **42hh** was inferred

by ^{1}H NMR analysis of the crude reaction mixture using trichloroethylene as the internal standard. An analytical amount of the pure compound was isolated by preparative TLC (70:30 hexanes/toluene) to obtain a colorless oil.

^{1}H NMR (400 MHz, CDCl$_3$) *1.1:1 mixture of diastereoisomers* δ 7.32 – 7.19 (m, 6H), 7.13 (dd, *J* = 2.9, 1.4 Hz, 0.5H), 6.99 (dd, *J* = 3.0, 1.4 Hz, 0.5H), 6.87 (dt, *J* = 5.1, 1.1 Hz, 1H), 5.79 (d, *J* = 10.5 Hz, 0.5H), 5.72 (d, *J* = 10.4 Hz, 0.5H), 5.62 (tq, *J* = 7.7, 2.4 Hz, 1H), 4.12 – 4.04 (m, 2H), 3.16 – 3.00 (m, 1H), 2.56 (dddd, *J* = 14.3, 11.8, 10.0, 4.6 Hz, 1H), 2.43 – 2.32 (m, 1H), 2.19 – 2.05 (m, 1H), 2.03 – 1.84 (m, 3H), 1.79 – 1.46 (m, 3H), 1.23 (td, *J* = 7.1, 4.1 Hz, 3H), 1.11 – 0.96 (m, 1H).

^{13}C NMR (101 MHz, CDCl$_3$) *1.1:1 mixture of diastereoisomers* δ 173.8, 146.5, 144.8, 144.4, 142.5, 129.7, 129.2, 129.1, 128.9, 128.9, 128.8, 128.7, 128.5, 127.9, 127.2, 126.1, 126.1, 124.5, 123.4, 122.4, 122.4, 60.3, 52.0, 51.9, 43.3, 42.5, 34.9, 33.7, 30.2, 30.2, 29.7, 25.0, 25.0, 24.6, 24.6, 22.3, 22.2, 14.1.

HRMS (ESI$^+$) Calculated for C$_{22}$H$_{26}$NaO$_2$S [M+Na]$^+$: 377.1546, found: 377.1547.

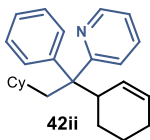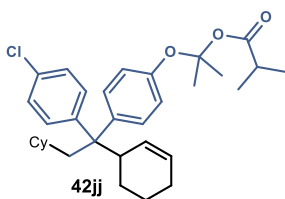### 2-(1-(cyclohex-2-en-1-yl)-2-cyclohexyl-1-phenylethyl)pyridine (42ii)

Prepared according to General Procedure B using radical precursor **1h** (41.1 mg, 0.1 mmol), cyclohexene **2a** (101 μL, 1.0 mmol), 2-(1-phenylvinyl)pyridine **41h** (21.7 mg, 0.12 mmol), and sodium hydrogen phosphate (14.2 mg, 0.1 mmol). The crude mixture was purified by column chromatography (SiO$_2$, 98:2 hexanes/EtOAc) to afford product **42ii** as a pale-yellow oil (21.7 mg, 63% yield, 1.3:1 *d.r.*, average of two runs).

^{1}H NMR (400 MHz, CDCl$_3$) *Major diastereoisomer* δ 8.66 (ddd, *J* = 4.8, 2.0, 0.9 Hz, 1H), 7.50 (td, *J* = 7.7, 1.9 Hz), 7.32 – 7.18 (m), 7.14 – 7.10 (m), 7.06 (ddt, *J* = 15.3, 8.1, 1.1 Hz), 5.78 (dt, *J* = 10.4, 2.0 Hz, 1H), 5.58 (dddt, *J* = 15.2, 10.3, 5.2, 2.5 Hz), 3.65 – 3.55 (m, 1H), 2.13 – 2.09 (m, 2H), 2.00 – 1.81 (m, 4H), 1.67 – 1.42 (m, 12H), 1.23 (tt, *J* = 11.1, 3.9 Hz, 1H), 1.17 – 1.09 (m, 2H), 1.01 (tdd, *J* = 14.0, 9.6, 6.0 Hz), 0.92 – 0.83 (m), 0.76 (td, *J* = 11.8, 5.6 Hz). *Minor diastereoisomer* δ 8.63 (ddd, *J* = 4.8, 2.0, 0.9 Hz, 1H), 7.50 (td, *J* = 7.7, 1.9 Hz), 7.32 – 7.18 (m), 7.14 – 7.10 (m), 7.06 (ddt, *J* = 15.3, 8.1, 1.1 Hz), 5.93 (dp, *J* = 10.4, 1.8 Hz, 1H), 5.58 (dddt, *J* = 15.2, 10.3, 5.2, 2.5 Hz), 3.43 – 3.34 (m, 1H), 2.20 (d, *J* = 4.4 Hz), 2.00 – 1.81 (m), 1.67 – 1.42 (m), 1.23 (tt, *J* = 11.1, 3.9 Hz), 1.17 – 1.09 (m), 1.01 (tdd, *J* = 14.0, 9.6, 6.0 Hz), 0.92 – 0.83 (m), 0.76 (td, *J* = 11.8, 5.6 Hz).

^{13}C NMR (126 MHz, CDCl$_3$) *1.3:1 mixture of diastereoiomers* δ 166.1, 164.7, 147.9, 147.4, 145.5, 143.6, 135.0, 134.3, 130.2, 129.8, 129.5, 129.4, 128.6, 128.1, 127.3, 126.8, 125.9, 125.7, 125.5, 125.4, 120.8, 120.7, 57.1, 57.0, 45.9, 45.8, 41.7, 40.9, 35.3, 35.3, 35.1, 35.0, 33.7, 33.4, 26.7, 26.6, 26.4, 26.3, 26.2, 25.1, 25.1, 24.9, 24.7, 22.5, 22.4.

HRMS (APCI$^+$) Calculated for C$_{25}$H$_{32}$N [M+H]$^+$: 346.2529 found: 346.2530.

UNIVERSITAT ROVIRA I VIRGILI
PHOTOCHEMISTRY AND ORGANOCATALYSIS FOR RADICAL-BASED CARBON-CARBON BOND-FORMING PROCESSES
Emilien Le Saux

137

2-(4-(1-(4-Chlorophenyl)-1-(cyclohex-2-en-1-yl)-2-cyclohexylethyl)phenoxy)propan-2-yl isobutyrate (42jj)

Prepared according to General Procedure B using radical precursor **1h** (61.7 mg, 0.15 mmol), cyclohexene **2a** (101 µL, 2.0 mmol), and 2-(4-(1-(4-chlorophenyl)vinyl)phenoxy)propan-2-yl isobutyrate **41i** (35.9 mg, 0.1 mmol). The crude mixture was purified by column chromatography (SiO$_2$, 80:1 hexanes/EtOAc) to afford product **42jj** as a colorless oil (38.2 mg, 73% yield,1.1:1 dr, average of two runs).

^{1}H NMR (500 MHz, CDCl$_3$) *1.1:1 mixture of diasteroisomers* δ 7.22 – 7.18 (m, 2H), 7.16 – 7.11 (m, 2H), 7.04 – 7.01 (m, 2H), 6.76 – 6.69 (m, 2H), 5.76 (dd, J = 20.8, 10.5 Hz, 1H), 5.58 – 5.52 (m, 1H), 5.08 (dtd, J = 12.5, 6.3, 2.3 Hz, 2H), 3.15 – 3.03 (m, 1H), 1.95 (ddd, J = 14.1, 6.4, 3.8 Hz, 1H), 1.90 – 1.78 (m, 3H), 1.59 (s, 3H), 1.56 (s, 3H), 1.52 – 1.39 (m, 5H), 1.22 (dd, J = 6.3, 0.9 Hz, 3H), 1.20 (dd, J = 6.2, 1.9 Hz, 3H), 1.05 (d, J = 12.6 Hz, 2H), 1.02 – 0.91 (m, 4H), 0.87 – 0.80 (m, 1H), 0.80 – 0.64 (m, 2H).

^{13}C NMR (126 MHz, CDCl$_3$) *1.1:1 mixture of diasteroisomers* δ 173.9, 173.8, 153.5, 153.3, 144.9, 143.2, 139.3, 137.4, 131.4, 131.3, 131.1, 131.1, 130.3, 130.1, 129.1, 129.0, 129.0, 128.9, 128.5, 128.3, 128.0, 127.7, 127.3, 126.8, 118.5, 118.3, 118.2, 117.1, 79.0, 78.9, 68.8, 68.8, 54.1, 54.0, 46.7, 46.6, 41.4, 41.3, 35.5, 35.4, 35.2, 35.2, 33.7, 33.6, 33.3, 26.6, 26.5, 26.5, 26.2, 26.2, 25.4, 25.3, 25.3, 25.2, 25.1, 25.0, 25.0, 25.0, 22.4, 22.3, 21.6, 21.5.

HRMS (ESI$^+$) Calculated for C$_{33}$H$_{43}$ClNaO$_3$ [M+Na]$^+$: 545.2793, found: 545.2787.
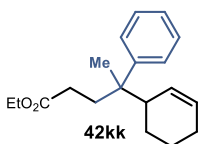
Ethyl 4-(cyclohex-2-en-1-yl)-4-phenylpentanoate (42kk)

Prepared according to General Procedure B using radical precursor **40b** (48.1 mg, 0.1 mmol), cyclohexene **2a** (202 µL, 2.0 mmol), α-methyl styrene **41j** (15.6 µL, 0.12 mmol), sodium hydrogen phosphate (14.2 mg, 0.1 mmol.), and catalyst **A5** (7.6 mg, 0.02 mmol). The crude mixture was purified by column chromatography (SiO$_2$, 75:25 hexanes/toluene) to afford product **42kk** as a colorless oil (13.7 mg, 42% yield, 1.1:1 *d.r.*, average of two runs).

[f1]H NMR (500 MHz, CDCl$_3$) *1.1:1 mixture of diastereoisomers* δ 7.30 (dt, J = 6.9, 4.5 Hz, 3H), 7.27 – 7.24 (m, 1H), 7.20 – 7.16 (m, 1H), 5.78 (s, 1H), 5.65 – 5.59 (m, 0.5H), 5.14 (dp, J = 10.4, 2.0 Hz, 0.5H), 4.05 (qdd, J = 6.9, 4.1, 2.4 Hz, 2H), 2.52 (dq, J = 8.4, 2.7 Hz, 0.5H), 2.46 (ddd, J = 8.8, 6.7, 4.7 Hz, 0.5H), 2.20 – 2.10 (m, 2H), 2.10 – 2.04 (m, 1H), 2.03 – 1.95 (m, 0.5H), 1.95 – 1.77 (m, 3H), 1.64 (ddd, J = 12.3, 6.0, 3.0 Hz, 0.5H), 1.50 (dddd, J = 19.9, 12.9, 7.9, 2.7 Hz, 0.5H), 1.45 – 1.30 (m, 1.5H), 1.29 – 1.22 (m, 2H), 1.25 (s, 3H) 1.22 – 1.17 (m, 3H), 1.07 (tdd, J = 13.1, 10.7, 3.1 Hz, 1H).

¹³C NMR (126 MHz, CDCl₃) *1.1:1 mixture of diastereoisomers* δ 174.2, 146.3, 146.0, 129.1, 128.9, 128.6, 128.3, 128.1, 126.9, 126.6, 125.7, 125.6, 60.2, 46.8, 46.7, 43.3, 34.6, 34.5, 29.9, 29.9, 29.7, 25.3, 25.3, 24.8, 24.3, 22.8, 22.7, 18.6, 14.2.

<u>HRMS</u> (ESI⁺) Calculated for C₁₉H₂₆NaO₂ [M+Na]⁺: 309.1825, found: 309.1829.

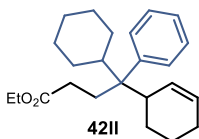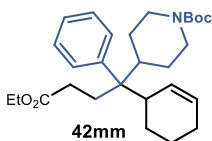**Ethyl 4-(cyclohex-2-en-1-yl)-4-cyclohexyl-4-phenylbutanoate (42ll)**

Prepared according to General Procedure B using radical precursor **40b** (48.1 mg, 0.1 mmol), cyclohexene **2a** (202 μL, 2.0 mmol), (1-cyclohexylvinyl)benzene **41k** (18.6 mg, 0.1 mmol), sodium hydrogen phosphate (14.2 mg, 0.1 mmol.), and catalyst **A5** (7.6 mg, 0.02 mmol). The crude mixture was purified by preparative TLC (SiO₂, 50:50 hexanes/toluene) to afford product **42ll** as a colorless oil (16.7 mg, 47% yield, 1.1:1 *d.r.*, average of two runs).

¹H NMR (500 MHz, CDCl₃) *1.1:1 mixture of diastereoisomers* δ 7.34 – 7.24 (m, 4H), 7.21 – 7.16 (m, 1H), 5.85 (d, *J* = 10.4 Hz, 0.5H), 5.69 – 5.64 (m, 0.5H), 5.51 – 5.44 (m, 0.5H), 5.34 (d, *J* = 10.5 Hz, 0.5H), 4.17 – 4.10 (m, 2H), 3.22 – 3.13 (m, 0.5H), 3.09 – 2.98 (m, 0.5H), 2.62 (t, *J* = 13.9 Hz, 0.5H), 2.59 – 2.48 (m, 1H), 2.44 – 2.39 (m, 0.5H), 2.39 – 2.25 (m, 1H), 2.21 – 2.07 (m, 1H), 2.04 – 1.94 (m, 2H), 1.94 – 1.87 (m, 1H), 1.86 – 1.79 (m, 2H), 1.79 – 1.45 (m, 4H), 1.31 – 1.23 (m, 3H), 1.04 – 0.91 (m, 2H), 0.91 – 0.80 (m, 2H), 0.80 – 0.69 (m, 1H), 0.57 – 0.46 (m, 0.5H), 0.28 (q, *J* = 12.3 Hz, 0.5H).

¹³C NMR (126 MHz, CDCl₃) *1.1:1 mixture of diastereoisomers* δ 174.5, 174.4, 143.6, 132.1, 129.8, 128.8, 128.0, 127.5, 127.4, 126.3, 125.5, 125.4, 60.3, 60.2, 49.2, 48.1, 45.6, 42.2, 40.3, 38.6, 30.9, 30.6, 30.3, 29.7, 28.6, 28.5, 28.3, 28.1, 28.0, 27.5, 27.4, 27.3, 26.6, 26.4, 25.6, 25.5, 25.4, 24.1, 23.5, 23.3, 14.3.

<u>HRMS</u> (ESI⁺) Calculated for C₂₄H₃₄NaO₂ [M+Na]⁺: 377.2451, found: 377.2455.

Ethyl 4-(benzo[d][1,3]dioxol-5-yl)-4-(cyclohex-2-en-1-yl)-4-phenylbutanoate (42mm)

Prepared according to General Procedure B using radical precursor **40b** (72.2 mg, 0.15 mmol), cyclohexene **2a** (101 μL, 1.0 mmol), tert-butyl 4-(1-phenylvinyl)piperidine-1-carboxylate **41l** (28.7 mg, 0.1 mmol), sodium hydrogen phosphate (14.2 mg, 0.1 mmol.), and catalyst **A5** (7.6 mg, 0.02 mmol). The crude mixture was purified by column chromatography (SiO₂, 90:10 hexanes/Et₂O) to afford product **42mm** as a colorless oil (20.0 mg, 44% yield, 1.1:1 *d.r.*, average of two runs).

¹H NMR (500 MHz, CDCl₃) *1.1:1 mixture of diastereoisomers* δ 7.36 – 7.29 (m, 3H), 7.27 – 7.20 (m, 2H), 5.86 (d, *J* = 10.6 Hz, 0.5H), 5.73 (dd, *J* = 10.5, 3.4 Hz, 0.5H), 5.52 (dd, *J* = 10.4, 3.4 Hz, 0.5H), 5.34 (d, *J* = 11.1 Hz, 0.5H), 4.20 – 4.01 (m, 4H), 3.11 (d, *J* = 51.5 Hz, 1H),

UNIVERSITAT ROVIRA I VIRGILI
PHOTOCHEMISTRY AND ORGANOCATALYSIS FOR RADICAL-BASED CARBON-CARBON BOND-FORMING PROCESSES
Emilien Le Saux

139

2.68 – 2.52 (m, 4H), 2.37 (td, J = 14.8, 14.1, 10.2 Hz, 1H), 2.23 – 2.13 (m, 1H), 2.08 – 1.90 (m, 5H), 1.75 (dd, J = 9.9, 5.6 Hz, 3H), 1.40 (d, J = 10.8 Hz, 9H), 1.31 – 1.27 (m, 4H), 0.91 – 0.84 (m, 1H).

^{13}C NMR (101 MHz, CDCl$_3$) *1.1:1 mixture of diastereoisomers* δ 174.3, 174.1, 154.7, 154.6, 142.6, 140.0, 131.6, 129.1, 128.7, 128.2, 127.9, 127.8, 127.7, 126.7, 125.9, 125.7, 79.2, 79.2, 60.4, 60.3, 48.6, 47.6, 44.2, 41.2, 40.0, 38.5, 31.5, 30.6, 30.5, 28.4, 28.3, 28.3, 27.9, 25.6, 25.4, 25.4, 24.1, 23.4, 23.2, 22.6, 14.2, 14.1.

HRMS (ESI) Calculated for C$_{28}$H$_{41}$NNaO$_4$ [M+Na]$^+$: 478.2928, found: 478.2927.

Ethyl 4-(cyclohex-2-en-1-yl)-4-phenyl-4-(4,4,5,5-tetramethyl-1,3,2-dioxaborolan-2-yl)butanoate (42nn)
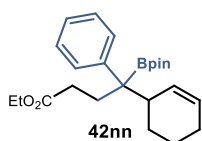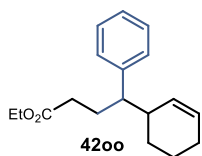
Prepared according to General Procedure B using radical precursor **40b** (48.1 mg, 0.1 mmol), cyclohexene **2a** (101 µL, 1.0 mmol), 4,4,5,5-tetramethyl-2-(1-phenylvinyl)-1,3,2-dioxaborolane **41m** (23.0 mg, 0.1 mmol), and catalyst **A5** (7.6 mg, 0.02 mmol). The crude mixture was purified by two successive separations on column chromatography (SiO$_2$, 90:10 hexanes:CH$_2$Cl$_2$ and then 50:50 hexanes/toluene) to afford product **42nn** as a colorless oil (19.8 mg, 50% yield, 1.1:1 dr, average of two runs).

^{1}H NMR (500 MHz, CDCl$_3$) *1.1:1 mixture of diastereoisomers* δ 7.37 – 7.33 (m, 4H), 7.31 – 7.27 (m, 4H), 7.20 – 7.15 (m, 2H), 5.81 (dp, J = 10.3, 1.7 Hz, 1H), 5.74 – 5.68 (m, 1H), 5.66 – 5.59 (m, 2H), 4.08 (qd, J = 7.1, 1.1 Hz, 4H), 2.82 – 2.74 (m, 1H), 2.70 – 2.62 (m, 1H), 2.45 (ddd, J = 14.6, 12.5, 4.7 Hz, 1H), 2.40 – 2.27 (m, 2H), 2.25 – 2.17 (m, 1H), 2.17 – 2.08 (m, 2H), 2.06 – 1.98 (m, 2H), 1.97 – 1.88 (m, 4H), 1.77 (dd, J = 4.6, 2.5 Hz, 1H), 1.74 – 1.65 (m, 2H), 1.58 – 1.46 (m, 1H), 1.45 – 1.38 (m, 2H), 1.30 (s, 12H), 1.27 (d, J = 3.7 Hz, 12H), 1.23 (td, J = 7.1, 2.1 Hz, 6H), 0.93 – 0.82 (m, 2H).

^{13}C NMR (101 MHz, CDCl$_3$) *1.1:1 mixture of diastereoisomers* δ 174.4, 143.8, 143.1, 130.7, 129.5, 128.8, 128.7, 128.6, 128.0, 127.9, 127.3, 125.4, 125.4, 83.5, 83.4, 60.1, 60.0, 43.9, 42.5, 31.5, 31.1, 30.6, 29.1, 26.0, 25.4, 25.3, 25.3, 25.0, 25.0, 24.8, 24.8, 24.6, 23.0, 22.8, 14.2.

HRMS (ESI$^+$) Calculated for C$_{24}$H$_{35}$NaBO$_4$ [M+Na]$^+$: 420.2557, found: 420.2551.
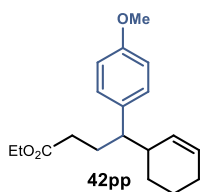
Ethyl 4-(cyclohex-2-en-1-yl)-4-phenylbutanoate (42oo)

Prepared according to General Procedure B using radical precursor **40b** (48.1 mg, 0.1 mmol), cyclohexene **2a** (202 µL, 2.0 mmol), styrene **41n** (14 µL, 0.12 mmol), sodium hydrogen phosphate (14.2 mg, 0.1 mmol.), and catalyst **A5** (7.6 mg, 0.02 mmol). The crude mixture was purified by column

chromatography (SiO$_2$, 75:25 hexanes/toluene) to afford product **42oo** as a colorless oil (12.6 mg, 42% yield, 1.1:1 *d.r.*, average of two runs).

<u>^{1}H NMR</u> (500 MHz, CDCl$_3$)) *1.1:1 mixture of diastereoisomers* δ 7.28 (t, *J* = 7.6 Hz, 2H), 7.22 – 7.17 (m, 1H), 7.13 (td, *J* = 8.0, 7.6, 1.3 Hz, 2H), 5.89 (dd, *J* = 10.3, 2.5 Hz, 0.5H), 5.78 – 5.71 (m, 0.5H), 5.66 – 5.58 (m, 0.5H), 5.35 (d, *J* = 10.2 Hz, 0.5H), 4.09 – 4.03 (m, 2H), 2.45 – 2.33 (m, 1H), 2.27 (dtd, *J* = 16.8, 8.1, 3.5 Hz, 1H), 2.21 – 2.13 (m, 0.5H), 2.09 – 2.04 (m, 2H), 1.97 – 1.83 (m, 3H), 1.77 – 1.68 (m, 0.5H), 1.62 (dq, *J* = 11.2, 4.3, 3.7 Hz, 0.5H), 1.53 – 1.37 (m, 1H), 1.36 – 1.27 (m, 1H), 1.20 (td, *J* = 7.0, 1.8 Hz, 3H), 1.14 – 1.06 (m, 0.5H).

<u>^{13}C NMR</u> (126 MHz, CDCl$_3$) 1.1:1 *mixture of diastereoisomers* δ 173.8, 173.7, 143.2, 143.1, 130.2, 129.6, 128.5, 128.4, 128.3, 128.3, 128.3, 127.9, 127.5, 126.2, 60.1, 50.8, 50.7, 41.1, 40.6, 32.8, 32.6, 28.0, 27.6, 27.3, 27.0, 25.4, 25.3, 21.9, 21.1, 14.2.

<u>HRMS</u> (ESI$^+$) Calculated for C$_{18}$H$_{24}$NaO$_2$ [M+Na]$^+$: 295.1669, found: 295.1672.

Ethyl 4-(cyclohex-2-en-1-yl)-4-(4-methoxyphenyl)butanoate (42pp)

Prepared according to General Procedure B using radical precursor **40b** (48.1 mg, 0.1 mmol), cyclohexene **2a** (202 μL, 2.0 mmol), 1-methoxy-4-vinylbenzene **41o** (16.2 μL, 0.12 mmol), sodium hydrogen phosphate (14.2 mg, 0.1 mmol.), and catalyst **A5** (7.6 mg, 0.02 mmol). The crude mixture was purified by column chromatography (SiO$_2$, 33:66 hexanes/toluene) to afford product **42pp** as a colorless oil (11.8 mg, 40% yield, 1.1:1 *d.r.*, average of two runs).

<u>^{1}H NMR</u> (500 MHz, CDCl$_3$) *1.1:1 mixture of diastereoisomers* δ 7.06 – 7.01 (m, 2H), 6.85 – 6.80 (m, 2H), 5.86 (dd, *J* = 10.2, 2.5 Hz, 0.5H), 5.77 – 5.69 (m, 0.5H), 5.62 (dq, *J* = 10.0, 3.3, 2.9 Hz, 0.5H), 5.36 (ddd, *J* = 10.3, 2.3, 1.2 Hz, 0.5H), 4.06 (qd, *J* = 7.2, 1.5 Hz, 2H), 3.79 (s, 6H), 2.39 – 2.29 (m, 1H), 2.24 (dddd, *J* = 13.1, 8.9, 7.2, 3.7 Hz, 1H), 2.17 – 2.09 (m, 0.5H), 2.09 – 2.03 (m, 2H), 1.93 (dp, *J* = 7.4, 1.7 Hz, 2H), 1.88 – 1.78 (m, 1H), 1.71 (dq, *J* = 9.0, 4.6 Hz, 0.5H), 1.67 – 1.55 (m, 2H), 1.54 – 1.45 (m, 0.5H), 1.41 (tdd, *J* = 11.7, 6.1, 2.9 Hz, 1H), 1.34 – 1.24 (m, 3H), 1.20 (td, *J* = 7.1, 1.7 Hz, 3H), 1.10 (dddd, *J* = 13.1, 10.4, 7.6, 2.5 Hz, 0.5H), 0.91 – 0.79 (m, 0.5H).

<u>^{13}C NMR</u> (126 MHz, CDCl$_3$) 1.1:1 *mixture of diastereoisomers* δ 173.9, 173.8, 158.0, 158.0, 135.2, 135.1, 130.2, 129.8, 129.4, 129.3, 129.1, 128.3, 127.8, 113.8, 113.6, 113.6, 60.1, 55.2, 49.9, 49.8, 41.2, 40.7, 32.8, 32.6, 29.7, 28.2, 27.7, 27.2, 27.1, 25.4, 25.3, 21.9, 21.1, 14.2.

<u>HRMS</u> (ESI$^+$) Calculated for C$_{19}$H$_{29}$NaO$_3$ [M+Na]$^+$: 325.1774, found: 325.1778.

UNIVERSITAT ROVIRA I VIRGILI
PHOTOCHEMISTRY AND ORGANOCATALYSIS FOR RADICAL-BASED CARBON-CARBON BOND-FORMING
PROCESSES
Emilien Le Saux

141

3.8.6 Telescoped three-component allylic C-H benzylation

The telescoped three-component reaction was performed as depicted in Figure 3.36, starting from carboxylic acids **43**.
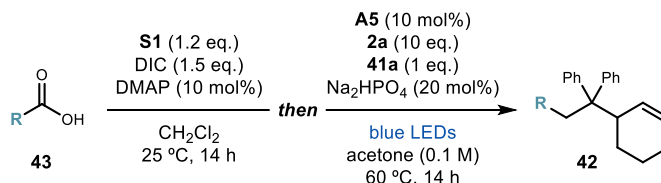
Figure 3.36. Telescoped three-component allylic benzylation.

General procedure C. An oven-dried glass vial, was charged with carboxylic acid **43** (0.12 mmol, 1.2 equiv.), **S1** (36.1 mg, 1.2 equiv.), and DMAP (1.2 mg, 0.1 equiv.). The vial was purged with argon before adding 1 mL of degassed solvent, followed by dropwise addition of DIC (23.5 µL, 1.5 equiv.). The vial was sealed with parafilm and the reaction stirred at 25 ºC for 14 h. The solvent was evaporated under reduced pressure. **A5** (3.8 mg, 0.01 mmol, 0.1 equiv.) and Na_2HPO_4 (2.8 mg, 0.02 mmol, 0.2 equiv.) were sequentially added and the vial purged with argon. 1,1-diphenylethylene **41a** (17.7 µL, 0.1 mmol) and cyclohexene **2a** (101 µL, 1 mmol, 10 equiv.) were finally added, followed by 800 µL (0.1 M) of argon-sparged HPLC grade acetone. The vial was sealed with Parafilm, and then placed in the irradiation setup, maintained at a temperature of 60 ºC. The reaction was stirred for 14 h, then the solvent was evaporated and the crude mixture purified by column chromatography (SiO_2, pentane) to afford products **42**.
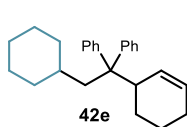
(1-(cyclohex-2-en-1-yl)-2-cyclohexylethane-1,1-diyl)dibenzene (42e)

Prepared according to General Procedure C using cyclohexane carboxylic acid (15.4 mg, 0.12 mmol) in CH_2Cl_2. The crude mixture was purified by column chromatography (SiO_2, pentane) to afford product **42e** as a colorless oil (19.3 mg, 56% yield).
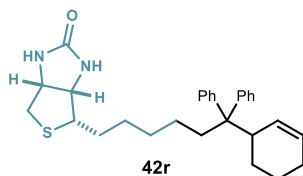
(3aS,4S,6aR)-4-(6-(cyclohex-2-en-1-yl)-6,6-diphenylhexyl)tetrahydro-1H-thieno[3,4-d]imidazol-2(3H)-one (42r)

Prepared according to General Procedure C using D-biotin (29.3 mg, 0.12 mmol) in DMF. Multiple purifications by column chromatography resulted in poor separation from several unidentified byproducts. The yield (37%, average of two runs, 1.1:1 *d.r.*) of **42r** was inferred by ^{1}H NMR analysis of the crude reaction mixture using trichloroethylene as the internal standard. An analytical amount of the pure compound was isolated by preparative TLC (70:30 hexanes/toluene) to obtain a colorless oil.

^{1}H NMR (400 MHz, MeOD) δ 7.36 – 7.29 (m, 6H), 7.26 (dd, J = 7.9, 4.1 Hz, 4H), 5.88 (d, J = 10.6 Hz, 1H), 5.67 – 5.56 (m, 1H), 4.53 (ddd, J = 7.9, 5.0, 1.0 Hz, 1H), 4.30 (dd, J = 7.9, 4.5 Hz, 1H), 3.30 (s, 1H), 3.18 (dt, J = 8.7, 5.3 Hz, 1H), 3.01 – 2.94 (m, 1H), 2.76 (d, J = 12.7 Hz, 1H), 2.19 (dd, J = 10.7, 5.9 Hz, 1H), 1.94 (t, J = 18.0 Hz, 2H), 1.74 – 1.59 (m, 4H), 1.57 – 1.48 (m, 1H), 1.35 (d, J = 15.3 Hz, 6H), 1.15 – 0.95 (m, 4H).

^{13}C NMR (101 MHz, MeOD) δ 163.2, 144.7, 142.6, 128.1, 127.8, 127.7, 126.3, 125.5, 125.0, 123.9, 123.8, 60.4, 58.7, 54.2, 52.6, 39.4, 39.3, 38.1, 37.5, 28.2, 27.8, 27.2, 26.7, 26.6, 23.2, 23.0, 22.4, 20.6.
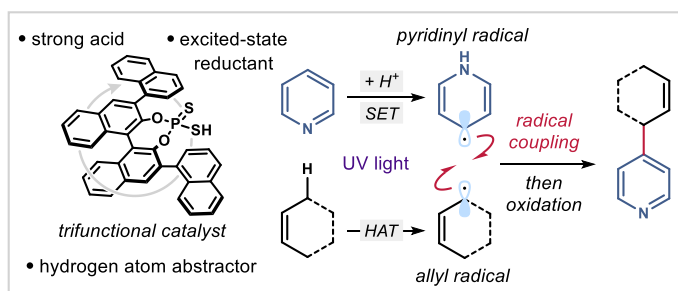
HRMS (ESI$^+$) Calculated for $C_{29}H_{36}N_2NaOS$ [M+Na]$^+$: 483.2441, found: 483.243.

Chapter IV

Photochemical Organocatalytic Functionalization of Pyridines via Pyridinyl Radicals

Target

To develop a new strategy for the C-H functionalization of pyridines by exploiting catalytically generated pyridinyl radicals as key intermediates in a radical coupling process.

- strong acid • excited-state reductant
trifunctional catalyst
- hydrogen atom abstractor
pyridinyl radical
+ H⁺ / SET
UV light
− HAT
allyl radical
radical coupling
then oxidation

Tool

An evolved dithiophosphoric acid catalyst that can perform three distinct activating roles: protonation of pyridine; single-electron reduction of pyridine to afford a pyridinyl radical; and hydrogen atom abstraction for the generation of allylic radicals from simple alkenes.[1]

4.1 General introduction

Azines are a ubiquitous class of heterocycles found in many biologically active molecules, with pyridine standing-out as the most abundant heteroaromatic ring across all FDA-approved drugs.[2] A common strategy in drug discovery is to substitute a benzene ring for the

---

[1] The project discussed in this chapter has been conducted in collaboration with Eleni Georgiou, Igor A. Dmitriev, and Dr. Will C. Hartley. I performed the initial experiments which led to the discovery of the reaction and was involved in the optimization, the investigation of the scope of the reaction, and in the mechanistic elucidation. This study has been published: Le Saux, E.; Georgiou, E.; Dmitriev, I. A.; Hartley, W. C.; Melchiorre, P. "Photochemical Organocatalytic Functionalization of Pyridines via Pyridinyl Radicals" *J. Am. Chem. Soc*. **2023**, *145,* 47.

[2] (a) Vitaku, E.; Smith, D. T.; Njadarson, J. T. "Analysis of the Structural Diversity, Substitution Patterns, and Frequency of Nitrogen Heterocycles among U.S. FDA Approved Pharmaceuticals" *J. Med. Chem*. **2014**, *57*, 10257; (b) Bhutani, P.; Joshi, G.; Raja, N.; Bachhav, N.; Rajanna, P. K.; Bhutani, H.;

isoelectronic and structurally similar pyridine ring, since this can have a drastic effect on the candidate's pharmacokinetic properties and potency.[3] Pyridines are also widely used as ligands for transition metal and photoredox catalysis (Figure 4.1).
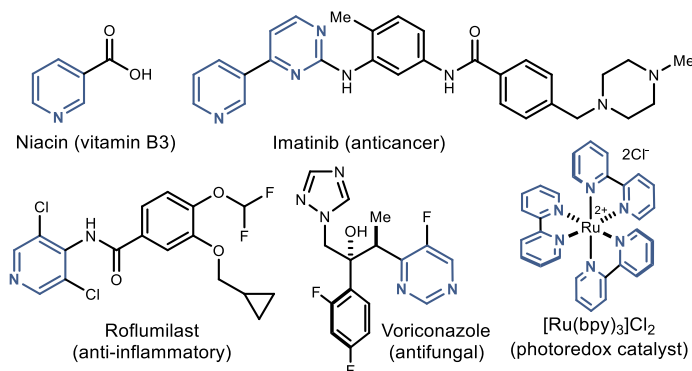

Figure 4.1. Examples of bio-relevant compounds and catalysts containing pyridine and diazine units.

The biological importance of pyridines has been a long-standing motivation for synthetic chemists to develop new methods for their construction and modification. Historically, multicomponent condensation reactions, pioneered by Knoevenagel and Hantzsch, have been the most common way for the *de novo* synthesis of pyridine rings.[4] In spite of the robustness of these strategies, the harsh reaction conditions usually required (>100 °C) have limited the complexity of the fragments amenable to such transformations. Thus, post-modification of the ring has become a desirable strategy. In this context, the C-H functionalization of pyridines has gained attention, as it offers rapid and direct modification of pre-formed scaffolds and is particularly useful for the late-stage modification of complex intermediates.[5]

One of these strategies consists in the addition of a carbon-centered radical to a heteroaromatic base. This process is referred to as the *Minisci reaction*, and constitutes a versatile tool for the C-H functionalization of pyridines and other azines.[6] As depicted in Figure 4.2, Minisci reactions are usually performed under acidic conditions in order to activate pyridine **1a** in the form of a pyridinium ion **I**. This intermediate has the energy level of its lowest unoccupied molecular orbital (LUMO) lowered compared to the neutral pyridine, which facilitates the

Paul, A. T.; Kumar, R. "U.S. FDA Approved Drugs from 2015−June 2020: A Perspective" *J. Med. Chem.* **2021**, *64*, 2339.

[3] Ling, Y.; Hao, Z-Y.; Liang, D.; Zhang, C-L.; Liu, Y-F.; Wang, Y. "The Expanding Role of Pyridine and Dihydropyridine Scaffolds in Drug Design" *Drug. Des. Devel. Ther.* **2021**, *15*, 4289.

[4] Allais, C.; Grassot, J-M.; Rodriguez, J.; Constantieux, T. "Metal-Free Multicomponent Syntheses of Pyridines" *Chem. Rev.* **2014**, *114*, 10829.

[5] Murakami, K.; Yamada, S.; Kaneda, T.; Itami, K. "C-H Functionalization of Azines" *Chem. Rev.* **2017**, *117*, 9302.

[6] Proctor, R. S. J.; Phipps, R. J. "Recent Advances in Minisci-Type Reactions" *Angew. Chem., Int. Ed.* **2019**, *58*, 13666.

UNIVERSITAT ROVIRA I VIRGILI
PHOTOCHEMISTRY AND ORGANOCATALYSIS FOR RADICAL-BASED CARBON-CARBON BOND-FORMING
PROCESSES
Emilien Le Saux

145

addition of an alkyl radical **II** to the ring. The major drawback of this chemistry is its poor regioselectivity, which usually leads to mixtures of products. C2-alkylation is generally favored, but C4-functionalized product is also formed as both these positions are similarly activated. Minisci reactions have found numerous applications in medicinal chemistry, but the regioselectivity issue usually makes products' purification challenging, thus hampering a more widespread use in an industrial context.[7]
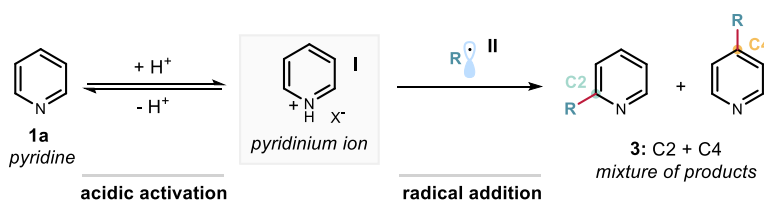

Figure 4.2. The Minisci reaction and the associated challenge of regioselectivity.

In the radical domain, the Minisci reaction is the only strategy available for functionalizing azines C-H bonds. This prompted us to investigate a new radical-based method for the functionalization of native pyridines. Specifically, we focused on neutral pyridinyl radicals **III** (Figure 4.3.a) as a possible handle to functionalize pyridines. This intermediate has been used as a one-electron shuttle for the catalytic reduction of carbon dioxide.[8] A report on electrochemical formation of dimers from this radical was disclosed in 1998 (Figure 4.3.b).[9] In this work, the authors observed that dimerization mainly occurred at the C4-position, unless prevented by a C4-substituent. It was suggested that the electron spin density distribution across the pyridinyl radical dictated the regioselectivity of the process, unless outweighed by steric hindrance effects. Apart from this example, these radicals have been neglected in synthetic chemistry. We sought that the unexplored reactivity of pyridinyl radicals **III** could offer new opportunities for the radical functionalization of pyridines.

---

[7] Duncton, M. A. J. "Minisci Reactions: Versatile CH-Functionalizations for Medicinal Chemists" *Med. Chem. Commun.* **2011**, *2*, 1135.

[8] (a) Seshadri, G.; Lin, C.; Bocarsly, A. B. "A New Homogeneous Electrocatalyst for the Reduction of Carbon Dioxide to Methanol at Low Overpotential" *J. Electroanal. Chem*. **1994**, *372*, 145; (b) Barton Cole, E.; Lakkaraju, P. S.; Rampulla, D. M.; Morris, A. J.; Abelev, E.; Bocarsly, A. B. "Using a One-Electron Shuttle for the Multielectron Reduction of CO_2 to Methanol: Kinetic, Mechanistic, and Structural Insights" *J. Am. Chem. Soc*. **2010**, *132*, 11539.

[9] Carelli, V.; Liberatore, F.; Casini, A.; Tortorella, S.; Scipione, L.; Di Rienzo, B. "On the Regio- and Stereoselectivity of Pyridinyl Radical Dimerization" *New J. Chem*. **1998**, *22*, 999.
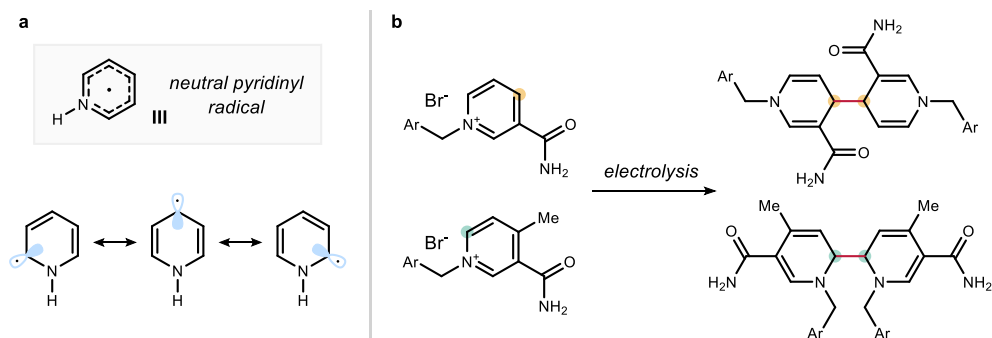
Figure 4.3. (a) Neutral pyridinyl radical **III** and its resonance structures. **(b)** The reported dimerization of pyridinyl radicals under electrochemical conditions (Ref. 9).

This chapter details how this target has been achieved, reporting a new radical method for the C-H functionalization of pyridines **1** (Figure 4.4). The process harnesses the largely unexplored reactivity of pyridinyl radicals **III**, which are generated catalytically upon protonation and sequential single-electron transfer (SET) reduction of the resulting pyridinium ion **I**. A radical cross-coupling between the pyridinyl intermediate **III** and a second radical **IV**, derived from allylic C-H bonds, affords the C-H functionalized pyridine **3** after rearomatization. The protocol offers good to complete regioselectivity depending on the substitution of the pyridine substrate, which has been linked to both steric factors and spin-density of the pyridinyl radical intermediate. In the case of simple pyridine **1a**, the reaction offers a positional selectivity diverging from classical Minisci chemistry, delivering the C4-adduct as the major product. The net process couples two unmodified substrates via functionalization of a C-H bond on each partner.
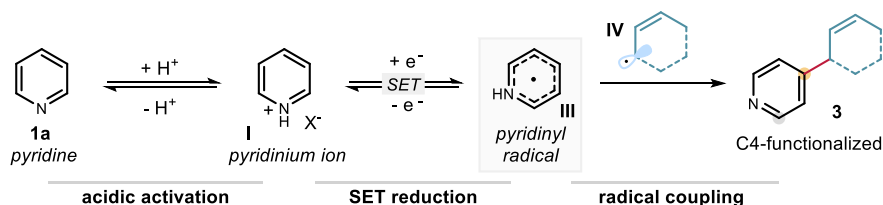

Figure 4.4. Pyridinyl radical-mediated C-H functionalization of pyridines.

In the following sections, the literature precedents on radical functionalization of pyridines and other azines will be discussed, as well as the scientific background and previous studies that were essential to the development of the present research project.

UNIVERSITAT ROVIRA I VIRGILI
PHOTOCHEMISTRY AND ORGANOCATALYSIS FOR RADICAL-BASED CARBON-CARBON BOND-FORMING
PROCESSES
Emilien Le Saux

147

4.2 Background

4.2.1 Radical addition to azines

Contemporary radical chemistry has provided inroads for new functionalization strategies of pyridines. The venerable Minisci reaction is arguably the most explored and versatile radical method for the functionalization of pyridines and related heterocycles. The process is generally used as a benchmark reaction to test the efficiency of new radical generation strategies.[6] The Minisci reaction consists of the addition of a carbon-centered radical **II** to a heteroaromatic substrate **1** followed by formal loss of a hydrogen atom (Figure 4.5.a). As early as 1964, it was found that aryl radicals **VI**, generated from aryldiazonium salts upon heating, could undergo addition to pyridines at the C2-, C3-, and C4-positions (Figure 4.5.b).[10] Lynch made the observation that the proportion of C2-product could be increased significantly by using a higher concentration of diazonium salts. The authors concluded that pyridine underwent *N*-activation in the form of pyridinium ion **VII** upon addition to the diazonium salt, thus favoring C2-regioselectivity. This interpretation was based on previous theoretical work that predicted higher reactivity at the C2-position of pyridinium ions in radical substitution reactions.[11] In subsequent work, the group of Lynch confirmed the implication of pyridinium ions in the reaction by using acetic acid to activate pyridine through protonation.[12] In an analogous fashion to iminium ion activation, the energy of the LUMO is lowered when pyridine is protonated. After describing the addition of alkyl radicals to heteroaromatics using new radical precursors,[13] Minisci and co-workers disclosed in 1971 what is now referred to as the Minisci protocol, in which alkyl radicals **II** are generated through oxidation of carboxylic acids **4** by a combination of silver salts and persulfates as co-oxidant (Figure 4.5.c).[14]

[10] (a) Abramovitch, R. A.; Saha, J. G. "Reaction of Pyridine with *ortho*-Substituted Phenyl Radicals, and the Influence of Oxygen upon Isomer Ratios in the Gomberg-Hey Reaction" *J. Chem. Soc.* **1964**, 2175; (b) Lynch, B. M.; Chang, H. S. "Concentration-Dependent Orientations in Free-Radical Phenylations of Heteroaromatic Compounds" *Tetrahedron Lett.* **1964**, *5*, 2965.

[11] Brown, R. D.; Heffernan, L. N. "The Chemistry of Pyridine, Pyrimidine, and Pyrazine" *Austral. J. Chem.* **1956**, *9*, 83.

[12] Dou, H. J. M.; Lynch, B. M. "Selective Free-Radical Phenylations: nitrogen-Heteroatomic Compounds in Acidic Media" Tetrahedron Lett. **1965**, 6, 897.

[13] (a) Minisci, F.; Galli, R.; Cecere, M.; Malatesta, V.; Caronna, T. "Nucleophilic Character of Alkyl Radicals: New Syntheses by Alkyl Radicals Generated in Redox Processes" *Tetrahedron Lett.* **1968**, *9*, 5609; (b) Minisci, F.; Galli, R.; Malatesta, V.; Caronna, T. "Nucleophilic Character of Alkyl Radicals – II: Selective Alkylation of Pyridine, Quinoline and Acridine by Hydroperoxides and Oxaziranes" *Tetrahedron*, **1970**, *26*, 4083.

[14] Minisci, F.; Bernardi, R.; Bertini, F.; Galli, R.; Perchinummo, M. "Nucleophilic Character of Alkyl Radicals – VI A New Convenient Selective Alkylation of Heteroaromatic Bases" *Tetrahedron* **1971**, *27*, 3575.
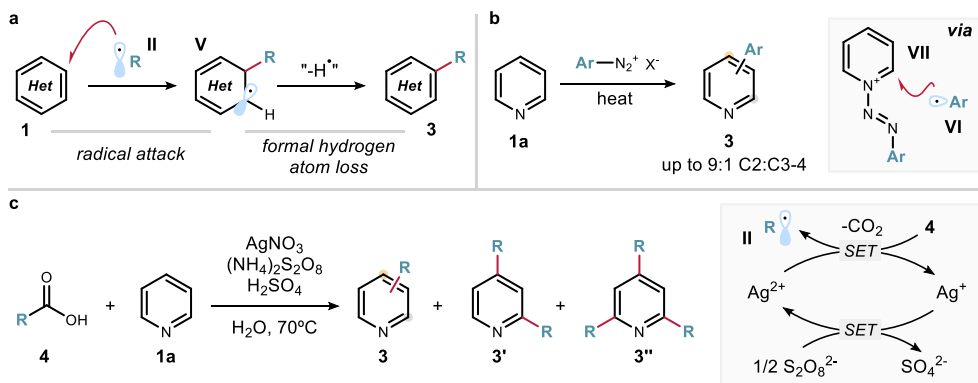
Figure 4.5. (**a**) General concept of the Minisci reaction. (**b**) Seminal reports on the radical arylation of azines. (**c**) The Minisci protocol using carboxylic acids.

In these seminal reports, fundamental aspects of this chemistry were already apparent: (*i*) nucleophilic radicals are required, (*ii*) acidic activation influences the regioselectivity but C2- and C4-mixtures of products are formed, and (*iii*) overalkylation is observed and difficult to control.

Mechanistically, the majority of Minisci reactions are proposed to follow the pathway illustrated in Figure 4.6. The nucleophilic radical **II** adds to pyridinium ion **I** (at the C2-position in this case) to afford the radical cation **VIII**. The proton adjacent to the aminium radical sees its acidity enhanced, resulting in facile deprotonation and formation of the α-amino radical **V**. The latter is eventually oxidized ($E_{red} \sim$ -0.6 V vs Ag^+/Ag) to afford C-H functionalized product **3**.
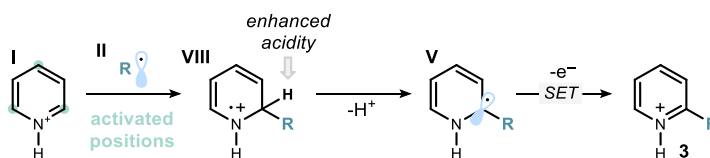

Figure 4.6. Mechanism for Minisci reactions.

This mechanistic rationale highlights the need for oxidative conditions to promote the re-aromatization step. Despite significant progress in the scope of radical precursors, stoichiometric oxidants and elevated temperatures were usually needed for this chemistry. More recently, the development of photoredox catalysis[15] has allowed for the generation of radicals under mild conditions, leading to a re-investigation of the Minisci reaction. In particular, the use of photocatalysts acting sequentially as oxidant and reductant (or *vice versa*) enabled the development of redox-neutral alkylations of azines. The first report of this

---

[15] Shaw, M. H.; Twilton, J.; MacMillan, D. W. C. "Photoredox Catalysis in Organic Chemistry" *J. Org. Chem.* **2016**, *81*, 6898.

UNIVERSITAT ROVIRA I VIRGILI
PHOTOCHEMISTRY AND ORGANOCATALYSIS FOR RADICAL-BASED CARBON-CARBON BOND-FORMING PROCESSES
Emilien Le Saux

149

kind came from DiRocco and colleagues at Merck in 2014.[16] A Minisci protocol was required for the late-stage functionalization of biologically active heterocycles, like Voriconazole **5**, but classical conditions were too harsh for their compounds of interest. Instead, attention was turned to photoredox catalysis to avoid the use of strong oxidants. Specifically, they used an iridium photocatalyst **PC** and visible light irradiation (Figure 4.7). The excited state of the photocatalyst *Ir^{III} reduced protonated *tert*-butyl peracetate **IX** in a SET event to afford acetic acid as a byproduct, and a *tert*-butoxyl radical **X**. The latter released acetone upon β-scission, along with a methyl radical **II** which underwent addition to the protonated heterocycle **I**. After deprotonation, the resulting α-amino radical **V** was oxidized to the methylated product **7** by Ir^{IV}, thus regenerating the ground state Ir^{III} catalyst. The redox-neutral reaction only required 1 mol% of photoredox catalyst and was performed at ambient temperature. Such mild conditions allowed the methylation of a variety of complex heterocycles in moderate to good yields, albeit with the inherent overalkylation problem still present.
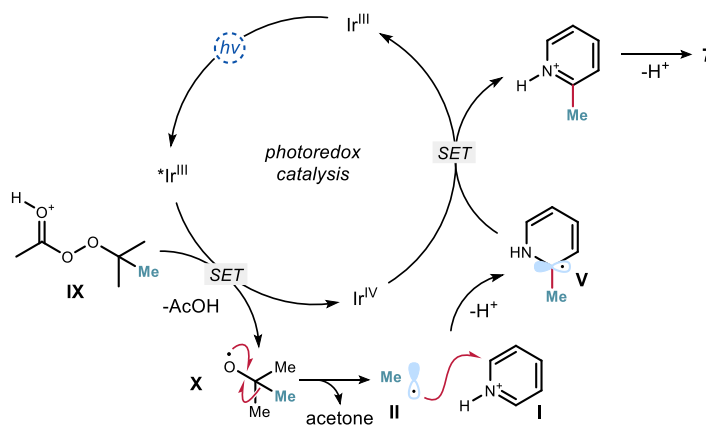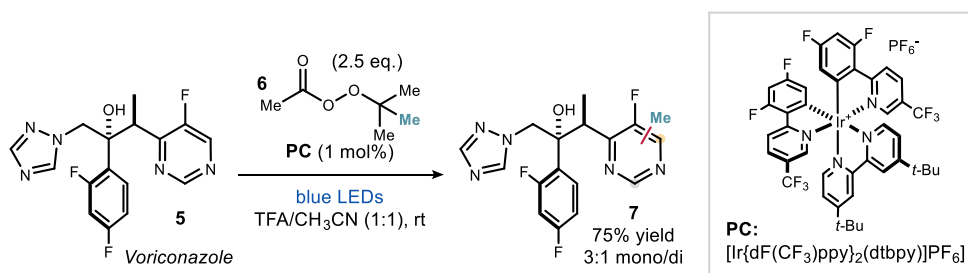

Figure 4.7. Photocatalytic Minisci reaction.

Besides expanding the scope of radicals amenable to Minisci reactions, the use of photoredox catalysis has also enabled HAT strategies to be employed for generating radicals. These

---

[16] DiRocco, D. A.; Dykstra, K.; Krska, S.; Vachal, P.; Conway, D. V.; Tudge, M. "Late-Stage Functionalization of Biologically Active Heterocycles Through Photoredox Catalysis" *Angew. Chem. Int. Ed.* **2014**, *53*, 4802.

approaches depend on C-H bond dissociation energies and polarity of the substrates, not on their redox properties (Figure 4.8). A limitation of this chemistry is the poor reactivity associated with benzylic or allylic radicals, which has hampered the corresponding functionalization of azines. Three protocols on azine benzylation are available, but they are limited to isoquinolines,[17] benzothiazole,[18] and 4-cyanopyridines[19] as acceptors.

non-stabilized alkyl   alpha to heteroatom   acyl and carbamoyl

challenging

aryl and trifluoromethyl   benzyl (3 reports)
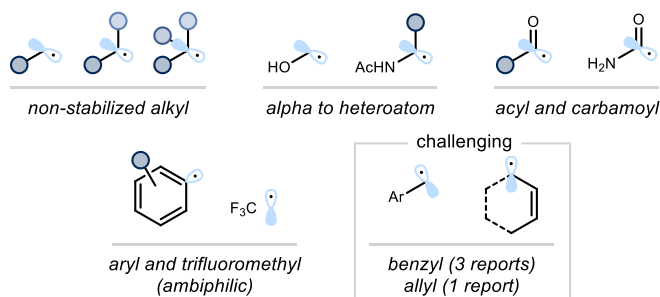(ambiphilic)   allyl (1 report)

Figure 4.8. Radicals amenable to Minisci reactions.

Furthermore, only one protocol has been reported for the radical allylation of pyridines.[20] Specifically, semiconductor quantum dots (QDs) in combination with visible light was used to generate allylic radicals **IV** from alkenes **2** through oxidation and deprotonation (Figure 4.9). Upon excitation with blue LEDs, an electron hole was formed in the valence band and an electron in the conduction band. The hole triggered oxidation of **2**, which then formed the allylic radical by deprotonation. This proton was immediately captured by an electron in the conduction band to form a hydrogen atom, which was ultimately released as hydrogen gas. The mechanism of addition of the allylic radical **IV** to the heteoarene **1** was not detailed by the authors. The products were obtained in good yields, but the scope was mostly limited to isoquinolines.

[17] Wan, M.; Lou, H.; Liu, L. "C1-Benzyl and Benzoyl Isoquinoline Synthesis Through Direct Oxidative Cross-Dehydrogenative Coupling with Methyl Arenes" *Chem. Commun.*, **2015**, *51*, 13953.

[18] Li, Z.-E.; Jin, L.-K.; Cai, C. "Efficient Synthesis of 2-Substituted Azoles: Radical C–H Alkylation of Azoles with Dicumyl Peroxide, Methylarenes and Cycloalkanes Under Metal-Free Condition" *Org. Chem. Front.*, **2017**, *4*, 2039.

[19] Georgiou, E.; Spinnato, D.; Chen, K.; Melchiorre, P. "Switchable Photocatalysis for the Chemodivergent Benzylation of 4-Cyanopyridines" *Chem. Sci.*, **2022**, *13*, 806.

[20] Huang, C.; Qiao, J.; Ci, R.-N.; Wang, X.-Z.; Wang, Y.; Wang, J.H.; Chen, B.; Tung, C.-H.; Wu, L.-Z. "Quantum Dots Enable Direct Alkylation and Arylation of Allylic C(sp^3)-H Bonds with Hydrogen Evolution by Solar Energy" *Chem* **2021**, *7*, 1244.

UNIVERSITAT ROVIRA I VIRGILI
PHOTOCHEMISTRY AND ORGANOCATALYSIS FOR RADICAL-BASED CARBON-CARBON BOND-FORMING
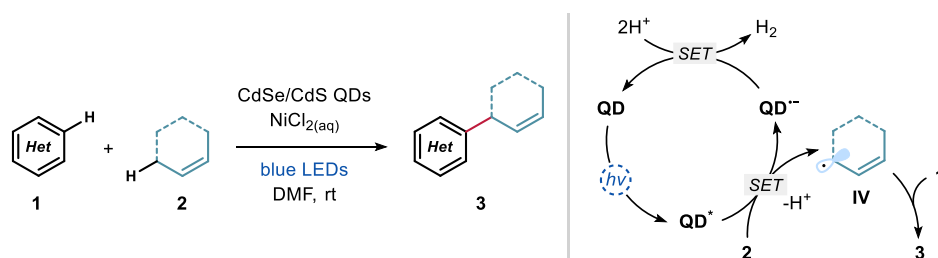PROCESSES
Emilien Le Saux

151

Figure 4.9. Quantum dot enabled allylation of heteroarenes.

Overall, the addition of radicals to heteroarenes is a powerful tool to rapidly modify aromatic heterocycles without the need for prefunctionalization. However, Minisci chemistry is generally associated with poor regioselectivity and over-alkylation when more than one position is available for functionalization.[21]

Pre-modified *N*-activated pyridines exhibit enhanced electrophilic character due to a lowered LUMO energy. In addition, this activation also influenced the regioselectivity of subsequent functionalization processes. It was shown that bulky activating groups, or *blocking groups*, could offer excellent to complete C2- or C4-selectivity in polar functionalization processes.[22] A similar strategy has been translated to the radical domain by employing such *N*-activated pyridines in Minisci-type reactions (Figure 4.10). The bulky *N*-activating group hinders the C2- and C6-positions, enabling greater C4-regioselectivity. Hong and coworkers found that *N*-aminopyridiniums **8a** acted as excellent substrates for C4-selective radical functionalization. Upon addition of a radical at the unhindered C4-position, the weak *N-N* bond was cleaved to release an *N*-centered radical with concomitant rearomatization of the pyridine system. The *N*-centered radical then propagated the reaction by promoting HAT from a suitable C-H precursor, generating a carbon-centered nucleophilic radical able of adding to another molecule of the *N*-activated pyridinium **8a**.[23] This strategy furnished the neutral C4-functionalized pyridine product without the need for *N*-deprotection. However, unsubstituted

---

[21] O'Hara, F.; Blackmond, D. G.; Baran, P. S. "Radical-Based Regioselective C−H Functionalization of Electron-Deficient Heteroarenes: Scope, Tunability, and Predictability" *J. Am. Chem. Soc.* **2013**, *135*, 12122.

[22] (a) Nakao, Y.; Yamada, Y.; Kashihara, N.; Hiyama, T. "Selective C-4 Alkylation of Pyridine by Nickel/Lewis Acid Catalysis" *J. Am. Chem. Soc.* **2010,** *132*, 13666; (b) Tsai, C.-C.; Shih, W.-C.; Fang, C.-H.; Li, C.-Y.; Ong, T.-G.; Yap, G. P. A. "Bimetallic Nickel Aluminum Mediated Para-Selective Alkenylation of Pyridine: Direct Observation of η^2,η^1-Pyridine Ni(0)− Al(III) Intermediates Prior to C−H Bond Activation" *J. Am. Chem. Soc.* **2010**, *132*, 11887; (c) Fier, P. S. "A Bifunctional Reagent Designed for the Mild, Nucleophilic Functionalization of Pyridines" *J. Am. Chem. Soc.* **2017**, *139*, 9499; (d) Obradors, C.; List, B. "Azine Activation via Silylium Catalysis" *J. Am. Chem. Soc.* **2021**, *143*, 6817.

[23] (a) Moon, Y.; Park, B.; Kim, I.; Kang, G.; Shin, S.; Kang, D.; Baik, M. H.; Hong, S. "Visible Light Induced Alkene Aminopyridylation using N-aminopyridinium Salts as Bifunctional Reagents" *Nat. Commun.* **2019**, *10*, 4117; (b) Jung, S.; Shin, S.; Park, S.; Hong, S. "Visible-Light-Driven C4-Selective Alkylation of Pyridinium Derivatives with Alkyl Bromides" *J. Am. Chem. Soc.* **2020**, *142*, 11370; (c) Lee, W.; Jung, S.; Kim, M.; Hong, S. "Site Selective Direct C-H Pyridylation of Unactivated Alkanes by Triplet Excited Anthraquinone" *J. Am. Chem. Soc.* **2021**, *143*, 3003.

pyridine could not be used, and in some cases poor C4/C2-selectivity was observed. In another strategy using a bulky *N*-activator, the Baran group devised *N*-alkylated pyridinium salts **8b** as radical traps.[24] This activation offered complete C4-selectivity, but an additional step was required to remove the blocking group, and *ortho*-substituted pyridines were not amenable to the reaction. For both **8a** and **8b**, two additional steps were needed to install the blocking groups.
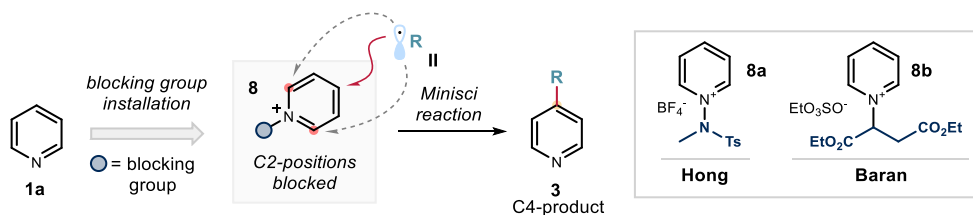

Figure 4.10. General concept of blocking group strategies for regioselective addition of radicals to pyridines.

4.2.2 Radical *ipso*-substitutions

An alternative radical strategy for the site-selective functionalization of azines is the *ipso*-substitution, which can be performed on pyridines **9** bearing a cyano or triphenylphosphonium group at the C2- or C4-position (Figure 4.11). The most common cyano group possesses both electron-withdrawing properties and good leaving group ability, which is key for the success of this radical-radical coupling strategy.[25] SET reduction of the pyridine substrate affords radical anion **XI**, which benefits from significant stabilization due to the neighboring π-systems. This persistent radical intermediate can couple efficiently with another open-shell species **II** to generate intermediate **XII**, which rearomatizes to the functionalized pyridine **3** through elimination of the leaving group.
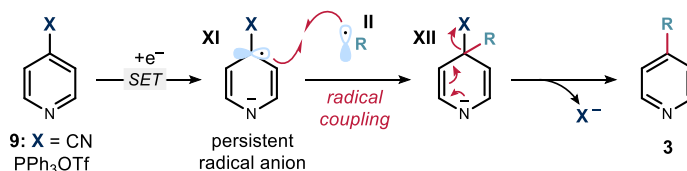

Figure 4.11. General mechanism for radical *ipso*-substitution reactions.

---

[24] Choi, J.; Laudadio, G.; Godineau, E.; Baran, P. S. "Practical and Regioselective Synthesis of C-4-Alkylated Pyridines" *J. Am. Chem. Soc.* **2021**, *143*, 11927.

[25] Tong, S.; Li, K.; Ouyang, X.; Song, R.; Li, J. "Recent Advances in the Radical-Mediated Decyanative Alkylation of Cyano(hetero)arene" *Green Synth. Catal.* **2021**, *2*, 145.

UNIVERSITAT ROVIRA I VIRGILI
PHOTOCHEMISTRY AND ORGANOCATALYSIS FOR RADICAL-BASED CARBON-CARBON BOND-FORMING
PROCESSES
Emilien Le Saux

153

In the late 1960s and early 1970s, several research groups independently reported the direct photoexcitation of azines using high energy UV light (λ <300 nm).[26] While neutral azines such as **1a** underwent $n \rightarrow \pi^*$ electronic transitions, granting HAT reactivity to the azine, protonated heterocycles **I** were turned into strong oxidants *via* $\pi \rightarrow \pi^*$ transitions (Figure 4.12.a). These processes afforded alkylation products **3** albeit in low yield (usually <20%) and poor regioselectivity. However, when 4-cyanopyridine **9a** was used in a similar process with alkenols **10**, *ipso*-substituted products **11** and **12** were formed in moderate yield but complete regioselectivity (Figure 4.12.b).[27] Under neutral conditions, HAT between excited **9a** and alcohol **10** led to pyridylation adjacent to the alcohol group. In contrast, product **12** was obtained under acidic conditions (1 equiv. HCl) *via* SET oxidation of the alkene moiety in **10**. These studies indicated the tendency of the radical anion **XIII** to undergo *ipso*-substitution via radical coupling and displacement of the CN moiety.
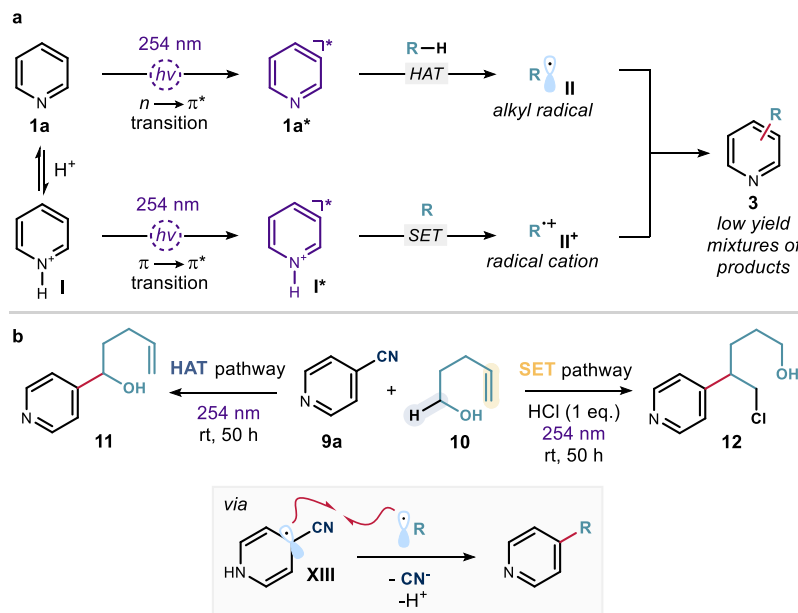

Figure 4.12. (**a**) Photoexcitation of azines with UV light. (**b**) Photoexcitation of cyanopyridine **9a** with UV light.

[26] (a) Stermitz, F. R.; Seiber, R. P.; Nicodem, D. E. "Imine Photoalkylations. Papaverine, Phenanthridine, and a General Mechanism" *J. Org. Chem.* **1968**, *33*, 1136; (b) Stermitz, F. R.; Wei, C. C.; O'Donnel, C. M. "Photochemistry of N-Heterocycles. Photochemistry of Quinoline and Some Substituted Quinoline Derivatives" *J. Am. Chem. Soc.* **1970**, *92*, 2745; (c) Noyori, R.; Katô, M. "Photochemical Reaction of Benzopyridines with Alkanoic Acids. Novel Reductive Alkylation of Acridine, Quinoline, and Isoquinoline under Decarboxylation" *Tetrahedron,* **1969**, *25*, 1125.
[27] Caronna, T.; Clerici, A.; Coggiola, D.; Morrocchi, S. "Photoreactions of 4-Cyanopyridine with Alkenols. Influence of the Medium on the Reaction Mechanism and Photoproducts Formation" *Tetrahedron Lett.* **1981**, *22*, 2115.

This reductive pathway has now become a widely employed strategy to engage cyanopyridines and other cyanoarenes into radical *ipso*-substitution reactions, in particular in combination with photoredox catalysis. A seminal report came from the MacMillan group in 2011 (Figure 4.13).[28] The strongly reducing excited state of Ir(ppy)$_3$ ($E^*(Ir^{IV}/*Ir^{III})$ = -1.9 V vs SCE) reduced cyanopyridine **9a** (E_{red} = -1.6 V vs SCE) to give the persistent radical anion **XI**. Concurrently, α-amino radicals **XIV** were generated by SET oxidation of anilines **13** by Ir^{III}, which after deprotonation of the radical cation **XVI** coupled with the radical anion **XI**.
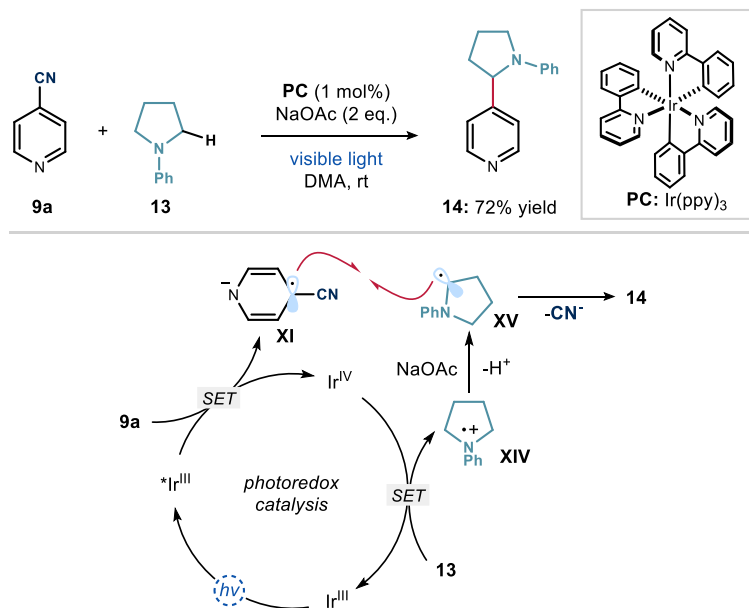

Figure 4.13. Photocatalytic synthesis of α-arylamines using cyanopyridines.

Since then, research in this area has flourished, mainly focusing on expanding the scope of radicals capable of coupling with cyanopyridines. While persistent and stabilized α-amino, benzylic, allylic radicals have been widely employed for this chemistry, the use of non-stabilized alkyl radicals is rare.[29]

The major drawback in using cyanopyridines is their synthesis. Cyanation of pyridines tends to be poorly regioselective, leading to multiple regioisomers that cannot be separated. Furthermore, cyanation protocols are generally not suitable for complex pyridines typically found in pharmaceutical and agrochemical candidates.[30] McNally and coworkers developed

---

[28] McNally, A.; Prier, C. K.; MacMillan, D. W. C. "Discovery of an α-Amino C-H Arylation Reaction using the Strategy of Accelerated Serendipity" *Science* **2011**, *334*, 1114.

[29] Lipp, B.; Nauth, A. M.; Opatz, T. "Transition-Metal-Free Decarboxylative Photoredox Coupling of Carboxylic Acids and Alcohols with Aromatic Nitriles" *J. Org. Chem.* **2016**, *81*, 6875.

[30] (a) Yu, X.; Tang, J.; Jin, X.; Yamamoto, Y.; Bao, M. "Manganese-Catalyzed C-H Cyanation of Arenes with N-Cyano-N-(4-methoxy)phenyl-p-toluenesulfonamide" *Asian J. Org. Chem.* **2018**, *7*, 550; (b)

UNIVERSITAT ROVIRA I VIRGILI
PHOTOCHEMISTRY AND ORGANOCATALYSIS FOR RADICAL-BASED CARBON-CARBON BOND-FORMING PROCESSES
Emilien Le Saux

155

pyridine phosphonium salts **9b** as an alternative to cyanopyridine, which can be prepared in a single step from pyridines **1** with complete C4-regioselectivity (Figure 4.14). Originally, these phosphonium salts **9b** were used for polar cross-coupling reactions with nucleophiles.[31] Later, these substrates were found to be amenable to radical processes through SET reduction (E_{red} = -1.5 V vs SCE). The resulting α-phosphonium radicals **XVI** behaved similarly to cyanopyridine radical anions, and coupled efficiently with other persistent or stabilized open-shell intermediates (Figure 4.14.a). Firstly, B$_2$pin$_2$ was applied as an electron transfer reagent for the C4-selective pyridine-pyridine cross-coupling.[32] Soon after, photoredox catalysis was used to develop a benzylation reaction using potassium tetrafluoroborate salts **15** as radical precursors.[33] Complex pyridines could be functionalized in good yield using this strategy (Figure 4.14.b).
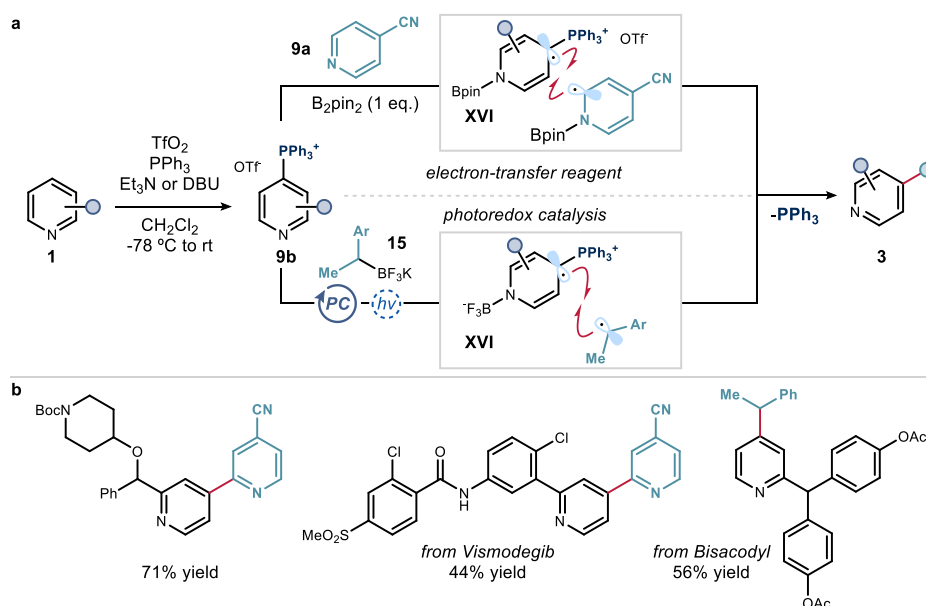

Figure 4.14. (**a**) Pyridine triphenylphosphonium salts **9b** as an alternative to cyanopyridines. (**b**) Selected examples from the scope.

Zhao, D.; Xu, P.; Ritter, T. "Palladium-Catalyzed Late-Stage Direct Arene Cyanation" *Chem*, **2019**, *5*, 97.

[31] (a) Anderson, R. G.; Jett, B. M.; McNally, A. "A Unified Approach to Couple Aromatic Heteronucleophiles to Azines and Pharmaceuticals" *Angew. Chem. Int. Ed.* **2018**, 57, 12514; (b) Patel, C.; Mohnike, M.; Hilton, M. C.; McNally, A. "A Strategy to Aminate Pyridines, Diazines, and Pharmaceuticals via Heterocyclic Phosphonium Salts" *Org. Lett.* **2018**, *20*, 2607.

[32] Koniarczyk, J. L.; Greenwood, J. W.; Alegre-Requena, J. V.; Paton, R. S.; McNally, A. "A Pyridine−Pyridine Cross-Coupling Reaction via Dearomatized Radical Intermediates" *Angew. Chem., Int. Ed.* **2019**, *58*, 14882.

[33] Greenwood, J. W.; Boyle, B. T.; McNally, A. "Pyridylphosphonium Salts as Alternatives to Cyanopyridines in Radical−Radical Coupling Reactions" *Chem. Sci.* **2021**, *12*, 10538.

Overall, *ipso*-substitutions constitute a powerful alternative to Minisci-type reactions as they benefit from complete regioselectivity, and are usually high yielding. Nevertheless, the requirement for prefunctionalization somehow lowers the attractiveness of the method.

4.2.3 Pyridyl radicals

In comparison to the aforementioned radical strategies, an underexplored approach is the use of neutral pyridyl radicals as intermediates for the functionalization of pyridines. SET reduction of pyridyl halides **16** can generate the corresponding pyridyl radicals **XVII**, which have similar reactivity to aryl radicals. Because of the high bond dissociation energy (BDE) of aromatic C-H bonds (113 kcal·mol^{-1} for benzene), aryl radicals are excellent hydrogen atom abstractors.[34] Consequently, those intermediates are highly reactive and difficult to engage in C-C bond-forming events. Notwithstanding, limited examples of pyridine functionalization via pyridyl radicals have been reported (Figure 4.15).
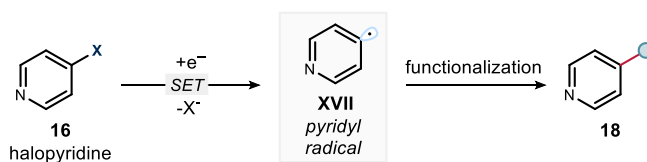

Figure 4.15. Reductive generation of pyridyl radicals **XVII** and addition to π-systems.

In 2015, Weaver reported a photoredox-catalyzed method for the alkylation of perfluoroarenes **16a** with alkenes **17** via pyridyl radicals (Figure 4.16).[35] Functionalized pyridines **18** were obtained in good yields, but as mixtures with the hydrodefluorination product **18'** (**18**/**18'** <3:1). Excess of alkene **17** was necessary to limit the formation of the reduced product **18'**, which came from rapid quenching of the pyridyl radical **XVII** *via* HAT. It was proposed that the reaction could occur *via* either an oxidative or a reductive quenching cycle, although the former manifold is more likely when using Ir(ppy)$_3$.

The excited photoredox catalyst (E*(Ir^{IV}/*Ir^{III}) = -1.9 V vs SCE) reduced **16a** to a radical anion (E_{red} = -2.2 V vs SCE) in an endergonic SET event. After defluorination, the emerging pyridyl radical **XVII** could either abstract a hydrogen atom (probably from the reaction solvent) leading to undesired **18'**, or add to alkene **17**. The latter option afforded an alkyl radical **XVIII** which delivered the final product **18** upon HAT. SET oxidation of DIPEA by

---

[34] Kvasovs, N.; Gevorgyan, V. "Contemporary Methods for Generation of Aryl Radicals" *Chem. Soc. Rev.*, **2021**, *50*, 2244.

[35] Sing, A.; Kubik, J. J.; Weaver, J. D. "Photocatalytic C–F Alkylation; Facile Access to Multifluorinated Arenes" *Chem. Sci.*, **2015**, *6*, 7206.

UNIVERSITAT ROVIRA I VIRGILI
PHOTOCHEMISTRY AND ORGANOCATALYSIS FOR RADICAL-BASED CARBON-CARBON BOND-FORMING
PROCESSES
Emilien Le Saux

157

Ir^{IV} turned over the photocatalyst. In a subsequent report, similar conditions were used for the synthesis of biaryls by replacing the alkene with arenes as radical traps.[36]
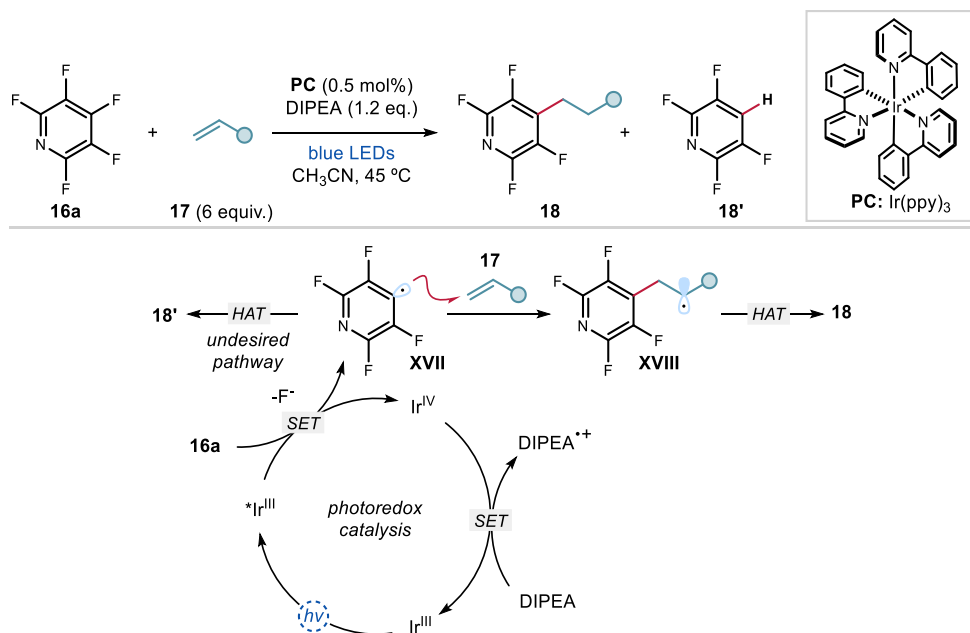

Figure 4.16. Photocatalytic alkylation of perfluoropyridine.

The addition of pyridyl radicals to electron-poor and unactivated alkenes was extensively studied by Jui and co-workers. Specifically, various catalytic systems have been developed for the use of bromo- and iodo-pyridines **16** as pyridyl radical precursors. The first report described the pyridyl radical conjugate addition to Michael acceptors **17a** (Figure 4.17), which took place under a similar mechanistic regime to that proposed by Weaver.[37] Using 3 equivalents of the radical trap, functionalized azines **18** were obtained in good to excellent yield. The presence of water as a cosolvent inhibited the formation of the undesired hydrodehalogenation side-product. In a subsequent report, the scope was expanded to include unactivated olefins **17b**.[38]

[36] Senaweera, S.; Weaver, J. D. "Dual C−F, C−H Functionalization via Photocatalysis: Access to Multifluorinated Biaryls" *J. Am. Chem. Soc.* **2016**, *138*, 2520.

[37] Aycock, R. A.; Wang, H.; Jui, N. T. "A Mild Catalytic System for Radical Conjugate Addition of Nitrogen Heterocycles" *Chem. Sci.*, **2017**, *8*, 3121.

[38] Byington, A. J.; Riu, M.-L. Y.; Jui, N. T. "Anti-Markovnikov Hydroarylation of Unactivated Olefins via Pyridyl Radical Intermediates" *J. Am. Chem. Soc.* **2017**, *139*, 6582.
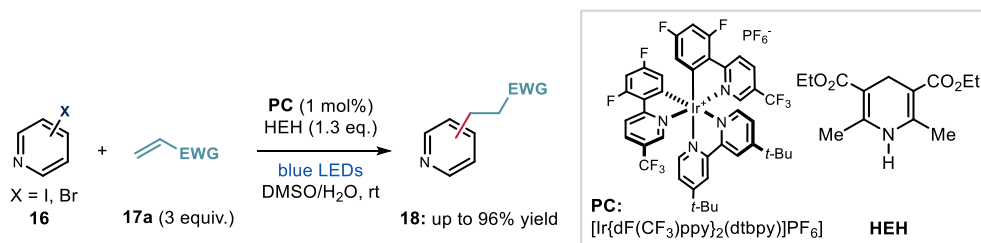
Figure 4.17. Photocatalytic conjugate addition of pyridyl radicals.

Overall, current radical strategies for the functionalization of pyridines are not suitable to achieve regioselectivity using non-functionalized substrates. While Minisci-type reactions are straightforward and allow the direct functionalization of C-H bonds, they lead to mixtures of products and are rarely productive with stabilized radicals. Regioselective approaches require pre-functionalization, either to install blocking groups on the nitrogen, or leaving groups on the ring for *ipso*-substitutions or pyridyl radical generation.

4.2.4 Pyridinyl radicals

As introduced earlier in this chapter, pyridinyl radicals (not to be confused with pyridyl radicals, see section 4.2.3) are neutral open-shell species in which the radical is delocalized across the π-system of the pyridine ring. They are sometimes proposed as intermediates in some biological processes. For example, while the nicotinamide adenine dinucleotide NADH/NAD$^+$ cofactor is mostly known for hydride transfer chemistry in living cells, the pyridinyl radical NAD$^\bullet$ may also play a role in some biological processes as a SET donor (Figure 4.18).[39]
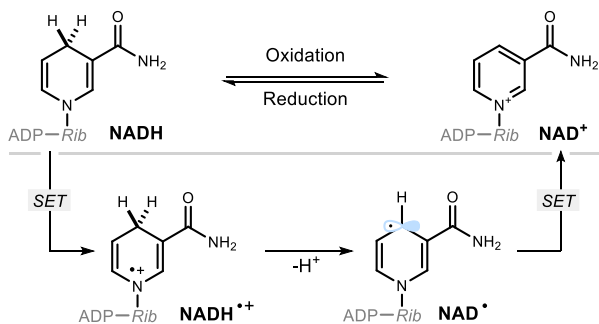

Figure 4.18. The two oxidation states of NAD and intermediacy of NAD$^\bullet$ in on-electron processes. Rib: ribose; ADP: adenine diphosphate.

---

[39] (a) Carlson, B. W.; Miller, L. L. "Oxidation of NADH by Ferrocenium Salts, Rate-Limiting One-Electron Transfer" *J. Am. Chem. Soc.,* **1983**, *105*, 7454; (b) Powell, M. F.; Wu, J. C.; Bruice, T. C. "Ferricyanide Oxidation of Dihydropyridines and Analogues" *J. Am. Chem. Soc.,* **1984**, *106,* 3850.

UNIVERSITAT ROVIRA I VIRGILI
PHOTOCHEMISTRY AND ORGANOCATALYSIS FOR RADICAL-BASED CARBON-CARBON BOND-FORMING
PROCESSES
Emilien Le Saux

159

Experimental studies using titration calorimetry and electrochemistry have shown that in this intermediate the spin density is higher at the C4-position.[40]

Pyridinyl radicals can be generated by SET reduction of pyridinium ions. Both sodium metal and electrochemical reduction have been used to generate the pyridinyl radical (Figure 4.19.a), and when a C4-ester substituted *N*-alkyl pyridinium salt is reduced, the subsequent pyridinyl radical is stable enough to be isolated by distillation.[41] In 1973 Fessenden reported the detection of the simple pyridinyl radical **III** by electron paramagnetic resonance (EPR) spectroscopy (Figure 4.19.b).[42] From the measured hyperfine coupling constants, the electronic distribution for each atom could be calculated, which showed that the C4-position, in analogy to NAD•, is the position with the greatest spin density.
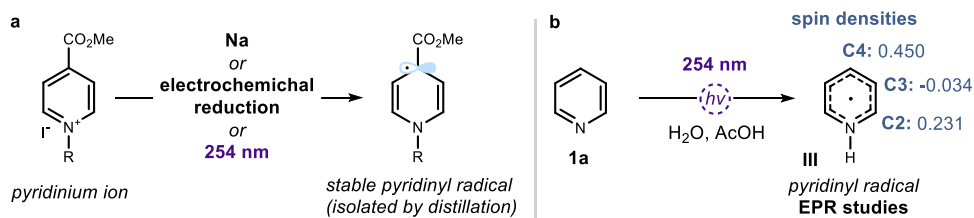

Figure 4.19. Early studies on pyridinyl radicals. (**a**) Reduction of pyridinium ions; (**b**) EPR studies and experimental spin density values on the pyridinyl radical **III**.

4.3 Design and target of the project

The development of the project discussed in this chapter was motivated by the idea to expand the radical strategies available to directly functionalize pyridines and other azines. Radical C-H functionalization methods are limited to Minisci reactions, which are typically poorly selective.

Specifically, we wondered whether pyridinyl radicals **III** could be used to functionalize unactivated pyridines. This intermediate could be generated in a catalytic process through SET reduction of pyridinium ions **I**. At the outset, we recognized that the catalytic activity of dithiophosphoric acid **A1** discussed in Chapter III makes it a suitable candidate to promote this pathway (Figure 4.20). Indeed, the high acidity[43] and reducing properties of the catalyst

[40] Zhu, X.-Q.; Li, H.-R.; Li, Q.; Ai, T.; Lu, J.-Y.; Yang, Y.; Cheng, J.-P. "Determination of the C4-H Bond Dissociation Energies of NADH Models and Their Radical Cations in Acetonitrile" *Chem. Eur. J.* **2003**, *9*, 871.

[41] Kosower, E. M. "Stable Pyridinyl Radicals" *Top. Curr. Chem.* **1983**, *112*, 117.

[42] Fessenden, R. W.; Neta, P. "ESR Spectra of Radicals Produced by Reduction of Pyridine and Pyrazine" *Chem. Phys. Lett.* **1973**, *18*, 14.

[43] Yang, C.; Xue, X.-S.; Jin, J.-L.; Li, X.; Cheng, J.-P. "Theoretical Study on the Acidities of Chiral Phosphoric Acids in Dimethyl Sulfoxide: Hints for Organocatalysis" *J. Org. Chem.* **2013**, *78*, 7076.

could secure the formation of pyridinium ions **I** from **1a**, and their sequential SET reduction to pyridinyl radicals **III**. In analogy to our previous system, the catalyst could be turned over by generating an allylic radical **IV** from a simple alkene **2** in a HAT event. Radical coupling between **III** and **IV** would afford the dihydropyridine intermediate **XIX** as formal product of the reaction. We surmised that a facile rearomatization step, leading to the C-H allylated pyridine **3**, would occur as non-substituted dihydropyridines are not stable.[44] The reports discussed in sections 4.1 and 4.2.4 on spin density distribution in pyridinyl radicals suggest that the radical coupling step could selectively occur at the C4-position.[9,40,42]
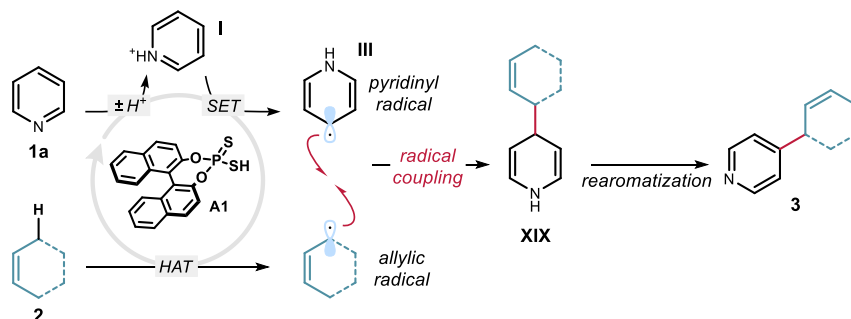

Figure 4.20. Our proposed strategy for pyridinyl radical-mediated C-H allylation of pyridines.

4.4 Results and discussion

4.4.1 Preliminary studies

The Melchiorre group has a strong interest in using light to unveil new excited-state reactivity for catalytic intermediates with an established polar behavior. For instance, electron-rich enamines are nucleophilic in the ground state, but they can act both as donors in photoactive EDA complexes[45] *and* strong reductant upon photoexcitation (see chapter I).[46] An important difference between these two photochemical activation pathways is the wavelength of irradiation. In the first case, blue light (455 nm) is sufficient to excite the EDA complex; but for the direct excitation of enamines, higher energy light is required (405 nm). By analogy, we wondered if dithiophosphoric acid **A1** which also acts as a donor in EDA complexes

---

[44] (a) Stout, D. M.; Meyers, A. I. "Recent Advances in the Chemistry of Dihydropyridines" *Chem. Rev.* **1982**, *82*, 223; (b) Lavilla, R. "Recent Developments in the Chemistry of Dihydropyridines" *J. Chem. Soc., Perkin Trans. 1*, **2002**, 1141.

[45] Arceo, E.; Jurberg, I. D.; Álvarez-Fernández, A.; Melchiorre, P. "Photochemical Activity of a Key Donor-Acceptor Complex Can Drive Stereoselective Catalytic α-Alkylation of Aldehydes" *Nat. Chem.* **2013**, *5*, 750.

[46] Silvi, M.; Arceo, E.; Jurberg, I. D.; Cassani, C.; Melchiorre, P. "Enantioselective Organocatalytic Alkylation of Aldehydes and Enals Driven by the Direct Photoexcitation of Enamines" *J. Am. Chem. Soc.* **2015**, *137*, 6120.

UNIVERSITAT ROVIRA I VIRGILI
PHOTOCHEMISTRY AND ORGANOCATALYSIS FOR RADICAL-BASED CARBON-CARBON BOND-FORMING
PROCESSES
Emilien Le Saux

161

(Chapter III), could potentially turn into a strong reductant upon excitation with more energetic light. This idea was first tested by reproducing an *ipso*-substitution reaction between dicyanobenzene **19** and cyclohexene **2a** originally reported by the MacMillan group using an external photoredox catalyst to reduce **19**.[47] We used **A1** as the sole catalyst instead of the originally used combination of thiol (which served for HAT) and photoredox catalyst. The anion of **A1** absorbs light in the near-UV region, so a wavelength of 365 nm was selected to run this experiment. Upon irradiation, the desired C-H arylation product **20** was formed almost quantitatively, while the use of visible light (455 nm) completely shut down the process (Figure 4.21).
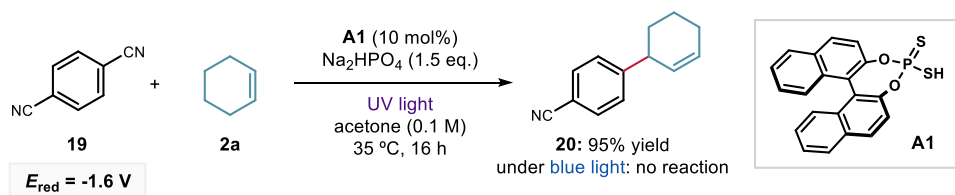

Figure 4.21. Initial discovery of the direct excitation of dithiophosphoric acid **A1**.

After showing in Chapter III that the sulfur anion of **A1** could activate specific substrates by EDA complex formation, this preliminary result indicated that upon UV light excitation the catalyst could also activate substrates that do not engage in EDA complex formation *via* a SET mechanism from an electronically excited state. Cognizant of the two distinct photochemical activation pathways available to catalyst **A1**, we performed preliminary UV-vis studies with our substrate of interest in this Chapter, pyridine **1a** (Figure 4.22). Equimolar mixtures of **A1** with an inorganic base (purple line, absorption of **A1**⁻) and pyridine **1a** (green line) displayed the same absorption profiles, thus excluding the formation of a photoactive ion pair or EDA complex between **A1** and **1a**.[48] Instead, these absorption spectra show that in the presence of pyridine, the catalyst is deprotonated and forms **A1**⁻ which absorbs light up to approximately 370 nm.

[47] Cuthbertson, J. D.; MacMillan, D. W. C. The Direct Arylation of Allylic *sp*³ C-H Bonds via Organic and Photoredox Catalysis. *Nature* **2015**, *519*, 74.

[48] Crisenza, G. E. M.; Mazzarella, D.; Melchiorre, P. "Synthetic Methods Driven by the Photoactivity of Electron Donor–Acceptor Complexes" *J. Am. Chem. Soc.* **2020**, *142*, 5461.
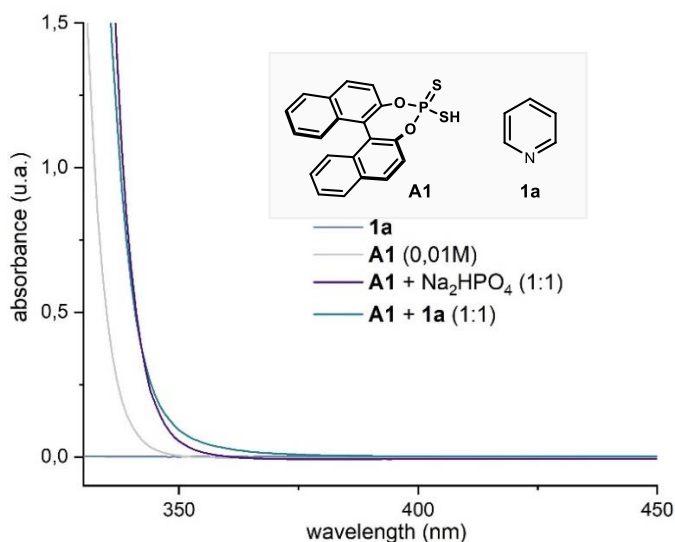
Figure 4.22. Preliminary UV-vis studies.

The notion that the deprotonated catalyst **A1** could absorb in the near-UV region to become a strong SET reductant prompted us to evaluate the feasibility of reducing protonated pyridine, to form the target pyridinyl radical. We probed the need for acidic activation of **1a** using cyclic voltammetry experiments (Figure 4.23). While pyridine **1a** displays an onset of reduction at -1.8 V, pyridinium ion **I** displays a much more favorable and reversible reduction wave at approximately -0.6 V. The reversibility of the SET event suggests that the reduced species, the pyridinyl radical **III**, is kinetically stable.[49]
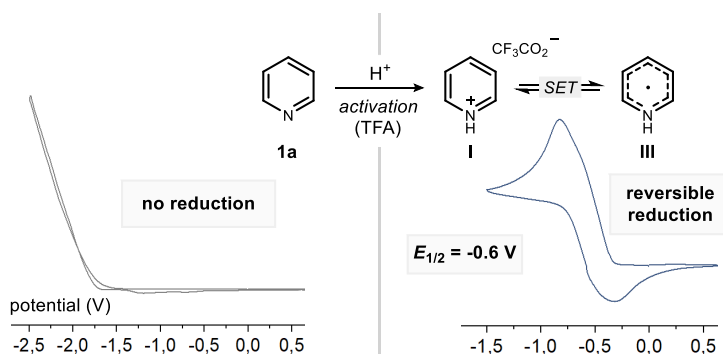

Figure 4.23. Electrochemical studies of pyridine **1a** and pre-formed pyridinium ion **I**. AgCl/Ag reference electrode in CH_3CN.

Considering these preliminary experiments, a plausible mechanism for the desired transformation is shown in Figure 4.24. Protonation of pyridine **1a** by the dithiophosphoric

---

[49] Elgrishi, N.; Rountree, K. J.; McCarthy, B. D.; Rountree, E. S.; Eisenhart, T. T.; Dempsey, J. L. "A Practical Beginner's Guide to Cyclic Voltammetry" *J. Chem. Educ.* **2018**, *95*, 197.

UNIVERSITAT ROVIRA I VIRGILI
PHOTOCHEMISTRY AND ORGANOCATALYSIS FOR RADICAL-BASED CARBON-CARBON BOND-FORMING
PROCESSES
Emilien Le Saux

163

acid catalyst **A** affords pyridinium **I** and the photoactive anion **A⁻**, which reaches a strongly reducing excited state **[A⁻]*** upon absorption of UV light. SET reduction of pyridinium ion **I** by **[A⁻]*** delivers the key pyridinyl radical **III** and sulfur-centered radical **A•**, which is known to undergo exergonic C−H abstraction from cyclohexene derivative **2** to deliver allylic radical **IV**. This HAT step is the turnover event of the catalytic cycle, since it regenerates acid **A**. Radical cross-coupling between **III** and **IV** affords the functionalized pyridine **3** after rearomatization.
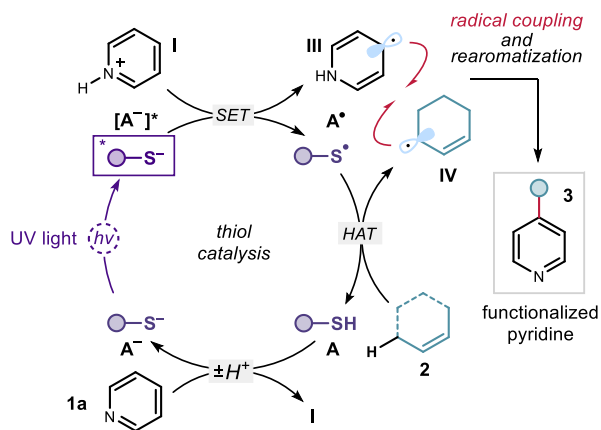

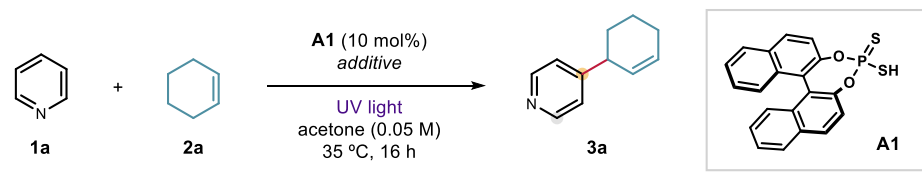**Figure 4.24.** Proposed reaction mechanism.

Here, the dithiophosphoric acid **A** plays three catalytic tasks, sequentially acting as a Brønsted acid for pyridine protonation, as SET reductant for pyridinium ion reduction, and a HAT activator for allylic C-H bonds. This novel mechanism for pyridine functionalization, based on the underexplored reactivity of pyridinyl radical **III**, heralds potential for enabling distinct positional selectivity that diverges from classical Minisci chemistry.

4.4.2 Optimization

We began our studies by selecting simple pyridine **1a** as the model substrate, with cyclohexene **2a** as the allylic radical precursor and dithiophosphoric acid **A1** as the catalyst. After irradiation under 365 nm light for 16 h, the formation of product **3a** was observed in 17% yield with a 8:1 regioisomeric ratio in favor of the C4-adduct over the C2 allylation (Table 4.1, entry 1). Changing the wavelength from UV (365 nm) to less energetic 390 nm or 460 nm light sources shut down the reactivity (entries 2 and 3). We then investigated the effect of additives. An inorganic base slightly increased the overall yield (entry 4), while a tertiary amine base gave no product (entry 5). As demonstrated by cyclic voltammetry studies (Figure 4.23), protonation of pyridine **1a** to the pyridinium ion **I** ($pK_a = 5.3$) is essential to ensure a thermodynamically feasible SET reduction. Therefore, the effect of acids was next evaluated.

Benzoic acid (pK_a = 4.2) was detrimental (entry 6), while the much stronger acid TFA (pK_a = 0.2) completely inhibited the process (entry 7). We found that inclusion of 2,4,6-collidine significantly increased the yield of the reaction from 17% to 41% (entry 8),[50] albeit with a decreased regioselectivity. A substoichiometric amount of collidine provided the same boost in reactivity (entry 9). Control experiments under air and without **A1** afforded no product **3a** (entries 10 and 11). Finally, an attempt at restoring reactivity under blue light using an external photoredox catalyst was successful (entry 12), with product **3a** formed in 47% yield.

Table 4.1. Preliminary optimization campaign.

entry	additive	other variations	yield **3a** (%)[a]	C4:C2[a]
1	-	-	17	8:1
2	-	465 nm	n.d.	n.d.
3	-	390 nm	traces	-
4	Na$_2$HPO$_4$ (1.5 eq.)	-	23	4:1
5	DIPEA (1.5 eq.)	-	n.d.	-
6	benzoic acid (1.5 eq)	-	14	6:1
7	TFA (80 mol%)	-	n.d.	-
8	2,4,6-collidine (1.5 eq.)	-	41	4:1
9	**2,4,6-collidine (50 mol%)**	-	**40**	**4:1**
10	-	O$_2$ atmosphere	n.d.	-
11	-	no catalyst	n.d.	-
12	**4CzIPN (5 mol%)**	**465 nm**	**47**	**4:1**

Reaction performed on a 0.2 mmol scale using 10 equiv. of **2a** under irradiation with a 365 nm EvoluChem LED spotlight. [a]Yields and regioisomeric ratios of **3a** determined by ^{1}H NMR analysis of the crude reaction mixtures using trichloroethylene as the internal standard. 4CzIPN: 1,2,3,5-Tetrakis(carbazol-9-yl)-4,6-dicyanobenzene; n.d.: not detected.

The results from entries 9 and 12 motivated us to pursue further reaction optimization with two sets of conditions: (*i*) under UV light irradiation, and (*ii*) under blue light irradiation using an external photocatalyst. After assessing additives, we turned our attention to the structural evaluation of the dithiophosphoric acid catalyst (Figure 4.25). A series of 3,3'-substituted derivatives of **A1** were synthesized and tested in the reaction. The 1-naphtyl-substituted catalyst **A2** afforded the best results, with **3a** formed in 67% yield with a 6:1 ratio in favor of

---

[50] The role of 2,4,6-collidine as an additive is discussed later in the chapter.

UNIVERSITAT ROVIRA I VIRGILI
PHOTOCHEMISTRY AND ORGANOCATALYSIS FOR RADICAL-BASED CARBON-CARBON BOND-FORMING PROCESSES
Emilien Le Saux

165

the C4 regioisomer.[51] Importantly, after purification by column chromatography, **3a** was obtained as a single regioisomer. We were pleased to observe such selectivity, as a typical Minisci pathway would afford a mixture of mainly C2- along with C4-functionalized pyridines.[6] Other dithiophosphoric acids **A3-7** were all competent in catalyzing the reaction, without outcompeting **A2**. Thiophosphoric acid (**A8**) and imide (**A9**) were ineffective.
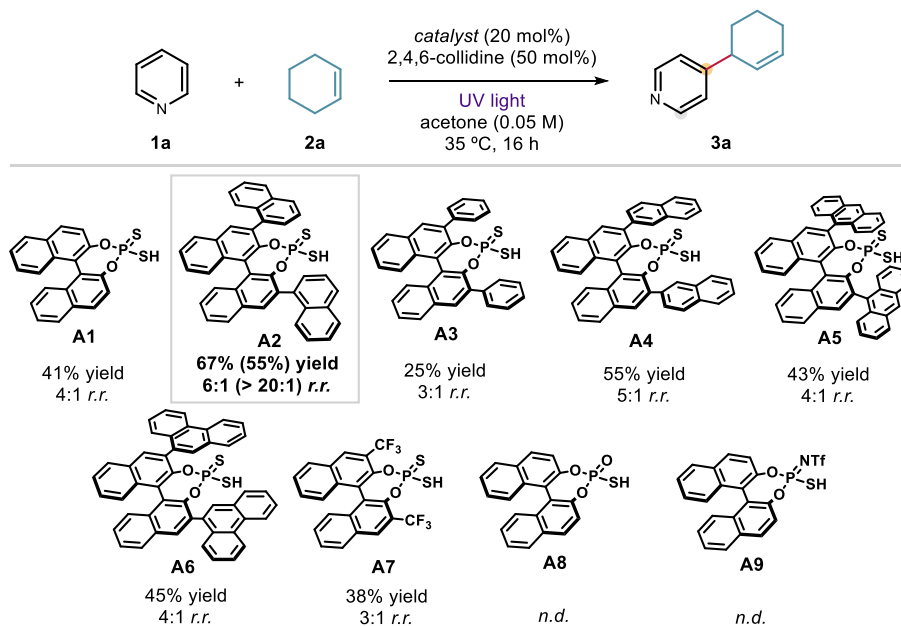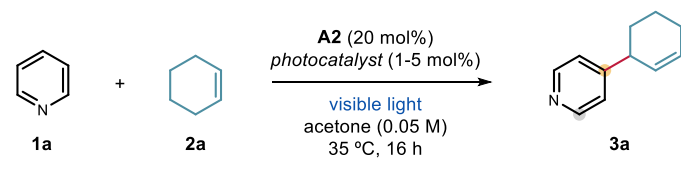

Figure 4.25. Screening of substituted dithiophosphoric acids in the UV light-mediated allylation of pyridine and control experiments with thiophosphoric acid and imide. Reaction performed on a 0.2 mmol scale using 10 equiv. of **2a** under irradiation with a 365 nm EvoluChem LED spotlight. Yields and ratios of regioisomers of **3a** were determined by ^{1}H NMR analysis of the crude reaction mixtures using trichloroethylene as the internal standard. Yields and regioisomeric ratios of isolated **3a** are reported in parentheses. *n.d.:* not detected.

Using catalyst **A2** (10 mol%), different photoredox catalysts were evaluated under blue light irradiation (Table 4.2). Other than 4CzIPN (entry 1), cationic iridium polypyridyl complexes exhibited reactivity (entries 4 and 5), with [(Ir(ppy)$_2$dtbbpy)PF$_6$] being the best performing (**3a** formed in 79% yield and 4:1 selectivity). Although the inclusion of a photoredox catalyst secured a higher chemical yield, the approach based on the direct excitation of the dithiophosphoric acid catalyst **A2** with UV light was taken forward for investigation of the reaction scope.

Conceptually, using a single catalyst to perform several catalytic roles is more interesting, and in this case offered better regioselectivity. For both sets of conditions, acetone was the best solvent, with acetonitrile and DCE delivering the product in <30% yield.

---

[51] A possible rationale for the higher reactivity offered by **A2** in comparison to **A1** is given in section 4.5.2.

Table 4.2. Screening of photoredox catalysts.

entry	photocatalyst	yield **3a** (%)[a]	C4:C2[a]
1	4CzIPN	51	2:1
2	Ir(ppy)$_3$	n.d.	-
3	Mes-Acr$^+$BF$_4^-$	n.d.	-
4	(Ir[dF(CF$_3$)ppy]$_2$(dtbbpy))PF$_6$	23	4:1
5	**(Ir(ppy)$_2$dtbbpy)PF$_6$**	**79 (65)**	**4:1 (> 20:1)**
6[b]	(Ir(ppy)$_2$dtbbpy)PF$_6$	n.d.	-

Reaction performed on a 0.2 mmol scale using 10 equiv. of **2a** under irradiation with a 455 nm 14 W LEDs strip. [a]Yields and ratios of regioisomers of **3a** were determined by ^{1}H NMR analysis of the crude reaction mixtures using trichloroethylene as the internal standard. Yields and regioisomeric ratios of isolated **3a** are reported in parentheses. [b]No **A2**. *n.d.:* not detected.

4.4.3 Generality of the system

Using the optimized conditions highlighted in Figure 4.25, the scope of the C-H allylation process was evaluated (Figure 4.26). *Ortho*-substituted pyridines were converted in good yields and C4-allylated products **3b-c** were isolated exclusively. The introduction of *meta* halogen substituents led to the formation of C4-functionalized pyridines **3d** and **3e** with high regioselectivity. Electron-withdrawing CF$_3$ and CN *meta* substituents were also tolerated, giving the C4 products **3f** and **3g** in good yield. The introduction of a bulkier aryl *meta* substituent caused a switch of regioselectivity in favor of the C6 position (**3i**). The reactivity of niacin (vitamin B3) derivatives was then tested. These substrates afforded products **3j-s** in good yield and a positional preference for C6 functionalization. A series of amino acid nicotinates proved suitable substrates, highlighting the method's potential for the functionalization of complex pyridines (entries **3t-w**). Other azines, including isoquinolines (**3x** and **3y**), pyrimidines (**3z-bb**), and pyridazine (**3cc**), also delivered the allylated products with high regioselectivity and modest yields.
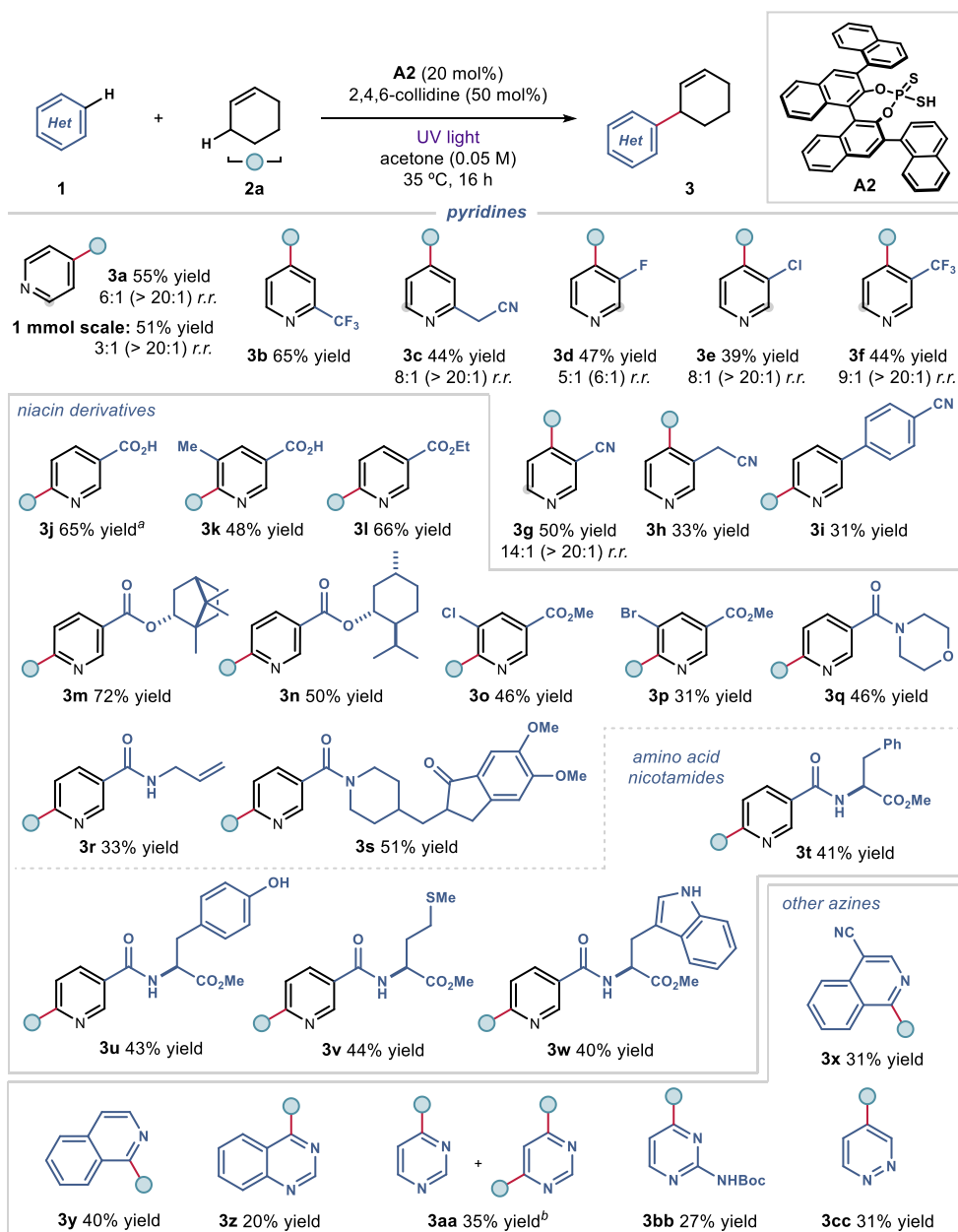
UNIVERSITAT ROVIRA I VIRGILI
PHOTOCHEMISTRY AND ORGANOCATALYSIS FOR RADICAL-BASED CARBON-CARBON BOND-FORMING PROCESSES
Emilien Le Saux

167

Figure 4.26. Scope of azines. Reactions performed on a 0.2 mmol scale using 10 equiv. of **2a**. Yields refer to isolated products **3** after purification. Products **3** were obtained as single regioisomers (>20:1 r.r.), unless otherwise stated. When more than one regioisomer was observed, the minor site of functionalization is highlighted by a gray circle. In these cases, the regioisomeric ratio (*r.r.*) of the crude mixture is specified, and the *r.r.* after isolation is reported in parentheses. When applicable, *d.r.* was ~1:1. [a]Yield determined by ^{1}H NMR analysis. [b]Using the visible light conditions described in Table 4.2 entry 5. Boc: *tert*-butyloxycarbonyl.

Next, we turned our attention to the direct functionalization of pharmaceuticals (Figure 4.27).

The *ortho*-substituted pyridine *Bisacodyl* (stimulant laxative drug) afforded the C4-allylated

product in moderate yield (product **3dd**). Three niacin derivatives, *i.e. Nicoboxil* (rubefacient), *Picamilon* (dietary supplement), and *Etofibrate* (hypolipidemic agent) were successfully functionalized in good yields with exclusive C6 regioselectivity (products **3ee-gg**). Finally, the pyrimidine-based *Voriconazole* (antifungal) afforded the C4-allylated adduct in synthetically useful yields (product **3hh**).
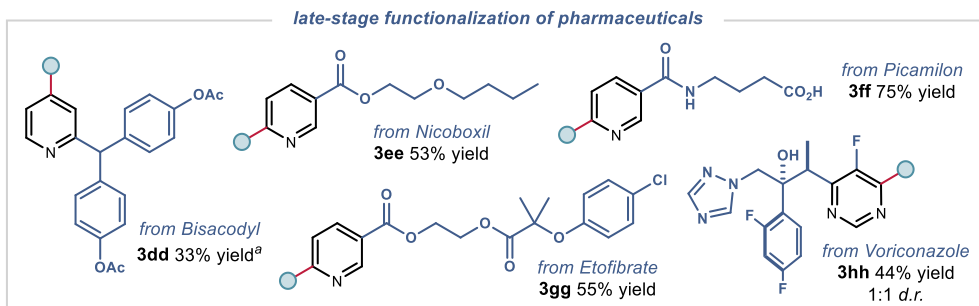

Figure 4.27. C-H allylation of pharmaceuticals. Reactions performed on a 0.2 mmol scale using 10 equiv. of **2a**. Yields refer to isolated products **3** after purification. Products **3** were obtained as single regioisomers (>20:1 r.r.). [a]Using the visible light conditions described in Table 4.2 entry 5.

We then evaluated other allylic C-H partners that could serve as radical precursors for the functionalization of 2-CF$_3$ pyridine **1b** (Figure 4.28). Cyclic alkenes of different ring sizes and substitution patterns afforded the desired products with complete C4-positional selectivity (products **3ii-mm**). Tetramethylethylene (**3nn**) and heterocycles, including dihydropyran (**3oo**) and a protected piperidine (**3pp**), were also suitable allylic precursors. Finally, benzylic precursors such as tetrahydronaphtalene and acenaphthylene were successfully reacted, affording adducts **3qq** and **3rr**, respectively.
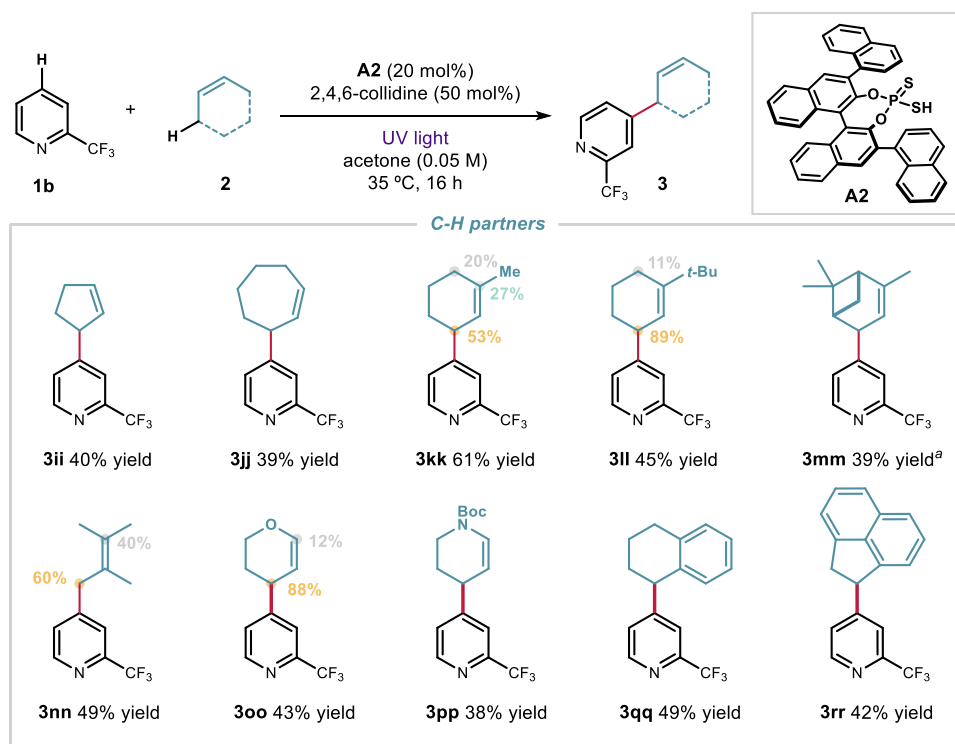
UNIVERSITAT ROVIRA I VIRGILI
PHOTOCHEMISTRY AND ORGANOCATALYSIS FOR RADICAL-BASED CARBON-CARBON BOND-FORMING
PROCESSES
Emilien Le Saux

169

Figure 4.28. Scope of C-H partners **2**. Reactions performed on a 0.2 mmol scale using 10 equiv. of **2**. Yields refer to isolated products **3** after purification. Products **3** were obtained as single regioisomers (> 20:1 r.r.), unless otherwise stated. When applicable, *d.r.* was ~1:1. [a]Yield determined by ^{1}H NMR analysis. Boc: *tert*-butyloxycarbonyl.

4.4.4 Limitations

In spite of the good reactivity offered by various substrates, the protocol does have some limitation with respect to the scope of pyridines and allylic C-H substrates (Figure 4.29). A general trend we observed is that pyridines bearing electron-donating substituents (by inductive or mesomeric effects) are poorly reactive. Conjugated substituents or halogens at the C2-position are not suitable either. Finally, when using C4-substituted pyridines, C2-functionalization did not occur.

The scope of allylic C-H partner was mostly limited to cyclic allylic and benzylic substrates, with the exception of tetramethylethylene. Linear alkenes, or more nucleophilic radicals from benzyl methyl ether or tetrahydroisoquinoline were not suitable. Simple THF or benzaldehyde did not afford any product either.
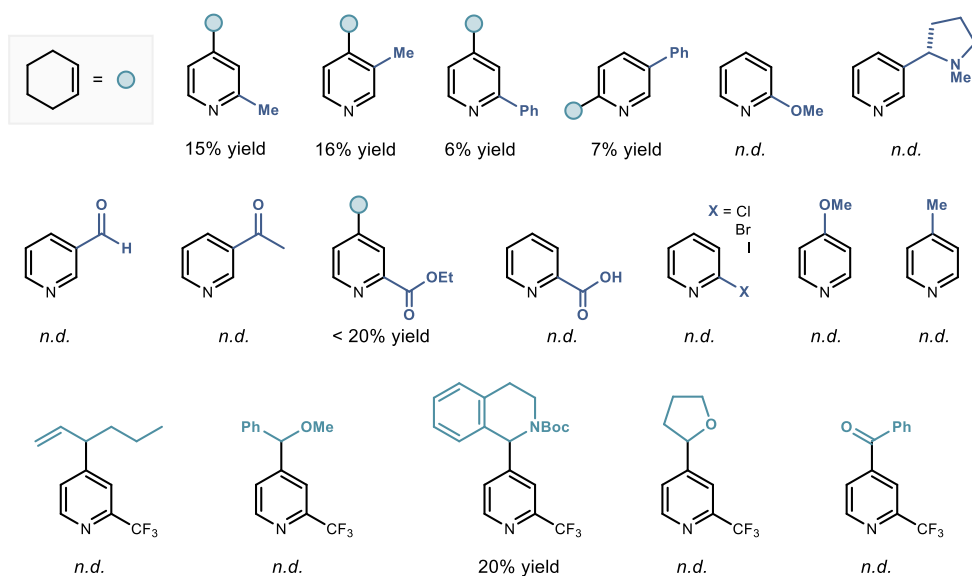
Figure 4.29. Moderately successful and unsuccessful substrates. Yields were determined by ^{1}H NMR analysis using trichloroethylene as the internal standard. *n.d.*: not detected.

4.5 Mechanistic investigations

4.5.1 Origin of regioselectivity

The origin of regioselectivity in the pyridine functionalization path could be rationalized on the spin density distribution of the key pyridinyl radicals, with radical coupling occurring preferentially at the position exhibiting the greatest localization of the electron. We evaluated the electronic properties of the pyridinyl radical **III** with DFT calculations, performed using uB3LYP/6-31G+(d) level of theory. Greater spin density was found at C4 compared to the C2 position (Figure 4.30), which is in agreement with the spin densities inferred by EPR hyperfine coupling constants of **III**.[42] Natural bond orbital (NBO) analysis revealed that the singly occupied molecular orbital (SOMO) is localized preferentially at the C4 position. These results are coherent with the experimentally observed C4 positional selectivity.

For all pyridines, greater spin density is found at C4, however nicotinic acid derivatives all afforded the C6-products. For these compounds, the difference between the C4- and C6-spin densities is not as large as for other pyridines, probably due to conjugation effects from the C3-carbonyl system. However, the strongly electron-withdrawing cyano group at the pyridine C3-position afforded the C4-regioisomer, unlike the nicotinic acid derivatives. The main difference compared to nicotinic esters is the size of the cyano group, which is much smaller than the methyl ester, e.g., steric factors: $A(CN) = 0.17$ against $A(CO_2Me) = 1.23$. For other azines (isoquinoline, pyridimidine and pyridazine), the spin densities are consistent with the

UNIVERSITAT ROVIRA I VIRGILI
PHOTOCHEMISTRY AND ORGANOCATALYSIS FOR RADICAL-BASED CARBON-CARBON BOND-FORMING
PROCESSES
Emilien Le Saux

171

observed product distribution. Overall, the selectivity seems to arise from an interplay between electronics and sterics.
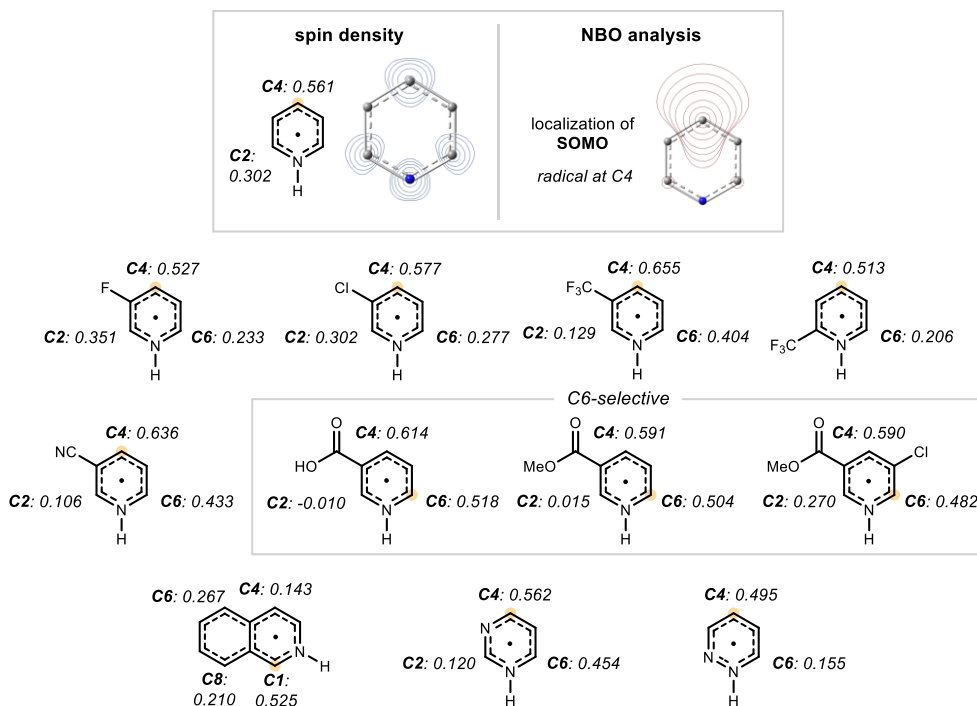

Figure 4.30. Calculated spin densities for representative examples from the scope. The major reactive sites are highlighted by a yellow circle.

4.5.2 Photophysical studies

To better understand the excited-state chemistry of dithiophosphoric acids, we characterized the excited state of **A2⁻** using photophysical studies. These experiments were essential to a better understanding of the overall reaction mechanism.

Estimation of the excited-state potential of A2⁻

The excited-state potential of **A2⁻** could be estimated using the Rehm-Weller equation (Figure 4.31, Equation 1).[52] This value was calculated from the ground-state potential $E(\mathbf{A2}^\bullet/\mathbf{A2}^-)$ measured by cyclic voltammetry (CV) and the excited-state energy $E_{00}([\mathbf{A2}^-]^*/\mathbf{A2}^-)$, which

---

[52] Buzzetti, L.; Crisenza, G. E. M.; Melchiorre, P. "Mechanistic Studies in Photocatalysis" *Angew. Chem., Int. Ed.* **2019**, *58*, 3730.

could be estimated by including the long wavelength tail of the absorption spectrum (λ_{tail}, obtained spectroscopically) into Equation 2 (Figure 4.31). [53]
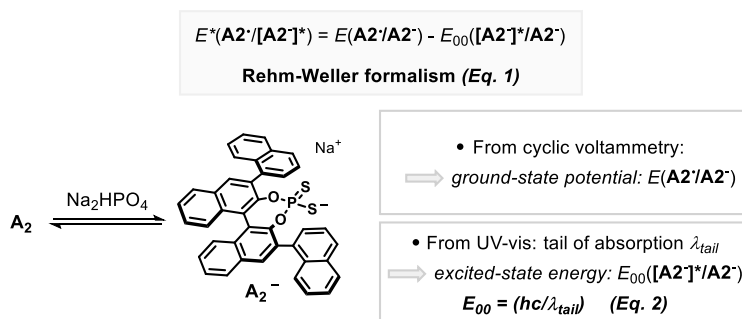

$$E^*(\textbf{A2}^{\cdot}/[\textbf{A2}^-]^*) = E(\textbf{A2}^{\cdot}/\textbf{A2}^-) - E_{00}([\textbf{A2}^-]^*/\textbf{A2}^-)$$

Rehm-Weller formalism *(Eq. 1)*

• From cyclic voltammetry:
ground-state potential: $E(\textbf{A2}^{\cdot}/\textbf{A2}^-)$

• From UV-vis: tail of absorption λ_{tail}
excited-state energy: $E_{00}([\textbf{A2}^-]^*/\textbf{A2}^-)$
$$E_{00} = (hc/\lambda_{tail}) \quad \textit{(Eq. 2)}$$

Figure 4.31. Determination of the excited-state potential of **A2**$^-$ using the Rehm-Weller equation. **A2**$^-$ was formed by mixing **A2** with 1 equiv. of Na$_2$HPO$_4$ followed by filtration. h: Planck's constant.

$E(\textbf{A2}^\bullet/\textbf{A2}^-) = 1.12$ V was measured by CV. Using UV-vis spectroscopy, λ_{tail} was found at 370 nm, which translates into an excited-state energy $E_{00}([\textbf{A2}^-]^*/\textbf{A2}^-) = 3.350$ V.

Using these data, the following potential was calculated for the excited anion of **A2** using Equation 1:

$$E^*(\textbf{A2}^\bullet/[\textbf{A2}^-]^*) = 1.12 - 3.35 = \textbf{-2.23 V} \text{ (vs AgCl/Ag)}$$

This value indicates that SET reduction of pyridinium **I** to the pyridinyl radical **III** by **[A2**$^-$**]*** is highly exergonic ($E_{1/2}$(**I/III**) = -0.6 V).

Transient Absorption Spectroscopy (TAS)[54]

Excited states are reached upon light absorption and are transient in character. The lifetime of an excited state (τ_0) is usually very short and cannot be observed with classical experimental methods that require rather long detection times. Measurement of τ_0 is useful for interpreting photochemical reaction mechanisms, and may support hypotheses based on how likely the excited-state species is to engage in bimolecular processes (SET or EnT, for example). The experimental technique that is usually employed to measure the lifetime of an excited species is *transient absorption spectroscopy* (TAS), also called *flash photolysis*. Two measuring methods can be used: (*i*) the spectrographic mode to record the absorption spectrum of the transient species, and (*ii*) the kinetic mode to observe the decay of the excited state over time at a given wavelength. This second mode is the one that was used to measure the lifetime of **[A2**$^-$**]***. In a typical experiment, a solution of **A2**$^-$ in acetone was irradiated with a short and intense light pulse. The light emitted by the sample, which contained the excited species, was

---

[53] Details about CV and UV-vis studies can be found in the experimental section.
[54] Balzani, V., Ceroni, P., Juris, A. "Photochemistry and Photophysics: Concept, Research and Applications" Weinheim, Wiley-VCH, 2014.

UNIVERSITAT ROVIRA I VIRGILI
PHOTOCHEMISTRY AND ORGANOCATALYSIS FOR RADICAL-BASED CARBON-CARBON BOND-FORMING
PROCESSES
Emilien Le Saux

173

then recorded and compared to the signal before excitation. The variation of optical density (ΔOD) was measured as a function of time and plotted in Figure 4.32. The excited state of **A2⁻** displayed a first-order exponential decay with a half-life of approximately **½ τ_0 = 5 µs**.

This value indicates that **[A2⁻]*** is sufficiently long-lived to engage in bimolecular photochemical processes.
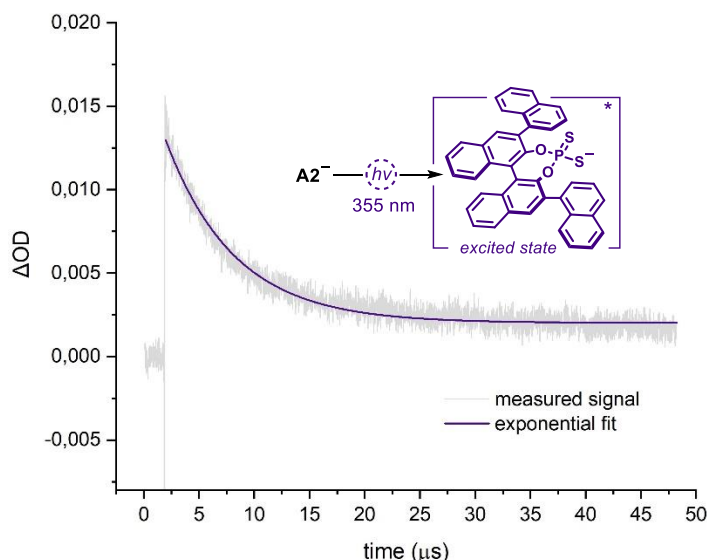
Figure 4.32. Absorption at 625 nm of the transient excited state of **A2⁻** generated upon excitation with a 355 nm laser. A first order exponential fit (purple line) was applied to the signal to facilitate the lifetime measurement. ΔOD: optical density variation.

In an additional TAS experiment, we attempted to measure the lifetime of the excited state of the unsubstituted catalyst **A1**. Wavelengths from 400 nm to 700 nm were inspected, down to 10 ns scale, but no signal was detected. This result suggests that the 3,3'-substituents significantly increase the excited state lifetime of the dithiophosphoric acid catalyst, thus facilitating productive SET with pyridinium ions **I**.

Luminescence quenching studies

Cognizant of the ability of **[A2⁻]*** to engage in a bimolecular process, we aimed at collecting evidence in support of our initial mechanistic hypothesis: that is, **[A2⁻]*** could engage in an exergonic SET with pyridinium **I**. To this end, we performed Stern-Volmer quenching studies. In Chapter II, the concept of dynamic quenching was introduced: this is experimentally quantified by measuring a decrease in emission of the excited species. This decrease is due to depopulation of the excited state, for instance because of a bimolecular SET event from the excited state. The linear relationship between I_0/I (I and I_0 are the luminescence intensities at a selected wavelength with and without quencher respectively) and the concentration of quencher in solution is reminded (Equation 3).

$$I_0/I = 1 + k_q\tau_0[Q] = 1 + K_{SV}[Q] \qquad \textbf{(Eq. 3)}$$

where k_q is the kinetic constant of the quenching process, while τ_0 is the excited-state lifetime in the absence of quencher. The product $k_q\tau_0$ is usually referred to as the Stern-Volmer constant, K_{SV}.

The preformed salts **A2·Et₃N** and **1a·HCl** were used so that the species in solution were **A2⁻** and **I**. The emission of the excited state of **A2⁻** was first recorded, by dissolving **A2·Et₃N** in thoroughly degassed acetone, and irradiating with 350 nm light (Figure 4.33).
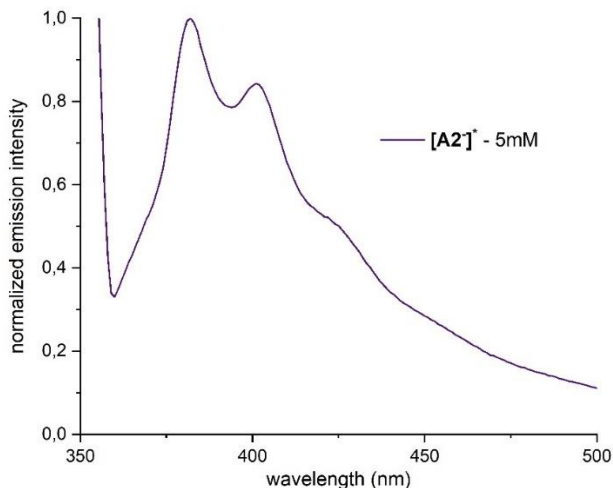
Figure 4.33. Normalized emission of **[A2⁻]*** upon irradiation at 350 nm of a 5 mM **A2·Et₃N** solution in acetone.

Emission quenching studies of the excited state of **A2⁻** were performed using pyridinium salt **I** as the quencher. Experimentally, a 5×10^{-3} M solution of **A2·Et₃N** in thoroughly degassed acetone was used. Sequential addition of a solution of **1a·HCl** resulted in sequential decrease in emission intensity (Figure 4.34, left panel). The Stern-Volmer plot was constructed (Figure 4.34, right panel), which highlighted a linear correlation between I_0/I and **[I]**. From this data, a Stern-Volmer constant of $K_{SV} = \textbf{346 M}^{-1}$ was determined.

No change in the absorption spectrum of ground-state **A2⁻** was observed upon additions of **I**, thus excluding a possible ground-state association between these two species, which would lead to a decrease in emission intensity.

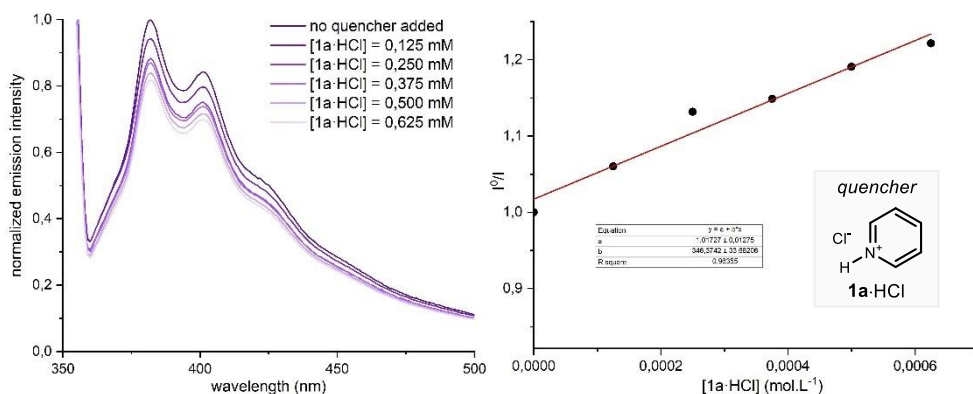UNIVERSITAT ROVIRA I VIRGILI
PHOTOCHEMISTRY AND ORGANOCATALYSIS FOR RADICAL-BASED CARBON-CARBON BOND-FORMING PROCESSES
Emilien Le Saux

175

Figure 4.34. Quenching of **A2**⁻emission (5×10^{-3} M in acetone) in the presence of increasing amounts of pyridinium **I**.

Under the same conditions, the effect of collidinium **XX** as a quencher was evaluated using 2,4,6-collidine hydrochloride. As shown in Figure 4.35, quenching was observed as well, with a Stern-Volmer constant $K_{SV} = \mathbf{283\ M^{-1}}$.
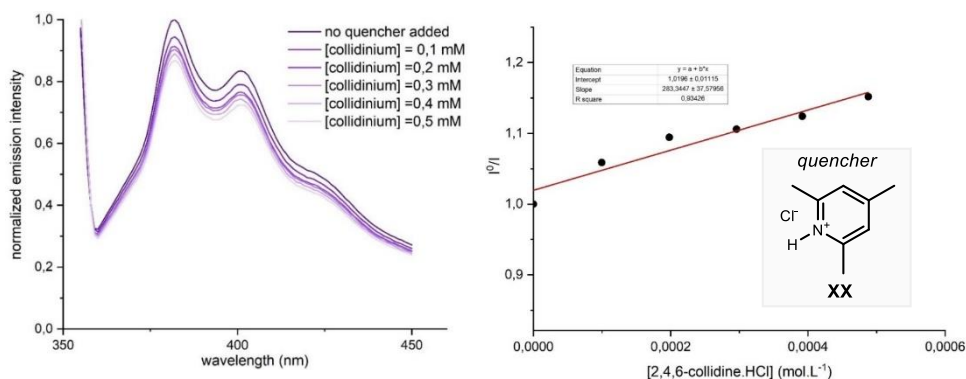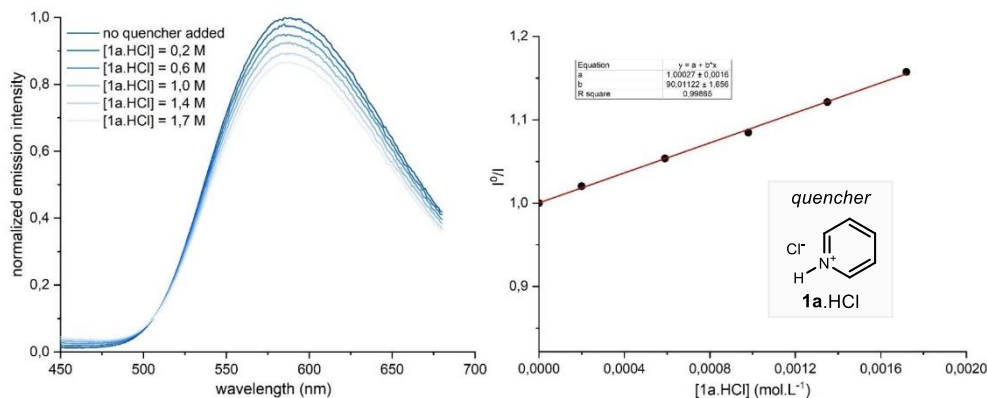

Figure 4.35. Quenching of **A2**⁻emission (5×10^{-3} M in acetone) in the presence of increasing amounts of collidinium **XX**.

These results indicate that both pyridinium ion **I** and collidinium **XX** can quench the excited state of **A2**⁻, therefore confirming the feasibility of an SET event taking place. The value of the Stern-Volmer constants suggests a faster quenching with **I**, although they are in the same order of magnitude. The role of collidine in the process will be discussed later (section 4.5.4).

Since the reaction can also be performed under blue light irradiation with an external photoredox catalyst, luminescence quenching studies under these conditions were performed. Upon irradiation of a 5×10^{-6} M solution of [(Ir(ppy)₂dtbbpy)PF₆] in thoroughly degassed acetone with a 390 nm light, emission of the photocatalyst was detected with a maximum around 600 nm. Sequential addition of a solution of **1a·HCl** caused a decrease in emission intensity (Figure 4.36, left panel). The Stern-Volmer plot was constructed (Figure 4.36, right

panel) and highlighted a linear correlation between I_0/I and [**I**]. From this data, a Stern-Volmer constant of $\boldsymbol{K_{SV}} = \textbf{90 M}^{\textbf{-1}}$ was determined. The quenching constant $\boldsymbol{k_q} = \textbf{1.6} \cdot \textbf{10}^{\textbf{8}} \textbf{ M}^{\textbf{-1}} \cdot \textbf{s}^{\textbf{-1}}$ was calculated considering the lifetime of [(Ir(ppy)$_2$dtbbpy)PF$_6$] in the excited state (0.557 μs).[55]

No change in the absorption spectrum of [(Ir(ppy)$_2$dtbbpy)PF$_6$] was observed upon additions of **I**, thus excluding a possible ground-state association between these two species, which would lead to a decrease in emission intensity.

Figure 4.36. Quenching of [(Ir(ppy)$_2$dtbbpy)PF$_6$]emission (5 × 10^{-6} M in acetone) in the presence of increasing amounts of pyridinium **I**.

4.5.3 Formation of the pyridinyl radical

Additional spectroscopic and synthetic mechanistic experiments were undertaken to identify the key pyridinyl radical **III** and understand the role of 2,4,6-collidine.

Electron Paramagnetic Resonance (EPR)[56]

EPR spectroscopy, also known as electron spin resonance (ESR) spectroscopy, is related to NMR spectroscopy but it serves for the detection of unpaired electrons in open-shell species. Instead of chemical shifts in ppm, the magnetic field strength expressed in Gauss (G) constitutes the *x*-axis. The Zeeman coupling factor *g* is a constant that characterizes the property of an electron in a defined environment, and appears in the following Equation 4:

$$h\nu = g\beta H \qquad \textbf{(Eq. 4)}$$

[55] Wu, Y.; Kim, D.; Teets, T., S. "Photophysical Properties and Redox Potentials of Photosensitizers for Organic Photoredox Transformations" *Synlett*, **2022**, *33*, 1154.

[56] McMillan, J. A. "Electron Paramagnetic Resonance of Free Radicals" *J. Chem. Educ.* **1961**, *38*, 438.

UNIVERSITAT ROVIRA I VIRGILI
PHOTOCHEMISTRY AND ORGANOCATALYSIS FOR RADICAL-BASED CARBON-CARBON BOND-FORMING PROCESSES
Emilien Le Saux

177

with h Planck's constant, ν the microwave frequency, β the Bohr magneton constant, and H the magnetic field.

Determining the *g*-factor is one of the main objectives of EPR spectroscopy as it characterizes the chemical environment of a radical. Since ν and H are controlled by the operator, *g* can be deduced from Equation 4. The micro-environment of the electron is also influenced by neighboring fields, which results in *hyperfine* coupling, and these constants can be measured to further elucidate the environment of the unpaired electron.

To confirm the formation of pyridinyl radical **III** under irradiation with **A2**, we recorded the EPR spectrum of a 5:1 mixture of **1a**/**A2** before and after 15 min of irradiation at 77 K (Figure 4.37). The experimental setup is shown in Figure 4.37, left panel. After irradiation, a signal was detected with a calculated **g-value of 2.00324**, which is in accordance with the literature for the same radical.[42] This result indicates that the proposed pyridinyl radical **III** can indeed be generated from simple pyridine **1a** using photochemical activation of **A2**. The hyperfine coupling constants could not be calculated due to the poor resolution of the spectrum.
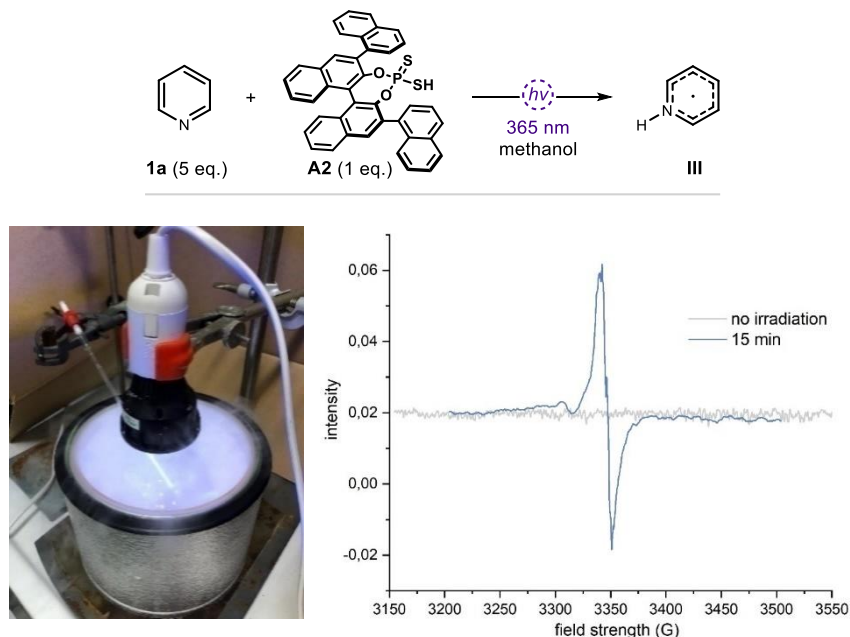
Figure 4.37. Experimental setup for the EPR experiment (*left*) and measured EPR spectra of a 5:1 mixture of **1a** and **A2** in methanol before and after 15 min of irradiation (*right*).

Radical-clock experiments

Taken together, the quenching and EPR experiments show that, upon photoexcitation, **A2⁻** can reduce pyridinium ion **I** to the pyridinyl radical **II**. We also wanted to get direct proof that the pyridinyl radical **III** is indeed formed *under the reaction conditions*. Therefore, we conducted the radical-clock experiments detailed in Figure 4.38, where we used tailored

pyridine substrates. Both C4- and C2- cyclopropyl pyridines (**21a** and **21b**) underwent ring opening under the standard conditions to give products **22a** and **22b** in 51% and 45% yield, respectively. The formation of these products is consistent with the intermediacy of **III**, which, upon ring opening to a highly stabilized benzylic radical **XXI**,[57] can undergo radical coupling with allylic radical **IV**.
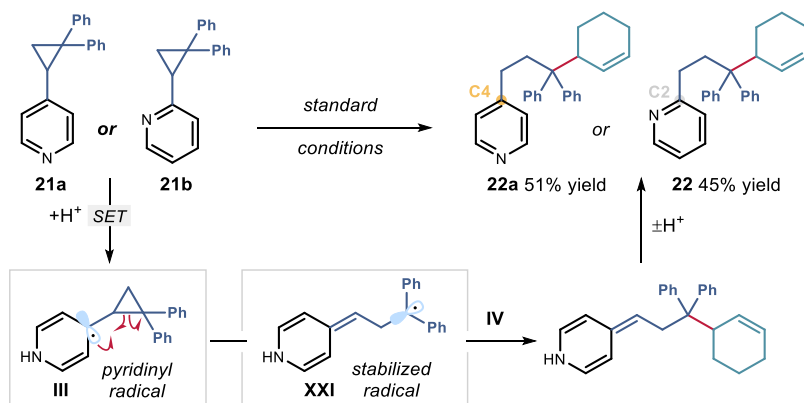

Figure 4.38. Probing the formation of pyridinyl radicals **III** under the reaction conditions.

4.5.4 Discussion on the role of collidine

The precise role of 2,4,6-collidine in the reaction is still unclear, but preliminary results allowed us to formulate a hypothesis. As for pyridine, collidine exhibited no reduction down to -2.5 V, while a reversible reduction wave was observed for the collidinium salt **XX** at -0.6 V (Figure 4.39).
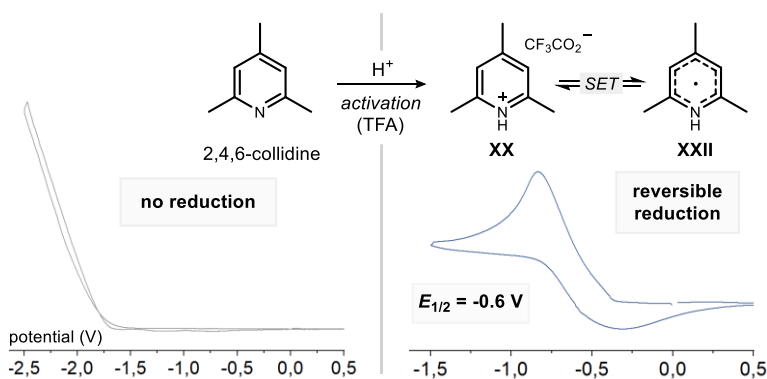
Figure 4.39. Electrochemical studies using collidine and pre-formed collidinium **XX**. AgCl/Ag reference electrode in CH_3CN.

---

[57] Griller, D.; Ingold, K. U. "Free-Radical Clocks" *Acc. Chem. Res*. **1980**, *13*, 317.

UNIVERSITAT ROVIRA I VIRGILI
PHOTOCHEMISTRY AND ORGANOCATALYSIS FOR RADICAL-BASED CARBON-CARBON BOND-FORMING
PROCESSES
Emilien Le Saux

179

Overall, collidine behaves in a similar way to pyridine **1a**, as demonstrated by quenching and cyclic voltammetry studies. However, radical coupling of **XXII** with an allylic radical **IV** is likely hampered by the steric profile of the methyl groups at *ortho* and *para* positions, thus avoiding any by-product formation. This led us to believe that collidine may act as an electron shuttle in the reaction (Figure 4.40). Accordingly, if **XXII** was to be formed, it could not couple with an allylic radical **IV** because of steric hindrance, but it could deliver an electron to pyridinium ion **I** to generate the productive intermediate radical **III**. Similar electron shuttling from Hantzsch pyridine has been proposed previously.[58]
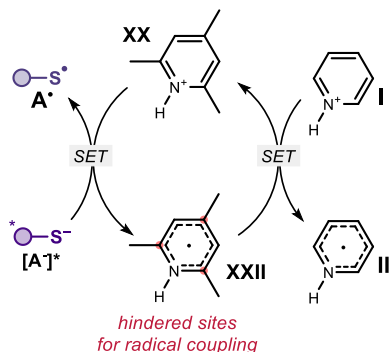
Figure 4.40. Possible role of collidine as a redox mediator.

4.5.5 Rearomatization of the dihydropyridine intermediate

As depicted in Figure 4.41, the formal product of the reaction is dihydropyridine **XIX**. However, this product was never observed directly in the course of this study. This section details a series of experiments performed to understand how the dihydropyridine **XIX** rearomatizes to the final product **3a**. An early observation was that isopropanol was formed during the reaction, most likely coming from reduction of the solvent: acetone. Thus, we concluded that acetone plays the role of an oxidant in the reaction, but the process through which **XIX** is oxidized needed clarification.

---

[58] Bieszczad, B.; Perego, L. A.; Melchiorre, P. "Photochemical C-H Hydroxyalkylation of Quinolines and Isoquinolines" *Angew. Chem. Int. Ed*. **2019**, *58*, 16878.
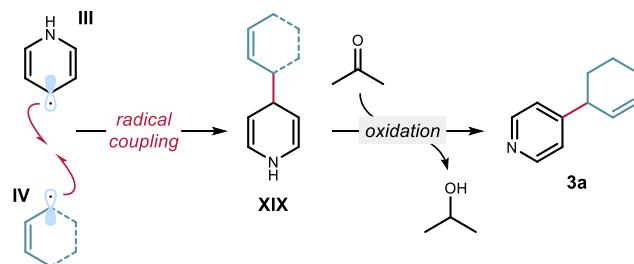
Figure 4.41. Oxidation of **XIX** by acetone and formation of isopropanol.

While the direct reduction of acetone by the excited state of **[A2⁻]*** is not thermodynamically favored (for cyclohexanone E_{red} = -2.33 V vs SCE < E_{red}^*(**A2⁻**) = -2.23 V),[59] the SET event leading to the formation of the ketyl radical **XXIV** is feasible for protonated acetone **XXIII**.[60] The resulting thiyl radical could then abstract the C4 hydrogen atom from the dihydropyridine intermediate **XIX** ((BDE (S-H) = 83.3 kcal mol^{-1} for **A1**, and for NADH analogues BDE(C4-H) ~ 69 kcal mol^{-1}).[40] After HAT events, the ketyl (**XXIV**) and pyridinyl (**XXV**) radicals would ultimately afford isopropanol and the final product (Figure 4.42).
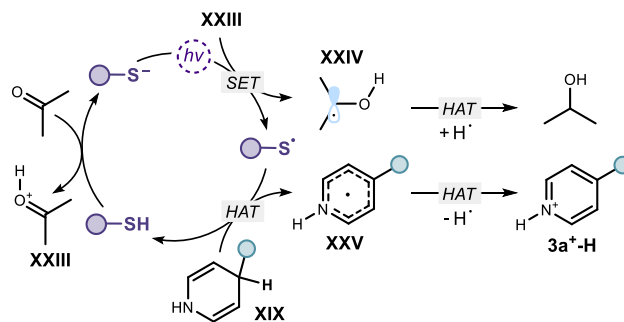
Figure 4.42. Tentative explanation for the re-aromatization of **XIX**.

This scenario was tested by submitting a stable dihydropyridine derivative, 9,10-dihydroacridine **23**, to the reaction conditions (Figure 4.43.a). Full consumption of the starting material was observed, along with the formation of acridine **24** in 60% yield and isopropanol in 40% yield. In the absence of light or catalyst, no conversion of **23** was observed. In order to confirm that the excited catalyst could reduce acetone, an experiment was conducted, excluding both 9,10-dihydroacridine and 2,4,6-collidine (Figure 4.43.b). 7% of dimer **25** and 17% of *i*-PrOH were formed during the reaction. The formation of isopropanol under these conditions supports the ability of the excited **A2⁻** to reduce acetone.

---

[59] Roth, H. G.; Romero, N. A.; Nicewicz, D. A. "Experimental and Calculated Electrochemical Potentials of Common Organic Molecules for Applications to Single-Electron Redox Chemistry" *Synlett*, **2016**, *27*, 714.

[60] Tarantino, K. T.; Liu, P.; Knowles, R. R. Catalytic Ketyl-Olefin Cyclizations Enabled by Proton-Coupled Electron Transfer. *J. Am. Chem. Soc*. **2013**, *135*, 10022.
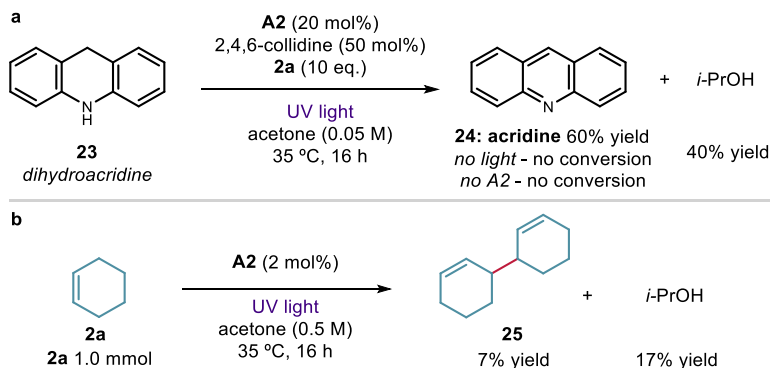
UNIVERSITAT ROVIRA I VIRGILI
PHOTOCHEMISTRY AND ORGANOCATALYSIS FOR RADICAL-BASED CARBON-CARBON BOND-FORMING
PROCESSES
Emilien Le Saux

181

Figure 4.43. (**a**) Oxidation of 9,10-dihydroacridine and reduction of acetone under the reaction conditions. (**b**) Reduction of acetone to isopropanol by [A2$^-$]*.

4.6 Conclusions

In this chapter, we described the development of a new radical strategy for the C-H functionalization of pyridines and related azines, which harnesses the reactivity of previously overlooked intermediates: pyridinyl radicals. This photochemical process relies on the direct excitation of a dithiophosphoric acid catalyst with UV light, which accesses a strongly reducing excited state. The catalyst plays three tasks, sequentially acting as a Brønsted acid for pyridine protonation, a SET reductant for pyridinium ion reduction, and a HAT abstractor for the activation of allylic C-H bonds. The functionalization step relies on a highly regioselective coupling between pyridinyl and allylic radicals. Preliminary investigations indicate that the selectivity arises from an interplay between the spin density distribution in the pyridinyl radical, and steric effects. Extensive photophysical and mechanistic studies allowed us to identify and characterize the key intermediates of the transformation.

4.7 Experimental section

General information. The ^{1}H NMR, ^{19}F NMR, ^{13}C NMR spectra and UPC^2 traces are available in the literature[1] and are not reported in the present dissertation.

The NMR spectra were recorded at 300 MHz, 400 MHz and 500 MHz for ^{1}H or at 75 MHz, 101 MHz and 126 MHz for ^{13}C, 376 MHz for ^{19}F, 162 MHz for ^{31}P, respectively. The chemical shifts (δ) for ^{1}H and ^{13}C{^{1}H} are given in ppm relative to residual signals of the solvents (CHCl$_3$ @ 7.26 ppm ^{1}H NMR, 77.00 ppm ^{13}C NMR). Coupling constants are given in Hz. The following abbreviations are used to indicate the multiplicity: s, singlet; d, doublet; t, triplet; q, quartet; m, multiplet; br s, broad signal.

High-resolution mass spectra (HRMS) were obtained from the ICIQ High-Resolution Mass Spectrometry Unit on MicroTOF Focus and Maxis Impact (Bruker Daltonics) with electrospray ionization or atmospheric pressure chemical ionization. Cyclic voltammetry (CV) studies were carried out on a Princeton Applied Research PARSTAT 2273 potentiostat offering compliance voltage up to $\pm$ 100 V (available at the counter electrode), $\pm$ 10 V scan range and $\pm$ 2 A current range. UV-vis measurements were carried out on a Shimadzu UV-2401PC spectrophotometer equipped with photomultiplier detector, double beam optics and D2 and W light sources. The emission spectra were recorded using a Fluorolog Horiba Jobin Yvon spectrofluorimeter equipped with a photomultiplier detector, a double monochromator, and a 350W xenon light source.

Yield of isolated products refer to materials of > 95% purity as determined by ^{1}H NMR analysis.

General Procedures. All reactions were set up under an argon atmosphere in oven-dried glassware using standard Schlenk techniques, unless otherwise stated. Synthesis grade solvents were used as purchased. Anhydrous solvents were taken from a commercial SPS solvent dispenser. Chromatographic purification of products was accomplished using flash column chromatography (FC) on silica gel (35-70 mesh). For thin layer chromatography (TLC) analysis throughout this work, Merck precoated TLC plates (silica gel 60 GF$_{254}$, 0.25 mm) were used, using UV light as the visualizing agent and either phosphomolybdic acid in EtOH, or basic aqueous potassium permanganate (KMnO$_4$), and heat as developing agents. Organic solutions were concentrated under reduced pressure on a Büchi rotary evaporator (*in vacuo* at 40 ºC, ~5 mbar).

Determination of Diastereomeric Ratio. The diastereomeric ratios were determined by ^{1}H NMR analysis of the isolated materials through integration of diagnostic signals, or by UPC^2 analysis on chiral stationary phase using a Waters Acquity instrument. The exact conditions for the analyses are specified within the characterization section.

UNIVERSITAT ROVIRA I VIRGILI
PHOTOCHEMISTRY AND ORGANOCATALYSIS FOR RADICAL-BASED CARBON-CARBON BOND-FORMING
PROCESSES
Emilien Le Saux

183

Materials. Commercial grade reagents and solvents were purchased at the highest commercial quality from Sigma Aldrich, Fluka, Acros Organics, Fluorochem, or Alfa Aesar and used as received, unless otherwise stated. Catalysts **A1-7** were prepared from the corresponding (*S*)-(−)-1,1'-Bi(2-naphtol) using the procedure described in Chapter III. Thiophosphoric acid **A8** and imide **A9** were synthesized following reported procedures.[61]

4.7.1 Substrate synthesis

Most nicotinamides and nicotinic esters were synthesized from nicotinoyl chloride as depicted in Figure 4.44.
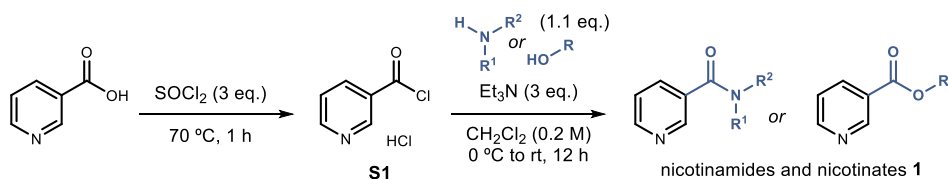
Figure 4.44. Synthesis of nicotinic acid derivatives from nicotinoyl chloride **S1**.

A suspension of nicotinic acid (1.0 equiv.) in thionyl chloride (3.0 equiv.) was stirred at 70 ºC for 1 h. The mixture was cooled-down to room temperature and concentrated under reduced pressure to afford the crude nicotinoyl chloride hydrochloride **S1** as a white solid which was used in the next step without further purification.

To an ice-cold suspension of **S1** (1.0 equiv.) in dichloromethane (0.2 M) was added the amine or alcohol (1.1 equiv.) in portions, followed by dropwise addition of triethylamine (3.0 equiv.). The reaction was allowed to warm-up to room temperature over 12 h. The mixture was washed with water, brine, dried over magnesium sulfate, filtered, and concentrated under reduced pressure. Purification by column chromatography afforded the pure nicotinamides and nicotinates **1**.

The amino acid-derived nicotinamides were prepared using EDCI hydrochloride as a coupling agent (Figure 4.45).

---

[61] Kato, S.; Saga, Y.; Kojima, M.; Fuse, H.; Matsunaga, S.; Fukatsu, A.; Kondo, M.; Masaoka, S.; Kanai, M. "Hybrid Catalysis Enabling Room-Temperature Hydrogen Gas Release from N-Heterocycles and Tetrahydronaphthalenes" *J. Am. Chem. Soc.* **2017**, *139*, 2204.
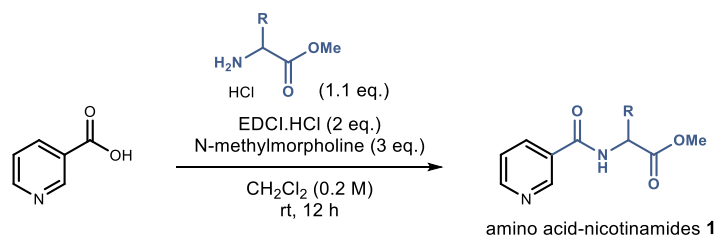
Figure 4.45. Synthesis of amino acid-derived nicotinamides.

To a suspension of nicotinic acid (1.0 equiv.) in dichloromethane (0.2 M) was added EDCI hydrochloride (2.0 equiv.), followed by *N*-methylmorpholine (3.0 equiv.) and the hydrochloride salt of the amino acid methyl ester (1.1 equiv.). The reaction mixture was stirred at room temperature overnight. The mixture was diluted with dichloromethane, washed with water, brine, dried over magnesium sulfate, filtered and concentrated under reduced pressure. Purification by column chromatography afforded the pure nicotinamides **1**.

The substrates for the radical clock experiments **21a** and **21b** were synthesized from the corresponding vinyl pyridines *via* cyclopropanation with diphenyldiazomethane (Figure 4.46).
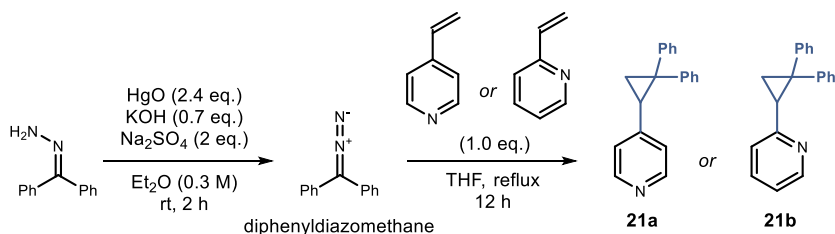
Figure 4.46. Synthesis of radical clock substrates **21a** and **21b**.

Diphenyldiazomethane. To benzophenone hydrazone (2.5 g, 12.7 mmol), anhydrous sodium sulfate (3.62 g, 2 equiv.), yellow mercuric oxide (II) (6.62 g, 2.4 equiv.), and potassium hydroxide (500 mg, 0.7 equiv., in 1 mL EtOH), was added 40 mL (0.3 M) of diethyl ether. The suspension was stirred at room temperature for 2 hours. The reaction mixture was filtered, and the filtrate concentrated under reduced pressure. The resulting dark red oil was dissolved in hexanes at 50 °C and filtered again. The solvent was evaporated under reduced pressure to obtain a dark red oil that was left to freeze overnight. Dark red crystals (2.47 g, quantitative yield) of diphenyldiazomethane formed when warmed-up to room temperature.

(2,2-diphenylcyclopropyl)pyridines) Diphenyldiazomethane (1.17 g, 6.0 mmol) and vinylpyridine (1.0 equiv.) were dissolved in THF (10 mL, 0.6 M). The solution was stirred under reflux overnight. After cooling down to room temperature, the dark solution was diluted with hexanes and filtered to remove the precipitate. The filtrate was concentrated under

UNIVERSITAT ROVIRA I VIRGILI
PHOTOCHEMISTRY AND ORGANOCATALYSIS FOR RADICAL-BASED CARBON-CARBON BOND-FORMING
PROCESSES
Emilien Le Saux

185

reduced pressure and the crude mixture purified by column chromatography to afford the pure (2,2-diphenylcyclopropyl)pyridines.
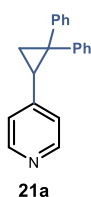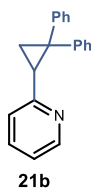

4-(2,2-diphenylcyclopropyl)pyridine (21a) Prepared using 4-vinylpyridine (643 µL, 6.0 mmol). Purification by column chromatography (SiO$_2$, 1:40:59 Et$_3$N/EtOAc/hexanes) afforded **21a** as a light-yellow wax (1.1 g, 65% yield).

^{1}H NMR (400 MHz, CDCl$_3$) δ 8.29 (d, $J = 6.2$ Hz, 2H), 7.31 (d, $J = 4.3$ Hz, 4H), 7.25 – 7.10 (m, 6H), 6.74 (d, $J = 6.2$ Hz, 2H), 2.81 (dd, $J = 8.8$, 6.4 Hz, 1H), 2.05 (dd, $J = 6.4$, 5.5 Hz, 1H), 1.93 (dd, $J = 8.8$, 5.5 Hz, 1H).

^{13}C NMR (101 MHz, CDCl$_3$) δ 148.9, 148.5, 146.0, 139.2, 131.0, 128.5, 128.3, 127.3, 126.8, 126.3, 123.0, 40.8, 31.4, 21.5.

HRMS (ESI$^+$) Calculated for C$_{20}$H$_{18}$N [M+H]$^+$: 272.1434 found: 272.1434.

2-(2,2-diphenylcyclopropyl)pyridine (21b) Prepared using 2-vinylpyridine (645 µL, 6.0 mmol). Purification by column chromatography (SiO$_2$, 1:40:59 Et$_3$N/EtOAc/hexanes) afforded **21b** as a light-yellow wax (1.0 g, 63% yield).

^{1}H NMR (400 MHz, CDCl$_3$) δ 8.35 (ddd, $J = 4.9$, 1.9, 0.9 Hz, 1H), 7.41 – 7.34 (m, 3H), 7.32 – 7.26 (m, 2H), 7.22 – 7.16 (m, 1H), 7.16 – 7.06 (m, 5H), 6.95 (ddd, $J = 7.5$, 4.9, 1.2 Hz, 1H), 6.80 (dt, $J = 7.9$, 1.1 Hz, 1H), 3.13 (dd, $J = 8.7$, 6.5 Hz, 1H), 2.34 (dd, $J = 6.5$, 5.1 Hz, 1H), 1.85 (dd, $J = 8.7$, 5.1 Hz, 1H).

^{13}C NMR (101 MHz, CDCl$_3$) δ 158.4, 148.6, 146.5, 140.2, 135.3, 131.0, 128.3, 127.9, 127.5, 126.2, 126.0, 122.3, 120.6, 40.2, 33.8, 20.3.

HRMS (ESI$^+$) Calculated for C$_{20}$H$_{18}$N [M+H]$^+$: 272.1434 found: 272.1433.
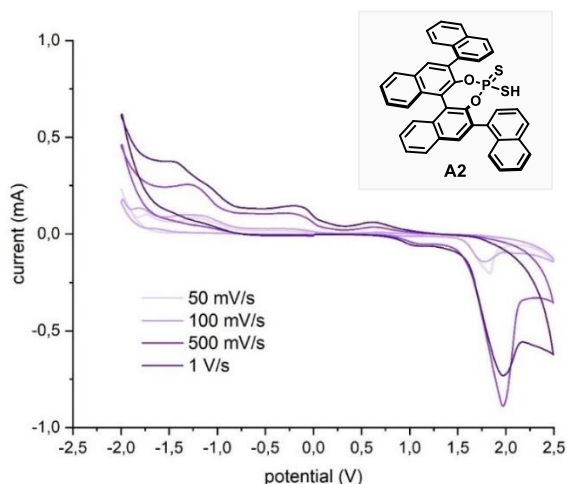
4.7.2 Electrochemical studies

Figure 4.47. Cyclic voltammogram for catalyst **A2** [0.02M] in [0.1 M] TBAPF$_6$ in CH$_3$CN. Measurement started by oxidation from 0 to +2.0 V and finishing at 0 V. Platinum disk working electrode, AgCl/Ag (NaCl 3 M) reference electrode, Pt wire auxiliary electrode. One irreversible oxidation observed at **+1.12 V**.

4.7.3 Absorption spectroscopy analysis

As for **A1**, no EDA complex between **A2** and pyridine **1a** was observed using absorption spectroscopy (Figure 4.48). The tail of absorption of **A2**$^-$ was located at approximately 370 nm (light blue, green, and orange lines).
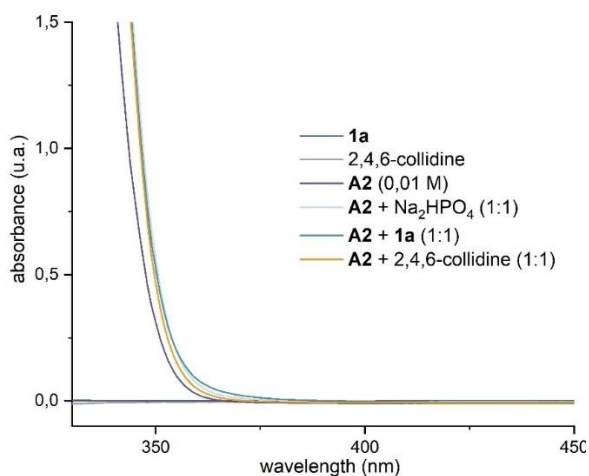
Figure 4.48. Optical absorption spectra of the reaction components under optimized conditions, recorded in acetone.

UNIVERSITAT ROVIRA I VIRGILI
PHOTOCHEMISTRY AND ORGANOCATALYSIS FOR RADICAL-BASED CARBON-CARBON BOND-FORMING
PROCESSES
Emilien Le Saux

187

4.7.4 General procedures for the photochemical reactions
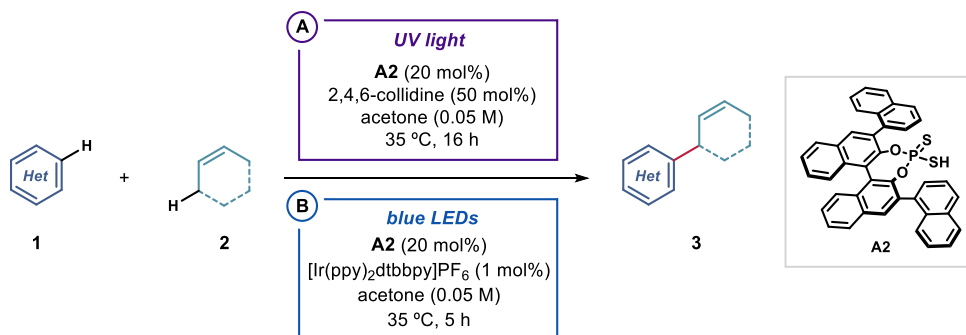
General Procedure A. To an argon-purged glass vial, containing dithiophosphoric acid catalyst **A2** (25.3 mg, 0.04 mmol), and pyridine derivative **1** (0.2 mmol), was added 2,4,6-collidine (13.2 µL, 0.1 mmol), followed by the allylic precursor **2** (2.0 mmol) and argon-sparged HPLC grade acetone (0.05 M). The vial was sealed with Parafilm, and placed in the 365 nm irradiation setup (Figure 4.49, left panel). The reaction was stirred for 16 h, then the solvent was evaporated and the crude mixture purified by flash column chromatography on silica gel to furnish the product **3**

General Procedure B. To an argon-purged glass vial, containing dithiophosphoric acid catalyst **A2** (25.3 mg, 0.04 mmol), [Ir(ppy)$_2$dtbbpy]PF$_6$ (1.8 mg, 2.0 µmol), and pyridine derivative **1** (0.2 mmol), was added the allylic precursor **2** (2.0 mmol) followed by argon-sparged HPLC grade acetone (0.05 M). The vial was sealed with Parafilm, and placed in the 455 nm irradiation setup (Figure 4.49, right panel). The reaction was stirred for 5 h, then the solvent was evaporated and the crude mixture purified by flash column chromatography on silica gel to furnish the product **3**.
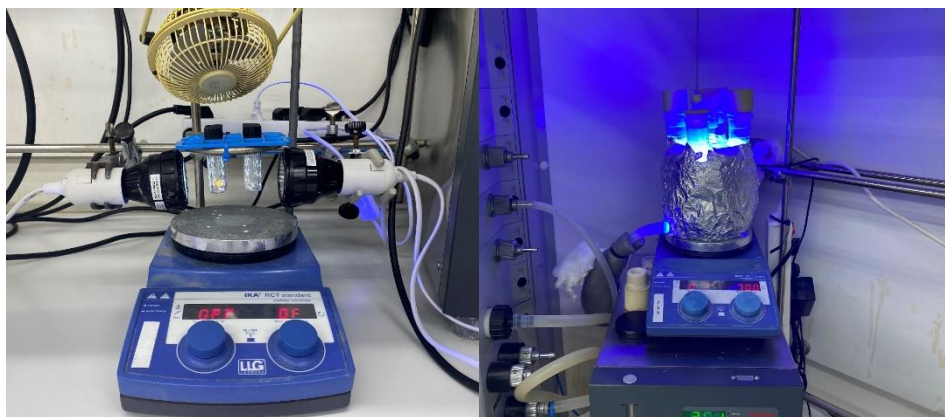
Figure 4.49. UV light (365 nm) setup using EvoluChem PF365 LED spotlights and a fan (*left*). Visible light (455 nm) setup using a 14 W LEDs strip and a minichiller to control the temperature (*right*).

4.7.5 Characterization of products 3
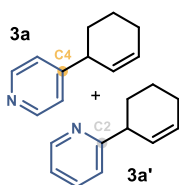
4-(cyclohex-2-en-1-yl)pyridine (3a) + 2-(cyclohex-2-en-1-yl)pyridine (3a')

Prepared according to General Procedure A using pyridine **1a** (16.2 µL, 0.2 mmol) and cyclohexene **2a** (203 µL, 2.0 mmol). The regioisomeric ratio **3a/3a'** (6:1) of the crude mixture was measured by ^{1}H NMR analysis. Purification by column chromatography (SiO$_2$, 1:10:89 Et$_3$N/EtOAc/hexanes) afforded product **3a** as a colorless oil (17.6 mg, 55% yield, > 20:1 *r.r.*). The minor regioisomer **3a'** was not isolated after column chromatography.

^{1}H NMR (400 MHz, CDCl$_3$) δ 8.53 – 8.49 (m, 2H), 7.17 – 7.14 (m, 2H), 5.97 (m, 1H), 5.70 – 5.65 (m, 1H), 3.40 (m, 1H), 2.16 – 2.09 (m, 2H), 2.08 – 1.98 (m, 1H), 1.80 – 1.71 (m, 1H), 1.69 – 1.61 (m, 1H), 1.61 – 1.51 (m, 1H).

^{13}C NMR (126 MHz, CDCl$_3$) δ 155.3, 149.7, 129.7, 128.2, 123.1, 41.1, 31.7, 24.9, 20.8.
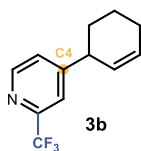

4-(cyclohex-2-en-1-yl)-2-(trifluoromethyl)pyridine (3b)

Prepared according to General Procedure A using 2-(trifluoromethyl)pyridine (23.0 µL, 0.2 mmol) and cyclohexene **2a** (203 µL, 2.0 mmol). No other regioisomer was detected in the crude mixture. Purification by column chromatography (SiO$_2$, 1:5:96 Et$_3$N/EtOAc/hexanes) afforded product **3b** as a colorless oil (29.3 mg, 65% yield, > 20:1 *r.r.*).

^{1}H NMR (500 MHz, CDCl$_3$) δ 8.64 (d, *J* = 5.0 Hz, 1H), 7.56 (d, *J* = 1.6 Hz, 1H), 7.36 (dd, *J* = 5.0, 1.6 Hz, 1H), 6.04 (m, 1H), 5.68 (m, 1H), 3.54 – 3.47 (m, 1H), 2.18 – 2.11 (m, 2H), 2.11 – 2.05 (m, 1H), 1.77 – 1.71 (m, 1H), 1.71 – 1.64 (m, 2H), 1.61 – 1.52 (m, 1H).

^{13}C NMR (126 MHz, CDCl$_3$) δ 157.5, 149.9, δ 148.3 (q, *J* = 34.0 Hz), 130.6, 127.1, 125.8, 119.8 (q, *J* = 2.9 Hz), 41.2, 31.8, 29.7, 24.8, 20.7.

^{19}F NMR (471 MHz, CDCl$_3$) δ -67.9.

HRMS (ESI$^+$) Calculated for C$_{12}$H$_{13}$F$_3$N [M+H]$^+$: 228.0995 found: 228.0988.
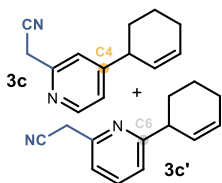
2-(4-(cyclohex-2-en-1-yl)pyridin-2-yl)acetonitrile (3c) + 2-(6-(cyclohex-2-en-1-yl)pyridin-2-yl)acetonitrile (3c')
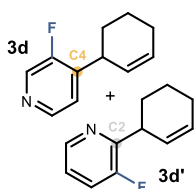
Prepared according to General Procedure A using 2-pyridylacetonitrile (23.6 mg, 0.2 mmol) and cyclohexene **2a** (203 µL, 2.0 mmol). The regioisomeric ratio **3c/3c'** (8:1) of the crude mixture was measured by ^{1}H NMR analysis. Purification by column chromatography (SiO$_2$, 1:50:49

UNIVERSITAT ROVIRA I VIRGILI
PHOTOCHEMISTRY AND ORGANOCATALYSIS FOR RADICAL-BASED CARBON-CARBON BOND-FORMING PROCESSES
Emilien Le Saux

189

Et$_3$N/EtOAc/hexanes) afforded product **3c** as a colorless oil (17.4 mg, 44% yield, > 20:1 *r.r.*). The minor regioisomer **3c'** was not isolated after column chromatography.

^{1}H NMR (500 MHz, CDCl$_3$) δ 8.48 (d, *J* = 5.1 Hz, 1H), 7.30 (s, 1H), 7.14 (dd, *J* = 5.1, 1.6 Hz, 1H), 6.06 – 5.97 (m, 1H), 5.71 – 5.62 (m, 1H), 3.94 (s, 2H), 3.49 – 3.39 (m, 1H), 2.17 – 2.09 (m, 2H), 2.08 – 2.00 (m, 1H), 1.80 – 1.70 (m, 1H), 1.70 – 1.61 (m, 1H), 1.60 – 1.50 (m, 1H).

^{13}C NMR (126 MHz, CDCl$_3$) δ 157.3, 150.4, 149.8, 130.2, 127.6, 122.5, 121.6, 117.2, 41.2, 31.7, 26.6, 24.8, 20.8.

HRMS (ESI$^+$) Calculated for C$_{13}$H$_{15}$N$_2$ [M+H]$^+$: 199.1230 found: 199.1229.

4-(cyclohex-2-en-1-yl)-3-fluoropyridine (3d) + 2-(cyclohex-2-en-1-yl)-3-fluoropyridine (3d')
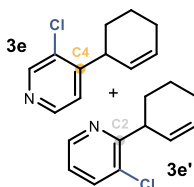
Prepared according to General Procedure A using 3-fluoropyridine (17.2 µL, 0.2 mmol) and cyclohexene **2a** (203 µL, 2.0 mmol). The regioisomeric ratio **3d/3d'** (5:1) of the crude mixture was measured by ^{1}H NMR analysis. Purification by column chromatography (SiO$_2$, 1:4:95 Et$_3$N/EtOAc/hexanes) afforded a mixture of products **3d** and **3d'** as a colorless oil (16.5 mg, 47% yield, 6:1 *r.r.*). An analytically pure sample of **3d** was obtained by preparative TLC (SiO$_2$, 1:4:95 Et$_3$N/EtOAc/hexanes, >20:1 *r.r.*). Only the major product **3d** is described.

^{1}H NMR (400 MHz, CDCl$_3$) δ 8.39 (s, 1H), 8.35 (d, *J* = 4.9 Hz, 1H), 7.21 (dd, *J* = 6.5, 4.9 Hz, 1H), 6.06 – 5.98 (m, 1H), 5.68 – 5.57 (m, 1H), 3.85 – 3.74 (m, 1H), 2.18 – 2.10 (m, 2H), 2.09 – 2.03 (m, 1H), 1.76 – 1.66 (m, 2H), 1.63 – 1.53 (m, 1H).

^{13}C NMR (126 MHz, CDCl$_3$) δ 145.7 (d, *J* = 5.1 Hz), 141.7 (d, *J* = 12.4 Hz), 137.7, 137.5, 130.45, 126.9, 123.8, 33.8, 29.8, 24.8, 20.6.

^{19}F{^{1}H} NMR (471 MHz, CDCl$_3$) δ -59.03, -134.28 (d, *J* = 6.4 Hz).

HRMS (APCI$^+$) Calculated for C$_{11}$H$_{13}$FN [M+H]$^+$: 178.1027 found: 178.1029.
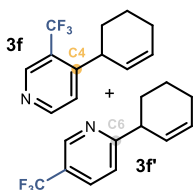

3-chloro-4-(cyclohex-2-en-1-yl)pyridine (3e) + 3-chloro-2-(cyclohex-2-en-1-yl)pyridine (3e')

Prepared according to General Procedure A using 3-chloro pyridine (22.7 mg, 0.2 mmol) and cyclohexene **2a** (203 µL, 2.0 mmol). Purification by column chromatography (SiO$_2$, 1:5:94 Et$_3$N/EtOAc/hexanes) afforded products **3e** + **3e'** (14.9 mg, 39% yield, 8:1 *r.r.*) as a colorless oil. Only the major product **3e** is described.

^{1}H NMR (400 MHz, CDCl$_3$) δ 8.54 (s, 1H), 8.41 (d, J = 5.0 Hz, 1H), 7.21 (d, J = 5.0 Hz, 1H), 6.09 – 6.02 (m, 1H), 5.67 – 5.58 (m, 1H), 3.91 – 3.83 (m, 1H), 2.17 – 2.06 (m, 3H), 1.73 – 1.65 (m, 2H), 1.58 – 1.44 (m, 1H).

^{13}C NMR (101 MHz, CDCl$_3$) δ 152.1, 149.3, 147.7, 131.7, 130.6, 127.2, 123.8, 37.6, 29.1, 24.9, 20.5.

HRMS (ESI$^+$) Calculated for C$_{11}$H$_{13}$ClN [M+H]$^+$: 194.0731 found: 194.0732.

### 4-(cyclohex-2-en-1-yl)-3-(trifluoromethyl)pyridine (3f) + 6-(cyclohex-2-en-1-yl)-3-(trifluoromethyl)pyridine (3f')

Prepared according to General Procedure A using 3-(trifluoromethyl)pyridine (23.0 µL, 0.2 mmol) and cyclohexene **2a** (203 µL, 2.0 mmol). The regioisomeric ratio **3f/3f'** (9:1) of the crude mixture was measured by ^{1}H NMR analysis. Purification by column chromatography (SiO$_2$, 1:4:95 Et$_3$N/EtOAc/hexanes) afforded product **3f** as a colorless oil (20.1 mg, 44% yield, > 20:1 *r.r.*). The minor regioisomer **3f'** was not isolated after column chromatography.

^{1}H NMR (500 MHz, CDCl$_3$) δ 8.84 (s, 1H), 8.70 (d, J = 5.2 Hz, 1H), 7.38 (d, J = 5.2 Hz, 1H), 6.08 – 5.95 (m, 1H), 5.62 – 5.51 (m, 1H), 3.87 – 3.80 (m, 1H), 2.20 – 2.13 (m, 2H), 2.13 – 2.08 (m, 1H), 1.88 – 1.77 (m, 1H), 1.77 – 1.65 (m, 1H), 1.51 – 1.43 (m, 1H).

^{13}C NMR (126 MHz, CDCl$_3$) δ 155.0, 152.9, 146.8 (q, J = 6.5 Hz), 130.0, 127.9, 124.0, 37.6 (d, J = 1.8 Hz), 31.9, 24.7, 21.2.

^{19}F{^{1}H} NMR (376 MHz, CDCl$_3$) δ -59.1, -59.1.

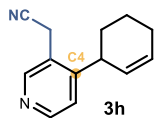HRMS (ESI$^+$) Calculated for C$_{12}$H$_{13}$F$_3$N [M+H]$^+$: 228.0995 found: 228.0987.
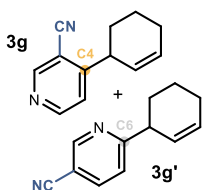
4-(cyclohex-2-en-1-yl)nicotinonitrile (3g) + 6-(cyclohex-2-en-1-yl)nicotinonitrile (3g')

Prepared according to General Procedure A using nicotinonitrile (20.8 mg, 0.2 mmol) and cyclohexene **2a** (203 µL, 2.0 mmol). The regioisomeric ratio **3g/3g'** (14:1) of the crude mixture was measured by ^{1}H NMR analysis. Purification by column chromatography (SiO$_2$, 1:4:95 Et$_3$N/EtOAc/hexanes) afforded product **3g** as a colorless oil (18.0 mg, 50% yield, > 20:1 *r.r.*). The minor regioisomer **3g'** was not isolated after column chromatography.

^{1}H NMR (400 MHz, CDCl$_3$) δ 8.81 (s, 1H), 8.69 (d, J = 5.3 Hz, 1H), 7.34 (d, J = 5.2 Hz, 1H), 6.10 – 6.05 (m, 1H), 5.63 – 5.58 (m, 1H), 3.86 – 3.80 (m, 1H), 2.20 – 2.11 (m, 3H), 1.76 – 1.67 (m, 2H), 1.58 – 1.49 (m, 1H).

^{13}C NMR (101 MHz, CDCl$_3$) δ 159.0, 153.2, 152.9, 131.6, 126.1, 123.0, 116.0, 110.1, 39.9, 30.9, 24.8, 20.7.

UNIVERSITAT ROVIRA I VIRGILI
PHOTOCHEMISTRY AND ORGANOCATALYSIS FOR RADICAL-BASED CARBON-CARBON BOND-FORMING PROCESSES
Emilien Le Saux

191

HRMS (APCI$^+$) Calculated for C$_{12}$H$_{13}$N$_2$ [M+H]$^+$: 185.1073 found: 185.1075.

2-(4-(cyclohex-2-en-1-yl)pyridin-3-yl)acetonitrile (3h)

Prepared according to General Procedure A using 3-pyridylacetonitrile (21.3 µL, 0.2 mmol) and cyclohexene **2a** (203 µL, 2.0 mmol) prolonging the reaction time to 48 hours. No other regioisomer was detected in the crude mixture. Purification by column chromatography (SiO$_2$, 1:9:90 Et$_3$N/EtOAc/hexanes) afforded product **3h** as a colorless oil (13.0 mg, 33% yield, > 20:1 *r.r.*).

^{1}H NMR (400 MHz, CDCl$_3$) δ 8.50 (d, *J* = 2.4 Hz, 1H), 7.64 (dd, *J* = 8.1, 2.4 Hz, 1H), 7.25 (d, *J* = 8.1 Hz, 1H), 6.00 – 5.93 (m, 1H), 5.81 – 5.75 (m, 1H), 3.74 (s, 2H), 3.64 – 3.57 (m, 1H), 2.17 – 2.04 (m, 3H), 1.79 – 1.63 (m, 3H).

^{13}C NMR (101 MHz, CDCl$_3$) δ 153.6, 150.2, 150.1, 130.7, 127.5, 124.2, 123.5, 117.2, 37.8, 30.5, 24.8, 21.0, 18.8.

HRMS (ESI$^+$) Calculated for C$_{13}$H$_{15}$N$_2$ [M+H]$^+$: 199.1230 found: 199.1233.
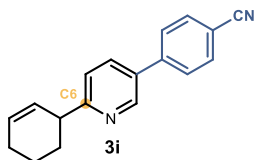

4-(6-(cyclohex-2-en-1-yl)pyridin-3-yl)benzonitrile (3i)

Prepared according to General Procedure A using 4-(pyridin-3-yl)benzonitrile **1i** (36.0 mg, 0.2 mmol) and cyclohexene **2a** (203 µL, 2.0 mmol).). No other regioisomer was detected in the crude mixture. Purification by column chromatography (SiO$_2$, 1:10:89 Et$_3$N/EtOAc/hexanes) afforded product **3i** as a white solid (16.1 mg, 31% yield, > 20:1 *r.r.*).

^{1}H NMR (400 MHz, CDCl$_3$) δ 8.81 (dd, *J* = 2.5, 0.9 Hz, 1H), 7.84 (dd, *J* = 8.1, 2.5 Hz, 1H), 7.80 – 7.76 (m, 2H), 7.72 – 7.68 (m, 2H), 7.35 (dd, *J* = 8.1, 0.8 Hz, 1H), 6.04 – 5.97 (m, 1H), 5.89 – 5.81 (m, 1H), 3.72 – 3.64 (m, 1H), 2.20 – 2.09 (m, 3H), 1.88 – 1.63 (m, 3H).

^{13}C NMR (101 MHz, CDCl$_3$) δ 165.9, 147.7, 142.5, 134.9, 132.8, 132.3, 129.4, 128.2, 127.6, 122.0, 118.7, 111.6, 43.8, 30.7, 25.0, 21.1.

HRMS (ESI$^+$) Calculated for C$_{18}$H$_{17}$N$_2$ [M+H]$^+$: 261.1386 found: 261.1398.
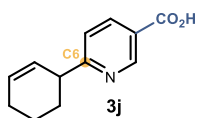
6-(cyclohex-2-en-1-yl)nicotinic acid (3j)

Prepared according to General Procedure A using nicotinic acid (24.6 mg, 0.2 mmol) and cyclohexene **2a** (203 µL, 2.0 mmol). No other regioisomer was detected in the crude mixture. The yield (65%, single regioisomer) of **3j** was inferred by ^{1}H NMR analysis of the crude reaction mixture using trichloroethylene as the internal standard. A 92% pure sample of **3j** (estimated by ^{1}H NMR integration) was obtained after purification by column chromatography (SiO$_2$, 1:4:95 AcOH/MeOH/CH$_2$Cl$_2$ as an off-white solid.

^{1}H NMR (400 MHz, MeOD) δ 9.10 (d, J = 1.4 Hz, 1H), 8.40 (dd, J = 8.2, 2.2 Hz, 1H), 7.51 (d, J = 8.2 Hz, 1H), 6.06 (dtd, J = 9.9, 3.7, 2.3 Hz, 1H), 5.88 – 5.79 (m, 1H), 3.73 (tq, J = 5.6, 2.8 Hz, 1H), 2.30 – 2.11 (m, 3H), 1.92 – 1.70 (m, 3H).

^{13}C NMR (101 MHz, MeOD) δ 169.3, 166.6, 149.6, 138.3, 129.4, 127.1, 125.0, 121.8, 43.7, 30.2, 24.5, 20.7.

HRMS (ESI$^+$) Calculated for $C_{12}H_{14}NO_2$ [M+H]$^+$: 204.1019 found: 204.1028.
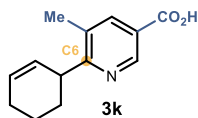
6-(cyclohex-2-en-1-yl)-5-methylnicotinic acid (3k)

Prepared according to General Procedure A using 5-methylnicotinic acid (27.4 mg, 0.2 mmol) and cyclohexene **2a** (203 μL, 2.0 mmol). No other regioisomer was detected in the crude mixture. Purification by column chromatography (SiO$_2$, 1:49:50 AcOH/EtOAc/hexanes) afforded product **3k** as a white solid (21.0 mg, 48% yield, > 20:1 *r.r.*).

^{1}H NMR (400 MHz, MeOD) δ 8.86 (d, J = 2.1 Hz, 1H), 8.14 (dd, J = 2.1, 0.9 Hz, 1H), 5.97 – 5.90 (m, 1H), 5.70 – 5.63 (m, 1H), 3.95 – 3.88 (m, 1H), 2.45 (s, 3H), 2.17 (ddd, J = 12.7, 6.1, 3.0 Hz, 2H), 2.07 – 1.99 (m, 1H), 1.90 (ddd, J = 11.9, 5.4, 2.9 Hz, 1H), 1.80 – 1.62 (m, 2H).

^{13}C NMR (101 MHz, MeOD) δ 168.4, 148.4, 140.9, 133.0, 129.7, 129.1, 41.8, 30.0, 25.8, 22.9, 18.6.

HRMS (ESI$^-$) Calculated for $C_{13}H_{14}NO_2$ [M-H]$^+$: 216.1030 found: 216.1027.
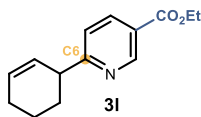
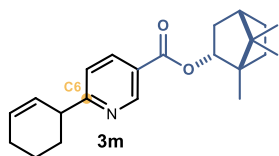**ethyl 6-(cyclohex-2-en-1-yl)nicotinate (3l)**

Prepared according to General Procedure A using ethyl nicotinate (27.3 μL, 0.2 mmol) and cyclohexene **2a** (203 μL, 2.0 mmol). No other regioisomer was detected in the crude mixture. Purification by column chromatography (SiO$_2$, 1:5:94 Et$_3$N/EtOAc/hexanes) afforded product **3l** as a yellowish oil (30.4 mg, 66% yield, > 20:1 *r.r.*).

^{1}H NMR (400 MHz, CDCl$_3$) δ 9.13 (dd, J = 2.2, 0.9 Hz, 1H), 8.19 (dd, J = 8.2, 2.2 Hz, 1H), 7.26 (dd, J = 8.2, 0.9 Hz, 1H), 5.95 (dtd, J = 9.8, 3.7, 2.2 Hz, 1H), 5.80 – 5.75 (m, 1H), 4.38 (q, J = 7.1 Hz, 2H), 3.67 – 3.61 (m, 1H), 2.17 – 2.02 (m, 3H), 1.79 – 1.60 (m, 3H), 1.38 (t, J = 7.1 Hz, 3H).

^{13}C NMR (101 MHz, CDCl$_3$) δ 169.9, 165.4, 150.6, 137.4, 129.5, 127.8, 123.9, 121.3, 61.1, 44.1, 30.5, 24.8, 21.0, 14.2.

HRMS: (ESI$^+$) calculated for $C_{14}H_{18}NO_2$ [M+H$^+$]: 232.1332, found 235.1326.

UNIVERSITAT ROVIRA I VIRGILI
PHOTOCHEMISTRY AND ORGANOCATALYSIS FOR RADICAL-BASED CARBON-CARBON BOND-FORMING PROCESSES
Emilien Le Saux

193

1,7,7-trimethylbicyclo[2.2.1]heptan-2-yl 6-(cyclohex-2-en-1-yl)nicotinate (3m)

Prepared according to General Procedure A using 1,7,7-trimethylbicyclo[2.2.1]heptan-2-yl nicotinate **1m** (52.0 mg, 0.2 mmol) and cyclohexene **2a** (203 µL, 2.0 mmol). No other regioisomer was detected in the crude mixture. Purification by column chromatography (SiO$_2$, 2:98 EtOAc/hexanes) afforded product **3m** as a colorless oil (49.0 mg, 72% yield, > 20:1 *r.r.*).

[underline]1H NMR[/underline] (500 MHz, CDCl$_3$) δ 9.19 (dd, *J* = 2.2, 0.8 Hz, 1H), 8.22 (dd, *J* = 8.2, 2.2 Hz, 1H), 7.29 (dd, *J* = 8.2, 0.9 Hz, 1H), 5.99 – 5.95 (m, 1H), 5.80 – 5.77 (m, 1H), 5.13 – 5.10 (m, 1H), 3.68 – 3.65 (m, 1H), 2.47 (dddd, *J* = 13.5, 9.9, 4.7, 3.3 Hz, 1H), 2.15 – 2.04 (m, 4H), 1.84 – 1.63 (m, 5H), 1.44 – 1.36 (m, 1H), 1.32 – 1.24 (m, 1H), 1.10 (ddd, *J* = 13.8, 3.5, 1.3 Hz, 1H), 0.96 (s, 3H), 0.90 (d, *J* = 4.8 Hz, 6H).

[underline]13C NMR[/underline] (126 MHz, CDCl$_3$) δ 170.0, 165.8, 150.8, 137.6, 129.6, 128.0, 124.5, 121.6, 81.0, 49.3, 48.0, 45.1, 44.3, 37.0, 30.7, 28.2, 27.5, 25.0, 21.2, 19.8, 19.0, 13.7.

[underline]HRMS[/underline]: (ESI$^+$) calculated for C$_{22}$H$_{30}$NO$_2$ [M+H$^+$]: 340.2271, found 340.2274.
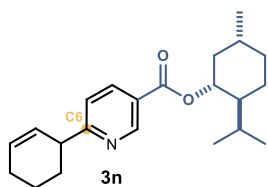
(1R,2S,5R)-2-isopropyl-5-methylcyclohexyl 6-(cyclohex-2-en-1-yl)nicotinate (3n)

Prepared according to General Procedure A using (1R,2S,5R)-2-isopropyl-5-methylcyclohexyl nicotinate **1n** (52.3 mg, 0.2 mmol) and cyclohexene **2a** (203 µL, 2.0 mmol). No other regioisomer was detected in the crude mixture. Purification by column chromatography (SiO$_2$, 1:99 EtOAc/hexanes) afforded product **3n** as a colorless oil (34.0 mg, 50% yield, > 20:1 *r.r.*).

[underline]1H NMR[/underline] (400 MHz, CDCl$_3$) δ 9.14 (dd, *J* = 2.2, 0.9 Hz, 1H), 8.20 (dd, *J* = 8.2, 2.2 Hz, 1H), 7.28 (d, *J* = 0.8 Hz, 1H), 5.99 – 5.94 (m, 1H), 5.80 – 5.75 (m, 1H), 4.93 (td, *J* = 10.9, 4.4 Hz, 1H), 3.68 – 3.62 (m, 1H), 2.14 – 2.06 (m, 4H), 1.96 – 1.88 (m, 1H), 1.80 – 1.65 (m, 6H), 1.58 – 1.51 (m, 2H), 1.17 – 1.05 (m, 2H), 0.91 (dd, *J* = 8.7, 6.8 Hz, 6H), 0.78 (d, *J* = 6.9 Hz, 3H).

[underline]13C NMR[/underline] (101 MHz, CDCl$_3$) δ 170.0, 165.1, 150.7, 137.6 (d1,d2), 129.6 (d1,d2), 128.0, 124.4, 121.6 (d1,d2), 75.4, 47.4, 44.3, 41.1, 34.4, 31.6, 30.7 (d1,d2), 26.7 (d1,d2), 25.0, 23.8(d1,d2), 22.1, 21.2(d1,d2), 20.9, 16.7(d1,d2).

[underline]HRMS[/underline]: (ESI$^+$) calculated for C$_{22}$H$_{32}$NO$_2$ [M+H$^+$]: 342.2428, found 342.2439.
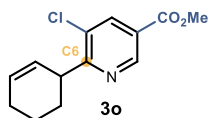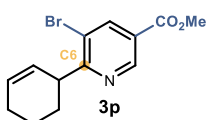
Methyl 5-chloro-6-(cyclohex-2-en-1-yl)nicotinate (3o)

Prepared according to General Procedure A using methyl 5-chloronicotinate (34.3 mg, 0.2 mmol) and cyclohexene **2a** (203 µL, 2.0 mmol). No other regioisomer was detected in the crude mixture. Purification by column

chromatography (SiO$_2$, 1:2:97 Et$_3$N/EtOAc/hexanes) afforded product **3o** as a colorless oil (23.0 mg, 46% yield, > 20:1 *r.r.*).

^{1}H NMR (400 MHz, CDCl$_3$) δ 9.05 (d, *J* = 1.9 Hz, 1H), 8.23 (d, *J* = 1.9 Hz, 1H), 6.03 – 5.96 (m, 1H), 5.77 – 5.70 (m, 1H), 4.17 – 4.09 (m, 1H), 3.94 (s, 3H), 2.24 – 2.05 (m, 3H), 1.93 – 1.85 (m, 1H), 1.77 – 1.64 (m, 2H).

^{13}C NMR (101 MHz, CDCl$_3$) δ 166.5, 165.0, 148.6, 137.9, 130.9, 129.2, 127.5, 125.1, 52.7, 40.6, 28.6, 24.8, 21.8.

HRMS (ESI$^+$) Calculated for C13H15ClNO2 [M+H]$^+$: 252.0786 found: 252.0785.

Methyl 5-bromo-6-(cyclohex-2-en-1-yl)nicotinate (3p)

Prepared according to General Procedure A using methyl 5-bromonicotinate (43.2 mg, 0.2 mmol) and cyclohexene **2a** (203 μL, 2.0 mmol) prolonging the reaction time to 24 hours. No other regioisomer was detected in the crude mixture. Purification by column chromatography (SiO$_2$, 1:2:97 Et$_3$N/EtOAc/hexanes) afforded product **3p** as a colorless oil (18.5 mg, 31% yield, > 20:1 *r.r.*).

^{1}H NMR (400 MHz, CDCl$_3$) δ 9.09 (d, *J* = 1.9 Hz, 1H), 8.41 (d, *J* = 1.9 Hz, 1H), 6.03 – 5.95 (m, 1H), 5.77 – 5.71 (m, 1H), 4.18 – 4.10 (m, 1H), 3.94 (s, 3H), 2.24 – 2.09 (m, 3H), 1.93 – 1.87 (m, 1H), 1.75 – 1.60 (m, 2H).

^{13}C NMR (101 MHz, CDCl$_3$) δ 167.6, 164.8, 149.2, 141.3, 129.1, 127.7, 125.2, 120.9, 52., 42.7, 28.8, 24.8, 21.8.

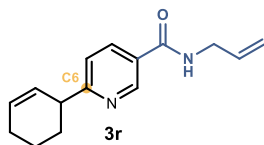HRMS (ESI$^+$) Calculated for C13H15BrNO2 [M+H]$^+$: 296.0281 found: 296.0283.
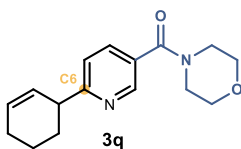
(6-(cyclohex-2-en-1-yl)pyridin-3-yl)(morpholino)methanone (3q)

Prepared according to General Procedure A using morpholino(pyridin-3-yl)methanone **1q** (38.4 mg, 0.2 mmol) and cyclohexene **2a** (203 μL, 2.0 mmol). No other regioisomer was detected in the crude mixture. Purification by column chromatography (SiO$_2$, 1:99 Et$_3$N/EtOAc) afforded product **3q** as a colorless oil (21.6 mg, 40% yield, > 20:1 *r.r.*).

^{1}H NMR (500 MHz, CDCl$_3$) δ 8.62 (d, *J* = 2.4 Hz, 1H), 7.71 (dd, *J* = 8.0, 2.3 Hz, 1H), 7.29 (d, *J* = 8.0, 1H), 6.03 – 5.94 (m, 1H), 5.82 – 5.76 (m, 1H), 3.95 – 3.40 (m, 9H), 2.17 – 2.05 (m, 3H), 1.82 – 1.74 (m, 1H), 1.73 – 1.64 (m, 2H).

^{13}C NMR (126 MHz, CDCl$_3$) δ 168.2, 167.3, 147.6, 135.7, 129.5, 128.6, 128.0, 121.8, 66.8, 44.0, 30.6, 24.9, 21.0.

HRMS (ESI$^+$) Calculated for C$_{16}$H$_{21}$N$_2$O$_2$ [M+H]$^+$: 273.1598 found: 273.1595.

UNIVERSITAT ROVIRA I VIRGILI
PHOTOCHEMISTRY AND ORGANOCATALYSIS FOR RADICAL-BASED CARBON-CARBON BOND-FORMING PROCESSES
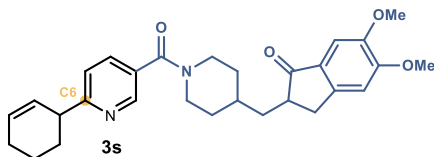Emilien Le Saux

195

N-allyl-6-(cyclohex-2-en-1-yl)nicotinamide (3r)

Prepared according to General Procedure A using *N*-allylnicotinamide **1r** (32.4 mg, 0.2 mmol) and cyclohexene **2a** (203 µL, 2.0 mmol). No other regioisomer was detected in the crude mixture. Purification by column chromatography (SiO$_2$, 1:9:90 Et$_3$N/EtOAc/hexanes to 1:24:75 Et$_3$N/EtOAc/hexanes) afforded product **3r** as a colorless oil (16.0 mg, 33% yield, > 20:1 *r.r.*).

^{1}H NMR (400 MHz, CDCl$_3$) δ 8.90 (dd, *J* = 2.4, 0.9 Hz, 1H), 8.05 (dd, *J* = 8.1, 2.4 Hz, 1H), 7.28 (dd, *J* = 8.1, 0.9 Hz, 1H), 6.24 (s, 1H), 5.99 – 5.88 (m, 2H), 5.80 – 5.74 (m, 1H), 5.27 (dq, *J* = 17.1, 1.6 Hz, 1H), 5.20 (dq, *J* = 10.2, 1.4 Hz, 1H), 4.10 (tt, *J* = 5.8, 1.6 Hz, 2H), 3.68 – 3.60 (m, 1H), 2.15 – 2.05 (m, 3H), 1.79 – 1.63 (m, 3H).

^{13}C NMR (101 MHz, CDCl$_3$) δ 169.0, 165.8, 147.5, 135.7, 134.0, 129.7, 128.1, 127.9, 121.9, 117.1, 44.2, 42.6, 30.7, 25.1, 21.2.

HRMS (ESI$^+$) Calculated for C$_{15}$H$_{19}$N$_2$O [M+H]$^+$: 243.1492 found: 243.1501.

2-((1-(6-(cyclohex-2-en-1-yl)nicotinoyl)piperidin-4-yl)methyl)-5,6-dimethoxy-2,3-dihydro-1H-inden-1-one (3s)

Prepared according to General Procedure A using donepezil nicotinate **1s** (78.9 mg, 0.2 mmol) and cyclohexene **2a** (203 µL, 2.0 mmol). No other regioisomer was detected in the crude mixture. Purification by column chromatography (SiO$_2$, 1:1:98 Et$_3$N/MeOH/CH$_2$Cl$_2$) afforded product **3s** (48.6 mg, 51% yield, > 20:1 *r.r.*) as a colorless oil.

^{1}H NMR (400 MHz, CDCl$_3$) δ 8.62 (dd, *J* = 2.3, 0.9 Hz, 1H), 7.71 (dd, *J* = 8.0, 2.3 Hz, 1H), 7.28 (d, *J* = 8.1 Hz, 1H), 7.18 (s, 1H), 6.88 (s, 1H), 6.02 – 5.95 (m, 1H), 5.86 – 5.76 (m, 1H), 4.74 (br s, 1H), 3.98 (s, 3H), 3.92 (s, 3H), 3.88 – 3.73 (m, 1H), 3.70 – 3.59 (m, 1H), 3.29 (dd, *J* = 17.4, 8.0 Hz, 1H), 3.10 (br s, 1H), 2.85 (br s, 1H), 2.77 – 2.68 (m, 2H), 2.17 – 2.06 (m, 3H), 2.02 – 1.82 (m, 3H), 1.82 – 1.64 (m, 2H), 1.48 – 1.37 (m, 2H).

^{13}C NMR (101 MHz, CDCl$_3$) δ 207.2, 168.0, 166.8, 155.6, 149.6, 148.6, 147.4, 135.5, 129.5, 129.4, 129.2, 128.1, 121.7, 107.3, 104.4, 56.3, 56.1, 44.0, 30.6, 24.9, 21.1.

HRMS: (ESI$^+$) calculated for C$_{29}$H$_{34}$N$_2$NaO$_4$ [M+Na$^+$]: 497.2411, found 497.2415.
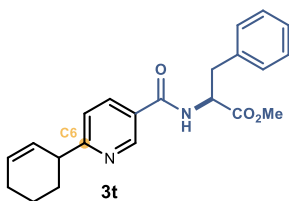
Methyl (6-(cyclohex-2-en-1-yl)nicotinoyl)-L-phenylalaninate (3t)

Prepared according to General Procedure A using methyl nicotinoyl-L-phenylalaninate **1t** (26.0 mg, 0.2 mmol) and cyclohexene **2a** (203 μL, 2.0 mmol). No other regioisomer was detected in the crude mixture. Purification by column chromatography (SiO$_2$, 1:9:90 Et$_3$N/EtOAc/hexanes to 1:19:80 Et$_3$N/EtOAc/hexanes) afforded product **3t** as a white solid (30.0 mg, 41% yield, 1:1 *d.r.*, > 20:1 *r.r.*). The diastereomeric ratio was determined by UPC^2 analysis on a Daicel Chiralpak ID-3 column (gradient: 1 min 100% CO$_2$; 5 min from 100% CO$_2$ to 60% CO$_2$ - 40% MeOH; flow rate 2.0 mL/min; λ = 268 nm: τ$_1$ = 5.6 min, τ$_2$ = 5.9 min).

^{1}H NMR (400 MHz, CDCl$_3$) δ 8.83 (dt, *J* = 2.2, 1.0 Hz, 1H), 7.95 (dd, *J* = 8.2, 2.4 Hz, 1H), 7.31 – 7.22 (m, 4H), 7.13 – 7.11 (m, 2H), 6.57 (d, *J* = 7.6 Hz, 1H), 5.99 – 5.94 (m, 1H), 5.79 – 5.74 (m, 1H), 5.07 (dt, *J* = 7.6, 5.6 Hz, 1H), 3.77 (s, 3H), 3.65 – 3.60 (m, 1H), 3.24 (qd, *J* = 13.9, 5.6 Hz, 2H), 2.13 – 2.04 (m, 3H), 1.77 – 1.63 (m, 3H).

^{13}C NMR (101 MHz, CDCl$_3$) δ 172.0, 169.2, 165.4, 147.8, 147.8, 135.7, 135.6, 129.6, 129.4, 128.9, 128.0, 127.5, 127.3, 121.8, 53.6, 52.6, 44.2, 37.9, 30.7, 25.0, 21.1.

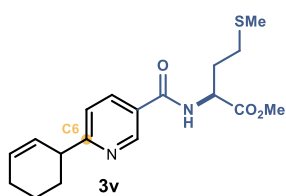HRMS: (ESI$^+$) calculated for C$_{22}$H$_{25}$N$_2$O$_3$ [M+H$^+$]: 365.1860, found 365.1864.
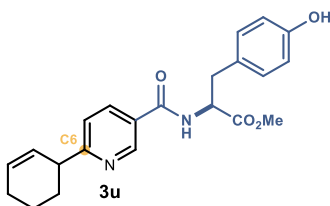
Methyl (6-(cyclohex-2-en-1-yl)nicotinoyl)-L-tyrosinate (3u)

Prepared according to General Procedure A using methyl nicotinoyl-L-tyrosinate **1u** (60.0 mg, 0.2 mmol) and cyclohexene **2a** (203 μL, 2.0 mmol). No other regioisomer was detected in the crude mixture. Purification by column chromatography (SiO$_2$, 1:29:70 Et$_3$N/acetone/hexanes) afforded product **3u** as a white solid (31.8 mg, 42% yield, 1:1 d.r., > 20:1 *r.r.*). The diastereomeric ratio was determined by UPC^2 analysis on a Daicel Chiralpak ID-3 column (gradient: 1 min 100% CO$_2$; 5 min from 100% CO$_2$ to 60% CO$_2$ - 40% MeOH; flow rate 2.0 mL/min; λ = 268 nm: τ$_1$ = 10.8 min, τ$_2$ = 11.3 min).

^{1}H NMR (400 MHz, CDCl$_3$) δ 8.80 (d, *J* = 1.5 Hz, 1H), 8.03 (ddd, *J* = 8.1, 2.4, 1.5 Hz, 1H), 7.29 (d, *J* = 8.1 Hz, 1H), 6.98 – 6.94 (m, 2H), 6.76 – 6.71 (m, 2H), 6.65 (d, *J* = 7.8 Hz, 1H), 5.98 – 5.93 (m, 1H), 5.78 – 5.70 (m, 1H), 5.04 (dt, *J* = 7.7, 5.6 Hz, 1H), 3.78 (s, 3H), 3.69 – 3.60 (m, 1H), 3.16 (qd, *J* = 14.1, 5.7 Hz, 2H), 2.13 – 2.04 (m, 3H), 1.77 – 1.62 (m, 3H).

^{13}C NMR (101 MHz, CDCl$_3$) δ 172.2, 169.2, 165.4, 156.0, 147.3, 136.2, 130.5, 129.9, 127.7, 127.6, 126.9, 122.1, 115.9, 53.8, 52.7, 44.0, 37.1, 30.7, 25.0, 21.1.

HRMS: (ESI$^+$) calculated for C$_{22}$H$_{24}$N$_2$NaO$_4$ [M+Na$^+$]: 403.1628, found 403.1627.

UNIVERSITAT ROVIRA I VIRGILI
PHOTOCHEMISTRY AND ORGANOCATALYSIS FOR RADICAL-BASED CARBON-CARBON BOND-FORMING PROCESSES
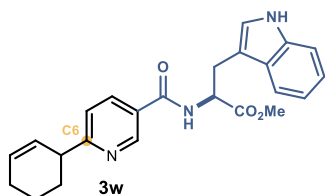Emilien Le Saux

197

Methyl (6-(cyclohex-2-en-1-yl)nicotinoyl)-L-methioninate (3v)

Prepared according to General Procedure A using methyl nicotinoyl-L-methioninate **1v** (53.7 mg, 0.2 mmol) and cyclohexene **2a** (203 μL, 2.0 mmol). No other regioisomer was detected in the crude mixture. Purification by column chromatography (SiO$_2$, 1:9:90 Et$_3$N/EtOAc/hexanes to 1:23:76 Et$_3$N/EtOAc/hexanes) afforded product **3v** as a white solid (31.0 mg, 44% yield, 1:1 *d.r.*, > 20:1 *r.r.*). The diastereomeric ratio was determined by UPC^2 analysis on a Daicel Chiralpak ID-3 column (gradient: 1 min 100% CO$_2$; 5 min from 100% CO$_2$ to 60% CO$_2$ - 40% EtOH; flow rate 2.0 mL/min; λ = 268 nm: τ_1 = 11.7 min, τ_2 = 12.0 min).

<u>^{1}H NMR</u> (400 MHz, CDCl$_3$) δ 8.96 (d, *J* = 2.4 Hz, 1H), 8.04 (dd, *J* = 8.1, 2.4 Hz, 1H), 7.27 (d, *J* = 8.2 Hz, 1H), 7.14 (d, *J* = 7.6 Hz, 1H), 5.98 – 5.93 (m, 1H), 5.78 – 5.74 (m, 1H), 4.91 (td, *J* = 7.3, 5.0 Hz, 1H), 3.78 (s, 3H), 3.65 – 3.60 (m, 1H), 2.58 (t, *J* = 7.2 Hz, 2H), 2.31 – 2.22 (m, 1H), 2.17-2.04 (m, 4H), 2.10 (s, 3H), 1.77 – 1.63 (m, 3H).

<u>^{13}C NMR</u> (101 MHz, CDCl$_3$) δ 172.5, 169.2, 165.6, 148.0, 135.7, 129.6, 128.0, 127.1, 121.8, 52.8, 52.3, 44.1, 31.3, 30.7, 30.3, 25.0, 21.1, 15.7.

<u>HRMS</u>: (ESI$^+$) calculated for C$_{18}$H$_{23}$N$_2$O$_3$S [M+H$^+$]: 347.1435, found 347.1439.

Methyl (6-(cyclohex-2-en-1-yl)nicotinoyl)-L-tryptophanate (3w)

Prepared according to General Procedure A using methyl nicotinoyl-L-tryptophanate **1w** (64.7 mg, 0.2 mmol) and cyclohexene **2a** (203 μL, 2.0 mmol). No other regioisomer was detected in the crude mixture. Purification by column chromatography (SiO$_2$, 1:19:80 Et$_3$N/EtOAc/hexanes to 1:59:40 Et$_3$N/EtOAc/hexanes) afforded product **3w** as a white solid (32.5 mg, 40% yield, 1:1 *d.r.*, > 20:1 *r.r.*). The diastereomeric ratio was determined by UPC^2 analysis on a Daicel Chiralpak IA-3 column (gradient: 1 min 100% CO$_2$; 5 min from 100% CO$_2$ to 60% CO$_2$ - 40% EtOH; flow rate 2.0 mL/min; λ = 268 nm: τ_1 = 6.9 min, τ_2 = 7.2 min).

<u>^{1}H NMR</u> (400 MHz, CDCl$_3$) δ 8.81 (ddd, *J* = 3.3, 2.3, 0.8 Hz, 1H), 8.40 (br s, 1H), 7.90 (dt, *J* = 8.2, 1.9 Hz, 1H), 7.53 (d, *J* = 7.9 Hz, 1H), 7.33 (d, *J* = 8.1 Hz, 1H), 7.20 (d, *J* = 8.2 Hz, 1H), 7.19 – 7.15 (m, 1H), 7.08 (ddd, *J* = 8.0, 7.0, 1.0 Hz, 1H), 6.99 (d, *J* = 2.4 Hz, 1H), 6.69 (d, *J* = 7.7 Hz, 1H), 5.98 – 5.93 (m, 1H), 5.78 – 5.73 (m, 1H), 5.12 (dt, *J* = 7.6, 5.3 Hz, 1H), 3.72 (s, 3H), 3.64 – 3.59 (m, 1H), 3.45 – 3.43 (m, 2H), 2.12 – 2.03 (m, 3H), 1.77 – 1.61 (m, 3H).

^{13}C NMR (101 MHz, CDCl$_3$) δ 172.4, 169.1, 165.5, 147.9, 147.9, 136.3, 135.7, 135.7, 129.7, 129.6, 128.0, 127.7, 127.3, 123.0, 122.5, 121.7, 119.9, 118.6, 111.5, 109.9, 53.5, 52.7, 44.1, 30.7, 30.7, 27.7, 25.0, 21.1.

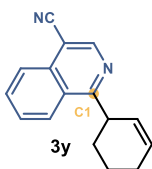HRMS: (ESI$^+$) calculated for C$_{24}$H$_{26}$N$_3$O$_3$ [M+H$^+$]: 404.1969, found 404.1979.

1-(cyclohex-2-en-1-yl)isoquinoline (3x)

Prepared according to General Procedure A using isoquinoline (23.5 µL, 0.2 mmol) and cyclohexene **2a** (203 µL, 2.0 mmol). No other regioisomer was detected in the crude mixture. Purification by column chromatography (SiO$_2$, 1:99 Et$_3$N/hexanes to 1:5:94 Et$_3$N/EtOAc/hexanes) afforded product **3x** as a colorless oil (16.6 mg, 40% yield, > 20:1 *r.r.*).

^{1}H NMR (500 MHz, CDCl$_3$) δ 8.51 (d, *J* = 5.7 Hz, 1H), 8.25 (d, *J* = 8.5 Hz, 1H), 7.82 (dt, *J* = 8.2, 1.0 Hz, 1H), 7.66 (ddd, *J* = 8.2, 6.9, 1.2 Hz, 1H), 7.58 (ddd, *J* = 8.3, 6.9, 1.4 Hz, 1H), 7.50 (dd, *J* = 5.7, 1.0 Hz, 1H), 6.04 – 5.99 (m, 1H), 5.95 (dtdd, *J* = 10.1, 2.5, 1.6, 1.1 Hz, 1H), 4.48 – 4.43 (m, 1H), 2.31 – 2.11 (m, 3H), 1.96 – 1.75 (m, 3H).

^{13}C NMR (126 MHz, CDCl$_3$) δ 164.6, 142.1, 136.5, 129.6, 129.1, 128.2, 127.6, 126.9, 126.5, 125.0, 119.2, 40.3, 30.2, 24.9, 22.1.

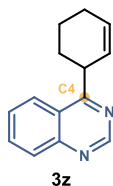HRMS: (ESI$^+$) calculated for C$_{15}$H$_{16}$N [M+H$^+$]: 210.1277, found 210.1271.

1-(cyclohex-2-en-1-yl)isoquinoline-4-carbonitrile (3y)

Prepared according to General Procedure A using isoquinoline-4-carbonitrile (30.8 mg, 0.2 mmol) and cyclohexene **2a** (203 µL, 2.0 mmol). No other regioisomer was detected in the crude mixture. Purification by column chromatography (SiO$_2$, 10:90 EtOAc/hexanes) afforded product **3y** as a white solid (14.6 mg, 31% yield, > 20:1 *r.r.*).

^{1}H NMR (400 MHz, CDCl$_3$) δ 8.87 (s, 1H), 8.35 (ddt, *J* = 8.5, 1.3, 0.7 Hz, 1H), 8.20 (ddd, *J* = 8.4, 1.3, 0.7 Hz, 1H), 7.89 (ddd, *J* = 8.3, 7.0, 1.3 Hz, 1H), 7.75 (dddd, *J* = 8.6, 7.0, 1.3, 0.3 Hz, 1H), 6.08 – 6.03 (m, 1H), 5.88 (dtdd, *J* = 10.1, 2.4, 1.8, 1.1 Hz, 1H), 4.54 – 4.46 (m, 1H), 2.30 – 2.12 (m, 3H), 1.97 – 1.74 (m, 3H).

^{13}C NMR (101 MHz, CDCl$_3$) δ 169.9, 147.7, 135.0, 132.2, 129.0, 128.8, 127.8, 125.7, 125.6, 125.1, 116.4, 104.3, 40.7, 30.2, 24.8, 21.8.

HRMS: (ESI$^+$) calculated for C$_{16}$H$_{15}$N$_2$ [M+H$^+$]: 235.1230, found 235.1234.

UNIVERSITAT ROVIRA I VIRGILI
PHOTOCHEMISTRY AND ORGANOCATALYSIS FOR RADICAL-BASED CARBON-CARBON BOND-FORMING PROCESSES
Emilien Le Saux

199

4-(cyclohex-2-en-1-yl)quinazoline (3z)

Prepared according to General Procedure A using quinazoline (26.0 mg, 0.2 mmol) and cyclohexene **2a** (203 µL, 2.0 mmol). No other regioisomer was detected in the crude mixture. Purification by column chromatography (SiO$_2$, 1:10:89 Et$_3$N/EtOAc/hexanes) afforded product **3z** (8.3 mg, 20% yield, > 20:1 *r.r.*) as a colorless oil.

<u>^{1}H NMR</u> (400 MHz, CDCl$_3$) δ 9.28 (s, 1H), 8.22 (d, *J* = 8.4 Hz, 1H), 8.06 (d, *J* = 8.5 Hz, 1H), 7.88 (ddd, *J* = 8.4, 6.9, 1.4 Hz, 1H), 7.64 (ddd, *J* = 8.3, 6.9, 1.3 Hz, 1H), 6.11 – 6.02 (m, 1H), 5.93 – 5.84 (m, 1H), 4.44 (ddp, *J* = 8.4, 5.6, 2.7 Hz, 1H), 2.31 – 2.11 (m, 3H), 2.02 – 1.71 (m, 3H).

<u>^{13}C NMR</u> (101 MHz, CDCl$_3$) δ 174.1, 154.9, 150.2, 133.4, 129.4, 129.3, 127.5, 127.4, 124.4, 123.5, 40.0, 29.9, 24.8, 21.8.

<u>HRMS</u> (ESI$^+$) Calculated for C$_{14}$H$_{15}$N$_2$ [M+H]$^+$: 211.1230 found: 211.1236.
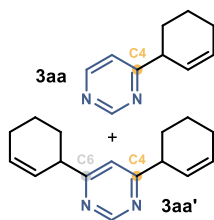
4-(cyclohex-2-en-1-yl)pyrimidine (3aa) + 4,6-di(cyclohex-2-en-1-yl)pyrimidine (3aa')

Prepared according to General Procedure B using pyrimidine (15.6 µL, 0.2 mmol) and cyclohexene **2a** (203 µL, 2.0 mmol). Purification by column chromatography (SiO$_2$, 1:5:94 Et$_3$N/EtOAc/hexanes) afforded product **3aa** (8.8 mg, 27% yield, > 20:1 *r.r.*) as a colorless oil.

<u>^{1}H NMR</u> (500 MHz, CDCl$_3$) δ 9.16 (d, *J* = 1.4 Hz, 1H), 8.65 (d, *J* = 5.2 Hz, 1H), 7.25 (dd, *J* = 5.2, 1.4 Hz, 1H), 6.08 – 5.97 (m, 1H), 5.86 – 5.75 (m, 1H), 3.59 – 3.52 (m, 1H), 2.21 – 2.07 (m, 3H), 1.81 – 1.65 (m, 3H).

<u>^{13}C NMR</u> (126 MHz, CDCl$_3$) δ 173.7, 158.8, 156.9, 130.2, 126.7, 119.5, 43.5, 29.9, 24.8, 20.8.

<u>HRMS</u> (ESI$^+$) Calculated for C$_{10}$H$_{13}$N$_2$ [M+H]$^+$: 161.1073 found: 161.1076.

Product **3aa'** (3.8 mg, 8% yield, > 20:1 *r.r.*) was also isolated as a colorless oil.

<u>^{1}H NMR</u> (500 MHz, CDCl$_3$) δ 9.09 (d, *J* = 1.3 Hz, 1H), 7.12 (d, *J* = 1.3 Hz, 1H), 6.07 – 5.99 (m, 2H), 5.82 – 5.74 (m, 2H), 3.59 – 3.47 (m, 2H), 2.22 – 2.04 (m, 6H), 1.86 – 1.63 (m, 6H).

<u>^{13}C NMR</u> (126 MHz, CDCl$_3$) δ 173.7, 158.5, 130.0, 127.1, 117.2, 43.5, 30.0, 24.9, 21.0.

<u>HRMS</u> (ESI$^+$) Calculated for C$_{16}$H$_{21}$N$_2$ [M+H]$^+$: 241.1699 found: 241.1699.

tert-butyl (4-(cyclohex-2-en-1-yl)pyrimidin-2-yl)carbamate (3bb)

Prepared according to General Procedure A using tert-butyl pyrimidin-2-ylcarbamate **1bb** (39.0 mg, 0.2 mmol) and cyclohexene **2a** (203 µL, 2.0 mmol). No other regioisomer was detected in the crude mixture. Purification by column chromatography (SiO$_2$, 1:10:89 Et$_3$N/EtOAc/hexanes) afforded product **3bb** (17.9 mg, 27% yield, > 20:1 *r.r.*) as a colorless oil.

^{1}H NMR (400 MHz, CDCl$_3$) δ 8.53 (d, *J* = 5.1 Hz, 1H), 7.54 (brs, 1H), 6.88 (d, *J* = 5.1 Hz, 1H), 6.04 – 5.93 (m, 1H), 5.80 – 5.72 (m, 1H), 3.54 – 3.40 (m, 1H), 2.17 – 2.04 (m, 3H), 1.82 – 1.63 (m, 3H), 1.55 (s, 9H).

^{13}C NMR (101 MHz, CDCl$_3$) δ 175.4, 158.2, 157.6, 150.6, 129.9, 126.9, 113.8, 81.2, 43.3, 29.6, 28.2, 24.8, 20.9.

HRMS (ESI$^+$) Calculated for C$_{15}$H$_{21}$N$_3$NaO$_2$ [M+Na]$^+$: 298.1526 found: 298.1522.
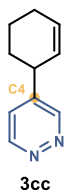
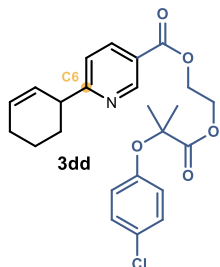### 4-(cyclohex-2-en-1-yl)pyridazine (3cc)

Prepared according to General Procedure A using pyridazine (14.5 µL, 0.2 mmol) and cyclohexene **2a** (203 µL, 2.0 mmol). No other regioisomer was detected in the crude mixture. Purification by column chromatography (SiO$_2$, 1:40:59 Et$_3$N/EtOAc/hexanes) afforded product **3cc** (10.0 mg, 31% yield, > 20:1 *r.r.*) as a brown oil.

^{1}H NMR (400 MHz, CDCl$_3$) δ 9.10 (s, 1H), 9.08 (d, *J* = 5.5 Hz, 1H), 7.33 (dd, *J* = 5.3, 2.4 Hz, 1H), 6.05 (dq, *J* = 9.8, 3.4 Hz, 1H), 5.70 – 5.61 (m, 1H), 3.45 (m, 1H), 2.17 – 2.11 (m, 2H), 2.10 – 2.04 (m, 1H), 1.77 – 1.62 (m, 2H), 1.61 – 1.52 (m, 1H).

^{13}C NMR (101 MHz, CDCl$_3$) δ 152.3, 151.1, 145.6, 131.1, 126.3, 125.2, 38.8, 31.3, 24.7, 20.4.

HRMS (ESI$^+$) Calculated for C$_{10}$H$_{13}$N$_2$ [M+H]$^+$: 161.1073 found: 161.1073.

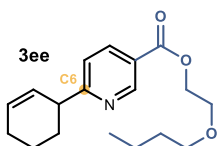### 2-((2-(4-chlorophenoxy)-2-methylpropanoyl)oxy)ethyl 6-(cyclohex-2-en-1-yl)nicotinate (3dd)

Prepared according to General Procedure A using Etofibrate **1dd** (72.8 mg, 0.2 mmol) and cyclohexene **2a** (203 µL, 2.0 mmol). No other regioisomer was detected in the crude mixture. Purification by column chromatography (SiO$_2$, 1:10:89 Et$_3$N/EtOAc/hexanes) afforded product **3dd** as a colorless oil (47.8 mg, 54% yield, > 20:1 *r.r.*).

^{1}H NMR (400 MHz, CDCl$_3$) δ 9.10 (dd, *J* = 2.3, 0.9 Hz, 1H), 8.07 (dd, *J* = 8.2, 2.2 Hz, 1H), 7.28 (dd, *J* = 8.2, 0.9 Hz, 1H), 7.13 – 7.08 (m, 2H), 6.79 – 6.74 (m, 2H), 6.05 – 5.97 (m, 1H),

UNIVERSITAT ROVIRA I VIRGILI
PHOTOCHEMISTRY AND ORGANOCATALYSIS FOR RADICAL-BASED CARBON-CARBON BOND-FORMING PROCESSES
Emilien Le Saux

201

5.85 – 5.77 (m, 1H), 4.58 – 4.49 (m, 4H), 3.73 – 3.63 (m, 1H), 2.22 – 2.03 (m, 3H), 1.86 – 1.65 (m, 3H), 1.60 (s, 6H).

^{13}C NMR (101 MHz, CDCl$_3$) δ 173.9, 170.5, 165.1, 153.9, 150.7, 137.4, 129.6, 129.1, 127.8, 127.2, 123.1, 121.5, 120.2, 79.4, 63.0, 62.5, 44.2, 30.5, 25.3, 24.9, 21.0.

HRMS (ESI$^+$) Calculated for C$_{24}$H$_{27}$ClNO$_5$ [M+H]$^+$: 444.1572 found: 444.1565.

2-butoxyethyl 6-(cyclohex-2-en-1-yl)nicotinate (3ee)

Prepared according to General Procedure A using Nicoboxil **1ee** (44.7 mg, 0.2 mmol) and cyclohexene **2a** (203 μL, 2.0 mmol). No other regioisomer was detected in the crude mixture. Purification by column chromatography (SiO$_2$, 1:2:97 Et$_3$N/EtOAc/hexanes) afforded product **3ee** as a light-yellow oil (32.3 mg, 53% yield, > 20:1 *r.r.*).

^{1}H NMR (500 MHz, CDCl$_3$) δ 9.19 (d, *J* = 2.2 Hz, 1H), 8.25 (dd, *J* = 8.1, 2.2 Hz, 1H), 7.30 (d, *J* = 8.2 Hz, 1H), 6.05 – 5.96 (m, 1H), 5.88 – 5.79 (m, 1H), 4.53 – 4.45 (m, 2H), 3.81 – 3.75 (m, 2H), 3.72 – 3.65 (m, 1H), 3.53 (t, *J* = 6.6 Hz, 2H), 2.22 – 2.06 (m, 3H), 1.83 – 1.64 (m, 3H), 1.64 – 1.55 (m, 2H), 1.45 – 1.35 (m, 2H), 0.93 (t, *J* = 7.4 Hz, 3H).

^{13}C NMR (126 MHz, CDCl$_3$) δ 170.1, 165.5, 150.8, 137.6, 129.6, 127.9, 123.7, 121.4, 71.3, 68.5, 64.4, 44.2, 31.7, 30.6, 24.9, 21.0, 19.3, 13.9.

HRMS (ESI$^+$) Calculated for C$_{18}$H$_{26}$NO$_3$ [M+H]$^+$: 304.1907 found: 304.1904.
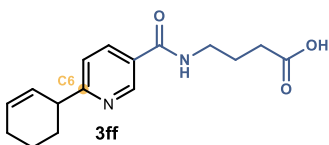
4-(6-(cyclohex-2-en-1-yl)nicotinamido)butanoic acid (3ff)

Prepared according to General Procedure A using Picamilon (41.6 mg, 0.2 mmol) and cyclohexene **2a** (203 μL, 2.0 mmol). No other regioisomer was detected in the crude mixture. Purification by column chromatography (SiO$_2$, 1:40:59 AcOH/EtOAc/hexanes to 1:99 AcOH/EtOAc) afforded product **3ff** as a white solid (43.4 mg, 75% yield, > 20:1 *r.r.*).

^{1}H NMR (400 MHz, Acetone) δ 9.05 (d, *J* = 2.7 Hz, 1H), 8.39 (s, 1H), 8.27 (dd, *J* = 8.2, 2.4 Hz, 1H), 7.37 (d, *J* = 8.2 Hz, 1H), 5.95 – 5.89 (m, 1H), 5.82 – 5.75 (m, 1H), 3.71 – 3.61 (m, 1H), 3.52 (q, *J* = 6.7 Hz, 2H), 2.43 (t, *J* = 7.0 Hz, 2H), 2.07 (p, *J* = 2.2 Hz, 4H), 1.93 (p, *J* = 7.1 Hz, 2H), 1.83 – 1.71 (m, 2H), 1.70 – 1.59 (m, 1H).

^{13}C NMR (101 MHz, Acetone) δ 147.8, 136.1, 128.8, 128.1, 121.3, 54.1, 43.5, 39.2, 24.6, 20.8.

HRMS (ESI$^+$) Calculated for C$_{16}$H$_{21}$N$_2$O$_3$ [M+H]$^+$: 289.1547 found: 289.1543.
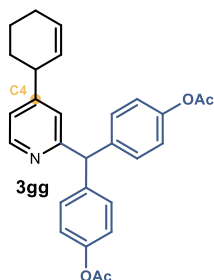
((4-(cyclohex-2-en-1-yl)pyridin-2-yl)methylene)bis(4,1-phenylene) diacetate (3gg)

Prepared according to General Procedure B using bisacodyl (72.3 mg, 0.2 mmol) and cyclohexene **2a** (203 μL, 2.0 mmol). No other regioisomer was detected in the crude mixture. Purification by column (SiO$_2$, 1:9:90 Et$_3$N/EtOAc/hexanes) afforded product **3gg** as a colorless oil (29.0 mg, 33% yield, > 20:1 *r.r.*).

^{1}H NMR (400 MHz, CDCl$_3$) δ 8.48 (d, *J* = 5.1 Hz, 1H), 7.21 – 7.17 (m, 4H), 7.03 – 6.98 (m, 6H), 5.94 – 5.89 (m, 1H), 5.63 – 5.59 (m, 2H), 3.35 – 3.30 (m, 1H), 2.27 (s, 6H), 2.09 – 2.04 (m, 2H), 2.00 – 1.94 (m, 1H), 1.73 – 1.63 (m, 2H), 1.62 – 1.59 (m, 1H), 1.52 – 1.42 (m, 1H).

^{13}C NMR (101 MHz, CDCl$_3$) δ 169.6, 162.5, 156.4, 149.6, 149.4, 140.4, 140.3, 130.4, 130.4, 129.8, 128.2, 123.5, 121.5, 121.2, 58.2, 41.3, 31.9, 25.0, 21.3, 21.0.

HRMS: (ESI$^+$) calculated for C$_{28}$H$_{28}$NO$_4$ [M+H$^+$]: 442.2013, found 442.2031.
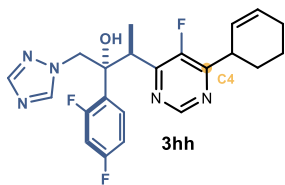
3-(6-(cyclohex-2-en-1-yl)-5-fluoropyrimidin-4-yl)-2-(2,4-difluorophenyl)-1-(1H-1,2,4-triazol-1-yl)butan-2-ol (3hh)

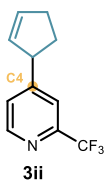Prepared according to General Procedure A using voriconazole (69.9 mg, 0.2 mmol) and cyclohexene **2a** (203 μL, 2.0 mmol). No other regioisomer was detected in the crude mixture. Purification by column chromatography (SiO$_2$, 1:50:49 Et$_3$N/EtOAc/hexanes) afforded product **3hh** (37.6 mg, 44% yield, 1:1 *d.r.*, > 20:1 *r.r.*) as an off-white solid.

^{1}H NMR (400 MHz, CDCl$_3$) *1:1 mixture of diastereoisomers* δ 8.85 (dd, *J* = 7.4, 1.8 Hz, 1H), 7.99 (d, *J* = 4.3 Hz, 1H), 7.67 – 7.58 (m, 1H), 7.54 (d, *J* = 5.2 Hz, 1H), 6.90 – 6.79 (m, 2H), 6.73 (s, 0.5H), 6.68 (s, 0.5H), 6.10 – 6.02 (m, 1H), 5.77 – 5.67 (m, 1H), 4.72 (dd, *J* = 14.2, 3.5 Hz, 1H), 4.32 (dd, *J* = 17.3, 14.1 Hz, 1H), 4.19 – 4.10 (m, 1H), 4.04 – 3.92 (m, 1H), 2.27 – 2.14 (m, 2H), 2.14 – 2.05 (m, 1H), 1.99 – 1.89 (m, 1H), 1.86 – 1.71 (m, 2H), 1.12 – 1.08 (m, 3H).

^{13}C NMR (101 MHz, CDCl$_3$) *1:1 mixture of diastereoisomers* δ 164.1, 163.9, 162.1, 162.0, 162.0, 161.9, 161.6, 161.5, 159.8, 159.7, 158.1, 158.0, 157.4, 157.3, 155.1, 153.0, 152.9, 152.9, 152.8, 152.5, 152.5, 150.8, 144.0, 143.9, 130.7, 130.7, 130.7, 130.6, 130.3, 130.2, 125.4, 125.4, 123.6, 123.6, 111.7, 111.5, 104.3, 104.1, 103.8, 57.5, 57.5, 37.3, 37.1, 36.5, 28.2, 28.1, 24.5, 21.3, 21.2, 16.2.

^{19}F{^{1}H} NMR (376 MHz, CDCl$_3$) *1:1 mixture of diastereoisomers* δ -109.17 (d, *J* = 8.2 Hz), -109.19 (d, *J* = 8.0 Hz), -110.55 (d, *J* = 8.1 Hz), -138.87, -139.00.

HRMS (ESI$^+$) Calculated for C$_{22}$H$_{23}$F$_3$N$_5$O [M+H]$^+$: 430.1849 found: 430.1854.

UNIVERSITAT ROVIRA I VIRGILI
PHOTOCHEMISTRY AND ORGANOCATALYSIS FOR RADICAL-BASED CARBON-CARBON BOND-FORMING
PROCESSES
Emilien Le Saux

203

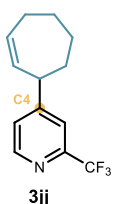### 4-(cyclopent-2-en-1-yl)-2-(trifluoromethyl)pyridine (3ii)

Prepared according to General Procedure A using 2-(trifluoromethyl)pyridine (23.0 μL, 0.2 mmol) and cyclopentene (183 μL, 2.0 mmol). No other regioisomer was detected in the crude mixture. Purification by column chromatography (SiO$_2$, 5:95 EtOAc/hexanes) afforded product **3ii** as colorless oil (17.1 mg, 40% yield, > 20:1 *r.r.*).

^{1}H NMR (400 MHz, CDCl$_3$) δ 8.60 (d, J = 5.0 Hz, 1H), 7.49 (d, J = 1.7 Hz, 1H), 7.30 (dd, J = 5.0, 1.7 Hz, 1H), 6.09 – 6.05 (m, 1H), 5.76 – 5.72 (m, 1H), 4.00 – 3.93 (m, 1H), 2.60 – 2.40 (m, 3H), 1.77 – 1.67 (m, 1H).

^{13}C NMR (101 MHz, CDCl$_3$) δ 157.5, 150.0, 148.4 (q, J = 34.1 Hz), 134.4, 131.6, 125.2, 121.7 (q, J = 274.2 Hz), 119.3 (q, J = 2.8 Hz), 50.6, 33.1, 32.4.

^{19}F NMR (376 MHz, CDCl$_3$) δ -68.0.

HRMS: (ESI$^+$) calculated for C$_{11}$H$_{11}$F$_3$N [M+H]$^+$: 214.0838, found 214.0829.

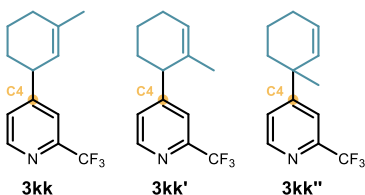### 4-(cyclohept-2-en-1-yl)-2-(trifluoromethyl)pyridine (3jj)

Prepared according to General Procedure A using 2-(trifluoromethyl)pyridine (23.0 μL, 0.2 mmol) and cycloheptene (233 μL, 2.0 mmol) with a reaction time of 24 hours. No other regioisomer was detected in the crude mixture. Purification by column chromatography (SiO$_2$, 5:95 EtOAc/hexanes) afforded product **3jj** as colorless oil (21.2 mg, 44% yield, > 20:1 *r.r.*).

^{1}H NMR (400 MHz, CDCl$_3$) δ 8.62 (d, J = 5.0 Hz, 1H), 7.55 (d, J = 2.2 Hz, 1H), 7.35 (dd, J = 5.0, 1.9 Hz, 1H), 5.96 (dddd, J = 11.3, 6.9, 5.5, 2.3 Hz, 1H), 5.64 (dddt, J = 11.3, 4.2, 1.9, 0.8 Hz, 1H), 3.66 – 3.60 (m, 1H), 2.29 – 2.19 (m, 2H), 1.97 – 1.88 (m, 1H), 1.88 – 1.66 (m, 4H), 1.53 – 1.42 (m, 1H).

^{13}C NMR (101 MHz, CDCl$_3$) δ 158.2, 150.1, 148.4 (q, J = 34.1 Hz), 133.9, 133.6, 125.3, 121.7 (q, J = 274.5 Hz), 119.5 (q, J = 2.9 Hz), 46.3, 35.2, 29.7, 28.7, 26.6.

^{19}F NMR (376 MHz, CDCl$_3$) δ -68.03.

HRMS: (ESI$^+$) calculated for C$_{13}$H$_{15}$F$_3$N [M+H]$^+$: 242.1151, found 242.1157.

4-(3-methylcyclohex-2-en-1-yl)-2-(trifluoromethyl)pyridine (3kk) + 4-(2-methylcyclohex-2-en-1-yl)-2-(trifluoromethyl)pyridine (3kk') + 4-(1-methylcyclohex-2-en-1-yl)-2-(trifluoromethyl)pyridine (3kk'')
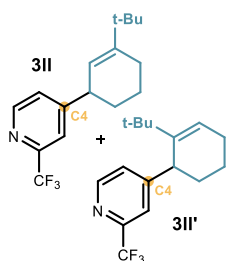
Prepared according to General Procedure A using 2-(trifluoromethyl)pyridine (23.0 µL, 0.2 mmol) and 1-methylcyclohex-1-ene (237 µL, 2.0 mmol). Purification by column chromatography (SiO$_2$, 1:99 Et$_3$N/hexanes) afforded a mixture of products **3kk, 3kk', and 3kk''** as a colorless oil (29.7 mg, 61% yield, 2:0.75:1 allylic *r.r.*). For NMR characterization, when possible, the signals are assigned to the corresponding isomer (COSY and HSQC spectra used for assignment).

<u>^{1}H NMR</u> (400 MHz, CDCl$_3$) δ 8.61 (dm, *J* = 5.0 Hz, 1H, **3kk'**), 8.61 (dm, *J* = 5.0 Hz, 1H, **3kk''**), 8.60 (dp, *J* = 5.0 Hz, 0.7 Hz, 1H, **3kk**), 7.65 (dd, *J* = 1.8, 0.8 Hz, 1H, **3kk''**), 7.52 – 7.51 (m, 1H, **3kk**), 7.51 – 7.50 (m, 1H, **3kk'**), 7.46 (ddq, *J* = 5.2, 1.8, 0.6 Hz, 1H, **3kk''**), 7.32 (ddt, *J* = 5.0, 1.7, 0.6 Hz, 1H, **3kk**), 7.30 (ddt, *J* = 5.0, 1.6, 0.5 Hz, 1H, **3kk'**), 5.96 (dtd, *J* = 10.1, 3.7, 0.6 Hz, 1H, **3kk''**), 5.79 (tp, *J* = 3.9, 1.4 Hz, 1H, **3kk'**), 5.64 (dtd, *J* = 10.1, 2.2, 1.1 Hz, 1H, **3kk''**), 5.36 (ddtd, *J* = 2.9, 2.2, 1.5, 0.7 Hz, 1H, **3kk**), 3.45 (ddp, *J* = 8.0, 5.5, 2.5 Hz, 1H, **3kk**), 3.32 (t, *J* = 5.9 Hz, 1H, **3kk'**), 2.15 – 1.26 (m, 6H, CH$_2$) 1.77 – 1.76 (m, 3H, **3kk**), 1.50 – 1.49 (m, 3H, **3kk'**), 1.40 (s, 3H, **3kk''**)

<u>^{13}C NMR</u> (101 MHz, CDCl$_3$) δ 161.0, 158.2, 156.7, 149.8, 149.8, 149.7, 148.2 (q, *J* = 34.0 Hz), 148.2 (q, *J* = 34.0 Hz, **3kk**), 148.1 (q, *J* = 33.6 Hz), 137.9, 132.5 (**3kk''**), 131.9, 128.9 (**3kk''**), 126.4 (**3kk'**), 125.8 (q, *J* = 1.0 Hz), 124.6 (q, *J* = 1.1 Hz, **3kk''**), 121.8 (q, *J* = 273.9 Hz, **3kk''**), 121.7 (q, *J* = 274.2 Hz, **3kk**), 121.7 (q, *J* = 274.1 Hz, **3kk'**), 121.4 (**3kk**), 120.4 (q, *J* = 2.5 Hz), 119.8 (q, *J* = 2.5 Hz), 118.6 (q, *J* = 2.8 Hz), 45.4 (**3kk'**), 41.6 (**3kk**), 39.7 (**3kk''**), 38.3, 31.9, 31.5 (**3kk**), 29.7, 28.5 (**3kk''**), 25.1, 24.8, 23.9 (**3kk**), 22.5 (**3kk'**), 21.1 (**3kk**), 18.8, 18.3 (**3kk'**).

<u>^{19}F NMR</u> (376 MHz, CDCl$_3$) δ 67.9 (**3kk''**), 68.0 (**3kk'**), 68.0 (**3kk**)

<u>HRMS</u>: (ESI$^+$) calculated for C$_{13}$H$_{15}$F$_3$N [M+H]$^+$: 242.1151, found 242.1152.

4-(3-(tert-butyl)cyclohex-2-en-1-yl)-2-(trifluoromethyl)pyridine (3ll) and 4-(2-(tert-butyl)cyclohex-2-en-1-yl)-2-(trifluoromethyl)pyridine (3ll')
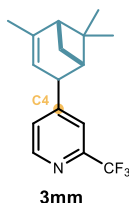
Prepared according to General Procedure A using 2-(trifluoromethyl)pyridine (23.0 µL, 0.2 mmol) and 1-(tert-butyl)cyclohex-1-ene (330 µL, 2.0 mmol). Purification by column chromatography (SiO$_2$, 5:95 EtOAc/hexanes) afforded products **3ll + 3ll'** as colorless oil (25.8 mg, 46% yield, 8:1 allylic *r.r.*). Only characterization data for the major product **3ll** is described.

<u>^{1}H NMR</u> (400 MHz, CDCl$_3$) δ 8.61 (dt, *J* = 5.0, 0.7 Hz, 1H), 7.50 (dt, *J* = 1.5, 0.7 Hz, 1H), 7.31 (ddt, *J* = 5.0, 1.7, 0.7 Hz, 1H), 5.44 – 5.42 (m, 1H), 3.49 (ddq, *J* = 8.4, 5.5, 2.7 Hz, 1H), 2.16 – 2.09 (m, 2H), 2.00 (dtd, *J* = 13.1, 6.6, 2.8 Hz, 1H), 1.79 – 1.69 (m, 1H), 1.65 – 1.55 (m, 1H), 1.44 (dddd, *J* = 13.1, 10.6, 8.2, 3.0 Hz, 1H), 1.09 (s, 9H).

UNIVERSITAT ROVIRA I VIRGILI
PHOTOCHEMISTRY AND ORGANOCATALYSIS FOR RADICAL-BASED CARBON-CARBON BOND-FORMING
PROCESSES
Emilien Le Saux

205

^{13}C NMR (101 MHz, CDCl$_3$) δ 158.5, 149.8, 149.5, 148.2 (q, J = 34.0 Hz), 125.7, 121.7 (q, J = 273.9 Hz), 119.9 (q, J = 2.8 Hz), 41.6, 35.6, 31.6, 30.0, 29.1, 24.3, 21.5.

^{19}F NMR (376 MHz, CDCl$_3$) δ -68.0.

HRMS: (ESI$^+$) calculated for C$_{16}$H$_{21}$F$_3$N [M+H]$^+$: 284.1621, found 284.1623.

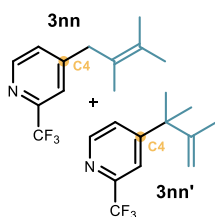### 2-(trifluoromethyl)-4-(4,6,6-trimethylbicyclo[3.1.1]hept-3-en-2-yl)pyridine (3mm)

Prepared according to General Procedure A using 2-(trifluoromethyl)pyridine (23.0 μL, 0.2 mmol) and alpha-Pinene (318 μL, 2.0 mmol) with a reaction time of 60 hours. The yield (39%, single regioisomer) of **3mm** was inferred by ^{1}H NMR analysis of the crude reaction mixture using trichloroethylene as the internal standard. A 90% pure sample of **3mm** (estimated by ^{1}H NMR integration) was obtained after purification by column chromatography (SiO$_2$, 3:97 Et$_2$O/hexanes) as a colorless oil.

^{1}H NMR (400 MHz, CDCl$_3$) δ 8.60 (dt, J = 5.0, 0.7 Hz, 1H), 7.54 (dt, J = 1.6, 0.7 Hz, 1H), 7.35 (ddt, J = 5.1, 1.7, 0.7 Hz, 1H), 5.32 (td, J = 2.9, 1.6 Hz, 1H), 3.62 (h, J = 2.3 Hz, 1H), 2.17 – 2.13 (m, 1H), 1.81 (t, J = 1.9 Hz, 3H), 1.35 (s, 3H), 1.21 – 1.14 (m, 1H), 1.01 (s, 3H).

^{13}C NMR (101 MHz, CDCl$_3$) δ 156.3, 149.6, 148.6, 148.0 (q, J = 34.3 Hz), 126.4, 121.8 (q, J = 274.1 Hz), 120.5 (q, J = 2.6 Hz), 115.6, 47.6, 46.8, 45.1, 42.1, 26.3, 26.2, 23.2, 20.5.

^{19}F NMR (376 MHz, CDCl$_3$) δ -67.5.

HRMS: (ESI$^+$) calculated for C$_{16}$H$_{19}$F$_3$N [M+H]$^+$: 282.1464, found 282.1473.

4-(2,3-dimethylbut-2-en-1-yl)-2-(trifluoromethyl)pyridine (3nn) and 4-(2,3-dimethylbut-3-en-2-yl)-2-(trifluoromethyl)pyridine (3nn')

Prepared according to General Procedure A using 2-(trifluoromethyl)pyridine (23.0 μL, 0.2 mmol) and tetramethylethylene (238 μL, 2.0 mmol) with a reaction time of 60 hours. Purification by column chromatography (SiO$_2$, 5:95 EtOAc) afforded the mixture of products **3nn** + **3nn'** as a colorless oil (22.4 mg, 43% yield, 3:2 allylic *r.r.*).

^{1}H NMR of **3nn** (400 MHz, CDCl$_3$) δ 8.58 (dt, J = 5.0, 0.7 Hz, 1H), 7.47 – 7.42 (m, 1H), 7.27 – 7.24 (m, 1H), 3.47 – 3.45 (m, 2H), 1.76 – 1.75 (m, 6H), 1.63 – 1.56 (m, 3H).

^{13}C NMR of **3nn** (101 MHz, CDCl$_3$) δ 152.4, 149.8, 148.2 (q, J = 34.2 Hz), 128.5, 126.3 (q, J = 1.1 Hz), 123.6, 121.7 (q, J = 274.5 Hz), 120.5 (q, J = 2.7 Hz), 39.6, 20.7, 20.6, 18.5.

^{19}F NMR of **3nn** (376 MHz, CDCl$_3$) δ -68.1.

[1H] NMR of **3nn'** (400 MHz, CDCl3) δ 8.62 (dp, *J* = 5.1, 0.6 Hz, 1H), 7.59 (dd, *J* = 1.8, 0.7 Hz, 1H), 7.41 (ddq, *J* = 5.1, 1.8, 0.6 Hz, 1H), 5.03 (dq, *J* = 1.4, 0.7 Hz, 1H), 5.00 (p, *J* = 1.4 Hz, 1H), 1.52 (dd, *J* = 1.4, 0.7 Hz, 3H), 1.44 (s, 6H).

[13C] NMR of **3nn'** (101 MHz, CDCl3) δ 159.9, 149.9, 149.8, 148.3 (q, *J* = 34.0 Hz), 124.1 (q, *J* = 1.1 Hz), 121.7 (q, *J* = 274.1 Hz), 118.2 (q, *J* = 2.7 Hz), 111.7, 44.2, 27.6, 20.0.

[19F] NMR of **3nn'** (376 MHz, CDCl3) δ -67.9.

HRMS of **3nn + 3nn'**: (ESI+) calculated for $C_{12}H_{15}F_3N$ [M+H]+: 230.1151, found 230.1161.

3oo
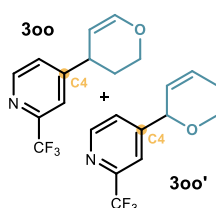
4-(3,4-dihydro-2H-pyran-4-yl)-2-(trifluoromethyl)pyridine (3oo) + 4-(5,6-dihydro-2H-pyran-2-yl)-2-(trifluoromethyl)pyridine (3oo')
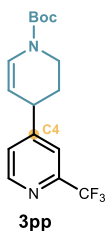
3oo'

Prepared according to General Procedure A using 2-(trifluoromethyl)pyridine (23.0 μL, 0.2 mmol) and 3,4-dihydropyran (182 μL, 2.0 mmol). Purification by column chromatography (SiO2, 10:90 EtOAc/hexanes) afforded products **3oo + 3oo'** as a colorless oil (19.8 mg, 43% yield, 7:1 allylic *r.r.*). Only the major product **3oo** is described.

[1H] NMR (400 MHz, CDCl3) δ 8.65 – 8.63 (m, 1H), 7.60 – 7.58 (m, 1H), 7.40 (m, 1H), 6.64 (dd, *J* = 6.3, 1.9 Hz, 1H), 4.72 (dddd, *J* = 6.3, 3.3, 1.0, 0.7 Hz, 1H), 4.03 (dddt, *J* = 11.0, 8.0, 3.0, 0.4 Hz, 1H), 3.96 (ddd, *J* = 11.1, 6.9, 3.2 Hz, 1H), 2.25 (dddddd, *J* = 13.8, 6.9, 6.3, 3.0, 1.1, 0.5 Hz, 1H), 1.84 (m, 1H).

[13C] NMR (101 MHz, CDCl3) δ 156.6, 150.0, 148.4 (q, *J* = 34.3 Hz), 146.3, 125.6, 121.6 (q, *J* = 274.2 Hz), 119.7 (q, *J* = 2.7 Hz), 100.7, 63.4, 35.8, 31.1.

[19F] NMR (376 MHz, CDCl3) δ -68.0.

HRMS: (ESI+) calculated for $C_{11}H_{11}F_3NO$ [M+H]+: 230.0787, found 230.0788.

tert-butyl 2'-(trifluoromethyl)-3,4-dihydro-[4,4'-bipyridine]-1(2H)-carboxylate (3pp)

Prepared according to General Procedure A using 2-(trifluoromethyl)pyridine 23.0 μL, 0.2 mmol) and tert-butyl 3,4-dihydropyridine-1(2H)-carboxylate (367 mg, 2.0 mmol). Purification by column chromatography (SiO2, 5:95 to 12:88 EtOAc/hexanes) afforded product **3pp** as colorless oil (24.8 mg, 38% yield, 20:1

3pp

allylic *r.r.*) and recovered olefin (311 mg, 1.7 mmol). Due to presence of N-Boc rotamers the [1H] NMR and [13C] NMR spectra were recorded at 328K which produced singular broad singlets for these signals.

UNIVERSITAT ROVIRA I VIRGILI
PHOTOCHEMISTRY AND ORGANOCATALYSIS FOR RADICAL-BASED CARBON-CARBON BOND-FORMING
PROCESSES
Emilien Le Saux

207

^{1}H NMR (500 MHz, CDCl$_3$, 328K) δ 8.63 (d, J = 5.0 Hz, 1H), 7.55 (d, J = 2.0 Hz, 1H), 7.36 (dd, J = 5.0, 1.9 Hz, 1H), 7.08 (br. s, 1H), 4.82 (br. s, 1H), 3.67 – 3.51 (m, 3H), 2.19 (dtd, J = 13.4, 6.2, 3.6 Hz, 1H), 1.82 (dtd, J = 13.5, 7.4, 4.0 Hz, 1H), 1.52 (s, 9H).

^{13}C NMR (126 MHz, CDCl$_3$, 328K) δ 156.3, 152.2, 150.1, 148.8 (q, J = 34.5 Hz), 128.1, 125.5, 121.7 (q, J = 274.3 Hz), 119.7 (q, J = 2.7 Hz), 104.5, 81.3, 39.7, 37.8, 30.4, 28.3.

^{19}F NMR (376 MHz, CDCl$_3$) δ -68.0.

HRMS: (ESI$^+$) calculated for C$_{16}$H$_{20}$F$_3$N$_2$O$_2$ [M+H]$^+$: 329.1471, found 329.1471.
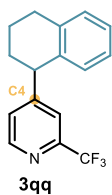
4-(1,2,3,4-tetrahydronaphthalen-1-yl)-2-(trifluoromethyl)pyridine (3qq)
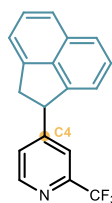
Prepared according to General Procedure A using 2-(trifluoromethyl)pyridine (23.0 µL, 0.2 mmol) and 1,2,3,4-tetrahydronaphthalene (273 µL, 2.0 mmol). No other regioisomer was detected in the crude mixture. Purification by column chromatography (SiO$_2$, 1:100 Et$_3$N/hexanes to 1:3:96 Et$_3$N/EtOAc/hexanes) afforded product **3qq** as pale-yellow oil (27.3 mg, 49% yield, > 20:1 *r.r.*).

^{1}H NMR (400 MHz, CDCl$_3$) δ 8.60 (d, J = 5.0 Hz, 1H), 7.46 (d, J = 1.7 Hz, 1H), 7.21 – 7.17 (m, 3H), 7.12 – 7.05 (dt, J = 7.7, 4.2 Hz, 1H), 6.75 (dd, J = 7.6, 1.0 Hz, 1H), 4.23 (t, J = 6.4 Hz, 1H), 3.00 – 2.82 (m, 2H), 2.27 – 2.17 (m, 1H), 1.90 – 1.77 (m, 3H).

^{13}C NMR (101 MHz, CDCl$_3$) δ 158.5, 149.9, 148.3 (q, J = 34.1 Hz), 137.6, 136.2, 129.8, 129.5, 126.9, 126.7, 126.1, 121.6 (q, J = 274.3 Hz), 120.6 (q, J = 2.7 Hz), 45.1, 32.6, 29.4, 20.4.

^{19}F NMR (376 MHz, CDCl$_3$) δ -68.0.

HRMS: (ESI$^+$) calculated for C$_{16}$H$_{15}$F$_3$N [M+H]$^+$: 278.1151, found 278.1152.

4-(1,2-dihydroacenaphthylen-1-yl)-2-(trifluoromethyl)pyridine (3rr)

Prepared according to General Procedure A using 2-(trifluoromethyl)pyridine (23.0 µL, 0.2 mmol) and 1,2-dihydroacenaphthylene (308 mg, 2.0 mmol). No other regioisomer was detected in the crude mixture. Purification by column chromatography (SiO$_2$, 5:95 EtOAc/hexanes) afforded product **3rr** as colorless oil (25.4 mg, 42% yield, > 20:1 *r.r.*).

^{1}H NMR (400 MHz, CDCl$_3$) δ 8.66 – 8.62 (m, 1H), 7.75 (t, J = 7.2 Hz, 2H), 7.60 – 7.54 (m, 2H), 7.51 (t, J = 7.6 Hz, 1H), 7.37 (d, J = 7.1 Hz, 1H), 7.31 – 7.27 (m, 1H), 7.12 (d, J = 7.1 Hz, 1H), 5.00 – 4.94 (m, 1H), 4.04 (dd, J = 17.6, 8.8 Hz, 1H), 3.39 (d, J = 17.3 Hz, 1H).

^{13}C NMR (101 MHz, CDCl$_3$) δ 156.5, 150.3, 148.6 (q, J = 34.3 Hz), 145.8, 142.5, 138.6, 131.6, 128.4, 128.1, 125.5, 123.9, 123.0, 121.5 (q, J = 274.3 Hz), 120.2, 119.8, 119.7 (q, J = 2.8 Hz), 48.7, 41.0.

^{19}F NMR (376 MHz, CDCl$_3$) δ -67.6.

HRMS: (ESI$^+$) calculated for C$_{18}$H$_{13}$F$_3$N [M+H]$^+$: 300.0995, found 300.0997.

4.7.6 Procedure for the 1 mmol reaction

To an argon-purged glass vial, containing dithiophosphoric acid catalyst **A2** (127 mg, 0.2 mmol), and pyridine **1a** (81 µL, 1 mmol), was added 2,4,6-collidine (66 µL, 0.5 mmol), followed by cyclohexene **2a** (1 mL, 10 mmol) and argon-sparged HPLC grade acetone (20 mL, 0.05 M). The vial was sealed with Parafilm, and placed in the 365 nm irradiation setup (Figure 4.49, left panel). The reaction was stirred for 16 h, then the solvent was evaporated. The regioisomeric ratio **3a/3a'** (2.6:1) of the crude mixture was measured by ^{1}H NMR analysis. Purification by column chromatography (SiO$_2$, 1:10:89 Et$_3$N/EtOAc/hexanes) afforded product **3a** as a light-yellow oil (81.2 mg, 51% yield, > 20:1 *r.r.*). The minor regioisomer **3a'** was not isolated after column chromatography.

Chapter V

General Conclusions

The work carried out in this doctoral thesis has shown that the combination of photo- and organocatalysis can be used to design new reactions for the formation of $C(sp^3)$-$C(sp^3)$ and $C(sp^2)$-$C(sp^3)$ bonds, which cannot be achieved with thermal activation. Specifically, the application of distinct mechanisms of photochemical activation grants access to key organic radical intermediates, which can be engaged in various synthetic transformations.

In chapter II, it was shown that electrophilic ground-state chiral iminium ions were able to intercept radicals generated by a visible-light-activated organic photoredox catalyst with high levels of stereoselectivity. An electron-poor *gem*-difluorinated secondary amine catalyst and a highly oxidizing acridinium-based photocatalyst were essential for the development of this dual-catalytic platform. The amine catalyst secured the formation of highly reactive iminium ion intermediates, which could overcome a fast racemic background process. In concert, the oxidative power of the photocatalyst permitted the use of a wide variety of non-nucleophilic radical precursors, such as organosilanes, organotrifluoroborate salts, organosilicates, Hantzsch esters, and cyclopropanols.

Chapter III detailed the first example of an organocatalytic allylic benzylation reaction. This chemistry relies on a new class of dithiophosphoric acid catalysts, which were found to act as donors in photoactive electron donor-acceptor (EDA) complexes while simultaneously activating allylic C-H bonds through hydrogen atom transfer (HAT). These two modes of activation allowed the formation of benzylic and allylic radicals from readily available starting materials upon visible light irradiation. Cross-coupling between these two open-shell intermediates eventually afforded the target allylic-benzylic C-C bond, albeit with concurrent formation of dimeric side-products. This undesired competitive pathway was suppressed by designing a three-component version of the reaction, which greatly expanded the scope of the chemistry.

Finally, it was found that these same dithiophosphoric acids could be activated with UV light to reveal a strongly reducing excited state, thus permitting the activation of substrates that do not engage in EDA complexes formation. Chapter IV delineates how this feature was used to design a regioselective allylation of pyridines, proceeding *via* the formation of neutral pyridinyl radicals. The organic catalyst performed three roles; (*i*) as a Brønsted acid to activate pyridine by protonation; (*ii*) as an excited-state reductant to generate pyridinyl radicals from pyridinium ions; and (*iii*) as a HAT catalyst to generate allylic radicals from simple alkenes. The functionalized pyridines were obtained after regioselective radical coupling between

these intermediates and facile rearomatization. The mechanistic proposal was supported by experimental, computational, and photophysical studies.

UNIVERSITAT ROVIRA I VIRGILI
PHOTOCHEMISTRY AND ORGANOCATALYSIS FOR RADICAL-BASED CARBON-CARBON BOND-FORMING
PROCESSES
Emilien Le Saux

UNIVERSITAT
ROVIRA i VIRGILI